CERN 69-3
Intersecting Storage
Rings Division
12 March, 1969.

ORGANISATION EUROPÉENNE POUR LA RECHERCHE NUCLÉAIRE
CERN EUROPEAN ORGANIZATION FOR NUCLEAR RESEARCH

GENERAL PROPERTIES OF FIELDS AND BEAM DYNAMICS IN A LINAC GAP

B. Schnizer*)

GENEVA
1969

SUMMARY

An extensive and detailed derivation of non-relativistic and relativistic difference equations describing the motion of a single proton through an Alvarez structure linac gap is given extending the difference equations given by P. Lapostolle at the Frascati Conference (1965). Integral representations of the field in such a gap are derived and their properties are discussed as well as those of the field amplitude which is proportional to the transit time factor. Beam dynamics coefficients are defined which are Fourier transforms of the fields. There are two types of them : T-coefficients which are known as soon as the transit time factor is given and which occur in difference equations describing the change of particle coordinates across the whole gap. In difference equations across the first half of it enter in addition the S-coefficients which are much more complicated.

Beam dynamics equations are derived by first order perturbation theory regarding as perturbation the influence of the radio frequency field (with angular frequency ω) on free particle motion. This is equivalent to solving the equations of motion by iteration starting from free particle motion, but the present method is more definite. The magnitude of the perturbation is described by the parameter $\kappa = (eE_1/\omega)/(m\dot{z}_o)$, (< 0.1) the impulse transmitted to the particle by the radio frequency RF field (with average strength E_1 across the gap) divided by the free particle momentum $m\dot{z}_o$. Results can be interpreted as if the particle interacts in the gap mainly with those waves travelling with its own velocity. Relativistic corrections (due to the magnetic RF field and the mass variation) are of the order $\kappa\beta^2$.

There are some chapters of an introductory nature. One deals with the motion of a proton in a uniform time-harmonic field. In another are described the methods of solving equations of motion approximately and the thin lens approximation. At the end are given tables of beam dynamics coefficients and of non-relativistic and relativistic beam dynamics difference equations across the whole gap and across the first half of it.

Remarks on the Presentation of the Material

"Mine is a long and sad tale" said the Mouse, turning to Alice and sighing. "It is a long tail, certainly" said Alice, looking down with wonder at the Mouse's tail; "but why do you call it sad?"

(Lewis Caroll, Alice's Adventures in Wonderland)

In the present report the author tried to reconcile two somewhat opposing aims, wishing to give the detailed rigorous derivations of beam dynamics equations without burying the technically useful equations among the haberdashery of mathematical proofs and lengthy calculations. Therefore the treatment is explained and the whole work is reviewed in the introduction (chapter 1); and tables for beam dynamics coefficients and beam dynamics difference equations are given at the end of the report. In addition, in chapters 2 to 5 the more intricate discussions and lengthy calculations of each section have been deferred to the end of it as appendices. It was intended to do this separation in such a way that the

section presenting the main train of thought is still understandable and readable without the need of consulting the appendices. In the latter the discussion goes into considerable detail in order to make the report as a whole rather self-contained. This philosophy made more frequent repetitions and cross references unavoidable.

TABLE OF CONTENTS

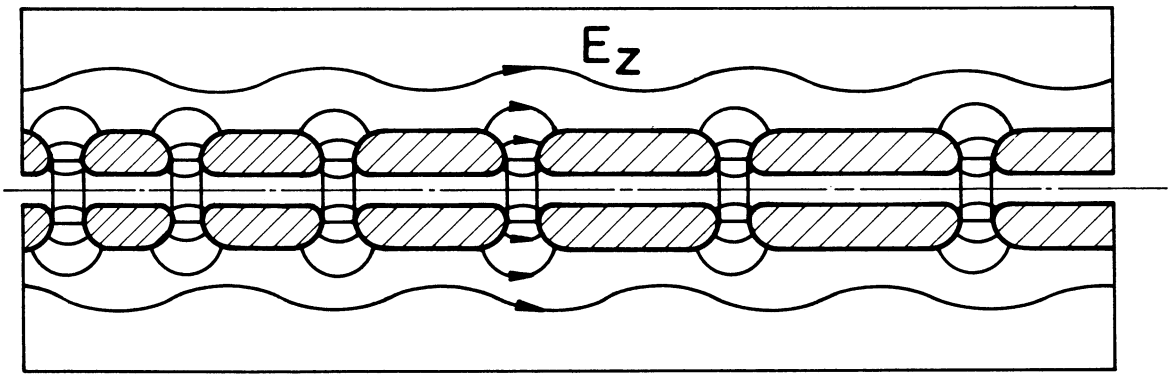

Fig. 1.1.1. Schematic sketch of an Alvarez structure linac.

1. Introduction and Review

The Alvarez structure of linear accelerators (Fig. 1.1.1.) consists of a resonant cylindrical cavity. Typical values of it are : characteristic frequency of the lowest mode $\omega/2\pi \simeq 200$ MHz (free space wave length $\lambda_o \simeq 1.5$ m), cavity radius $\simeq 0.5$ m, length some meters. Along the axis of this cavity passes the beam of particles to be accelerated. For this purpose drift tubes are aligned along the axis whose length and distance is adjusted in accordance with the particle velocity in a way to screen the particles from the radio frequency field during about three quarters of a period. In the remaining quarter the particles pass through the gaps between the drift tubes where they are accelerated by the microwave field. The direction of the latter is favourable to acceleration during half a period, however, the additional condition of phase stability restricts the useful time to a quarter.

For the detailed analysis of the electromagnetic field and of particle dynamics in such a structure, the whole tank is firstly split up into single cells of length L_n by inserting plates in the middle between gaps. This is done at those places where the transverse electrical field is zero so that the field distribution is not changed by these septates. In practice, the method of investigation is applied in reversed order. First the field in single cell cavities is investigated theoretically and experimentally and all cells are tuned to the same resonant frequency. Then the whole linac is designed by assembling cells (without faces) and matching the current flowing along the cylindrical wall.

To these two steps correspond two levels of treating particle dynamics. Firstly, the motion of a particle through a single field region is investigated. The ensuing results are used to trace particles through the whole linac. Each linac comprises various regions where different fields of force are acting upon the charged particle. In the interior of the drift tubes magnetic quadrupoles are inserted to focus the beam. They may be separated from the central region of the cell by some drift space. At the centre, between the drift tubes there is the gap which is filled by the electromagnetic radio frequency field penetrating from the main cavity. The present report is centered on the investigation of the motion of a single heavy charged particle through such a gap. Interactions between particles, or space charge forces, are neglected.

The theory presented here is applicable to protons or heavy particles only. The underlying basic assumption is that there is an accelerating time-harmonic electromagnetic field along the beam direction, confined by gaps and drift tubes in which the field cannot penetrate. Thus, though the theory is particularly applicable to the Alvarez structure, this assumption is met in other accelerating structures.

The pioneering work by PANOFSKY [1] has been extended, modified and applied by many other authors. The works of J.S. BELL [2], R. TAYLOR [3], SWENSON [4], RICH [5]. PROME [6], LAPOSTOLLE [7][8] CARNE et al. [9], CARNE and LAPOSTOLLE [10] may be quoted. This list, of course, is by no means complete.

It is not possible to solve exactly the equations of motion of a particle moving in a field as complicated as that of an accelerating gap, and it is necessary to employ approximate methods. It is initially assumed that the field in the gap is exactly known and can be described by Fourier integrals with respect to z (cf. eq.(1)), the amplitude function being the transit time factor $T_o(k_z)$ (cf.(2)). The equations of motion are solved by treating the influence of the field upon the otherwise free particle as a perturbation. It then turns out that if first order results are satisfactory, there is no need for complete information about the field, but all beam dynamics equations integrated across the whole gap contain the transit time factor for only one value $k = \omega/\dot{z}_o$ ($\dot{z}_o$ = longitudinal velocity of the particle in the centre of the gap) of its argument k_z .

It may be worthwhile to describe this point already here in more detail. The field is given by :

$$E_z(z,r,\omega t) = \frac{E_1}{2\pi} \int_{-\infty}^{\infty} b(k_z)\left[I_o(k_r r)/I_o(k_r a)\right] e^{ik_z z}\, dk_z \cos(\omega t + \phi_o) \qquad (1.1.1)$$

$$k_r = \left[k_z^2 - (\omega/c)^2\right]^{\frac{1}{2}}$$

where a is the radius of the drift tubes terminating the gap and E_1 the average field strength across the gap. The amplitude function is proportional to the transit time factor :

$$T_o(k_z) \sim \frac{b(k_z)}{I_o(k_r a)} \sim \frac{\sin(k_z p/2)}{k_z p/2} \frac{1}{I_o(k_r a)} (1 + Y) . \qquad (1.1.2)$$

$p = g + 2 R_i$ is roughly equal to the gap length (cf. Fig. 2.1.4). Y is in general small compared to unity ($|Y| << 1$). The equations of motion, e.g.

$$m \ddot{z} = eE_z(z,r,\omega t) \qquad (1.1.3)$$

are solved by interation: Free particle motion :

$$z_{(o)} = \dot{z}_o t \qquad r_{(o)} = \dot{r}_o t + r_o \qquad (1.1.4)$$

is assumed as a zero order solution and inserted into the right hand side of (3). $E_z(z_{(o)}(t), r_{(o)}(t), \omega t)$ becomes a pure function of time t and the differential equation (3) can be solved by quadratures. If this is done with the representations like that in (1), this gives integral representations of the trajectories:

$$z_1(t) = \dot{z}_o t + \qquad (1.1.5)$$

$$+ \frac{eE_1}{m\dot{z}_o} \frac{1}{2\pi} \int_{\hat{C}} b(k_z) \frac{I_o(k_r r)}{I_o(k_r a)}\, dk_z \frac{1}{2}\left[e^{i\phi_o} \frac{e^{it(k_z \dot{z}_o + \omega)}}{k_z + \omega/\dot{z}_o} + e^{-i\phi_o} \frac{e^{-it(k_z \dot{z}_o - \omega)}}{k_z - \omega/\dot{z}_o} \right]$$

Radial motion is neglected for the present and radius is assumed as constant, $r \equiv r_o$. The path of integration $\hat{C}$ in the complex k_z -plane avoids the poles: $k_z = \pm k = \pm \omega/\dot{z}_o$ (see Fig. 2.2.1). These singularities give the main(or even only) contribution if the above integral is used to evaluate the change in velocity (for kinetic energy) across the whole gap (cf. eq. (7)). This suggests the following physical interpretation : The integral (1) is a superposition of partial waves and the particle mainly interacts with the waves moving with its own velocity. This statement, however, should not be taken too literally.

From this it results that beam dynamics can be completely described to that order of approximation if the transit time factor $T_o(k)$ and its derivatives $dT_o(k)/dk,...$ are known for the only value :

$$k = \omega/\dot{z}_o \tag{1.1.6}$$

These quantities depending on both the gap geometry and the field of the main cavity provide sufficient information about the field acting upon the particle. The change of all particle coordinates across the gap is expressed by $T_o(k)$, $dT_o/dk,..$. For example, the gain in kinetic energy is :

$$\Delta W = eV_o\, T_o(k)\, I_o(k_r r)\, \cos\phi_o + ... \tag{1.1.7}$$

$V_o \approx E_\perp p$ is the peak voltage across the gap.

The transit time factor :

$$T_o(k) = \int_{-\infty}^{\infty} E_z(z, r = 0, \omega t)\, \cos(kz)\, dz \Big/ \int_{-\infty}^{\infty} E_z(z, r = 0, \omega t)\, dz \tag{1.1.8}$$

is a measure of the longitudinal distribution of the longitudinal electric field E_z along the axis, and may be easily derived by numerical integration from solutions which have been obtained by solving the field equations numerically (mesh calculations). $T_o(k)$ is the Fourier transform of E_z and by this theorem the equivalence between the definition (8) and the statements of eqs.(1) and (2) can be shown.

The magnitude of the influence of the electric field upon the motion of the particle is determined by the parameter :

$$\kappa = eE_\perp/(m\omega\dot{z}_o) \tag{1.1.9}$$

This is suggested from the factor $eE_\perp/(m\dot{z}_o)$ preceeding the integral in eq. (5). The factor $1/\omega$ comes in if the derivative dz/dt is transformed into one with respect to phase, $\phi = \omega t$; this means that time is measured in units of the period of the accelerating radio

frequency field. $\kappa = (eE_1/\omega)/(m\dot{z}_o)$ may be interpreted as the ratio of two momenta : The numerator is a measure of the impact of the field whose force ($\sim eE_1$) is acting upon the particle during the time of one period ($\sim 1/\omega$). This is divided by the momentum of the free particle. The physical interpretation raises the hope that the effect of the field is even smaller, say $\kappa/3$ or so, since the particle sees the field only during a third or a quarter of a period. The value of κ is smaller than 0.1 at the entrance of a proton linac (0.5 MeV) and decreases with increasing energy. By use of this perturbation parameter it is possible to solve the equations of motion in a more systematic way. Perturbation series are assumed for the solutions :

$$z(t) = z^{(o)}(t) + \kappa z^{(1)}(t) + \kappa^2 z^{(2)}(t) + \ldots \qquad (1.1.10)$$

and the equations of motion (3) are split into a system of equations. It is reasonable to believe that the coefficients of the powers of κ in (10) are of about the same order of magnitude, so that the series (10) permits to estimate the accuracy attained. The order of magnitude of relativistic effects (force due to the magnetic radio frequency field and mass variation) is given by $\kappa(\dot{z}_o^2/c^2) = \kappa\beta^2$. The relative magnitude of these parameters depending on the velocity, $\beta c \approx \dot{z}_o$, is shown in Fig. 4.1.1.

In Chapter 2 are discussed the properties of the field in the gap and the beam dynamics coefficients. In Section 2.1 the field in the cavity and in the gap is described and explained by a few drawings of field distributions. The parameters describing the gap geometry are introduced and the concept of the effective gap length is mentioned. In Section 2.2 the field components E_r, E_z, H_θ are expressed by Fourier integrals with respect to the longitudinal (z-) direction (cf. eq. (1)). Their analytical properties can be discussed (Section 2.3) by expanding in a Fourier series the longitudinal component of the electric field applied along the circumference, r = a, of the gap, $|z| \leq p/2$:

$$E_z^a(z) = E_z(z, r = a) = E_1 2 \left[1/2 + \sum_{n=1}^{\infty} B_n \cos(2\pi n z/p) \right] \qquad (1.1.11)$$

It is assumed that E_z^a is continuous and symmetrical with respect to the centre, z = 0, and that its derivative $\partial E_z^a/\partial z$ is only weakly singular (so that it is still integrable). Then the series (11) is absolutely and uniformly convergent and operations of summation and integration may be interchanged. By means of a Green 's function the field in the interior is related to $E_z^a(z)$ and the field amplitude is found :

$$b(k_z) = \frac{\sin(k_z p/2)}{k_z p/2} \left[p - 2k_z^2 p^3 \sum_{n=1}^{\infty} B_n(-1)^n \Big/ \left[(2\pi n)^2 - (k_z p)^2 \right] \right] \qquad (1.1.12)$$

$p = g + 2R_i$ is gap length plus the radius of the drift tube rims. (See Fig. 2.1.4). The Fourier integrals representing E_z, E_r and H_θ are absolutely and uniformly convergent for $r < a$.

Therefore they are analytical functions in z and r (< a). In Section 2.5 are given series expansions of the fields in terms of the Fourier coefficients B_n . The series for $U = -rH_\theta$ may be fitted to the values $U_m(r = a)$ found by mesh calculations to give numerical values for a finite number of coefficients B_n. The quality of this method is discussed by comparing $U_m(r < a)$ with the calculated U_c . In Section 2.6 are defined the T-coefficients. They are even Fourier transforms of the three field components (cf. (8))and can be simply expressed as products of the transit time factor T_o with modified Bessel functions. They serve for expressing the change of particle coordinates across the whole gap. The S-coefficients (Section 2.7) are odd Fourier integrals along the half-line $0 \leq z \leq \infty$. They serve for beam dynamics formulae across the first half of the gap. S-coefficients are complicated functions of k and r and their expressions contain besides the T-coefficients series of modified Bessel functions.

In Section 2.8 another approach of fitting fields to the mesh values U is described. It starts from Fourier expansions of the magnetic field. This is used in Section 2.9 for the derivation of new expressions for T- and S-coefficients.

Chapter 3 deals with the motion of a proton in a time-harmonic spatially homogeneous field. This model for an accelerating gap is oversimplified but useful from the pedagogical point of view, since all solutions can be worked out easily. In Section 3.1 this problem is treated in the non-relativistic approximation. There the reasons appear for the introduction of the perturbation parameter $\kappa = eE_1/(m\omega\dot{z}_o)$; and the transition from approximate solutions found by interations to those arising from perturbation theory is described. In Section 3.2 is explained the practical application of beam dynamics formulae and the use of the longitudinal S-coefficient. Numerical examples given in Section 3.3 show that the accuracy of approximate formulae for energy gain is somewhat better if mid-gap conditions in place of input conditions are used to specify the solutions of the equations of motions. In Section 3.4 a method is demonstrated by which the relativistic mass variation can be taken into account approximately.

In Chapter 4 are discussed approximation schemes used in the treatment of particle dynamics. Two methods of solving equations of motion approximately, iterations and perturbation theory, are explained and compared in Section 4.1.Section 4.2 contains general comments on the thin lens approximation where real trajectories of the particles are replaced by step functions, as if the gap were reduced to its median plane.

In Chapter 5 are derived non-relativistic expressions for the particle motion. The equations of motion are solved in section 5.1 by the method whose main features have been described at the beginning of this introduction. The non-relativistic difference equations for the change of kinetic energy, phase, transversal position and velocity across a gap and across the first half of it are derived in Section 5.2 and 5.3, respectively. In Section 5.4 is considered a method where input values in place of mid-gap conditions are used to specify the solutions. This permits to avoid the complicated S-coefficients. But it is

then necessary to change the present linac design procedure.

In Chapter 6 the relativistic equations of motion are solved approximately and the two corresponding sets of difference equations are derived.

At the end of the report tables are given for the transit time factor T_o and its derivatives (Table I), for T- and S-coefficients (Table II), non-relativistic difference equations across the whole gap (Table III), across the first half of it (Table IV) and for the two corresponding sets where relativistic corrections are included (Table V and V1, respectively).

Applications of these (or similar) beam dynamics equations are described, for example, in refs. [10) - 12)].

2. General Properties of the Field. Beam Dynamics Coefficients

This chapter deals in considerable detail with the properties of the field representations and of the amplitude functions $b(k_z)$ proportional to the transit time factor $T_o(k_z)$ contained in them. For those who are mainly interested in the derivation of the beam dynamics equations it may suffice to have a look upon the field representations (2.2.11) to (2.2.13), the expression for the amplitude function $b(k_z)$, eq. (2.4.6)(cf. eqs.(1.1.11) and (1.1.12)),whose most important property is given in equations (2.4.9), and upon the definitions of beam dynamics coefficients described in Sections 2.6 and 2.7.

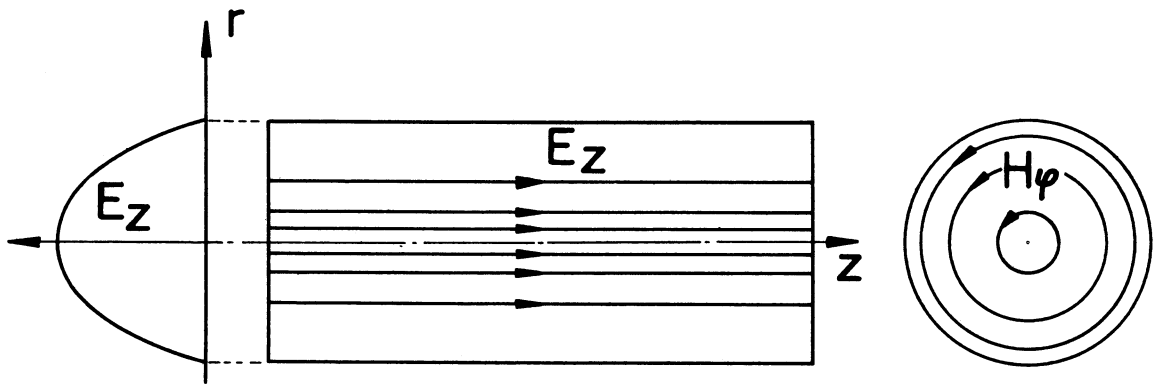

Fig. 2.1.1 Field Distribution of the basic TM-mode in a cylindrical cavity

2.1. General Description of the Cavity, of the Gap and of the Field

Before describing gap geometry and its characteristic parameters, it may be worthwhile to say a few words about the electromagnetic field in the whole cell. The lowest TM-mode of an empty cylindrical cavity (radius R) is (Fig. 2.1.1.) :

$$\begin{aligned} E_z(z,r,t) &= A\ J_o(j_{o,1} r/R) \cos(\omega t) \\ E_r(z,r,t) &= 0 \\ -c\,\mu\, H_\theta(z,r,t) &= A\ J_1(j_{o,1} r/R) \sin(\omega t) \end{aligned} \qquad (2.1.1)$$

where $j_{o,1} = 2{,}405$ is the first zero of the Bessel function $J_o(x)$. The corresponding eigen frequency $\omega/2\pi$ is given by :

$$k_o = \omega/c = j_{o,1}/R \qquad (2.1.2)$$

The field distribution is homogeneous in the z-direction but decreases radially.

In the real Alvarez cavity (Fig. 1.1.1) the drift tubes aligned along the axis, r = 0, disturb the field there, but in the outer regions, $R \geq r \geq R/3$, the field distribution is not so different from that in the empty cavity. The longitudinal electrical field E_z is displayed in Figs. 2.1.2 and 2.1.3. Figure 2.1.2 shows the field $E_z(z=0,r,t=0)$ in the centre plane for the instant t=0 (peak field). The field strength is considerably increased in the region of the drift tubes. This may be discussed using the static approximation which is valid for distances from the metallic boundaries which are small in comparison with the free space wave length $\lambda_o = 2\pi\, k_o \simeq 1.5$ m. The potential $\int E_z\, dz$ between opposite walls is then constant. If the distance between metallic surfaces is decreased, as is the case for the drift tube region, the field strength is increased. The same reasoning explains the drop in the field strength within the drift tubes, r < a. Figure 2.1.3 gives the longitudinal distribution of $E_z(z,r,t=0)$ along various lines r = const. The field cannot penetrate into the drift tube bores, the field distribution is roughly rectangular for $r \simeq a$. The decay is less steep along the axis, r = 0. (The longitudinal distribution of E_z within the gap varies to a certain extent with increasing gap length. This is discussed in Section 2.5.) Just between the cylinders of the drift tubes the field strength E_z is highest. Outside of them it decreases with increasing radius; its homogeneity in the z-direction is gradually restored, and is almost perfect for r > R/3. The eigen frequency of the cavity is lowered by the insertion of the drift tubes, e.g. an empty cavity with the same outer dimensions as that whose field is displayed in Fig. 2.1.2 and 2.1.3, has an eigen frequency of 215 MHz while the real Alvarez cavity has 203 MHz.

Gap geometry and the parameters characterizing it are shown in Fig. 2.1.4. The rims of the drift tubes are rounded to prevent sparking. Therefore the numerical value of the gap length is a somewhat ambiguous quantity. In the present work the gap and the adjoining

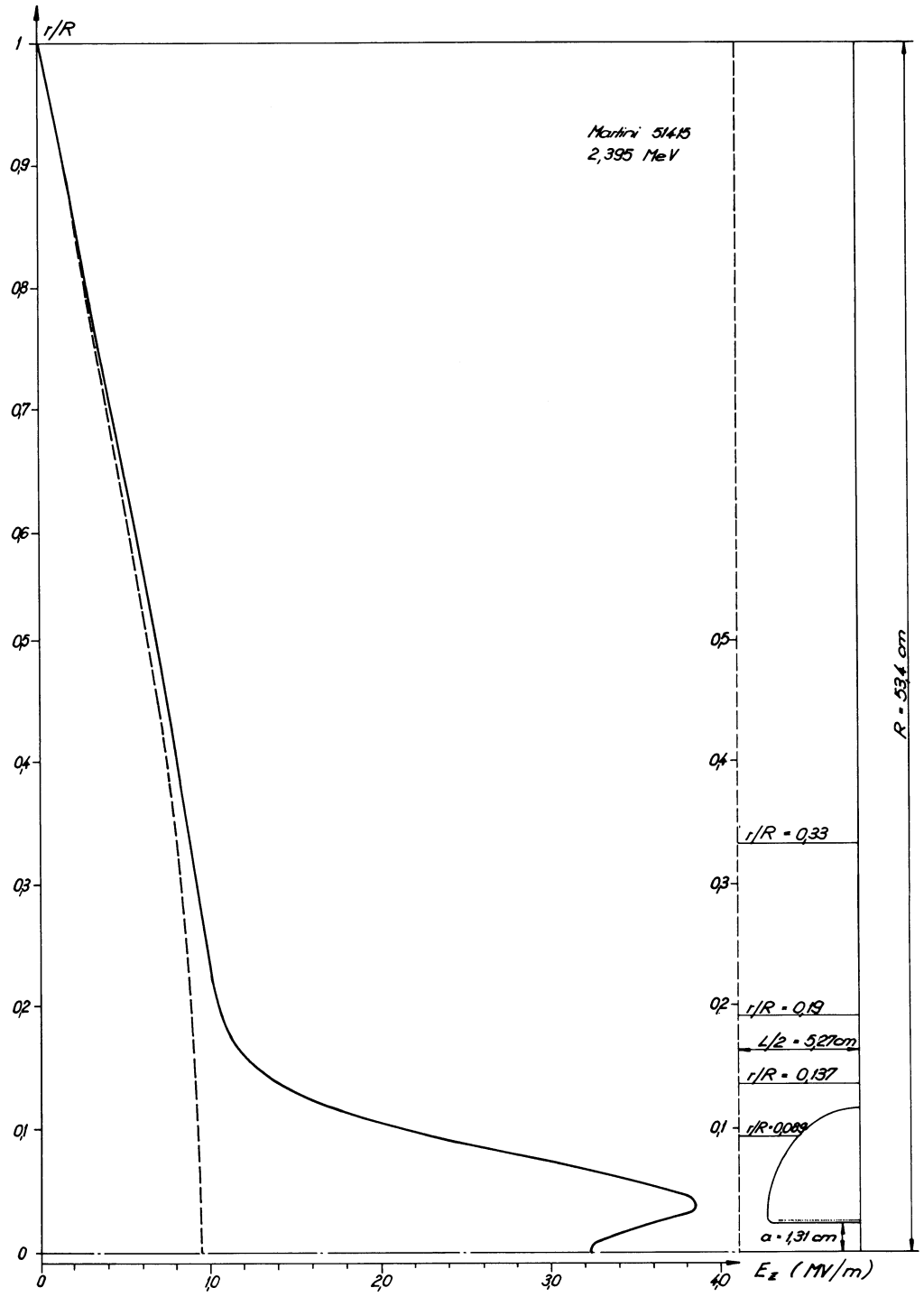

Fig. 2.1.2. Longitudinal electric field, $E_z(z=0,r)$ in the centre plane of an Alvarez cell versus relative radius, r/R. Cavity MARTINI 51415 : Energy 2.395 Mev, transit time factor $T_o = 0.762$, $\omega/2\pi = 202.99$ MHz. Normalization : Average Field strength $E_o = 1$ MV/m. Drift tube dimensions are given in Fig. 2.1.3. The dashed line gives the field E_z of an empty cavity with same radius R = 53.4 cm ($\omega/2\pi = 215$ MHz), eq. (2.1.1), A = 0.95 MV/m. The geometry of the half cell is given at right, dashed line is symmetry (centre) plane.

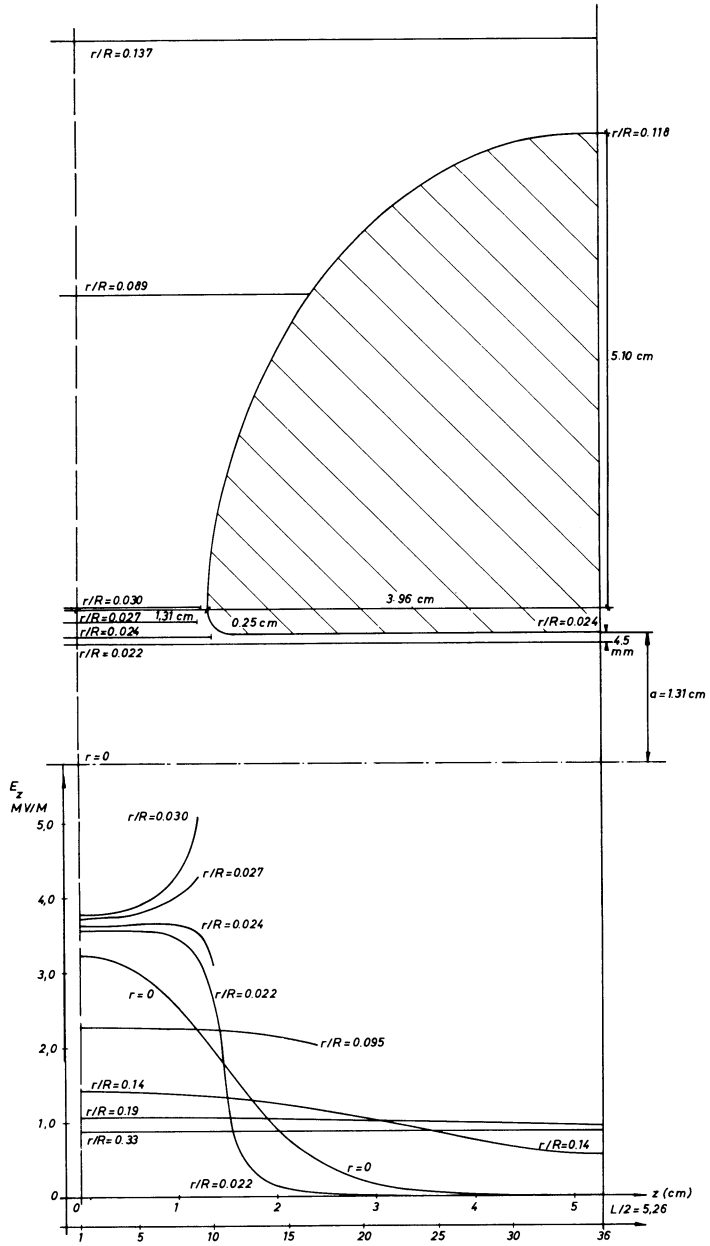

Fig. 2.1.3. Longitudinal electric field, $E_z(z,r)$, along various lines r/R = const. versus longitudinal coordinate z. The position of the lines r = const. chosen is indicated in the upper part of the figure displaying cavity geometry. Cavity MARTINI 51415 : Energy = 2.395 MeV, transit time factor T_o = 0.762, $\omega/2\pi$ = 202,99 MHz, normalization: average field strength E_o = 1 Mv/m. Radius R = 53.5 cm, cell length L = 10.53 cm. The cross section of the drift tube is bounded by a circle (R_1 = 0.25 cm) in the lower part and (approximately) by an ellipse (semi-axes 3.96 cm and 5.10 cm)in the upper part. Radius of drift tube bore a = 1.31 cm. Values of E_z have been found by interpolation starting from the potential $U(z,r) = -rH_\theta$ found by a mesh calculation. For lines $r \leq a$ the method described in section 2.5 has been used. For other lines a rather rough approximation is introduced by replacing in eq. (2.3.4) differential quotients by differences : $E_z \sim (1/r)\,\Delta U/\Delta r$ where ΔU is the potential difference between adjoining mesh lines and $\Delta r \approx 1.5$ mm mesh line distance.

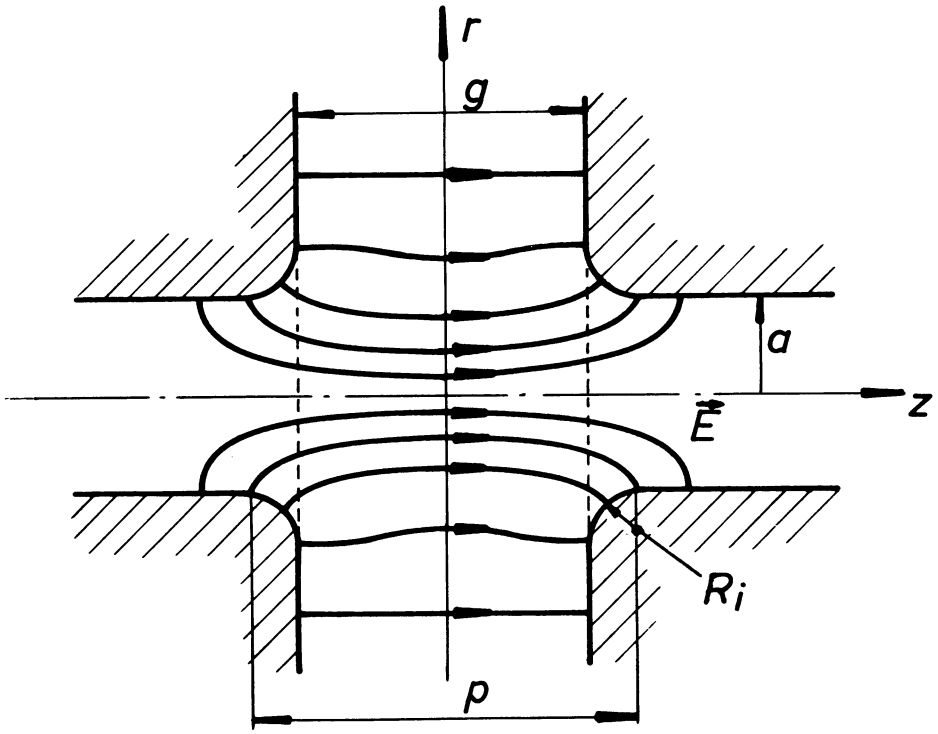

Fig. 2.1.4 Configuration of an accelerating gap and its field.

drift tubes are described by an infinitely long circular wave guide of radius a (= radius of the drift tube bore) with a circumferential slot at r = a, $-p/2 \leq z \leq p/2$, where

$$p = g + 2\,R_i \tag{2.1.3}$$

is the real distance (wall to wall) at r = a. If it is assumed that the electrical field is rather homogeneous, E_z = const. in that portion r > a of the gap where the distance of the metallic surfaces is smallest (=g) and where they are straight and parallel, then the roundening of the rims will introduce a certain distortion of the field E_z at r = a. Here this is not taken into account by physical considerations, but it is implicitely contained in the coefficients B_n of the Fourier series :

$$|z| \leq p/2 : \qquad E_z(z,r = a) = 2\,E_1 \left[B_o/2 + \sum_{n=1}^{\infty} B_n \cos(2\pi n z/p) \right] \tag{2.1.4}$$

into which the tangential electrical field is expanded (Section 2.4).

In earlier works [3), 10),13)] some effective gap length has been introduced :

$$g' = g + \alpha\,R_i \tag{2.1.5}$$

g' is not a geometrical parameter, it is empirically adjusted in such a way that the transit time factor found by numerical integration of the defining integral :

$$T_o = \int_{-L/2}^{L/2} E_z(z,r = 0) \cos(2\pi z/L)\, dz \Big/ \int_{-L/2}^{L/2} E_z(z,r = 0)\, dz \tag{2.1.6}$$

where the real field on the axis is used, equals that (T_{oo}) for a homogeneous field E_z = const. applied along the slot r = a, $-g'/2 \leq z \leq g'/2$:

$$T_{oo} = \frac{\sin(2\pi g'/L)}{2\pi g'/L} \cdot \frac{1}{I_o\left(a\sqrt{(2\pi/L)^2 - (\omega/c)^2}\right)} \tag{2.1.7}$$

Various numerical values have been proposed for α, e.g. $\alpha = 1/2$ [3)], $= 1$ [10)], $= 0.85$ [13)]. However, this approximation is not used here. Its merits are discussed at the end of Section 6.2.

2.2. Field Equations and Field Representations.

Throughout this report practical MKSA units will be used. In general, instead of time t time-angle (phase) :

$$\phi = \omega t \tag{2.2.1}$$

is employed. (ω = angular frequency of the accelerating radio frequency field.) Axially symmetrical, source-free, time-harmonic electromagnetic field TM-fields will only be regarded :

$$E_\theta = H_r = H_z = 0 \qquad \partial/\partial\theta = 0$$

$$-\frac{\partial H_\theta}{\partial z} = \varepsilon \frac{\partial E_r}{\partial t} = \varepsilon\omega \frac{\partial E_r}{\partial \phi}$$

$$\frac{1}{r}\frac{\partial}{\partial r}(rH_\theta) = \varepsilon \frac{\partial E_z}{\partial t} = \varepsilon\omega \frac{\partial E_z}{\partial \phi} \tag{2.2.2}$$

$$\frac{\partial E_r}{\partial z} - \frac{\partial E_z}{\partial r} = -\mu \frac{\partial H_\theta}{\partial t} = -\mu\omega \frac{\partial H_\theta}{\partial \phi}$$

$$\nabla\cdot\vec{E} = \frac{1}{r}\frac{\partial}{\partial r}(rE_r) + \frac{\partial E_z}{\partial z} = 0 \qquad \nabla\cdot\vec{H} = \frac{1}{r}\frac{\partial H_\theta}{\partial \theta} = 0$$

The field components of E_r, E_z, H_θ of such a field may be derived from an electric Hertz vector $\vec{\pi} = \vec{e}_z\, V(z,r,\phi)$ [14] where V is a solution of the scalar Helmholtz equation

$$\Delta V - \frac{1}{c^2}\frac{\partial^2 V}{\partial t^2} = \frac{\partial^2 V}{\partial r^2} + \frac{1}{r}\frac{\partial V}{\partial r} + \frac{\partial^2 V}{\partial z^2} + k_o^2 V = 0 \tag{2.2.3}$$

with

$$k_o^2 = \varepsilon\mu\,\omega^2 = \omega^2/c^2 \tag{2.2.4}$$

Field components are given by :

$$E_z = \left(\frac{\partial^2}{\partial z^2} + k_o^2\right) V = -\left(\frac{\partial^2}{\partial r^2} + \frac{1}{r}\frac{\partial}{\partial r}\right) V$$

$$E_r = \frac{\partial^2 V}{\partial z \partial r} \tag{2.2.5}$$

$$H_\theta = -\varepsilon \frac{\partial^2 V}{\partial t \partial r} = -\varepsilon\omega \frac{\partial^2 V}{\partial r \partial \phi}$$

Along the metallic wall (of infinite conductivity) of a wave guide or cavity (radius a) the tangential electrical field E_z vanishes. This implies for V the boundary condition :

$$r = a : \qquad V = 0 \tag{2.2.6}$$

Of course, this is not true along the circumferential slot ($-p/2 \leq z \leq p/2$) where the gap leads to the main cavity.

In the applications considered here the frequency $\omega/2\pi$ ($\approx$ 202 MHz) lies far below the lowest cut-off frequency $\omega_{cl}/2\pi$ of the wave guide ($\omega \approx \omega_{cl}/50$ to $\omega_{cl}/100$, cf.(2.4.39) or (2.5.1)) so that all modes are evanescent. At the infinitely remote faces of the wave guide may therefore be prescribed :

$$|z| = \infty \qquad V = 0 \tag{2.2.7}$$

If, however, the wave guide is closed by plates perpendicular to the z-axis say at $z = -\ell_1$ and at $z = \ell_2$, the condition :

$$z = -\ell_1, \ \ell_2 \qquad \frac{\partial V}{\partial n} = \mp \frac{\partial V}{\partial z} = 0 \tag{2.2.8}$$

applies. It is also appropriate for the quasi-periodic field of an Alvarez structure driven in the zero mode.

Imagine the field distribution (cf. Fig. 2.5.3) corresponding to an instant where phase stable particles are crossing a gap. E_r is then positive at the end of it and negative at the entrance of the next gap, and so on. It has to change sign somewhere between these gaps, say at $z = -\ell_1$, and $z = \ell_2$. The field is not altered if there plates are inserted. In this way the whole linac tank may be split into single cells, each containing one gap and (roughly) a half of the anterior and of the posterior drift tube. Since the point $z = 0$ is defined by the electric gap centre, the coordinates of the planes $E_r = 0$ differ in sign and may have different distances from it.

In a closed cavity with boundary conditions (6) and (8) the spectrum of eigen frequencies is discrete. In a wave guide where (6) and (7) apply, the spectrum is continuous and this brings the advantage that the fields may be described by integral representations.*) Since the field decreases fast within the drift tube bores the difference in the field distributions (cf. Section 2.5) due to the difference in boundary conditions (7) or (8) is expected to be negligible as far as beam dynamics is concerned. As the fields in the wave guide decay exponentially ($\omega << \omega_{cl}$!) for $|z| \to \infty$, it is appropriate to represent them by Fourier integrals:

---

*) There arises the additional difficulty that the complete system of eigen functions of a cavity contains such ones which cannot be generated by an electric or a magnetic Hertz vector $\vec{\pi} = \vec{e}_z \vec{V}$ [15], so that the Green 's function analogous to that used in Section 2.3, is more complicated.

$$V(z,r,\phi) = V(z,r)\cos(\phi + \phi_o)$$

$$= \frac{E_1}{2\pi}\int_{\bar{C}} \frac{b(k_z)}{\gamma^2 J_o(\gamma a)}\, J_o(\gamma r)\, e^{ik_z z}\, dk_z \cos(\phi + \phi_o) \qquad (2.2.9)$$

with

$$\gamma = \gamma_1 + i\,\gamma_2 = ik_r = (k_o^2 - k_z^2)^{1/2},\ \gamma_2 \geq 0 \qquad (2.2.10)$$

ϕ_o is just a phase constant. The partial waves $J_o(\gamma r)\, e^{ik_z z}$ are solutions of (3) for any (complex)k_z ; so is their superposition with an arbitrary amplitude function. The latter has been written down in a fashion anticipating some of the results of Sect. 2.4. The path of integration $\bar{C}$ (cf. Fig. 2.2.1) avoids the singularities $k_z = \pm k_o$ ($\gamma = 0$). Here it does not matter whether the indentations go upwards or downwards, since the poles $k_z = \pm k_o$ do not contribute to the electromagnetic field. (cf. eqs. (11) to (13)). - The choice is important e.g. in the case where V represents the velocity potential of an acoustical field ($\sim$ grad V).- The poles $J_o(\gamma a) = 0$ lie off the real k_z -axis if $\omega < \omega_{cl}$, i.e. $k_o < j_{o,1}/a$ (cf.(2.4.39)). $b(k_z)$ is continuous and bounded for any real k_z . The branch $\gamma_2 \geq 0$ of the square root γ (10) is chosen. (cf. Fig. 2.2.1). This ensures convergence of the integrals (9), (11) to (13), as discussed in Section 2.4.C. No integral contains an odd power of γ(e.g. $J_o(\gamma r)/(\gamma^2 J_o(\gamma a))$, $J_1(\gamma r)/(\gamma J_o(\gamma a)),\ldots$); each is a single-valued function of k_z. In the following representations for the field components derived from (9) according to (5), integration may be performed along the real k_z-axis, where the integrands are regular :

$$E_z(z,r,\phi) = E_z(z,r)\cos(\phi + \phi_o) = E_z(z,r)\cos(\omega t + \phi_o)$$

$$= \frac{E_1}{2\pi}\int_{-\infty}^{\infty} \frac{b(k_z)}{J_o(\gamma a)}\, J_o(\gamma r)\, e^{ik_z z}\, dk_z \cos(\phi + \phi_o) \qquad (2.2.11)$$

$$E_r(z,r,\phi) = E_r(z,r)\cos(\phi + \phi_o)$$

$$= -i\,\frac{E_1}{2\pi}\int_{-\infty}^{\infty} b(k_z)\, \frac{k_z J_1(\gamma r)}{\gamma J_o(\gamma a)}\, e^{ik_z z}\, dk_z \cos(\phi + \phi_o) \qquad (2.2.12)$$

$$\mu H_\Theta(z,r,\phi) = \mu H_\Theta(z,r)\sin(\phi + \phi_o) = \varepsilon\mu\omega\ \partial V(z,r)/\partial r \sin(\phi + \phi_o)$$

$$= -\frac{E_1}{2\pi}\,\frac{k_o}{c}\int_{-\infty}^{\infty} b(k_z)\, \frac{J_1(\gamma r)}{\gamma J_o(\gamma a)}\, e^{ik_z z}\, dk_z \sin(\phi + \phi_o) \qquad (2.2.13)$$

The correspondence with analogous representations used in earlier treatments [7)-9)] will be established by Eq. (2.6.10).

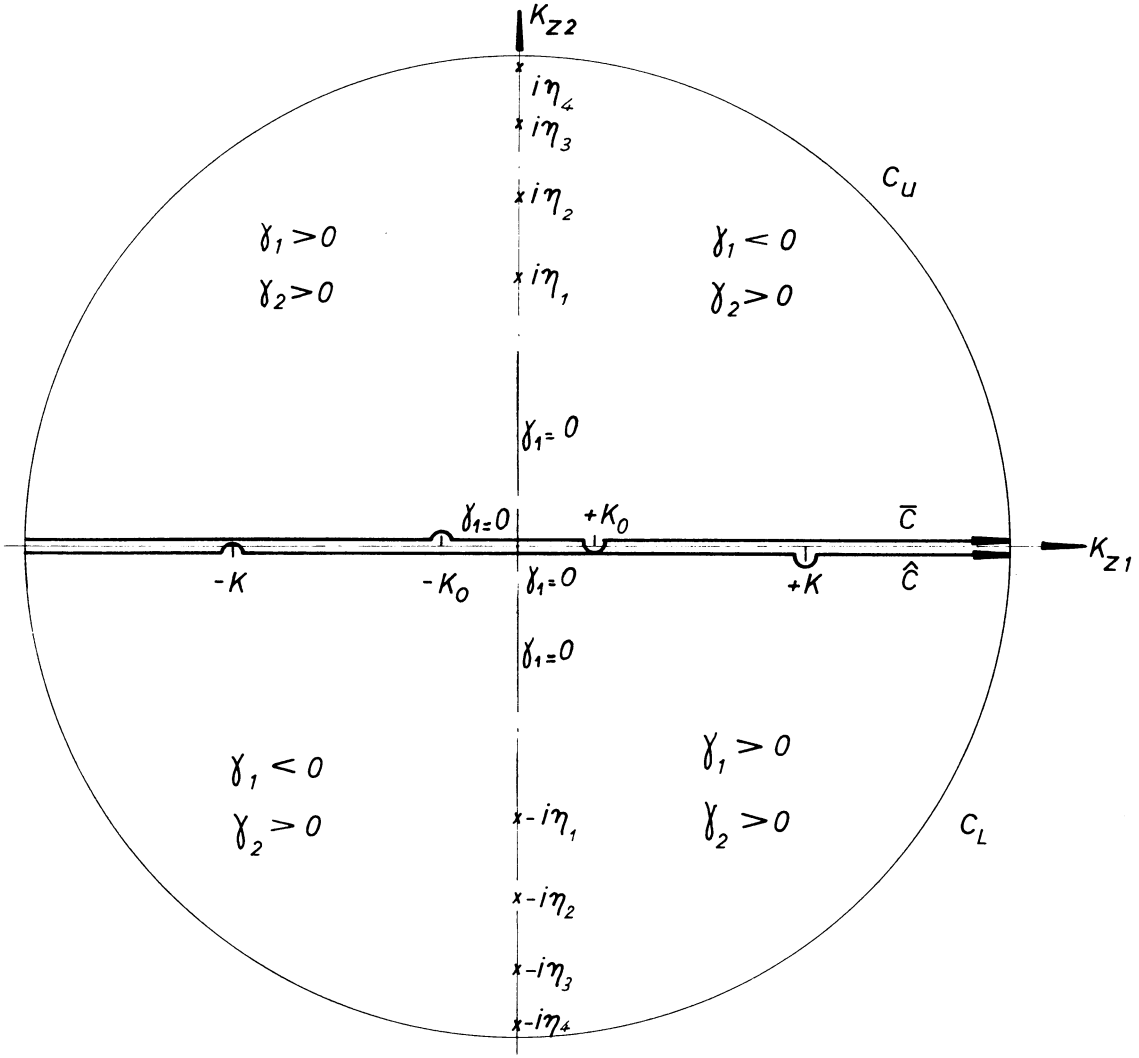

Fig. 2.2.1. The complex k_z-plane and the contours $\bar{C}$, $\hat{C}$, C_U, C_L.
$\bar{C}$ and $\hat{C}$ follow the real k_z-axis, except that they are indented at $k_z = \pm k_o(\bar{C})$ and at $k_z = \pm k\ (\hat{C})$ resp. C_U (C_L) are semi-circles whose radii tend to infinity. The integrals (2.2.9) till (2.2.13), (5.1.13) till (5.1.16), (5.2.11) and (5.2.15) have simple poles for $k_z = \pm i\eta_\nu$, since there is $J_o(\gamma a) = 0$.

2.3. The Potential $U = - r H_\Theta$.

The electric Hertz vector $\vec{e}_z V$ has the disadvantage that the boundary condition :

$$0 = \vec{E}_{tang} = \vec{n} \times \vec{E} = (\vec{n} \times \vec{e}_r)\partial^2 V/\partial z \partial r + (\vec{n} \times \vec{e}_z)(k_o^2 + \partial^2/\partial z^2)V \qquad (2.3.1)$$

assumes a form as simple as (2.2.6) or (2.2.8) only if the wall coincides with a coordinate surface, ($\vec{n} = \vec{e}_z$ or $\vec{e}_r$). In the general case the explicit expression for it is on the contrary somewhat more complicated than that, eq. (7) below, the condition $E_{tang} = 0$ assumes for the potential U(z,r) defined by [16] *):

$$U(z,r) \equiv - r H_\Theta(z,r) = - \varepsilon\omega r \ \partial V(z,r)/\partial r \qquad (2.3.2)$$

For that reason this potential is preferred when the field in a complicated but still axially symmetrical configuration (as for instance a cell for the Alvarez structure) is calculated by numerical methods (mesh calculations) [4] [13] [17].

The field equation for U is :

$$\mathcal{L}U + k_o^2 U = \partial^2 U/\partial r^2 - 1/r \ \partial U/\partial r + \partial^2 U/\partial z^2 + k_o^2 U = 0 \qquad (2.3.3)$$

It is obtained from the equation for V, $\Delta V + k_o^2 V = 0$, by use of the definition (2) and with the help of the relation $r \ \partial/\partial r(\Delta V) = \mathcal{L}(r \ \partial V/\partial r)$ which can be derived by straightforward calculation.

From (2.2.5) and (2.2.11) to (2.2.13) E_r and E_z are found :

$$E_z(z,r) = (\varepsilon\omega r)^{-1} \ \partial U(z,r)/\partial r \qquad (2.3.4)$$

$$E_r(z,r) = -(\varepsilon\omega r)^{-1} \ \partial U(z,r)/\partial z \qquad (2.3.5)$$

which may be combined to

$$\vec{E}(z,r) = - (\varepsilon\omega r)^{-1} \ \vec{e}_\Theta \times \nabla U(z,r) \qquad (2.3.6)$$

$\vec{e}_\Theta = (- \sin\Theta, \cos\Theta, 0)$ is a unit vector tangential to the circles r = const.
From

$$0 = \vec{E}_{tang} = \vec{n} \times \vec{E} = - (\varepsilon\omega r)^{-1} \vec{n} \times (\vec{e}_\Theta \times \nabla U) = - (\varepsilon\omega r)^{-1} \vec{e}_\Theta(\vec{n}, \nabla U)$$

---

*) The minus sign in this definition has been adopted so that simultaneously $E_z(z,r) > 0$ for any z and $U(z,r) > 0$ for $0 \leq z \leq \infty$, if the cavity is excited in the lowest mode.

($(\vec{e}_\theta, \vec{n}) = 0$ by the supposed axial symmetry) follows the boundary condition :

$$\text{along walls (or planes of symmetry): } \partial U/\partial n = (\vec{n}, \nabla U) = 0 \tag{2.3.7}$$

E_r and E_z must be finite at $r = 0$, so (4) and (5) give the additional condition :

$$r = 0 : U = 0 \tag{2.3.8}$$

(more exactly : $\lim_{r\to 0} rU(z,r) < \infty$). By integration of (4) it is shown that $U(z,r)$ is proportional to the electric flux through a tube with radius r :

$$\varepsilon\omega \int_0^r E_z(z,\rho)\rho \, d\rho = \int_0^r \partial U(z,\rho)/\partial\rho \, d\rho = U(z,r) \, . \tag{2.3.9}$$

2.4. Analytical Properties of the Field Amplitude and of the Field Representations

As it is intended to evaluate integrals (2.2.9) to (2.2.13) and others derived from them, by Cauchy's residue theorem, some insight into the analytical properties of the amplitude $b(k_z)$ regarded as a function of complex k_z, is needed. The results of this investigation will allow to state that the field representations mentioned above are analytic in the variables r and z in the interior of the drift tube space $r < a$. Simultaneously is prepared the ground for a method elaborated in the next section which permits to determine $b(k_z)$ approximately from cavity fields found by mesh calculations. In order to achieve these goals the fact is exploited that the accelerating gap is approximated by a wave guide in which a field is excited by an "external" field $E_z^a(z)$ applied along the circumferential slot $r = a$, $-p/2 \leq z \leq p/2$:

$$-p/2 \leq z \leq p/2: \quad E_z(z,a) = E_z^a(z) \tag{2.4.1}$$

$$|p/2| > z: \quad E_z(z,a) = 0 \tag{2.4.2}$$

The field in the interior $r < a$ is related to that given by (1) and (2) along the cylinder $r = a$, by means of a Green 's function as demonstrated in Appendix 2.4D, eq. (43):

$$E_z(z,r) = \frac{1}{2\pi} \int_{-\infty}^{\infty} dk_z \left[\int_{-p/2}^{p/2} d\bar{z}\, E_z^a(\bar{z})\, e^{-ik_z\bar{z}} \right] e^{ik_z z}\, J_o(\gamma r)/J_o(\gamma a) \quad r \leq a \tag{2.4.3}$$

Comparison with (2.2.11) yields an expression for the amplitude function :

$$E_1 b(k_z) = \int_{-p/2}^{p/2} d\bar{z}\, E_z^a(\bar{z})\, e^{-ik_z\bar{z}} \tag{2.4.4}$$

$E_z^a(z)$ which is assumed to be symmetrical, $E_z^a(-\bar{z}) = E_z^a(\bar{z})$, is expanded into a Fourier series :

$$E_z^a(\bar{z}) = 2E_1 \left[1/2 + \sum_{n=1}^{\infty} B_n \cos(2\pi n\bar{z}/p) \right] = E_1 \sum_{s=\infty}^{-\infty} B_s \cos(2\pi s\bar{z}/p) \tag{2.4.5}$$

$$B_o \equiv 1 \ , \ B_s \equiv B_{-s} \equiv B_n$$

Performing in (4) the integration with respect to $\bar{z}$ for this $E_z^a(\bar{z})$, eq. (5) gives :

$$b(k_z) = b(-k_z) = 2 \sum_{s=\infty}^{-\infty} B_s (-1)^s \frac{\sin(k_z p/2)}{k_z - 2\pi s/p} = -4\, k_z p^2 \sum_{n=o}^{\infty} \frac{B_n (-1)^n}{1 + \delta_{no}} \frac{\sin(k_z p/2)}{(2\pi n)^2 - (k_z p)^2}$$

(2.4.6)

where δ_{no} is the Kronecker symbol; it is unity if n equals zero, it vanishes otherwise. As indicated below (Appendix A), the inequality

$$|B_n| < \text{const.}/n^{1+\alpha} \qquad \alpha > 0,\ n \neq 0 \tag{2.4.7}$$

holds if $E_z^a(z)$ fulfils some reasonable conditions - in essence : $E_z^a(z)$ is continuous and bounded in $-p/2 \leq z \leq p/2$, it is symmetrical ($E_z^a(-z) = E_z^a(z)$) and $\partial E_z^a/\partial z$ is continuous except for $z = \pm p/2$ where it is not more singular than $\partial/\partial z((p/2)^2 - z^2)^{\alpha}$, $\alpha > 0$.(7) is a sufficient condition that the function $b(k_z)$ is continuous and analytical for any finite (real or complex) k_z and that it is permitted to interchange integrations and summations as performed above.

The behaviour of $b(k_z)$ at $|k_z| = \infty$ is determined by the essential singularity of the sine. Writing :

$$k_z = R\, e^{i\psi} \tag{2.4.8}$$

it can be stated that :

$$|b(k_z)\, e^{ik_z z}| \sim e^{-(z-p/2)R \sin\psi} \to 0$$

$$\text{if} \quad z > p/2, \quad 0 < \psi < \pi \qquad \text{and } R \to \infty \tag{2.4.9}$$

$$|b(k_z)\, e^{ik_z z}| \sim e^{(z+p/2) \sin\psi} \to 0$$

$$\text{if} \quad z < -p/2, \quad 0 > \psi > -\pi \qquad \text{and } R \to \infty$$

These are the most important properties of the amplitude function $b(k_z)$ upon which the greater part of the derivation of beam dynamics equations will be based. If $|z| < p/2$, the above limits (9) no longer hold since one of the exponentials of $\sin(k_z p/2)$ contained in $b(k_z)$ tends stronger to infinity than $e^{ik_z z}$, $e^{-ik_z z}$ go to zero. In this case $b(k_z)$ must be decomposed:

$$b(k_z) = b_+(k_z) + b_-(k_z)$$

$$b_+(k_z) = -i\, e^{ik_z p/2} \sum_{s=\infty}^{-\infty} B_s(-1)^s (k_z - 2\pi s/p)^{-1} = b_-(-k_z) \qquad (2.4.10)$$

$$b_-(k_z) = i\, e^{-ik_z p/2} \sum_{s=\infty}^{-\infty} B_s(-1)^s (k_z - 2\pi s/p)^{-1}$$

Then it is for $k_z = R\, e^{i\psi}$:

$$\begin{aligned} &\lim_{R\to\infty} |b_+(k_z)\, e^{ik_z z}| = 0 \quad \text{where} \quad -p/2 \le z \le p/2 \qquad 0 < \psi < \pi \\ &\lim_{R\to\infty} |b_-(k_z)\, e^{ik_z z}| = 0 \quad \text{where} \quad p/2 \ge z \ge -p/2 \qquad 0 > \psi > -\pi \end{aligned} \qquad (2.4.11)$$

$b_+(k_z)$ and $b_-(k_z)$ have simple poles at $k_z = 2\pi s/p$, $s = 0, \pm 1, \pm 2, \ldots$ with residues :

$$\mathrm{Res}(b_+(k_z), k_z = 2\pi s/p) = -\mathrm{Res}(b_-(k_z), k_z = 2\pi s/p) = B_s/i \qquad (2.4.12)$$

The integral representations (2.2.11) to(2.2.13) and any one which may be deduced from them by derivations with respect to z and r are analytical functions of z and r in the cylinder $0 \le r \le \delta < a$, $-\infty \le z \le \infty$.

This follows from the fact that these integrals are absolutely convergent since their integrands are bounded (they are non- singular on the finite part of the real k_z-axis) and vanish exponentially for $k_z \to \pm\infty$ (see appendix C).

2.4. A The asymptotic properties of the Fourier coefficients B_n.

The behaviour (for large n) of Fourier coefficients is intimately connected with the periodicity and continuity properties of the function they represent [18) 19)].

An interesting and useful example is provided by the expansion [20)]:

$$g(z) = (\pi^2 - z^2)^{\alpha} = \frac{\sqrt{\pi}}{2}\frac{\Gamma(\alpha+1)}{\Gamma(\alpha+3/2)} + \sqrt{\pi}\,\Gamma(\alpha+1)\sum_{n=1}^{\infty}\frac{J_{\alpha+1/2}(n\pi)}{(n\pi/2)^{\alpha+1/2}}\cos(nz) \qquad (2.4.13)^{*)}$$

$$= C_o/2 + \sum_{n=1}^{\infty} C_n \cos(nz)$$

$$|z| \leq \pi,\ \alpha > 0 \quad \text{or} \quad |z| < \pi,\ \alpha > -1$$

By use of the asymptotic formula of the Bessel functions: [21)]

$$J_v(x) \approx (2/\pi x)^{1/2} \cos(x - (v + \tfrac{1}{2})\tfrac{\pi}{2}),\ x >> 1,\ |\arg x| < \pi \qquad (2.4.14)$$

it is concluded that the Fourier coefficients behave for great n as :

$$C_n \approx \frac{\Gamma(\alpha+1)\,2^{\alpha+1}}{\pi^{\alpha+1/2}}\cos\left[(\alpha+1)\frac{\pi}{2}\right]\frac{(-1)^n}{n^{\alpha+1}},\ n >> 1,\ |C_n| < \frac{C}{n^{\alpha+1}} \qquad (2.4.15)$$

If $\alpha > 0$, then the function on the left hand side of (13) is continuous and the series on the right hand side is absolutely and uniformly convergent. If α is an integer, then all derivatives up to the α -th order are finite, $g^{(\alpha)}(z = \pm\pi)$ = finite, $g^{(\alpha+1)}(z = \pm\pi) = \infty$. If α is not an integer, put $\alpha = r + \mu$ where r is the greatest non-negative integer contained in α and $g^{(r)}(z = \pm\pi)$ = finite, $g^{(r+1)}(z = \pm\pi) = \infty$. This behaviour is exactly reflected by the sum of the series at this point.

A general discussion about the relation between the continuity of the function developed (limited to even functions) and the asymptotic behaviour of its Fourier-coefficients may start from the formula :

$$f(x) = A_o/2 + \sum_{n=1}^{\infty} A_n \cos(nz),\ A_n = \frac{1}{2\pi}\int_{-\pi}^{\pi} f(z)\cos(nz)\,dz \qquad (2.4.16)$$

---

*) For simplicity in this appendix A period π is assumed instead of p .

Performing partial integrations, taking into account possible finite jumps of f(z) at $z_1^{(o)}$, $z_2^{(o)}$, ... $z_\ell^{(o)}$ and of f' at $z_1^{(1)}$, $z_2^{(1)}$, ... $z_m^{(1)}$, gives :

$$2\pi A_n = \frac{1}{n}\left[(f(\pi) + f(-\pi))\sin(n\pi) + \sum_{\rho=1}^{\ell}(f(z_\rho + o) - f(z_\rho - o))\sin(nx_\rho)\right]$$

$$- \frac{1}{n}\int_{-\pi}^{\pi} f'(z)\sin(nz)\,dz$$

$$2\pi A_n = \frac{1}{n}\left[(f(\pi) + f(-\pi))\sin(n\pi) + \sum_{\rho=1}^{\ell}(f(z_\rho + o) - f(z_\rho - o))\sin(nx_\rho)\right] \quad (2.4.17)$$

$$+ \frac{1}{n^2}\left[(f'(\pi) - f'(-\pi))\cos(n\pi) + \sum_{\rho=1}^{m}(f'(z_\rho + o) - f'(z_\rho - o))\cos(nz_\rho)\right]$$

$$- \frac{1}{n^2}\int_{-\pi}^{\pi} f''(z)\cos(nz)\,dz$$

If f(z) has only finite jumps and f'(z) is integrable then A_n will tend to zero at least as $1/n$. If f(z) is continuous, $f(\pi) = f(-\pi)$, if f'(z) has only finite jumps and f"(z) is integrable, then $A_n \sim 1/n^2$ for great n, and so on. The assumption $f'(\pi)$ = finite demands already more than can be expected from the function f(z) (which will be identified with $E_z^a(z)$) on physical reasons. On the other hand there is no need of $|A_n| < C/n^2$, but only of $|A_n| < C/n^{1+\alpha}$, $\alpha > 0$. In addition, even the conditions ensuring $|A_n| < C/n^2$ can be relaxed in comparison with those which flow from the present discussion of equation (17). A proof employing more sophisticated methods (the second mean value theorem of the integral calculus) can come along without invoking properties of the second derivative. But the treatment becomes more involved, so there will be only quoted from reference [19] the necessary theorems together with their presuppositions.

A basic property of a function arising in this context is covered by the Dirichlet conditions: A function f(z) fulfils them, if it is bounded in the closed interval $[\pi, -\pi]$, and if this interval can be broken up into a finite number of open intervals, in each of which f(z) is monotonic (ref.[19], §93). There is the theorem (ibid., §104, III; ref.[18] Section 157): "If f(z) is bounded and continuous and otherwise satisfies Dirichlet's conditions in $-\pi < z < \pi$, while $f(\pi-o) = f(-\pi + o)$ and if f'(z) is bounded and otherwise satisfies Dirichlet's conditions in the same interval, the coefficients in the Fourier series for f(z) are less in absolute value than K/n^2, K = const."

However, the presuppositions of the above theorem are still too incisive. The function which is expanded into a Fourier series in the present discussion, is the tangential electrical field $E_z(z,r=a) = E_z^a(z) \equiv F(2z\pi/p)$. From physical considerations it is expected that its derivative $\partial E_z^a/\partial z$ is weakly singular at $z = \pm p/2$, at the places where the inner rim goes over into the cylindrical section of the drift tube bore. This means that F'(z) has the

same singularity at $z = \pm \pi$. Therefore it is not bounded and it does not fulfil the complete set of assumptions of the above theorem. But it is reasonable to expect that the singularity of $F'(z)$ (and of $\partial E_z^a(z)/\partial z$) is of the same nature as that of $\partial/\partial z(\pi^2 - z^2)^{\bar{\alpha}}$ with some $\bar{\alpha} > 0$. It is then possible to construct a function $f(z) = F(z) - A\,g(z)$ which fulfils the presuppositions of the above theorem, by subtracting out this singularity of the derivative of $F(z)$ with the help of a multiple of the function $g(z)$ (with $\alpha = \bar{\alpha}$) given in equation (13) . By this choice of the constants α and A it is achieved that $f'(z)$ is bounded and fulfils the Dirichlet conditions. The Fourier coefficients A_n of $f(z)$ therefore behave asymptotically as $1/n^2$. The asymptotic behaviour $1/n^{1+\alpha}$ of the coefficients C_n of $g(z)$ is given by (15). The asymptotic behaviour of the coefficients $B_n = A_n + AC_n$ is determined by the smaller of the two exponents 2 and $1+\alpha$. In general $\alpha < 1$, so $B_n < 1/n^{1+\alpha}$. This reasoning is summarized in the following equation:

$$
\begin{aligned}
f(z) &= A_o/2 + \sum_{n=1}^{\infty} A_n \cos(nz) && |A_n| < K/n^2 \\
A\,g(z) &= A\,C_o/2 + \sum_{n=1}^{\infty} AC_n \cos(nz) && |C_n| < C/n^{\alpha+1} \quad n > 0 \qquad (2.4.18) \\
\hline
F(z) &= f(z) + Ag(z) = B_o/2 + \sum_{n=1}^{\infty} B_n \cos(nz) && |B_n| < AC/n^{\alpha+1}
\end{aligned}
$$

From the preceding discussion it is concluded that the coefficients B_n of the Fourier Expansion (5) of the tangential electrical field $E_z^a(z)$ are governed by the inequality (7):

$$
E_z^a(z) = E_1 \sum_{s=-\infty}^{\infty} B_s \cos(2\pi sz/p), \quad |B_s| < \text{const.}/|s|^{1+\alpha} \quad \alpha > 0,\ s \neq 0 \qquad (2.4.19)
$$

if it is supposed :

1.) $E_z^a(z)$ fulfils Dirichlet's conditions in the closed interval $-p/2 \leq z \leq p/2$.

2.) $E_z^a(z) = E_z^a(-z)$ which ensures $E_z^a(-p/2) = E_z^a(p/2)$.

3.) $\partial E_z^a(z)/\partial z$ fulfils Dirichlet's conditions in $-p/2 < z < p/2$.

4.) $E_z^a(z)/\partial z$ is at $z = \pm p/2$ not more singular than the derivative $\partial/\partial z((p/2)^2 - z^2)^{\alpha}$ with $\alpha > 0$.

It is reasonable to believe that these conditions are fairly well reproduced by the real field existing in a linac gap. $E_z^a = E_z(z,a)$ will be continuous and bounded if there is no sharp corner at $z = \pm p/2$. Neither it nor $\partial E_z^a/\partial z = \partial/\partial z\, E_z(z,a)$ will have an infinite number of wiggles violating the condition of monotony in subintervals as demanded by Dirichlet's conditions. $\partial E_z^a/\partial z$ is permitted to have a weak singularity as might arise at $|z| = p/2$ where the curved rim joins the straight section of the interior of the drift tubes.

Finally, it should be indicated how the conditions listed above may be relaxed. The total symmetry $E_z^a(-z) = E_z^a(z)$ may be given up; similarly the weak singularity of $\partial E_z^a/\partial z$ may be different at $z = p/2$ and at $z = -p/2$, e.g. $\partial E_z^a(z = p/2)/\partial z \sim (p/2 - z)^{\alpha_1 - 1}$, $\partial E_z^a(z = -p/2)/\partial z \sim (p/2 + z)^{\alpha_2 - 1}$, $\alpha_1, \alpha_2 > 0$, so that the α in inequality (7) is the minimum of α_1 and α_2. However, (7) will fail if $E_z^a(-p/2) = E_z^a(p/2)$ is abandoned. I do not say that giving up this assumption principally excludes the possibility of a rigorous proof of beam dynamics equations like those developed in Chapter 5,but the treatment would probably become more complicated.

2.4.B Analytic Properties of the Amplitude function $b(k_z)$

The amplitude function :

$$b(k_z) = 2 \sum_{s=\infty}^{-\infty} B_s (-1)^s \sin(k_z p/2) \, (k_z - 2\pi s/p)^{-1} \qquad (2.4.6)$$

is continuous and bounded for any real k_z, because it consists of an absolutely and uniformly convergent series of continuous and bounded terms. The denominator of the coefficient of B_s vanishes at $k_z = 2\pi s/p$ ($s = 0, \pm, \pm 2, \ldots$); but so does the numerator, the ratio there being equal to $(-1)^s$ and this is the maximum value the modulus of the function considered assumes for any real k_z, i.e. $|\sin(k_z p/2)/(k_z - 2\pi s/p)| \leq 1$.

$$|b(k_z)| \leq \left| 2 \sum_{s=\infty}^{-\infty} B_s (-1)^s \frac{\sin(k_z p/2)}{k_z - 2\pi s/p} \right| < 4 \sum_{n=o}^{\infty} |B_n| \equiv K \qquad (2.4.20)$$

by the assumptions 1. - 4. on the electrical field $E_z^a(z) = E_z(z, r = a)$ listed at the end of the appendix A. Since the Fourier coefficients B_n behave asymptotically as $1/n^{1+\alpha}$ where $\alpha > 0$, the series $\sum B_n$ is absolutely convergent and its sum is a constant.
For complex $pk_z/2 \equiv u_1 + iu_2 \equiv (p/2) R e^{i\psi}$ it can be shown that

$$|b(k_z)| < pK \cosh(u_2) = pK \cosh\left(\frac{pR}{2} \sin\psi\right) \qquad (2.4.21)$$

This estimate results from :

$$\frac{(\sin u_1 \cosh u_2)^2}{(u_1 - \pi s)^2 + u_2^2} \leq (\cosh u_2)^2$$

$$\frac{(\cos u_1 \sinh u_2)^2}{(u_1 - \pi s)^2 + u_2^2} \leq \left(\frac{\sinh u_2}{u_2}\right)^2 \leq (\cosh u_2)^2$$

from which follows :

$$\left|\frac{\sin(k_z p/2)}{pk_z/2 - \pi s}\right| = \left[\frac{(\sin u_1 \cosh u_2)^2 + (\cos u_1 \sinh u_2)^2}{(u_1 - \pi s)^2 + u_2^2}\right]^{\frac{1}{2}} \leq 2 \cosh u_2$$

which finally gives :

$$\left|\frac{2}{p} b(k_z)\right| \leq 2 \sum_{s=\infty}^{-\infty} |B_s| \left|\frac{\sin(k_z p/2)}{pk_z/2 - \pi s}\right| \leq 4 \cosh u_2 \sum_{s=\infty}^{-\infty} |B_s| < \cosh u_2 \; 8 \sum_{n=o}^{\infty} |B_n| = 2K \cosh u_2$$

Using (21) it is concluded :

$$2\,|b(k_z)\,e^{ik_z z}| \leq pK\,e^{-(z-p/2)R\,\sin\psi} + e^{-(z+p/2)R\,\sin\psi} \to 0$$

$$\left.\begin{array}{ll} \text{if} & z > p/2,\quad 0 < \psi < \pi \\ \text{or} & z < -p/2,\quad 0 > \psi > -\pi \end{array}\right\} \text{ and } \quad R \to \infty \qquad (2.4.22)$$

When estimating $b_+(k_z)$ and $b_-(k_z)$, one may proceed in the following manner :

$$\left|\frac{2}{p}\,b_+(k_z)\right| < e^{-u_2} \sum_{s=\infty}^{-\infty} |B_s| \left[(u_1 - \pi s)^2 + u_2^2\right]^{-\frac{1}{2}} < \bar{K}\,e^{-u_2}$$

$$\frac{2}{p}\,b_-(k_z) < \bar{K}\,e^{u_2} \qquad (2.4.23)$$

where $\bar{K} = \sum_{s=\infty}^{-\infty} |B_s| / \text{Min}\left[(u_1 - \pi s)^2 + u_2^2\right]$. The final result is :

$$\frac{2}{p}|b_+(k_z)e^{ik_z z}| < \bar{K}\,e^{-(p/2+z)R\,\sin\psi} \to 0$$

$$\text{if} \qquad z > -p/2,\ 0 < \psi < \pi \quad \text{and } R \to \infty \ . \qquad (2.4.24)$$

$$\frac{2}{p}|b_-(k_z)\,e^{ik_z z}| < \bar{K}\,e^{(p/2-z)R\,\sin\psi} \to 0$$

$$\text{if} \qquad z < p/2\ ,\ 0 > \psi > -\pi \quad \text{and } R \to \infty \ .$$

2.4. C Absolute Convergence of Integrals Representing Fields

The integrands of the integrals (2.2.11) to (2.2.13) (and of any derivative with respect to r and/or z) are well behaved for any finite real k_z. $b(k_z)$ is continuous and bounded along the whole real k_z-axis, as explained just before. The zeros of $J_o(\gamma a)$ lie off the real k_z-axis if the frequency $\omega/2\pi$ is smaller than the lowest cut-off frequency ($\omega < \omega_{cl}$) (cf. Fig. 2.2.1 and appendix D, especially eq. (39)).

The discussion of the behaviour of the integrands for k_z tending to $\pm\infty$ is at first limited to that of E_z, (2.2.11). Use is made of the fact that for great real k_z the root γ is purely imaginary (cf.(2.2.10))and approximately proportional to $i|k_z|$:

$$\gamma = (k_o^2 - k_z^2)^{\frac{1}{2}} \approx (-k_z)^{\frac{1}{2}} = i|k_z| \qquad (2.4.25)$$

and

$$|J_n(\gamma r)| \approx |I_n(|k_z|r)| \qquad |k_z| >> k_o \qquad (2.4.26)$$

The modified Bessel function will be replaced by its asymptotic expression:[21]

$$I_n(x) \approx e^x/(2\pi x)^{\frac{1}{2}} \qquad |x| >> 1 \qquad |\arg x| < \pi/2 \qquad (2.4.27)$$

With these formulae and with (20) the modulus of the integrand of (2.2.11) is estimated for large real k_z to :

$$\begin{aligned} |b(k_z)\, e^{ik_z z}\, J_o(\gamma r)/J_o(\gamma a)| &\leq |b(k_z)|\,|I_o(|k_z|r)/I_o(|k_z|a)| \\ &< K\,(a/r)^{\frac{1}{2}}\; e^{-|k_z|\,(a-r)} \to 0 \\ &\text{if} \qquad a > r \qquad k_z \to \pm\infty \end{aligned} \qquad (2.4.28)$$

provided $r > 0$; otherwise $J_o(0) = 1$ and the second line of (28) reads as $K\,(2\pi|k_z|a)^{\frac{1}{2}}\, e^{-|k_z|\,a}$. It results that the integral (2.2.11) representing $E_z(z,r)$ is absolutely and uniformly convergent for any z and $r \leq \delta < a$. All other integrals are treated in a completely analogous fashion. Comparing those for E_r and H_θ to that of E_z, one recognizes that $J_o(\gamma r)$ is replaced by $k_z J_1(\gamma r)/\gamma$, $J_1(\gamma r)/\gamma$ resp.,which are finite even for $\gamma = 0$. Differentiating any one of these integrals with respect to z and/or r,the integrand will contain some powers of k_z, γ and some derivative of $J_n(\gamma r)$. Any integrand arising in this way is comprised within the following general expression estimated in the same manner as that for E_z above in (28).

$$m \geq 0, \quad s \geq -1, \quad n \geq 0, \quad n + s \geq 0, \quad \ell \geq 0, \quad m,n,s,\ell \text{ integers}$$

$$|b(k_z)\, e^{ik_z z}\, k_z^m \gamma^s\, J_n^{(\ell)}(\gamma r)/J_o(\gamma a)| < K|k_z|^{m+s}|I_n^{(\ell)}(|k_z|r)/I_o(|k_z|a)| \qquad (2.4.29)$$

$$< K\,(a/r)^{\frac{1}{2}}|k_z|^{m+s} e^{-|k_z|(a-r)} \to 0$$

$$\text{if} \quad a > r \qquad\qquad k_z \to \pm\infty$$

(26) and (27) are also valid for the ℓ-th derivative of $J_n(\gamma r)$, if $r \neq 0$. If $r = 0$, $J_n^{(\ell)}(\gamma r)$ is either zero (e.g. $J_o' \sim J_o^{(1)} \sim -J_1 = 0$ for $r = 0$) or some constant (e.g. $J_o'' \sim J_o^{(2)} \sim -J_1' \sim (J_2 - J_o)/2 = -1/2$ for $r = 0$) and does not produce any troubles in this context.

2.4 D Green 's function for a Wave Guide and Derivation of Eq. (2.4.3)

Here will be summarized expressions and properties of the Green 's function G_1 used in the course of the present derivations. This is done in a rather short fashion which should suffice for those acquainted with this technique. A detailed introduction will be given elsewhere [22], see also ref. [43].

To relate a vector field (as e.g. the electromagnetic field) in the interior of a domain to the corresponding field at the surrounding boundary, in general a Green 's tensor is necessary. However, in this simple case (among others) with axial symmetry where there is only one component of the tangential electrical field different from zero, one can emplay the scalar Green 's function $G_1(z,r;\bar{z},\bar{r})$ belonging to the differential equation :

$$\Delta G_1 + k_o^2 G_1 = - \delta(z - \bar{z})\ \delta(r - \bar{r})/r \tag{2.4.30}$$

where the δ-functions have their usual meaning : The integrals:

$$\int_\alpha^\beta \delta(z - \bar{z})\ dz = 1, \quad \int_\gamma^\delta \frac{\delta(r - \bar{r})}{r}\ r\ dr = \int_\gamma^\delta \delta(r - \bar{r})\ dr = 1 \tag{2.4.31}$$

if the interval of integration (α,β) ((γ,δ)) includes the point $\bar{z}$ ($\bar{r}$), and are zero otherwise. G_1 obeys the boundary conditions :

$$r = a : \qquad G_1 = 0 \tag{2.4.32}$$

and

$$\lim_{|z|\to\infty} G_1 = 0\ , \quad \lim_{|z|\to\infty} \partial G_1/\partial z = 0 \quad (\text{if } \omega < \omega_{c1}) \tag{2.4.33}$$

If into Green's second theorem :

$$\int_{z=-\infty}^{\infty} \int_{r=o}^{a} (G_1\ \bar{\Delta}\ V(\bar{z},\bar{r}) - V(\bar{z},\bar{r})\ \Delta G_1)\ \bar{r}d\bar{r}\ d\bar{z} = \int df\ (G_1 \frac{\partial V}{\partial n} - V\frac{\partial G_1}{\partial n}) =$$

$$= \int_{z=-\infty}^{\infty} \bar{r}\ d\bar{z}\ (G_1 \frac{\partial V}{\partial \bar{r}} - V \frac{\partial G_1}{\partial \bar{r}})\Big|_{\bar{r}=a} + \lim_{|\bar{z}|\to\infty} \int_{r=o}^{a} \bar{r}\ d\bar{r}\ (G_1\frac{\partial V}{\partial \bar{z}} - V\frac{\partial G_1}{\partial \bar{z}}) \tag{2.4.34}$$

$$+ \lim_{|\bar{z}|\to\infty} \int_{r=o}^{a} \bar{r}\ d\bar{r}\ (G_1 \frac{\partial V}{\partial(-\bar{z})} - V \frac{\partial G_1}{\partial(-\bar{z})})$$

$$= -\int_{\bar{z}=-\infty}^{\infty} \bar{r}\, d\bar{z}\; V(\bar{z},\bar{r})\; \partial G_1(z,r;\bar{z},\bar{r})/\partial\bar{r}\,\Big|_{\bar{r}=a}$$

G_1 as defined above, is inserted, the second and the third integral on the right hand side vanish by (33). In the first integral the first term is zero by (32). On the left hand side of (34) for V(z,r) some solution of the Helmholtz equation :

$$\bar{\Delta}V(\bar{z},\bar{r}) + k_o^2 V = 0 \tag{2.4.35}$$

is used and $\bar{\Delta}V$ and $\bar{\Delta}G_1$ are eliminated with the help of the differential equations (35) and (30):

$$\int_{\bar{z}=-\infty}^{\infty} \int_{\bar{r}=o}^{a} \bar{r}\, d\bar{r}\, d\bar{z}\; (G_1\, \bar{\Delta}\, V - V\, \bar{\Delta}\, G_1) =$$

$$\int_{\bar{z}=-\infty}^{\infty} \int_{\bar{r}=o}^{a} \bar{r}\, d\bar{r}\, d\bar{z}\; (-G_1\, k_o^2 V + V\, k_o^2 G_1 + V(\bar{z},\bar{r})\; \delta(z-\bar{z})\; \delta(r-\bar{r})/\bar{r}\;)$$

$$= V(z,r) \qquad r \leq a$$

$$= 0 \qquad r > a \tag{2.4.36}$$

Equating (34) and (36) finally gives :

$$V(z,r) = -a \int_{\bar{z}=-\infty}^{\infty} d\bar{z}\; V(\bar{z},\bar{r})\quad \partial G_1(z,r;\bar{z},\bar{r})/\partial\bar{r}\,\Big|_{\bar{r}=a} \qquad (r < a) \tag{2.4.37}$$

G_1 can be represented by a Fourier integral :

$$G_1(z,r;\bar{z},\bar{r}) = G_1(\bar{z},\bar{r};z,r) =$$

$$= \frac{i}{4} \int_{-\infty}^{\infty} dk_z e^{ik_z(z-\bar{z})} J_o(\gamma r_<) \left[J_o(\gamma a)\, H_o^{(1)}(\gamma r_>) - H_o^{(1)}(\gamma a)\, J_o(\gamma r_>) \right] / J_o(\gamma a) \tag{2.4.38}$$

with $\gamma = (k_o^2 - k_z)^{\frac{1}{2}}$, (2.2.10), and $r_< = r$, $r_> = \bar{r}$ if $\bar{r} \geq r$ and vice versa. This integral is a superposition of elementary waves $J_o(\gamma r)\exp(ik_z z)$, $(H_o^{(1)}(\gamma r) - J_o(\gamma r)\, H_o^{(1)}(\gamma a)/J_o(\gamma a))$ $\exp(ik_z z)$ resp. and is therefore a solution of (30) at least for $r \neq \bar{r}$, $z \neq \bar{z}$. The case $z = \bar{z}$, $r = \bar{r}$ is a bit more tricky and it is referred to ref.[22] for a detailed discussion. It is obvious that $G_1 = 0$ at $r = a$, for there $r = r_> = a$ and the square bracket in (38) is zero. The symmetry in the arguments (z,r) and $(\bar{z},\bar{r})$ indicated in eq. (38) and the property (33) can be seen if G_1 is expanded into a series of wave guide modes, eq. (40) The integrand

in (38) is single-valued: The only branch points could arise at $\gamma = 0$, since $H_o^{(1)}(x)$ contains a term proportional to logx; but in the square bracket of (38) the logy of $H_o^{(1)}(\gamma r_>)$ cancels against that of $H_o^{(1)}(\gamma a)$ if $\gamma \to 0$; this can be proved by putting $H_o = J_o + i\, N_o$ and inserting the series expansions of J_o and N_o. Since (38) is single-valued, it is permissible to evaluate it by Cauchy's residue theorem. The path of integration in the k_z-plane is closed by a semi-circle C_U (C_L) if $z - \bar{z} \geq 0$ (≤ 0) and the integrals along C_U (C_L) vanish if the radii of these semi-circles tend to infinity. (cf. Section 2.5. B). The integral $\int_{-\infty}^{\infty}$ equals $2\pi i$ times the sum of the residues of the poles enclosed by the paths real axis + C_U (real axis + C_L). (cf. Fig. 2.2.1). These simple poles lie at $k_z = \pm i\eta_\nu$:

$$J_o(\gamma a) = 0 : \quad \gamma a = j_{o,\nu} = j_\nu \ , \quad k_z = \pm i\eta_\nu = \pm i\left[(j_\nu/a)^2 - k_o^2\right]^{\frac{1}{2}} \qquad (2.4.39)$$

$$\eta_\nu > 0 \quad \text{if} \quad \omega = k_o c < j_\nu/a = \omega_{c\nu}$$

$\omega_{c\nu}/2\pi$ is the cut-off frequency of the ν-th circular TM-mode in a wave guide of radius a. Only the second term of the square bracket (38) contributes to these poles, in the first one the $J_o(\gamma a)$ of the numerator and that of the denominator cancel. For the calculation of the residues compare eq. (2.5.10).

With $H_o^{(1)}(j_\nu) = 2i/(J_1(j_\nu)\, \pi j_\nu)$ which follows from the Wronskian given below in (42), the residue series becomes :

$$G_1(z,r:\bar{z},\bar{r}) = \frac{1}{a^2} \sum_{\nu=1}^{\infty} \frac{J_o(j_\nu r/a)\, J_o(j_\nu \bar{r}/a)}{\eta_\nu J_1(j_\nu)}\, e^{-\eta_\nu |z-\bar{z}|} \qquad (2.4.40)$$

The symmetry $G_1(\bar{z},\bar{r},z,r) = G_1(z,r,\bar{z},\bar{r})$ is now obvious as well as (33). (33) is fulfilled as long as all η_ν are positive. Differentiating (38) ($r_< = r$, $r_> = \bar{r} = a$) gives :

$$\partial G_1(z,r,\bar{z},\bar{r})/\partial \bar{r}\,|_{\bar{r}=a} =$$

$$= \frac{i}{4} \int_{-\infty}^{\infty} dk_z\, e^{ik_z(z-\bar{z})}\, (-\gamma) J_o(\gamma a) \left[J_o(\gamma a)\, H_1^{(1)}(\gamma a) - H_o^{(1)}(\gamma a)\, J_1(\gamma a) \right] / J_o(\gamma a) \qquad (2.4.41)$$

$$= -\frac{1}{2\pi a} \int_{-\infty}^{\infty} dk_z\, de^{ik_z(z-\bar{z})} J_o(\gamma r)/J_o(\gamma a)$$

In order to arrive at the last equation, the Wronskian:

$$J_o(x)\, H_1^{(1)}(x) - J_1(x)\, H_o^{(1)}(x) = 2/(\pi i x) \qquad (2.4.42)$$

has been used.

With the aid of (41) equation (37) assumes its final form :

$$V(z,r) = \frac{1}{2\pi} \int_{\bar{z}=-\infty}^{\infty} d\bar{z}\, V(\bar{z},a) \int_{-\infty}^{\infty} dk_z e^{ik_z(z-\bar{z})} J_o(\gamma r)/J_o(\gamma a) \qquad (2.4.43)$$

Identifying $V(z,r)$ with $E_z(z,r)$ which as a Cartesian field component fulfils the homogeneous Helmholtz equation (35), gives equation (3).

2.4.E Different Expressions for E_z^a and $b(k_z)$.

Mesh calculations yield numerical values for the field at discrete points only. There arises the question of interpolation: fit some analytical expression to these values given along a line r = const., either $r \approx a$, $|z| \leq p/2$ or $r < a$, $|z| \leq L/2$. One possibility, exploited in the preceding parts of this section, consists of expanding $E_z(z,r=a)$ into a Fourier series. - To my opinion this is the most natural approach. - The amplitude function $b(k_z)$ which is by (4) a Fourier transform, turns out to be a convenient analytical function.

It has been investigated whether the Fourier transforms of other functions which could be used for fitting, are suitable from the point of view that the integrals (2.2.11) to (2.2.13) containing the corresponding $b(k_z)$ can be evaluated by Cauchy's residue theorem. The result is that all other functions considered have rather impractical Fourier transforms $b(k_z)$.

There have been considered some simple functions which come into mind at the inspection of field distributions (e.g. Figs. 2.5.3 , 2.5.4) :

a) A function which is easy to fit to given values is a polynomial. An even polynomial might be used to approximate the exciting fields in the gap circumference. (By reason of the symmetry supposed at the beginning, eq. (5), the tangential fields $U(z,a) = - a H_\theta(z,a)$ and $E_z(z,a)$ are even. It suffices to investigate just an even power, e.g. :

$$|z| \leq p/2 \qquad U(z) = z^{2n}$$

Its Fourier transform :

$$b(k) = \int_{-p/2}^{p/2} z^{2n} e^{-ikz} \, dz$$

$$= \left(\frac{p}{2}\right)^{2n+1} (2n)! \left[\frac{\sin(pk/2)}{pk/2} \sum_{v=o}^{n} \frac{1}{(2n-2v)!} \frac{(-2)^v}{(kp)^{2v}} + \cos(kp/2) \sum_{v=o}^{n-1} \frac{1}{(2n-v-1)!} \frac{(-2)^{v+2}}{(kp)^{2v+2}} \right]$$

has poles of order 2n at k = 0; evaluation of residues would be tedious if n > 1. Fields along a line r = const., $-L/2 \leq z \leq L/2$ situated within the drift tube space exhibit bell-like shapes. They might be approximated by:

b) a Gaussian times a polynomial. Its Fourier transform is again a Gaussian times a polynomial, now in k_z. $\exp(-k_z^2)$ grows indefinitely for $|k_z| \to \infty$ in the part $\pi/4 < |\arg(k_z)| < 3\pi/4$ of the complex k_z-plane. It is not possible to evaluate an integral $\int dk_z b(k_z)$ ... by Cauchy's residue theorem.

c) the inverse of an even polynomial, e.g. :

$$U(z) = (z^2 + c^2)^{-1} \qquad c > 0.$$

Its Fourier transform :

$$b(k_z) = (\pi/c)\, e^{-|k_z|c}$$

is not at all analytic in k_z.

2.5 Series Expansions of Fields

Series expansions for the various field components valid within the drift tube space $r < a$. are obtained by evaluating the integral representations (2.2.9) till (2.2.13) containing $b(k_z)$ given in equation (2.4.6) by means of Cauchy's residue theorem. If $z < -p/2$ ($z > p/2$) the path of integration ($\bar{C}$, or the real k_z-axis resp.) is closed by a semi-circle C_L (C_U) situated in the lower (upper) k_z-plane (cf. Fig. 2.2.1). By (2.4.9),(2.4.22) the integral along C_L (C_U) vanishes if the radius R of these semi-circles tends to infinity. The integral along the real axis therefore equals $2\pi i$ times the sum of the residues due to the simple poles enclosed :

$$J_o(\gamma a) = 0 : \quad \gamma a = j_{o,v} = j_v , k_z = \pm i\eta_v = + ((j_v/a)^2 - k_o^2)^{\frac{1}{2}} \qquad (2.5.1)$$

If $|z| < p/2$ the method just described fails, since one of the exponentials in $b(k_z)\, e^{ik_z z} \sim \left[e^{ik_z(p/2+z)} - e^{-ik_z(p/2-z)} \right]$ becomes infinite along C_U and C_L if R increases indefinitely. For this reason the path of integration is deformed into $\tilde{C}$(Fig. 2.5.1) and $b(k_z)$ afterwards split up into $b(k_z) = b_+(k_z) + b_-(k_z)$, see (2.4.10). The integrals containing $b_+(k_z)$, $b_-(k_z)$ resp. vanish along C_U, C_L resp. in the limit $R \to \infty$. The integral along $\tilde{C}$ is $2\pi i$ times the sum of the residues due to the two chains of simple poles, one given by (2.5.1), the other by $k_z = 2\pi s/p$, $s = 0, \pm 1, \pm 2, \ldots$.

Before listing these expansions, it may be worthwhile to recall that from the symmetry of the tangential electrical field

$$E_z^a(z) = E_z(z,a) = E_z(-z,a) = E_z^a(-z)$$

as assumed in eq. (2.4.5), result the following symmetries of the field components :

$$\begin{aligned} V(z,r) &= V(-z,r) \qquad H_\theta(z,r) = H_\theta(-z,r) \\ E_z(z,r) &= E_z(-z,r) \;, \; E_r(z,r) = -E_r(z,r) \end{aligned} \qquad (2.5.2)$$

One has

$$|z| \geq p/2: \qquad V(z,r) = \qquad (2.5.3a)$$

$$= 4 E_1 p^2 \sum_{n=o}^{\infty} \frac{B_n (-1)^n}{1+\delta_{no}} \sum_{v=1}^{\infty} \frac{J_o(j_v r/a)}{j_v J_1(j_v)} \frac{\sinh(\eta_v p/2)}{(p\eta_v)^2 + (2\pi n)^2} e^{-\eta_v |z|} + D_a$$

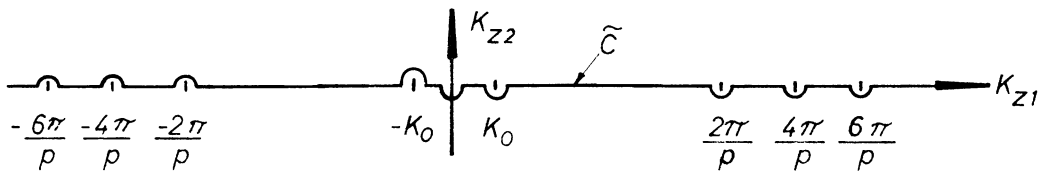

Fig. 2.5.1 The contour C. It is indented at $k_z = \pm 2\pi n/p$, n = 1, 2, ... and at $k_z = \pm k_o$. The integral representations of the field components E_z, E_r and H_θ are regular at $k_z = \pm k_o$ and these points do not give a contribution for them.

$|z| = p/2$: $V(|p/2|,r) =$

$$= E_1 p^2 \left[\frac{B_o}{2} \frac{1}{(k_o p)^2} \frac{J_o(k_o r)}{J_o(k_o a)} - \sum_{n=1}^{\infty} \frac{B_n (-1)^n}{(2\pi n)^2 - (k_o p)^2} \frac{I_o(\mu_n r/p)}{I_o(\mu_n a/p)} \right. \qquad (2.5.3b)$$

$$\left. - 2 \sum_{n=o}^{\infty} \frac{B_n (-1)^n}{1 + \delta_{no}} \frac{J_o(j_v r/a)}{j_v J_1(j_v)} \frac{e^{-\eta_v p}}{(p\eta_v)^2 + (2\pi n)^2} \right] + D_b$$

$|z| \leq p/2$: $V(z,r) =$

$$= 2 E_1 p^2 \left[\frac{B_o}{2} \frac{1}{(k_o p)^2} \frac{J_o(k_o r)}{J_o(k_o a)} - \sum_{n=1}^{\infty} \frac{B_n \cos(2\pi n z/p)}{(2\pi n)^2 - (k_o p)^2} \frac{I_o(\mu_n r/p)}{I_o(\mu_n a/p)} \right. \qquad (2.5.3c)$$

$$\left. - 2 \sum_{n=o}^{\infty} \frac{B_n (-1)^n}{1 + \delta_{no}} \sum_{v=1}^{\infty} \frac{J_o(j_v r/a)}{j_v J_1(j_v)} \frac{\cosh(\eta_v z)}{(p\eta_v)^2 + (2\pi n)^2} e^{-\eta_v p/2} \right] + D_c$$

with:

$$\mu_n = \left[(2\pi n)^2 - (k_o p)^2 \right]^{\frac{1}{2}} \qquad (2.5.4)$$

and

$$2 k_o D_a = - i E_1 b(k_o) e^{ik_o|z|} \qquad 2 k_o D_b = -i E_1 b_+(k_o) e^{ik_o p/2}$$

$$2 k_o D_c = -i E_1 \left[b_+(k_o) e^{ik_o z} + b_-(k_o) e^{-ik_o z} \right]$$

D_a , D_b and D_c do not contribute to the electromagnetic field. The expressions for the field components follow from the series listed above by use of (2.2.5) and (2.2.11 to 13)or by direct evaluation of the integral representations ($r \leq a$) :

$$|z| \geq \frac{p}{2} : \quad E_z(z,r) = 4E_1 \left(\frac{p}{a}\right)^2 \sum_{n=o}^{\infty} \frac{B_n (-1)^n}{1 + \delta_{no}} \sum_{v=1}^{\infty} \frac{J_o(j_v r/a)}{J_1(j_v)} \frac{j_v \sinh(\eta_v p/2)}{(p\eta_v)^2 + (2\pi n)^2} e^{-\eta_v |z|}$$

(2.5.5a)

$$|z| = \frac{p}{2} : \quad E_z\left(\frac{p}{2},r\right) = E_1 \left[\frac{B_o}{2} \frac{J_o(k_o r)}{J_o(k_o a)} + \sum_{n=1}^{\infty} B_n (-1)^n \frac{I_o(\mu_n r/p)}{I_o(\mu_n a/p)} + \bar{D}\, \delta_{ar} \right.$$

(2.5.5b)

$$- 2\left(\frac{p}{a}\right)^2 \sum_{n=o}^{\infty} \frac{B_n(-1)^n}{1+\delta_{no}} \sum_{v=1}^{\infty} \frac{J_o(j_v r/a)}{J_1(j_v)} \frac{j_v e^{-\eta_v p}}{(p\eta_v)^2 + (2\pi n)^2}$$

$$\delta_{ar} = \begin{cases} 0 & \text{if } a \neq r \\ 1 & \text{if } a = r \end{cases}$$

$$\bar{D}(z=p/2\pm o) = \bar{D}(z=-p/2\mp 0) = \mp \sum_{n=o}^{\infty} B_n(-1)^n (1+\delta_{no})^{-1}$$

$$|z| \leq \frac{p}{2} : E_z(z,r) = 2E_1 \left[\frac{B_o}{2} \frac{J_o(k_o r)}{J_o(k_o a)} + \sum_{n=1}^{\infty} B_n \cos(2\pi n z/p) \frac{I_o(\mu_n r/p)}{I_o(\mu_n a/p)} \right.$$

(2.5.5c)

$$\left. - 2\left(\frac{p}{a}\right)^2 \sum_{n=o}^{\infty} \frac{B_n(-1)^n}{1+\delta_{no}} \sum_{v=1}^{\infty} \frac{J_o(j_v r/a)}{J_1(j_v)} \frac{j_v \cosh(\eta_v z)}{(p\eta_v)^2 + (2\pi n)^2} e^{-\eta_v p/2} \right]$$

$$\begin{matrix} z > p/2 : \\ z < -p/2 : \end{matrix} E_r(z,r) = \mp 4E_1 \frac{p}{a} \sum_{n=o}^{\infty} \frac{B_n(-1)^n}{1+\delta_{no}} \sum_{v=1}^{\infty} \frac{J_1(j_v r/a)}{J_1(j_v)} \frac{p\eta_v \sinh(\eta_v p/2)}{(p\eta_v)^2 + (2\pi n)^2} e^{-\eta_v |z|}$$

(2.5.6a)

$$|z| < \frac{p}{2} : E_r(z,r) = 2E_1 \left[\sum_{n=1}^{\infty} B_n \frac{2\pi n}{\mu_n} \sin(2\pi n z/p) \frac{I_1(\mu_n r/p)}{I_o(\mu_n a/p)} \right. \qquad (2.5.6c)$$

$$\left. + 2\frac{p}{a} \sum_{n=o}^{\infty} \frac{B_n(-1)^n}{1+\delta_{no}} \sum_{v=1}^{\infty} \frac{J_1(j_v r/a)}{J_1(j_v)} \frac{p\eta_v \sinh(\eta_v z)}{(p\eta_v)^2 + (2\pi n)^2} e^{-\eta_v p/2} \right]$$

$$|z| \geq \frac{p}{2} : H_\theta(z,r) = -4E_1 \varepsilon\omega \frac{p^2}{a} \sum_{n=o}^{\infty} \frac{B_n(-1)^n}{1+\delta_{no}} \frac{J_1(j_v r/a)}{J_1(j_v)} \frac{\sinh(\eta_v p/2)}{(p\eta_v)^2 + (2\pi n)^2} e^{-\eta_v |z|}$$

(2.5.7a)

$$|z| = \frac{p}{2} : H_\theta\left(\frac{p}{2},r\right) = -E_1 \varepsilon\omega p \left[\frac{B_o}{2} \frac{1}{k_o p} \frac{J_1(k_o r)}{J_o(k_o a)} + \sum_{n=1}^{\infty} B_n(-1)^n \frac{1}{\mu_n} \frac{I_1(\mu_n r/p)}{I_o(\mu_n a/p)} \right. \qquad (2.5.7b)$$

$$\left. - 2\frac{p}{a} \sum_{n=0}^{\infty} \frac{B_n(-1)^n}{1+\delta_{no}} \sum_{v=1}^{\infty} \frac{J_1(j_v r/a)}{J_1(j_v)} \frac{e^{-\eta_v p}}{(p\eta_v)^2 + (2\pi n)^2} \right]$$

$$|z| \leq \frac{p}{2} : H_\theta(z,r) = -2E_1 \varepsilon\omega p \left[\frac{B_o}{2} \frac{1}{k_o p} \frac{J_1(k_o r)}{J_o(k_o a)} + \sum_{n=1}^{\infty} B_n \cos(2\pi n z/p) \frac{1}{\mu_n} \frac{I_1(\mu_n r/p)}{I_o(\mu_n a/p)} \right.$$

$$\left. - 2\frac{p}{a} \sum_{n=o}^{\infty} \frac{B_n(-1)^n}{1+\delta_{no}} \sum_{v=1}^{\infty} \frac{J_1(j_v r/a)}{J_1(j_v)} \frac{\cosh(\eta_v z)}{(p\eta_v)^2 + (2\pi n)^2} e^{-\eta_v p/2} \right]$$

(2.5.7c)

Remember that E_1 , $B_o \equiv 1$, B_n originate from the Fourier expansion of the tangential electrical field applied along the gap circumference :

$$E_z(z, r=a) = E_z^a(z) = 2E_1 \left[1/2 + \sum_{n=1}^{\infty} B_n \cos(2\pi nz/p) \right], 0 \leq z \leq p/2 \qquad (2.4.5)$$

How to find their numerical values is explained three paragraphs later. Series of type (a) represent superpositions of (evanescant) wave guide modes, in (b) and (c) there is a second sum (running over n only) directly related to the exciting field $E_z^a(z)$. Equation (5b) reproduces the jump of E_z assumed at the beginning in equations (2.4.1), (2.4.2) .

All the expressions (a) and (c) above are analytical functions in r and z provided $r < a$ and $|z| \neq p/2$. However, at and around $z = \pm p/2$ the series of v converge very slowly, the product of the exponential times the hyperbolic function which has a decisive influence upon a speedy decrease of terms, decaying dilatorily with increasing v . They are hardly tractable numerically in this region. In the series for V, E_z, H_θ but not in that for E_r the troublesome part can be summed at $|z| = p/2$ which procedure yields series (b). The derivatives of all these series are definitely or indefinitely divergent at $|z| = p/2$.

If $r > a$ the series (b) and (c) diverge, the n-th term being approximately proportional to $B_n \exp(-2\pi n(a-r))$. B_n which is expected to diminish only as an inverse power of n, cf. Section 2.4 A, cannot overcome the exponential growth of the modified Bessel function. It is completely natural that something goes wrong for $r > a$. The Green's function G_1 (2.4.38) is valid within the space $r \leq a$ only, the expression becomes infinite for $r > a$. The domain of integration in Green's theorem (2.4.34) is confined to the region $\bar{r} \leq a$ and the integral in equation (2.4.36) is zero if $r > a$, i.e. $V(z,r) = E_z(z,r) \equiv 0$ if $r > a$. The representation (2.4.36) describes a field excited by sources situated at $r = a$, $|z| \leq p/2$ which have been chosen in such a way to produce the field in the interior, but no field outside $r = a$. (Compare the analogous situation in electrostatics or potential theory, e.g. ref [35].) The series which is derived from the integral just described, should behave accordingly. For a series it is a rather difficult job to be zero for a continuous range of the argument r ($\infty > r > a$) without being identical zero for any r. So it has recourse to divergence,to bring its domain of validity in concordance with that of the generating integral. This statement should not be taken too literally. The use of Cauchy's residue theorem for the evaluation of the integrals (2.2.9) to (2.2.13) is impossible if $r > a$.

Just for fun we once evaluated some series (c) for $r > a$ with a finite number of terms in n. Already for modest $r - a > 0$ the sums oscillate between large positive and negative values. Series of type (a) have been investigated numerically [23]. In general they are convergent for $r > a$, they diverge only at some discrete points. But there seems to be no physical application of these expressions for $r > a$.

The above series contain the still unknown Fourier coefficients, E_1 , B_n. A finite number of them may be extracted from cavity fields calculated by numerical methods. Mesh calculations (e.g. [13), 17)] yield numerical values of $U = -rH_\Theta$ at discrete points within the whole cavity. One employs a truncated series for $-rH_\Theta(7c)$, inserts for r and z the coordinates of a point lying within the drift tube space $r \leq a$ and equates it to the corresponding mesh value U_m. In this way one sets up a system of linear equations for the unknown Fourier coefficients. We choose one mesh line situated very near to the edge of the drift tube, $r \approx a$, and take N terms, i.e. N Fourier coefficients, N being the number of mesh points in the region $o \leq z < p/2$. All the information needed concerning the field in the drift tube region can be derived in that way which has the advantage of introducing properties of an exact field but may lack some smoothing effect as is achieved when one is fitting a curve containing less disposable parameters than the number of values given.

Using these Fourier coefficients, $U = U_c$ may be calculated for all points within the space ($r < a$), and compared with the corresponding values U_m given by mesh calculation . For $z \leq p/2$ an agreement in U/r of about 1% is achieved. For $z > p/2$: $U_c/r < U_m/r$, the difference increases rapidly with increasing z, and amounts to about 50 to 60 percent at $z = L/2$.

This is not as serious as it appears since the values at $z = L/2$ are smaller by three to five orders of magnitude than their maximum values attained in the central region of the cell. To a large extent the difference between U_c and U_m is due to the fact that the above series describe the field in the wave guide rather than a cavity with end plates at $z = \pm L/2$. It is possible to give an approximate physical reasoning which leads to the result that at $|z| = L/2$ the wave guide field value is about half of the cavity field value. This is explained in Fig. 2.5.2.

With the aid of the series listed before, field distributions in a gap may be calculated. Examples are shown in Figs. 2.5.3, 2.5.4 and 2.1.3.

Agreement between the electric field along the axis, $E_z(z, r=0)$, computed in this way with that found by fitting a parabola to the mesh values and deriving this expression, is very satisfactory. In general, in the gap differences are not greater than 1%, often smaller than 1 °/oo. Outside it differences may be greater but are not serious. In some cavities where a column of mesh points is too near to the gap end, $z = p/2$, convergence of series at these points is insufficient for one or two points, and greater differences may occur. This affects particularly E_r which has just there its maximum. But this does not appreciably influence the values of the beam dynamics coefficients when these fields are used for their computation.

In conclusion it may be said that the method described is somewhat complicated and probably demands more computer and programmer's time than the simple interpolations usually employed. So its use seems to be justified only for tests of the quality of mesh calculations (where, however, the domain of comparison is restricted to the gap) and for computation of the Fourier coefficients B_n to find approximate expressions for $T_o(k)$ and the S-coefficients.

The electrical fields corresponding to the static approximation follow from the expressions above by the replacements:

$$k_o = 0 \qquad \mu_n \to 2\pi n \qquad p\eta_v \to j_v p/a \tag{2.5.8}$$

This is a very good approximation, since in (1):$(j_v/a)^2 >> k_o^2$, e.g.

$$(j_1/a)^2 \approx (2{,}4/10^{-2})^2 \approx 5{,}8 \times 10^4 >> 89{,}9 \approx (3\pi)^2 \approx (2\pi/\lambda)^2 \ ^{*)}$$

and in (4):$(2\pi n) >> (k_o p)^2$, e.g.

$$(2\pi)^2 >> (2\pi \times p/\lambda)^2 \approx (2\pi \times (0.02 \text{ to } 25)/150)^2$$

This reflects the well known fact that the static solution is good as long as the distances from metallic boundaries are small in comparison with λ. Further simplification to a homogeneous field across the gap ($B_s = 0$, $s \neq 0$) gives the results already given by R.TAYLOR.[3] The non-static field given in ref. [10] slightly differs from that in (2.5.5) and is only an approximate solution of Maxwell's equations.

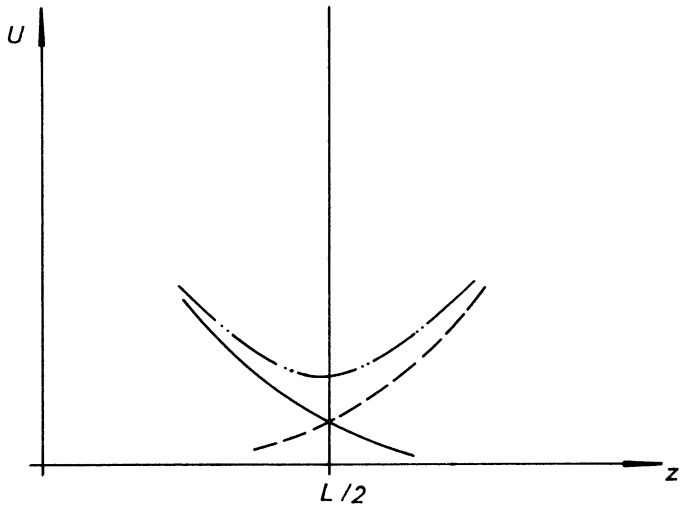

Fig. 2.5.2 The difference between cavity and wave guide field values at cell end, z = L/2. For fixed r the wave guide field $U_{w.g.}(z,r) = -rH_\theta(z,r)$, eq. (2.5.7a) decreases exponentially with increasing z (——). The cavity boundary condition $\partial U_{cav}/\partial z = 0$, eq. (2.3.7), can be approximately fulfilled by adding to $U_{w.g.}$ the field found from it by reflections(---). This procedure yields the field (-..-) which has at z = L/2 a value twice that of $U_{w.g.}$.

---

*) In the numerical expressions the dimension $(\text{metres})^{-2}$ is omitted.

2.5.A Evaluation of Residues

The calculation of the various residues rendering the above series (3) to (7) is easy since all poles are simple. The following formula is used :

$$\text{Res}\left(g(z)/(z - z_o) \; ; \; z = z_o \right) = g(z_o) \tag{2.5.9}$$

The residue of $g(k_z)/J_o(\gamma a)$ at the zeros, $\gamma a = j_v$, of the Bessel function is found with the aid of de l'Hospital's rule :

$$\gamma a = a\,(k_o^2 - k_z^2)^{\frac{1}{2}} = j_v \qquad k_z = \pm\, i\eta_v$$

$$\text{Res}\left(g(k_z)/J_o(\gamma a) \; ; \; k_z = \pm\, i\eta_v \right) = g(\pm\, i\eta_v) \lim_{k_z \to \pm\, i\eta_v} \left(\frac{k_z \mp i\eta_v}{J_o(\gamma a)} \right)$$

$$= g(\pm\, i\eta_v)\; d/dk_z \left(1/J_o(\gamma a) \right) \Big|_{k_z = \pm\, i\eta_v} = g(\pm\, i\eta_v) \left[J_o'(j_v)\; a^2(\mp\, i\eta_v)/j_v \right]^{-1} \tag{2.5.10}$$

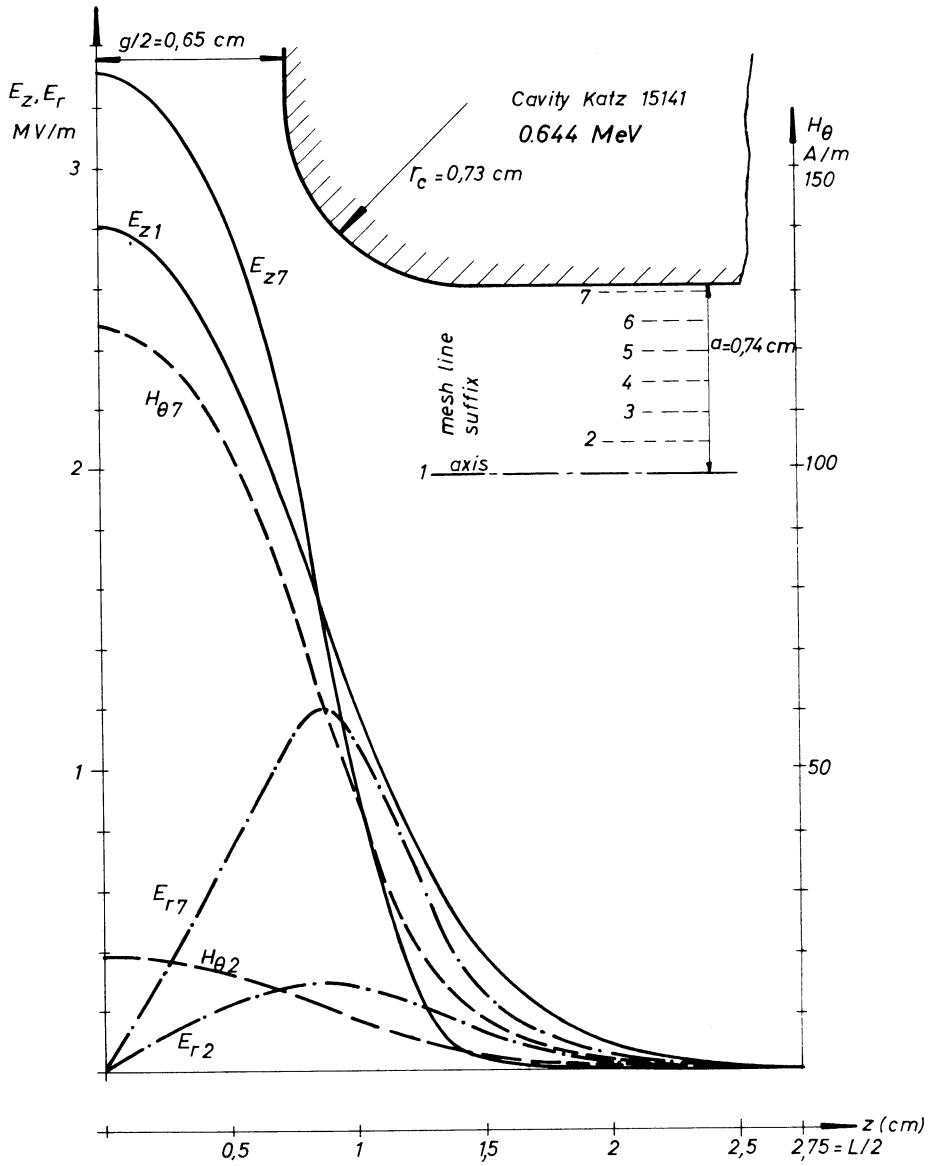

Fig. 2.5.3. Fields in the drift tube space of cavity KATZ 15141. Energy = .644 MeV, transit time factor T = .68 , $\omega/2\pi$ = 202.19 MHz, normalization : average field strength $E_o = V_o/L = 1$ MV/m. Cavity radius R = 48.1 cm, inner radius of drift tube a = 0.74 cm, outer diameter of drift tube = 17.9 cm, radius of curvature of outer rim = 1.94 cm, radius of curvature in inner rim R_i = .73 cm, distance of mesh-lines $\Delta z \simeq \Delta r \approx 2$ mm. Second index of fields indicates mesh line suffix.

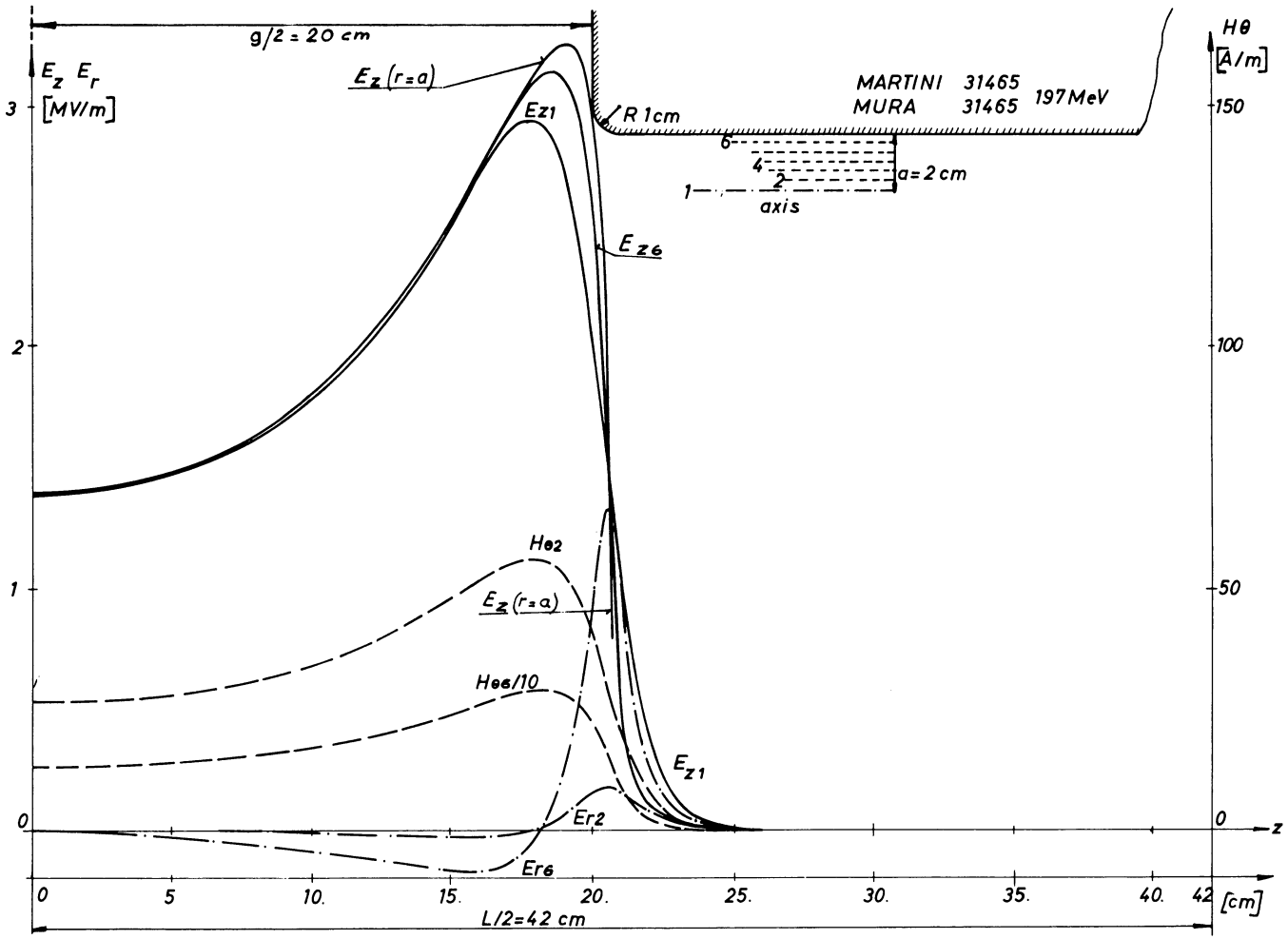

Fig. 2.5.4. Fields within gap and drift tube of cavity MARTINI 31465 (design MURA 31465 [26]). Energy = 197 MeV, transit time factor T_o = 0.56, $\omega/2\pi$ = 200.93 MHz. Normalization: average field strength E_o = 1 MV/m. Cavity radius R = 84 cm, inner radius of drift tube a_o = 2cm, outer diameter of drift tube = 16 cm, radius of curvature of outer rim = 4 cm, radius of curvature of inner rim R_i = 1 cm, mesh-line distance $\Delta r \approx \Delta z \approx 3.4$ mm. Second index of fields indicates mesh-line suffix. $H_{\theta 6}$ scaled down by a factor 1/10.

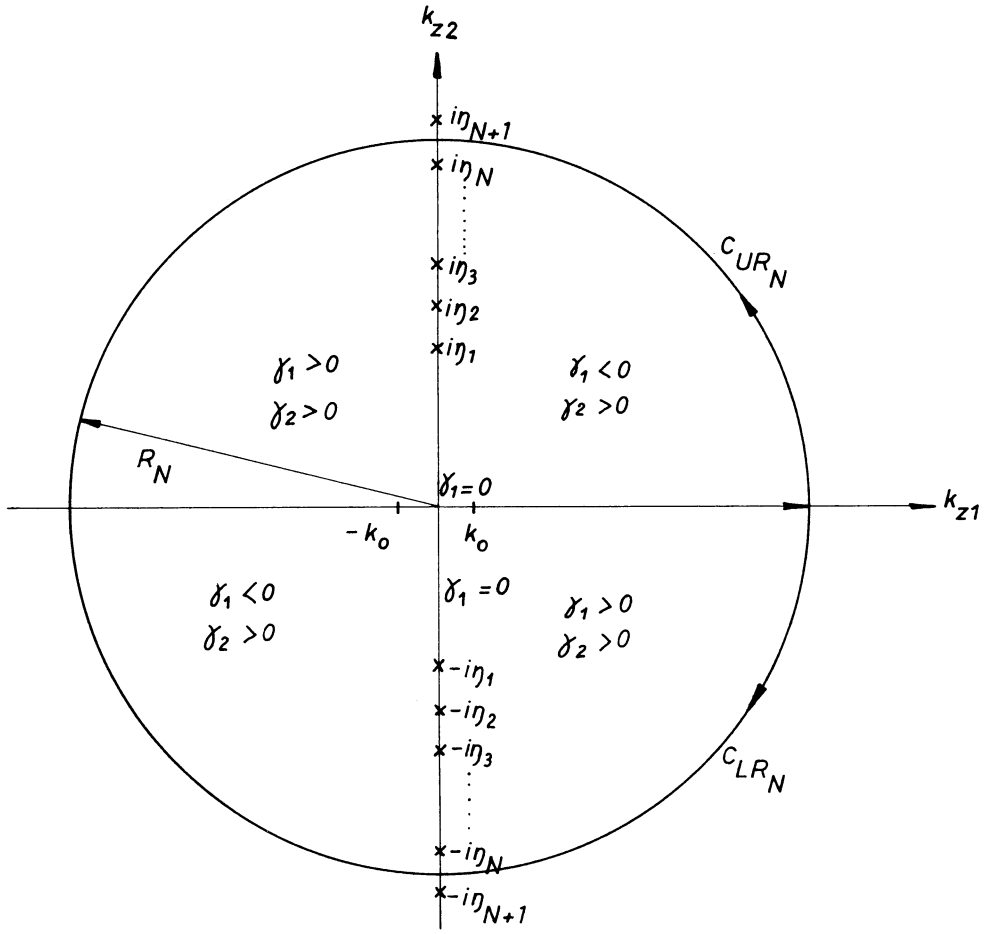

Fig. 2.5.5. The complex k_z-plane. The semi-circles C_{UR_N} and C_{LR_N} pass just between $\pm i\eta_N$ and $\pm i\eta_{N+1}$, the N-th and the (N+1)-th zero of the Bessel function $J_o(\gamma a) = 0$. The branch cuts $\gamma_1 = 0$ which ensure that the imaginary part γ_2 of the root $\gamma = \gamma_1 + i\gamma_2 = (k_z^2 - k_o^2)^{\frac{1}{2}}$ is positive throughout the whole plane, run along the real k_z-axis between $-k_o$ and $+k_o$ and along the whole imaginary k_z-axis. They are needed only for the estimate of the asymptotic behaviour of the integrand in (2.5.15). The integrals themselves are single-valued.

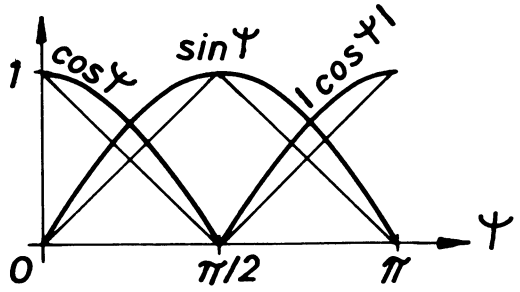

Fig. 2.5.6 Linear Approximations for Sine and Cosine

2.5.B Rigorous Demonstration of Expansion into a Residue Series

The procedure to be employed will be demonstrated on an example where the series (5a) of $E_z(z,r)$, $z > p/2$, will be derived from the corresponding integral representation (2.2.11). At first an integral around the semi-circle of finite radius R_N situated in the upper half of the complex k_z-plane is set up and evaluated by use of Cauchy's residue theorem (see Fig.2.5.5):

$$\int_{-R_N}^{R_N} f(k_z)\, dk_z + \int_{C_{UR_N}} f(k_z)\, dk_z = 2\pi i \sum_{\nu=1}^{N} \mathrm{Res}(f(k_z)\ ;\ k_z = + i\eta_\nu) \qquad (2.5.11)$$

The integrand:

$$f(k_z) = (E_1/2\pi)\, b(k_z)\, e^{ik_z z}\ J_o(\gamma r)/J_o(\gamma a) \qquad (2.5.12)$$

is regular within the domain enclosed except for the simple poles $J_o(\gamma a) = 0$.
R_N is defined as :

$$R_N = a(N + \tfrac{1}{4})\pi \qquad N = \text{integer} \qquad (2.5.13)$$

Then C_{UR_N} passes just half-way between the poles $k_z = i\eta_N \approx i\, j_N/a \approx i\,(N-\tfrac{1}{4})/a$ and $k_z = i\eta_{N+1} \approx i\,(N + 3/4)/a$ and never hits a singularity. If with increasing N i) the integral along C_{UR_N} vanishes, ii) the other integral in (11) assumes a definite value, iii) the series on the right hand side of (11) uniformly converges, then the integral $\int_{-\infty} f(k_z)\, dk_z$ equals $2\pi i$ times the residue series.

The proof of i) is as follows :

For sufficiently great N, k_z and γ are given along C_{UR_N} by:

$$k_z = R_N e^{i\psi} \qquad dk_z = R_N\, i\, e^{i\psi}\, d\psi$$

$$\gamma = \gamma_1 + i\gamma_2 = (k_o^2 - k_z^2)^{\frac{1}{2}} \approx ik_z = i\,R_N|\cos\psi| + R_N \sin\psi \quad (\gamma_2 \geq 0) \qquad (2.5.14)$$

The subscript N will now be dropped, but the limit $R \to \infty$ is always to be understood as $N \to \infty$. Employing (2.4.21) and (2.4.25) till (2.4.27) the second integral of (11) is estimated at :

$$\left| \int_{C_{UR}} f(k_z)\, dk_z \right| \leq 2K(a/r)^{\frac{1}{2}} \int_0^{\pi} \cosh\left(\frac{pR}{2}\sin\psi\right) e^{-zR\sin\psi}\, e^{-(a-r)R|\cos\psi|}\, R\, d\psi$$

$$\leq 2K(a/r)^{\frac{1}{2}}\,(I_1 + I_2 + I_3 + I_4)\ . \qquad (2.5.15)$$

The integral in the first line is split up into $\int_0^{\pi/2} + \int_{\pi/2}^{\pi}$ and cosh ( ) is decomposed into the exponentials. This yields 4 integrals as indicated. As the arguments of all exponentials are negative, the above inequality still holds when $\sin\psi$, $\cos\psi$ are replaced by the following smaller linear functions (cf. Fig. 2.5.6):

$$2\,\psi/\pi \le \sin\psi, \quad 1 - 2\,\psi/\pi \le |\cos\psi| \quad 0 \le \psi \le \pi/2$$
$$2 - 2\psi/\pi \le \sin\psi, \quad -1 + 2\,\psi/\pi \le |\cos\psi| \quad \pi/2 \le \psi \le \pi \tag{2.5.16}$$

These integrals may be evaluated :

$$I_{1,2} = R\, e^{-R(a-r)} \int_0^{\pi/2} e^{-R\left[(z \mp p/2) - (a-r)\right]} 2\psi/\pi \, d\psi = \pi \frac{e^{-R(z \mp p/2)} - e^{-(a-r)R}}{-2\left[(z \mp p/2) - (a-r)\right]} \tag{2.5.17}$$

$$I_{3,4} = R\, e^{-2R(z \mp p/2)}\, e^{R(a-r)} \int_{\pi/2}^{\pi} e^{R\left[(z \mp p/2) - (a-r)\right]} 2\psi/\pi \, d\psi =$$

$$= \pi \frac{e^{-R(a-r)} - e^{-R(z \mp p/2)}}{2\left[(z \mp p/2) - (a-r)\right]}$$

condition i) above is now obvious, for all four integrals and therefore (15) tend to zero if $R \sim N \to \infty$, provided $a-r > 0$ and $z > p/2$.
The residues are given by :

$$2\pi i\, \mathrm{Res}(\, f(k_z) \,;\, k_z = i\eta_\nu) = - E_1\, b(i\eta_\nu)\, e^{-\eta_\nu z}\; j_\nu J_0(j_\nu r/a)/(a^2 \eta_\nu J_1(j_\nu)^2) \tag{2.5.18}$$

$$= - 4\, E_1 \sinh(\eta_\nu p/2)\; e^{-\eta_\nu z}\, j_\nu J_0(j_\nu r/a)/(a^2 J_1(j_\nu)^2) \sum_{n=0}^{\infty} B_n (-1)^n (1+\delta_{no})^{-1} \times \left[\eta_\nu^2 + (2\pi n/p)^2\right]^{-1}$$

With:

$$|J_0(j_\nu r/a)| \le 1 \,, \quad J_1(j_\nu) \approx (2/\pi j_\nu)^{\frac{1}{2}} \cos\left[(\nu - 1)\pi\right]$$

and

$$\left| 4 \sum_{n=0}^{\infty} B_n (-1)^n (1 + \delta_{no})^{-1} \sqrt{j_\nu^3}/a^2 \left[\eta_\nu^2 + (2\pi n/p)^2\right]^{-1} \right| < 4 \sum_{n=0}^{\infty} |B_n| = K = \bar{K}\sqrt{2/\pi}$$

it is :

$$|2\pi \operatorname{Res}(f(k_z)\ ;\ k_z = i\eta_\nu)| \leq (E_1 \bar{K}/2) \left[e^{-\eta_\nu(z-p/2)} + e^{-\eta_\nu(z+p/2)} \right]$$

Here $z - p/2 < z + p/2$, therefore the modulus of the general term of the residue series (11) decreases faster than $\exp(-\eta_\nu(z-p/2)) \approx \exp(-j_\nu(z-p/2)/a) \approx \exp(-\nu\pi(z-p/2)/a)$. The latter produces a geometric series $\sum q^n$, with $q = -\pi(z-p/2)/a$. It can be concluded that the condition iii) above is fulfilled since residue series (11) is uniformly and absolutely convergent, if $z > p/2$. Condition ii) above has already been ascertained in Section 2.4.C. The proof of the expansion of the integral (2.2.11) into the series (5a) is now complete. Interchange of summation with regard to n and v is permissible, the series in n and v being uniformly and absolutely convergent in the interior of the drift tube space.

When $z < -p/2$, then a circle C_{LR_N} lying in the lower half of the complex k_z-plane is used to close the path running along the real axis and the whole game is played again mutatis mutandis.

When $|z| < p/2$ the path of the integrations is deformed into $\tilde{C}$. The choice of the indentations is arbitrary; the sole purpose is to avoid the singularities of $b_+(k_z)$ and $b_-(k_z)$ lying on the real axis. Afterwards the following equation is set up:

$$f_{\pm}(k_z) = b_{\pm}(k_z)\ e^{ik_z z}\ J_o(\gamma r)/J_o(\gamma a)$$

$$\int_{\tilde{C}} f(k_z)\, dk_z + \int_{C_U} f_+(k_z)\, dk_z + \int_{C_L} f_-(k_z)\, dk_z = \tag{2.5.19}$$

$$= 2\pi i \sum_{\nu=1}^{\infty} \left[\operatorname{Res}(f_+(k_z)\ ;\ k_z = i\eta_\nu) - \operatorname{Res}(f_-(k_z)\ ;\ k_z = -i\eta_\nu) \right]$$

$$+ 2\pi i \sum_{n=o}^{\infty} \operatorname{Res}(f_+(k_z)\ ;\ k_z = 2\pi n/p) - 2\pi i \sum_{n=1}^{\infty} \operatorname{Res}(f_-(k_z)\ ;\ k_z = -2\pi n/p)$$

$\int_{C_U}$ and $\int_{C_L}$ are shown to be zero by (2.4.11). (17) again applies to the series in v ; (9) and (2.4.12) serve for the calculation of the residues of the second chain. The first series in n contained in (3b), (3c),(5b), (5c), (6b), (6c), (7b) and (7c) uniformly converge ; for them bounding geometric series may be set up by use of :

$$B_n\, I_o(\mu_n r/p)/I_o(\mu_n a/p) \sim B_n\, e^{-2\pi n(a-r)} \quad , a > r \tag{2.5.20}$$.

and similar relations for the terms in I_1 .

2.5C Summation of series at $|z| = p/2$

At $|z| = p/2$ the expansions (a) valid for $|z| \geq p/2$ and (c) valid for $|z| \leq p/2$ join (except that for E_r, (2.5.6), whose behaviour at this point remains undetermined). In order to prove this fact the part of $2\cosh(\eta_v p/2)\exp(-\eta_v p/2) = 1 - \exp(-\eta_v p)$ or $\sinh(\eta_v p/2)\exp(-\eta_v p/2)$ no longer containing an exponential, must be summed. For this purpose the integral :

$$\lim_{R \to \infty} \int_{|k_z| = R} dk_z \frac{k_z J_o(\gamma r)}{\gamma^2 J_o(\gamma a)} \frac{1}{k_z^2 - (2\pi n/p)^2} = 0 \qquad (2.5.21)$$

is introduced. If the radius of the circle $|k_z| = R$, $C_U - C_L$ in Figs. 2.2.1 and 2.5.5, tends to infinity, then the integral vanishes as may be shown by the method described in equations (14) to (17). In consequence, the sum of all residues enclosed which are due to the simple poles at $k_z = \pm i\eta_v$, $\pm k_o$, $\pm 2\pi n/p$, is zero. This gives :

$$2 \sum_{v=1}^{\infty} \frac{J_o(j_v r/a)}{j_v J_1(j_v)} \frac{1}{(p\eta_v)^2 + (2\pi n)^2} = \qquad (2.5.22)$$

$$= \frac{I_o\left(\frac{r}{p}\left[(2\pi n)^2 - (k_o p)^2\right]^{\frac{1}{2}}\right)}{I_o\left(\frac{a}{p}\left[(2\pi n)^2 - (k_o p)^2\right]^{\frac{1}{2}}\right)} \frac{1}{(k_o p)^2 - (2\pi n)^2} - \frac{1}{(k_o p)^2 - (2\pi n)^2}$$

If $n = 0$, $I_0(x\sqrt{-k_o^2}) = J_o(k_o x)$. This expansion serves for summing (3), the series for U ; its derivative with respect to r is employed for H_θ , equations (7). The integral to be used for E_z, equations (5), gives a slightly different result :

$$\lim_{R \to \infty} \frac{1}{2\pi i} \oint_{|k_z| = R} dk_z \, k_z \, J_o(\gamma r) / \left[J_o(\gamma a)\,(k_z^2 - (2\pi n/p)^2)\right] = \delta_{ar} \qquad (2.5.23)$$

where $\delta_{ar} = 1$ if $r = a$, $\delta_{ar} = 0$ if $r \neq a$. The residue series belonging to (23) is :

$$2\left(\frac{p}{a}\right)^2 \sum_{v=1}^{\infty} \frac{J_o(j_v r/a)}{J_1(j_v)} \frac{j_v}{(p\eta_v)^2 + (2\pi n)^2} = -\delta_{ar} + \frac{I_o\left(\frac{r}{p}\left[(2\pi n)^2 - (k_o p)^2\right]^{\frac{1}{2}}\right)}{I_o\left(\frac{a}{p}\left[(2\pi n)^2 - (k_o p)^2\right]^{\frac{1}{2}}\right)} \qquad (2.5.24)$$

A trial to set up a similar integral to produce the corresponding series of $E_r(\frac{p}{2}, r)$ is not successful; residues due to $k_z = i\eta_v$, $2\pi n/p$ cancel against those arising from $k_z = -i\eta_v$, $-2\pi n/p$ respectively.

2.6 Voltage, Transit Time Factor, T-coefficients

The instantaneous peak voltage, measured at the instant $\omega t = \phi = -\phi_o$ along the line r = const is :

$$V(r) = \int_{-\infty}^{\infty} E_z(z,r)\, dz = E_1\, b(0)\, J_o(k_o r)/J_o(k_o a) = V_o J_o(k_o r) \qquad (2.6.1)$$

For the evaluation of this integral, the representation (2.2.11) of E_z has been inserted. $b(0) = p$ (cf. (2.4.6)) has been used; and the definitions :

$$V_1 = V(a) = E_1 p \qquad V_o = V(0) = E_o L = E_1 p/J_o(k_o a) \qquad (2.6.2)$$

have been adopted.

$V_1(V_o)$ is the "voltage" across the gap (along the axis), $E_1(E_o)$ the average field strength at the same lines. L is the length of the cell. In numerical results of field calculations, it is common to normalize the fields such that E_o = 1 MV/m. (In a linac under operation E_o = 1 - 3 MV/m.) In the static limit (k_o = 0) there is no r-dependence of the voltage (1), and in practice it is negligible, since (for example) $0 \leq k_o r \leq k_o a = 2\pi a/\lambda \approx 3\pi\ 10^{-2}$, $V_1 : V_o \leq 0{,}9988$.

When E_o is computed according to (2) with the help of E_1 found by the method described in Section 2.5, it does not exactly reproduce the normalization of 1 MV/m, but deviations of more than 1 or 2% are very exceptional.

When approximately solving the equations of particle motion, integrals like :

$$\int_0^{\infty} E_z(z,r)\cos(kz)\, dz \quad , \quad \int_0^{\infty} E_r(z,r)\sin(kz)\, dz$$
$$\int_0^{\infty} E_z(z,r)\sin(kz)\, dz \quad , \quad \int_0^{\infty} E_r(z,r)\cos(kz)\, dz \qquad (2.6.3)$$

will arise, where $k = \omega/\dot{z}_o$. ($\dot{z}_o$ = mid plane velocity of the particle). For this reason these integrals will be introduced as dynamical coefficients (T- and S-coefficients), and their properties will be discussed in this and the following section. For the present k may just be regarded as a parameter, $k > k_o$, whose connections with particle velocity does not matter.

The longitudinal T-coefficient $T_1(k,r)$ is defined as :

$$V_o\, T_1(k,r) = \int_{-\infty}^{\infty} E_z(z,r)\cos(kz)\, dz = V_o T_o(k)\, I_o(k_r r) \qquad (2.6.4.)$$

with

$$k_r = (k^2 - k_o^2)^{\frac{1}{2}} \tag{2.6.5}$$

The evaluation of the above integral containing $E_z(z,r)$ from (2.2.11) and $b(k_z)$ from (2.4.6) shows that the result factorizes in the way indicated on the right hand side. $T_o(k)$ is defined below.

The same factorization can be achieved in the following integral over the radial electrical field, called the transverse T-coefficient $T_r(k,r)$:

$$V_o\, T_r(k,r) = \int_{-\infty}^{\infty} E_r(z,r)\, \sin(kz)\ dz = V_o\, T_o(k)\, k\, I_1(k_r r)/k_r \tag{2.6.6}$$

and similarly in the integral over the magnetic field, called the magnetic T-coefficient $T_m(k,r)$:

$$V_o\, T_m(k,r) = -\frac{c}{k_o} \int_{-\infty}^{\infty} \mu H_\theta(z,r)\, \cos(kz)\, dz = V_o\, T_o(k)\, I_1(k_r r)/k_r \tag{2.6.7}$$

In (4),(6) and (7) use has already been made of the transit time factor, defined as :

$$T_o(k) = \frac{1}{V_o} \int_{-\infty}^{\infty} E_z(z,0)\, \cos(kz)\, dz \tag{2.6.8}$$

All T-coefficients are known as soon as k and the transit time factor T_o are given; they may just be regarded as convenient abbreviations.

Evaluation of the above integral with E_z from (2.2.11) and $b(k_z)$ from (2.4.6) gives :

$$T_o(k) = \frac{b(k)}{b(0)} \frac{J_o(k_o a)}{I_o(k_r a)} = T_{oo}(k)\, (1 + Y) \tag{2.6.9}$$

$$T_{oo}(k) = \frac{J_o(k_o a)}{I_o(k_r a)} \frac{\sin(kp/2)}{(kp/2)} \qquad Y = -\sum_{n=1}^{\infty} \frac{2(-1)^n B_n\, (kp)^2}{(2\pi n)^2 - (kp)^2}$$

This is rewritten with the help of (2) :

$$E_1\, b(k)/I_o(k_r a) = V_o\, T_o(k) \tag{2.6.10}$$

Inserting this into (2.2.11) to (2.2.13) gives the same field representations as used in earlier treatments [7)-9)].

In earlier work [1), 8)] the factor $J_o(k_o a) \approx 1$ is missing ; where $T_o(k)$ was taken from the static approximation, $k_o = 0$. In many cases the field $E_z(z,a)$ applied along the gap has been approximated by a homogeneous one, $E_z(z,a) = E_1$, and Y has been neglected.

The transit time factor has been introduced into the theory of linac particle dynamics by PANOFSKY[1)]. Together with its derivatives $T'_o(k)$, $T''_o(k)$, it plays a primary role in beam dynamics calculations treating the motion of a proton which crosses an accelerating gap (see Section 3.1 and Chapter 5). All these quantities are needed for the single value $k = \omega/z_o$, and may be easily obtained from fields given numerically by numerical integration of the integral defined in (8). Regarding the cell as a closed cavity, a common definition for T_o is, instead of (8) :

$$T_o = \int_{-L/2}^{L/2} E_z(z,0) \cos\frac{2\pi z}{L}\, dz \Big/ \int_{-L/2}^{L/2} E_z(z,0)\, dz \qquad (2.6.11)$$

The transit time factor $T_o(k)$ for any $k = \omega/\dot{z}_o$ is found from T_o, T'_o, .. with the help of a Taylor's series around $2\pi/L$:

$$T_o(k) = T_o + (k - 2\pi/L)\, T'_o + \frac{1}{2}(k - 2\pi/L)\, T''_o + \ldots \qquad (2.6.12)$$

$T_o(k)$ is a measure of the distribution of E_z in the longitudinal direction, and $0 \leq |T_o| \leq 1$. $T_o \sim 1$ for small ideal gaps, and decreases with increasing gap size. T_{oo} corresponds to an excitation by a purely homogeneous field $E_z = E_1$ across the boundary of the gap; Y accounts for the deviation from homogeneity. Y is expected to be not very large compared with unity, since the aim is to achieve a field as homogeneous as possible, i.e. $1 = B_o \gg B_n$ $(n > 1)$ (and since each term contains in addition a factor of order $1/n^2$).

The fields in the gaps of a number of Alvarez cells have been studied; and the transit time factor, T_o, and its derivatives have been evaluated by use of the formulae given in table II. k was computed from :

$$k = \omega/\dot{z}_o = (\omega/c)/(c/\dot{z}_o) = k_o \left[1 - (mc^2/W)\right]^{-\frac{1}{2}} \qquad (2.6.13)$$

where mc^2 is proton rest mass and W the mean kinetic energy of the cell [13)]. The list of cavities comprised some of the cavities of the CERN 3 MeV experimental linac [13) 24)], two cavities designed by KATZ[25)] and a number of MURA cavities.[26)27)]. The fields and beam dynamics coefficients of the latter have been re-calculated by MARTINI and WARNER [24)].

There appears quite a clear correlation between the value of Y (which in turn strongly depends on the value of B_1), the "uniformity" of the exciting field, $E_z^a(z) = E_z(z,r=a)$, and (at not too high energy) the ratio R_i/p (cf. Fig. 2.1.4). As a measure of the uniformity the ratio p_9/p may be introduced where $p_9/2$ is the distance where the field E_z^a has decayed to 90% of its maximum value. Numerical results are compared in table 2.6.1.

The following tentative conclusions can be drawn. In the 3 MeV linac cavities the field E_z^a attains a high degree of uniformity, very probably due to the small ratio R_i/p (and may be also due to a favourable shaping of the outer part of the drift tube). Y is small. The transit time factor, T_o, and its derivatives can be very well approximated by that of a uniform field, T_{oo}. In the two KATZ cavities R_i/p is greater, therefore Y is greater. T_o and especially T_o' cannot be approximated by that of a uniform field. In the low energy MURA cavities R_i/p is not small enough, the field uniformity parameter p_9/p is smaller than 0.8 and the differences between T_o and T_{oo} and also between the corresponding derivatives are quite appreciable. With increasing gap length (cf. the 63 MeV cavity) p_9/p again approaches 0.8, Y drops to .03 and agreement between T_o and T_{oo} and also between the derivatives becomes satisfactory. It is interesting that for the cavities in the range 47 to 83 MeV Y is small in spite of the central depression of E_z^a (this depression already appears in the 19 MeV Cell). In the 197 MeV cell Y,on the contrary, is again quite great. At not too great gap length, comparison of T_o found by numerical integration of $E_z(z,r=0)$ with the above T_{oo} may give an indication of the field distribution in the gap circumference. If $|Y| = |T_o - T_{oo}|/T_{oo}$ is small, the field E_z^a has either a plateau or a not too deep central depression, while a great Y indicates that the field soon begins to drop from the maximum which in that case is assumed at the gap centre or very near to it.

The value of T_o is strongly influenced by the gap geometry. Small radius of curvature of the inner drift tube rim may enhance the electrical field at the gap end, thereby increasing T_o at low energy or decreasing it at high energy.

Also the bore radius a is of importance. In practice, T_o may vary between about .50 and 0.85 . If transverse geometries are comparable, T_o first increases with energy. Then T_o is roughly constant between say 5 and 50 MeV and afterwards it again decreases, due to the deep central depression of the electrical field upon the axis.

Cavity	Energy (MeV)	B_1	Y	p_9/p	R_i/p	By numerical integration			From Fourier Coefficients					
						T_o	kT'_o	$k^2T''_o$	T_o	kT'_o	kT''_o	$\frac{T_o-T_{oo}}{T_o}$	$\frac{T'_o-T'_{oo}}{T'_o}$	$\frac{T''_o - T''_{oo}}{T''_o}$
3MeV linac	70 001	.558	.089	.0239	.80	.10	.690	-.512	-.101	.682	-.509	-.085	.023	.043	-.119
	70 203	.738	.105	.0286	.86	.08	.721	-.462	-.134	.716	-.469	-.129	.028	.058	-.065
	51 112	1.891	.070	.0105	.86	.07	.760	-.416	-.179	.757	-.419	-.177	.018	.057	-.002
	51 415	2.395	.065	.0175	.87	.08	.762	-.415	-.183	.756	-.420	-.181	.017	.048	+.001
	51 617	2.764	.060	.0164	.86	.08	.770	-.406	-.188	.764	-.410	-.187	.016	.047	+.004
KATZ	15 141	.644	.416	.2922	.32	.26	.679	-.526	-.119	.688	-.513	-.127	.226	+.398	-1.155
	15 034	7.981	.147	.0636	.71	.10	.786	-.391	-.246	.788	-.387	-.247	.060	+.168	.079
MURA	31 335	5.469	.292	.1253	.48	.16	.821	-.328	-.224	.819	-.335	-.228	.111	.457	.195
	20 241	10.860	.226	.101	.62	.11	.817	-.341	-.244	.818	-.340	-.243	.092	+.377	.183
	30 941	19.463	.149	.0662	.78	.09				.818	-.342	-.252	.062	.285	.135
	30 830	47.756	.054	.0263	.84	.06				.825	-.329	-.250	.026	.111	.056
	20 242	63.784	.003	.0144	.88	.05	.758	-.449	-.303	.757	-.448	-.302	.014	.035	-.019
	30 736	84.098	.040	.0055	.52	.04	.701	-.543	-.323	.748	-.464	-.307	-.006	-.022	-.051
	31 465	197.011	-.185	-.1202	.9	.01	.558	-.770	-.325	.557	-.768	-.324	-.138	-.166	-.108

TABLE VII

Table 2.6.1. Transit time factors of various cavities. Their geometrical and dynamical parameters are given in Table VII. $p_9/2$ is the distance along which the field E_z^a has dropped to 90% of its maximum value.

2.6.A Evaluation of Voltage and T-coefficients

The evaluation of the quantities $V(r)$, T_1, T_r, T_m and T_o defined above by integrals, is easily accomplished by methods of complex integration.

In the expression defining the voltage $V(r)$ (eq.(1)):

$$V(r) = \lim_{\ell \to \infty} \int_{-\ell}^{\ell} E_z(z,r)\, dz = \frac{E_1}{2\pi} \lim_{\ell \to \infty} \int_{-\ell}^{\ell} dz \int_{-\infty}^{\infty} dk_z\, b(k_z)\, e^{ik_z z}\, J_o(\gamma r)/J_o(\gamma a) \tag{2.6.14}$$

the path of integration in the complex k_z-plane is indented at $k_z = 0$ (C_o, see Fig. 2.6.1) before the integration with respect to z is performed :

$$V(r) = -i \frac{E_1}{2\pi} \lim_{\ell \to \infty} \int_{C_o} dk_z\, b(k_z) \frac{1}{k_z} e^{ik_z \ell}\, J_o(\gamma r)/J_o(\gamma a) + \int_{C_o} dk_z\, b(k_z) \frac{1}{k_z} e^{-ik_z \ell}\, J_o(\gamma r)/J_o(\gamma a) \tag{2.6.15}$$

In the first (second) integral the path C_o is completed by the addition of C_U (C_L) (Fig. 2.2.1) whose contribution vanishes, as usual (cf. (2.4.9) and (2.5.15) to (2.5.17)), if $\ell > p/2$. The integrals equal $2\pi i$ times the sum of the residues due to the simple poles enclosed. Those due to $k_z = +i\eta_\nu$ ($-i\eta_\nu$) ($J_o(\gamma a) = 0$) contain a factor $e^{-\eta_\nu \ell}$ (cf.(2.5.18)) and vanish in the limit $\ell \to \infty$. In the first integral remains the contribution due to $k_z = 0$ which does not depend on ℓ :

$$V(r) = E_1\, b(0)\, J_o(k_o r)/J_o(k_o a) = E_1 p\, J_o(k_o r)/J_o(k_o a) \tag{2.6.16}$$

$b(0) = p$ follows from (2.4.6): terms with $n \neq 0$ vanish for $k_z = 0$; that with $n = 0$ $(2 B_o \sin(k_z p/2))/(k_z p)$ yields in the limit $k_z \to 0$: $B_o p = p$.

To begin the treatment of the T_1-coefficient, $\hat{C}$ (Fig. 2.2.1) is used as path of integration in the complex k_z-plane ; this permits to perform the integration with respect to z :

$$V_o\, T_1(k,r) = \lim_{\ell \to \infty} \int_{-\ell}^{\ell} E_z(z,r) \cos(kz)\, dz$$

$$= \frac{E_1}{4\pi} \lim_{\ell \to \infty} \int_{\hat{C}} dk_z \left[\frac{e^{i\ell(k_z+k)} - e^{-i\ell(k_z+k)}}{i(k_z + k)} + \frac{e^{i\ell(k_z-k)} - e^{-i\ell(k_z-k)}}{i(k_z - k)} \right] \times \tag{2.6.17}$$

$$\times\, b(k_z)\, J_o(\gamma r)/J_o(\gamma a)$$

The four integrals, each one containing one exponential, are evaluated as before where $\hat{C}$ is closed by C_U (C_L) for $e^{i\ell(k_z \pm k)}$ ($e^{-i\ell(k_z \pm k)}$). Residues due to $k_z = \pm i\eta_v$ vanish if $\ell \to \infty$. In the second, third integral respectively, there remain the contributions due to $k_z = -k, +k$ resp., they are equal since $b(-k) = b(k)$, and yield :

$$V_o T_1(k,r) = E_1 \, (b(k)/I_o(k_r a)) \, I_o(k_r r) \qquad (2.6.18)$$

with $-i\gamma(k) = k_r = (k^2 - k_o^2)^{\frac{1}{2}} > 0$, eq. (5). $r = 0$ gives the <u>transit time factor</u> :

$$T_o(k) = T_1(k,r=0) = (E_1/V_o)\,(b(k)/I_o(k_r a)) = J_o(k_o a)\, b(k)/(pI_o(k_r a)) \qquad (2.6.19)$$

$E_1/V_o = E_1/V(0) = J_o(k_o a)/p$ has been taken from (2). Inserting $b(k)$ from (2.4.6) gives (9). $T_r(k,r)$ and $T_m(k,r)$ may be treated in the same way.

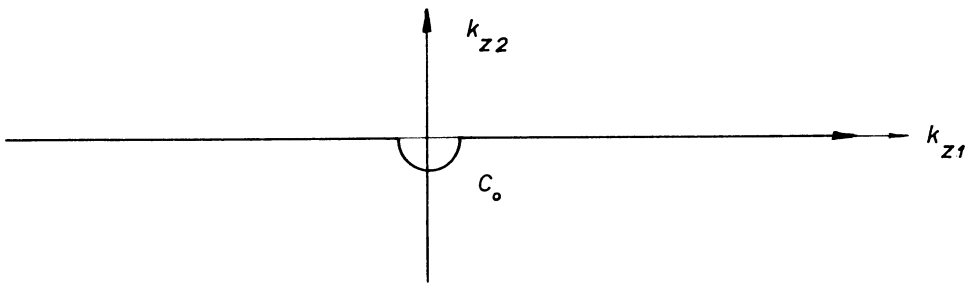

Fig. 2.6.1 The contour C_o .

2.7 The S-coefficients

Among the integrals listed in (2.6.3), two which are even functions in z by the symmetry properties (2.5.2) of the field, have been employed for the definition of the T-coefficients. It is this symmetry which permits the factorization of the radial dependence accomplished in equations (2.6.4) and (2.6.6). The odd functions give rise to the S-coefficients, needed for dynamical calculations in the first half of the gap. First attempts of this type have been started by LAPOSTOLLE [7)9)], and the present definitions of the S-coefficients are generalizations of his idea.

The longitudinal, the transverse and the magnetic S-coefficient are defined as :

$$V_o S_l(k,r) = 2 \int_0^\infty E_z(z,r) \sin(kz)\, dz \qquad (2.7.1)$$

$$V_o S_r(k,r) = 2 \int_0^\infty E_r(z,r) \cos(kz)\, dz \qquad (2.7.2)$$

$$V_o S_m(k,r) = \frac{-2c}{k_o} \int_0^\infty \mu H_\theta(z,r) \sin(kz)\, dz \qquad (2.7.3)$$

(It should be noted that the above S-coefficients are completely different from the S-factor (coupling-coefficient) defined by SWENSON [4)].)

S_l and S_r (as well as T_l and T_r) are dimensionless, while S_m (and T_m) have the dimension of a length. It may be tempting to introduce dimensionless definitions by multiplying the right hand sides of (2.6.7) and (2.7.3) by k. However, this brings disadvantages in the presentation of dynamical formulae, because it is then no longer possible to write $d/dk_z\, S_m(k_z,r)\big|_{k_z = k} = d/dk\, S_m(k,r)$.

On the other hand in numerics it is preferable to introduce some normalization. Without it S_m and T_m are smaller than the other T- and S-coefficients by a factor 10 to 100. It may be best to multiply T_m and S_m by $2\pi/L$ and to modify dynamical formulae in Tables IV to VI accordingly. In all these formulae S_m (or dS_m/dk, d^2S_m/dk^2) is preceded by k. Therefore the normalization can be done in the following way :

$$kS_m = (kL/2\pi) \times (2\pi\, S_m/L) = (kL/2\pi) \times S_{m\,norm}$$

where $kL/2\pi \approx 1$.

The various S-coefficients are related to each other by :

$$V_o \, \partial S_1(k,r)/\partial r = 2 \, \omega \mu \, H_\theta(0,r)/k - V_o \, k_r^2 \, S_r(k,r)/k \qquad (2.7.4)$$

$$V_o \, \partial S_r(k,r)/\partial r = 2 \, E_z(0,r) - V_o \, S_r(k,r)/r - k \, V_o \, S_1(k,r) \qquad (2.7.5)$$

$$V_o \, S_m(k,r) = \frac{2}{k} \frac{c}{k_o} \, \mu \, H_\theta(0,r) - \frac{1}{k} \, V_o \, S_r(k,r) \qquad (2.7.6)$$

Numerical values of the S-coefficients (with $k = \omega/\dot{z}_o$) may be found by numerical integration of the defining integrals. Regarding the cell as a closed cavity, a common definition for $S_1(k,r)$ is instead of (1) :

$$S_1(r) = 2 \int_0^{L/2} E_z(z,r) \sin\frac{2\pi z}{L} \, dz \Bigg/ \int_{-L/2}^{L/2} E_z(z,0) \, dz \qquad (2.7.7)$$

and similarly for the other two S-coefficients.*) It is expected that then the relations (4) to (6) are no longer exactly fulfilled, but that they represent a good approximation. For the evaluation of the radial derivatives of the S-coefficients (4) and (5) may be useful since they permit to circumvent the need of radial derivatives of the fields.

The S-coefficients do not exhibit such a simple dependence on r comparable to that of the T-coefficients. With $\bar{\bar{C}}$ as the path of integration in the k_z-plane (Fig. 2.7.1) it is possible to integrate with respect to z and evaluate the integrals in k_z in the same way as the field expression in the case $|z| < p/2$. This gives :

$$\begin{aligned} S_1(k,r) = & - T_o(k) \operatorname{ctg}(kp/2) \, I_o(k_r r) \\ & + \frac{J_o(k_o r)}{pk/2} - 4 \, J_o(k_o a) \sum_{n=1}^{\infty} \frac{pk \, B_n}{(2\pi n)^2 - (kp)^2} \frac{I_o(\mu_n r/p)}{I_o(\mu_n a/p)} \qquad (2.7.8) \\ & - 8 \, J_o(k_o a) \, (kp) \left(\frac{p}{a}\right)^2 \sum_{n=0}^{\infty} \frac{B_n (-1)^n}{1 + \delta_{no}} \sum_{v=1}^{\infty} \frac{J_o(j_v r/a)}{J_1(j_v)} \frac{\exp(-\eta_v p/2)}{(kp)^2 + (\eta_v p)^2} \frac{j_v}{(2\pi n)^2 + (\eta_v p)^2} \end{aligned}$$

with

$$\mu_n = \left[(2\pi n)^2 - (k_o p)^2 \right]^{\frac{1}{2}} \qquad (2.5.4)$$

and

$$\eta_v p = \left[(j_v p/a)^2 - (k_o p)^2 \right]^{\frac{1}{2}} \qquad (2.5.1)$$

---

*) $S_1(k,r) = S_1(r) + (k - 2\pi/L) \, S_1'(r) + \frac{1}{2} (k - 2\pi/L)^2 \, S_1''(r) + \ldots$

The expression in the first line of (8) may be rewritten as :

$$- T_1(k,r)\ \mathrm{ctg}(kp/2)$$

Equation (8) is rewritten in a different notation suitable for displaying numerical results:

$$\begin{aligned} S_1(r) &= S_{1m}(r) \\ &+ S_{1o}(r) + \sum_{n=1}^{\infty} S_{1n}(r) \\ &+ S_{1r}(r) \end{aligned} \qquad (2.7.8a)$$

$k = \omega/\dot{z}_o$ is taken from eq.(2.6.13)and is no longer indicated.

The series for the radial S-coefficient:

$$\begin{aligned} S_r(k,r) = {} & T_o(k)\ \mathrm{ctg}(kp/2)\ \frac{k}{k_r}\ I_1(k_r r) \\ & + 4\ J_o(k_o a) \sum_{n=1}^{\infty} \frac{B_n\ (2\pi n)^2}{(2\pi n)^2 - (kp)^2}\ \frac{1}{\mu_n}\ \frac{I_1(\mu_n r/p)}{I_o(\mu_n a/p)} \\ & - 8\ J_o(k_o a)\ \frac{p}{a} \sum_{n=0}^{\infty} \frac{B_n(-1)^n}{1+\delta_{no}} \sum_{v=1}^{\infty} \frac{J_1(j_v r/a)}{J_1(j_v)}\ \frac{\exp(-\eta_v p/2)}{(kp)^2 + (\eta_v p)^2}\ \frac{(\eta_v p)^2}{(kp)^2 + (\eta_v p)^2} \end{aligned} \qquad (2.7.9)$$

where the first line equals :

$$T_r(k,r)\ \mathrm{ctg}(kp/2),$$

is written in the same way as:

$$\begin{aligned} S_r(r) &= S_{rm}(r) \\ &+ \sum_{n=1}^{\infty} S_{rn}(r) \\ &+ S_{rr}(r) \end{aligned} \qquad (2.7.9a)$$

The magnetic S-coefficient is :

$$\begin{aligned} \frac{1}{p}\ S_m(k,r) = {} & - T_o(k)\ \mathrm{ctg}(kp/2)\ \frac{1}{k_r p}\ I_1(k_r r) \\ & + \frac{1}{kp/2}\ \frac{J_o(k_o r)}{k_o p} - 4\ J_o(k_o a)\ kp \sum_{n=1}^{\infty} \frac{B_n}{(2\pi n)^2 - (kp)^2}\ \frac{1}{\mu_n}\ \frac{I_1(\mu_n r/p)}{I_o(\mu_n a/p)} - \cdots \end{aligned} \qquad (2.7.10)$$

$$- 8\, J_o(k_o a)\, kp\, \frac{p}{a} \sum_{n=0}^{\infty} \frac{B_n (-1)^n}{1 + \delta_{no}} \sum_{\nu=1}^{\infty} \frac{J_1(j_\nu r/a)}{J_1(j_\nu)} \frac{\exp(-\eta_\nu p/2)}{(kp)^2 + (\eta_\nu p)^2} \frac{1}{(2\pi n)^2 + (\eta_\nu p)^2} \qquad (2.7.10)$$

The first term on the right hand side is :

$$- \frac{1}{p} T_m(k,r)\, \mathrm{ctg}(kp/2)$$

A programme has been prepared for the evaluation of the above series for $S_1(k,r)$ and $S_r(k,r)$ and for the derivatives dS_1/dk, $d/dk\ \partial S_1/\partial r$, dS_r/dk, $d/dk\ \partial S_r/\partial r$ for the single value k computed from(2.6.13). The Fourier coefficients, B_n, are found by the method described in Section 2.5. The behaviour of the various terms of these series depends much more sensitively upon the field distribution and the gap geometry, than is the case of the transit time factor, T_o . Therefore tables of results for some of the cavities are given using the notation introduced in equations (8a) and (9a). For sake of comparison the values of the beam dynamics coefficients computed by numerical integration are also given as well as the partial sums when only contributions due to the first three Fourier coefficients are retained, (S_{1a2}, S_{ra2}) . S_r/r is given since S_r behaves linearly for not too great r.

In the derivatives some terms show striking similarities with corresponding terms in S_1 and S_r . They have the same order of magnitude as their counterparts, often almost the same value. These correspondences are summarized in the following equations where the notations of equations (8a) and(9a) are used :

$$k\, dS_{1n}/dk \sim S_{1n} \qquad (a)$$

$$d/dk\ \partial S_{1n}/\partial r \sim -S_{rn} \qquad (b)$$

$$k\, dS_{rn}/dk \sim S_{rn}\ (1/3 - 1/100) \qquad (c) \qquad (2.7.11)$$

$$d/dk\ \partial S_{rn}/\partial r \sim -S_{1n} \qquad (d)$$

The sign $\sim$ in the above relations means that the expressions on both sides are of about the same order of magnitude. $k\, dS_{rn}/dk$ is smaller than S_{rn} and this is indicated by the numerical factor included in the bracket.

The following conclusions can be drawn. The terms S_{1m} , S_{rm} containing the transit time factor are almost always important, as well as their derivatives in dS_1/dk, $d/dk\ \partial S_1/\partial r$,.... The same can be said about S_{1o} . The magnitude of the terms S_{1n} , S_{rn} (and similarly that of their derivatives) generally decreases with increasing n. However, this decrease is less pronounced for higher energies. At low energy only the first, say two or three Fourier coefficients, B_n , are important. In the CERN 3 MeV experimental linac cavities (e.g. MARTINI 51415) the terms of type S_{1n} and S_{rn} are small due to the good uniformity of the field.

While the double series S_{lr} and S_{rr} are small in the KATZ and MURA cavities, they are not completely negligible in the 3 MeV linac cavities. There it may be even necessary to retain two terms of the series in v which exponentially decreases with increasing v. The convergence with respect to this index depends quite sensitively upon the ratio $p/a = (g + 2R_i)/a$.

In conclusion it can be said that at low energy only the first few harmonics of the field $E_z^a(z) = E_z(z,r=a)$ applied along the gap circumference, eq. (2.4.5) determine the behaviour of the beam dynamics coefficients. With increasing energy more and more harmonics become of equal importance in the S-coefficients. However, in the beam dynamics equations these coefficients are multiplied by ratios like eV_o/W(W = kinetic energy) and the contributions as a whole become increasingly smaller. For many applications it may suffice to use besides S_{lm} or S_{rm} the parts of the above expressions which contain the first two or three Fourier coefficients. Still the arising formulae are lengthy and the computation of derivatives is tedious. It is annoying that these simple (and in most cases monotonous) functions of r are given by such frightening expressions.

2.7.A Derivation of Relations Connecting the S-coefficients

These relations are found by expressing the fields by the Hertz potential $V(z,r)$ (equations (2.2.5) and (2.2.11) to 2.2.13)) and by partial integrations. Use is also made of the fact that all fields vanish at $|z| = \infty$.

Proof of (4):

$$V_o S_1(k,r) = 2 \int_o^\infty E_z(z,r) \sin(kz)\, dz = 2 \int_o^\infty \sin(kz)(k_o^2 + \partial^2/\partial z^2)\, V(z,r)\, dz$$

$$= - 2 \frac{k_o^2}{k} \cos(kz)\, V \Big|_{z=o}^{z=\infty} + 2 \frac{k_o^2}{k} \int_o^\infty \frac{\partial V}{\partial z} \cos(kz)\, dz \qquad (2.7.12)$$

$$+ 2 \frac{\partial V}{\partial z} \sin(kz) \Big|_{z=o}^{z=\infty} - 2 k \int_o^\infty \frac{\partial V}{\partial z} \cos(kz)\, dz$$

$$= 2 \frac{k_o^2}{k} V(0,r) - 2 k \left(1 - \frac{k_o^2}{k^2}\right) \int_o^\infty \frac{\partial V(z,r)}{\partial z} \cos(kz)\, dz$$

$$V_o\, \partial S_1(k,r)/\partial r = 2 k_o^2/k\, \partial V(0,r)/\partial r - 2 k_r^2/k \int_o^\infty \partial^2 V(z,r)/\partial r \partial z \cos(kz)\, dz$$

$$= 2 k\omega \mu H_\theta(0,r) - k_r^2/k\, V_o S_r(k,r) \qquad (2.7.12a)$$

When deriving the above formula with respect to k, the ω contained in the first term must be regarded as a constant independent of k.

Proof of (5) :

$$V_o\, \partial S_r(k,r)/\partial r + V_o S_r(k,r)/r = 2 \int_o^\infty \frac{\partial}{\partial z} \left(\frac{\partial^2 V(z,r)}{\partial r^2} + \frac{1}{r} \frac{\partial V}{\partial r}\right) \cos(kz)\, dz$$

$$= -2 \int_o^\infty \frac{\partial E_z(z,r)}{\partial z} \cos(kz)\, dz \qquad (2.7.13)$$

$$= -2 E_z \cos(kz) \Big|_{z=o}^{z=\infty} - 2 k \int_o^\infty E_z(z,r) \sin(kz)\, dz$$

$$= 2 E_z(0,r) - k V_o S_1(k,r)$$

r(cm)	r/a	S_{1m}	S_{10}	S_{11}	S_{12}	S_{13}	S_{14}	$\sum_{n=5}^{N-1} S_{1n}$	S_{1r}	S_{1a2}	S_1	S_{1w}	S_{1c}
KATZ 15141		.644 MeV											
.000	.000	.0067	.6327	-.0965	.0010	.0000	.0000	.0000	-.0005	.5434	.5434	.5421	
.120	.161	.0067	.6327	-.0983	.0011	.0000	.0000	.0000	.0005	.5417	.5417	.5405	
.239	.322	.0068	.6327	-.1038	.0013	.0000	.0000	.0000	.0004	.5366	.5366	.5353	
.359	.484	.0070	.6327	-.1133	.0018	.0000	.0000	.0000	.0003	.5278	.5278	.5264	
.479	.645	.0072	.6326	-.1273	.0025	.0000	.0000	.0000	.0002	.5149	.5149	.5134	
.599	.806	.0075	.6326	-.1466	.0038	.0000	.0000	.0000	.0001	.4972	.4972	.4956	
.718	.967	.0079	.6326	-.1724	.0060	.0001	-.0001	.0000	.0000	.4740	.4740	.4721	
KATZ 15034		7.981 MeV											
.000	.000	-.2959	.8254	-.0322	.0026	-.0003	.0001	-.0000	.0000	.5011	.4996	.4990	.4914
.253	.200	-.2964	.8254	-.0326	.0027	-.0004	.0001	-.0000	.0000	.5004	.4987	.4982	.4971
.506	.400	-.2979	.8253	-.0337	.0030	-.0005	.0001	-.0000	.0000	.4980	.4963	.4958	.4943
.760	.600	-.3004	.8252	-.0357	.0037	-.0008	.0002	-.0001	.0000	.4942	.4923	.4918	.4901
1.013	.800	-.3039	.8251	-.0385	.0048	-.0012	.0004	-.0002	.0000	.4888	.4866	.4860	.4690
1.266	1.000	-.3085	.8249	-.0422	.0065	-.0021	.0009	-.0005	.0000	.4819	.4791	.4796	
MARTINI 51415		2.395 MeV.											
.000	.000	-.5584	1.0697	-.0038	.0001	.0000	.0000	.0000	-.0082	.5003	.4994	.4942	.4967
.151	.115	-.5595	1.0697	-.0039	.0001	.0000	.0000	.0000	-.0080	.4992	.4983	.4931	.4961
.301	.231	-.5629	1.0696	-.0041	.0001	.0000	.0000	.0000	-.0076	.4961	.4952	.4897	.4924
.452	.346	-.5686	1.0696	-.0046	.0002	.0000	.0000	.0000	-.0068	.4907	.4898	.4839	.4867
.603	.462	-.5765	1.0695	-.0053	.0003	.0000	.0000	.0000	-.0059	.4831	.4821	.4756	.4788
.754	.577	-.5868	1.0694	-.0063	.0005	-.0001	.0000	.0000	-.0047	.4731	.4720	.4646	
.904	.692	-.5996	1.0693	-.0076	.0008	-.0001	.0000	.0000	-.0034	.4605	.4594	.4503	
1.055	.808	-.6148	1.0691	-.0093	.0013	-.0003	.0001	.0000	-.0021	.4453	.4440	.4319	
1.206	.923	-.6326	1.0690	-.0117	.0022	-.0007	.0002	-.0001	-.0008	.4272	.4256	.4062	

Table 2.7.1. Longitudinal S-coefficients for various cavities. S_{1a2} is the sum of the contributions due to the first three Fourier coefficients. (Note that this also influences the value of S_{1m}.) S_1 is the sum of the whole series. S_{1w} has been found by numerical integration of the fields derived in Sect. 2.5 (wave guide fields); S_{1c} is found by the usual interpolation of fields found by mesh calculations (cavity fields).

r(cm)	r/a	S_{1m}	S_{10}	S_{11}	S_{12}	S_{13}	S_{14}	$\sum_{n=5}^{N-1} S_{1n}$	S_{1r}	S_{1a2}	S_1	S_{1w}	S_{1c}
MURA (MARTINI)		31335	5.469 MeV										
.000	.000	-.2631	.7938	-.0708	.0040	-.0003	.0000	0	0	.4644	.4636	.4630	.4641
.160	.160	-.2634	.7938	-.0712	.0041	-.0003	.0000	0	0	.4639	.4630	.4623	.4635
.321	.321	-.2642	.7938	-.0725	.0044	-.0004	.0000	0	0	.4620	.4611	.4605	
.481	.481	-.2655	.7937	-.0747	.0049	-.0005	.0001	0	0	.4590	.4580	.4574	
.642	.642	-.2673	.7937	-.0779	.0057	-.0007	.0001	0	0	.4548	.4536	.4530	
.802	.802	-.2696	.7936	-.0821	.0069	-.0010	.0001	0	0	.4493	.4480	.4473	
.963	.962	-.2725	.7935	-.0873	.0084	-.0014	.0002	0	0	.4426	.4409	.4405	
MURA (MARTINI)		20241	10.863 MeV										
.000	.000	-.2658	.7959	-.0608	.0059	-.0009	.0002	.0000	0	.4761	.4744	.4741	.4745
.173	.173	-.2660	.7959	-.0610	.0060	-.0010	.0002	.0000	0	.4758	.4741	.4739	
.347	.347	-.2664	.7959	-.0617	.0062	-.0010	.0002	.0000	0	.4749	.4731	.4729	
.520	.520	-.2672	.7958	-.0628	.0067	-.0012	.0003	.0000	0	.4734	.4715	.4713	
.694	.694	-.2683	.7957	-.0644	.0074	-.0015	.0003	-.0001	0	.4714	.4692	.4690	
.867	.867	-.2696	.7956	-.0665	.0083	-.0019	.0005	-.0001	0	.4687	.4663	.4661	
MURA (MARTINI)		30941	19.463 MeV										
.000	.000	-.3138	.8304	-.0398	.0063	-.0014	.0003	-.0001	0	.4831	.4820	.4818	
.225	.225	-.3140	.8303	-.0399	.0064	-.0014	.0004	-.0001	0	.4830	.4818	.4816	
.450	.450	-.3145	.8303	-.0404	.0067	-.0016	.0004	-.0001	0	.4822	.4809	.4808	
.674	.674	-.3153	.8302	-.0411	.0072	-.0018	.0005	-.0001	0	.4810	.4796	.4794	
.899	.899	-.3165	.8301	-.0422	.0079	-.0022	.0008	-.0002	0	.4793	.4777	.4775	

The geometrical and dynamical parameters of the cavities are given in Table VII.

Table 2.7.1. (continued)

r(cm)	r/a	S_{rm}	S_{r1}	S_{r2}	S_{r3}	S_{r4}	$\sum_{n=5}^{N-1} S_{rn}$	S_{rr}	S_{ra2}	S_r	S_{rw}	S_{rc}	S_r/r
KATZ	15141	.644 MeV											
.120	.161	-.0005	.0264	-.0011	-.0000	.0000	-.0000	-.0003	.0245	.0245	.0246	.0240	.2047
.239	.322	-.0009	.0542	-.0025	-.0000	.0000	-.0000	-.0005	.0503	.0503	.0504	.0497	.2100
.359	.484	-.0014	.0850	-.0044	-.0001	.0000	-.0000	-.0007	.0786	.0786	.0787	.0777	.2187
.479	.645	-.0019	.1207	-.0073	-.0001	.0001	-.0000	-.0008	.1107	.1107	.1108	.1096	.2311
.599	.806	-.0024	.1632	-.0120	-.0002	.0003	-.0001	-.0008	.1479	.1480	.1480	.1466	.2473
.718	.967	-.0030	.2150	-.0197	-.0004	.0009	-.0002	-.0008	.1916	.1919	.1918		.2672
KATZ	15034	7.981 MeV											
.253	.200	.0123	.0090	-.0029	.0009	-.0003	.0001	-.0000	.0183	.0191	.0191	.0190	.0753
.506	.400	.0246	.0184	-.0062	.0022	-.0007	.0002	-.0000	.0366	.0383	.0383	.0384	.0757
.760	.600	.0371	.0284	-.0104	.0041	-.0016	.0005	-.0001	.0548	.0579	.0578	.0579	.0762
1.013	.800	.0497	.0393	-.0161	.0074	-.0036	.0012	-.0001	.0726	.0779	.0778	.0781	.0769
1.266	1.000	.0626	.0517	-.0241	.0132	-.0078	.0029	-.0001	.0898	.0985	.0989		.0778
MARTINI	51415	2.395 MeV											
.151	.115	.0251	19	-.0002	.0000	-.0000	.0000	.0034	.0233	.0235	.0234	.0236	.1557
.301	.231	.0504	40	-.0005	.0000	-.0000	.0000	.0067	.0471	.0473	.0472	.0478	.1571
.452	.346	.0760	64	-.0008	.0001	-.0000	.0000	.0095	.0717	.0721	.0718	.0729	.1594
.603	.462	.1020	92	-.0015	.0002	-.0000	.0000	.0119	.0974	.0980	.0976	.0992	.1626
.754	.577	.1287	126	-.0025	.0005	-.0001	.0000	.0136	.1252	.1256	.1249		.1667
.904	.692	.1561	169	-.0043	.0011	-.0003	.0001	.0145	.1536	.1551	.1539		.1715
1.055	.808	.1845	225	-.0075	.0026	-.0009	.0002	.0147	.1842	.1867	.1844		.1770
1.206	.923	.2140	296	-.0130	.0060	-.0029	.0009	.0140	.2160	.2207	.2148		.1830

Table 2.7.2. Radial S-coefficients for various cavities. S_{ra2} is the sum of the contributions due to the first three Fourier coefficients. (Note that this also changes the value of S_{rm}). S_r is the sum of the whole series. S_{rw} has been found by numerical integration of the fields derived in Section 2.5. (wave guide fields); S_{rc} is found by the usual interpolation of fields found by mesh calculations (cavity fields).

r(cm)	r/a	S_{rm}		S_{r1}	S_{r2}	S_{r3}	S_{r4}	$\sum_{n=5}^{N-1} S_{rn}$	S_{rr}	S_{ra2}	S_r	S_{rw}	S_{rc}	S_r/r
MURA (MARTINI)		31335		5.469 MeV										
.160	.160	.0083		.0139	-.0032	.0006	-.0001	.0000	0	.0190	.0195	.0195	.0194	.1217
.321	.321	.0166		.0281	-.0066	.0013	-.0002	.0000	0	.0380	.0392	.0391	.0389	.1221
.481	.481	.0250		.0427	-.0105	.0022	-.0004	.0000	0	.0571	.0591	.0590	.0587	.1227
.642	.642	.0334		.0582	-.0152	.0035	-.0006	.0001	0	.0763	.0793	.0792	.0788	.1236
.802	.802	.0419		.0747	-.0210	.0054	-.0012	.0002	0	.0955	.1000	.0999		.1217
.963	.962	.0506		.0927	-.0285	.0082	-.0020	.0004	0	.1147	.1214	.1211		.1261
MURA (MARTINI)		20241		10.863 MeV										
.173	.173	.0064		.0092	-.0036	.0013	-.0004	.0001	0	.0121	.0131	.0130	.0125	.0753
.347	.347	.0129		.0185	-.0074	.0027	-.0009	.0002	0	.0240	.0261	.0261	.0250	.0753
.520	.520	.0194		.0281	-.0114	.0043	-.0015	.0004	0	.0359	.0393	.0392		.0755
.694	.694	.0259		.0379	-.0160	.0065	-.0024	.0008	0	.0477	.0526	.0524		.0758
.867	.867	.0324		.0482	-.0213	.0092	-.0037	.0013	0	.0592	.0661	.0658		.0762
MURA (MARTINI)		30941		19.463 MeV										
.225	.225	.0074		.0064	-.0041	.0020	-.0009	.0000	0	.0097	.0112	.0111		.0497
.450	.450	.0148		.0128	-.0083	.0042	-.0019	.0001	0	.0192	.0224	.0221		.0498
.674	.674	.0222		.0194	-.0130	.0068	-.0034	.0001	0	.0286	.0337	.0332		.0500
.899	.899	.0297		.0262	-.0182	.0102	-.0054	.0001	0	.0376	.0452	.0443		.0503

Table 2.7.2. (continued)

Proof of (6):

$$V_o\, S_m(k,r) = -\,2\,\frac{c}{k_o}\int_o^\infty \mu H_\theta(z,r)\,\sin(kz)\,dz = -\,2\,\frac{c}{k_o}\,\varepsilon\mu\omega\int_o^\infty \frac{\partial V(z,r)}{\partial r}\,\sin(kz)\,dz$$

$$= 2\,\frac{c}{k_o}\,\frac{\varepsilon\omega\mu}{k}\,\cos(kz)\,\frac{\partial V}{\partial r}\Bigg|_{z=o}^{z=\infty} - 2\frac{c}{k_o}\,\frac{\varepsilon\omega\mu}{k}\int_o^\infty \frac{\partial^2 V}{\partial z\partial r}\,\cos(kz)\,dz \qquad (2.7.14)$$

$$= \frac{2}{k}\,\frac{c}{k_o}\,\mu H_\theta(0,r) - \frac{1}{k}\,V_o\,S_r(k,r)$$

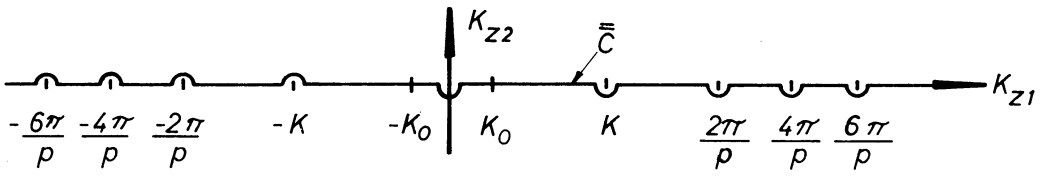

Fig. 2.7.1 The contour $\bar{\bar{C}}$. It is indented at $k_z = \pm k$ and at $k_z = \pm 2\pi n/p$, $n = 0,1,2,\ldots$

2.7.B Series Expansions for the S-coefficients

At first the integral representation (2.2.11) and the contour $\hat{C}$ (see Fig. 2.2.1) are used :

$$V_o\, S_1(k,r) = 2 \lim_{\ell\to\infty} \int_0^{\ell} E_z(z,r)\, \sin(kz)\, dz$$

$$= -i \frac{E_1}{2\pi} \lim_{\ell\to\infty} \int_0^{\ell} dz \int_{\hat{C}} dk_z\, b(k_z) \left(e^{iz(k_z+k)} - e^{iz(k_z-k)} \right) J_o(\gamma r)/J_o(\gamma a)$$

$$= -i \frac{E}{2\pi} \lim_{\ell\to\infty} \int_{\hat{C}} dk_z \left[\frac{e^{i\ell(k_z+k)} - 1}{i(k_z+k)} - \frac{e^{i\ell(k_z-k)} - 1}{i(k_z-k)} \right] b(k_z)\, J_o(\gamma r)/J_o(\gamma a)$$

The integrals containing $e^{i\ell(k_z \pm k)}$ are evaluated in the same way as those for the T-coefficients : $\hat{C}$ and C_U make up a closed contour and, in the limit $\ell \to \infty$, the contributions of all poles enclosed vanish except that arising from $k_z = +k$:

$$V_o\, S_1(k,r) = i\, E_1 b(k) \frac{I_o(k_r r)}{I_o(k_r a)} + \frac{E_1}{2\pi} \int_{\hat{C}} dk_z \left[\frac{1}{k_z + k} - \frac{1}{k_z - k} \right] b(k_z) \frac{J_o(\gamma r)}{J_o(\gamma a)}$$

$$= i\, V_o\, T_1(k,r) \quad + \ldots \qquad (2.7.15)$$

Now the contour $\hat{C}$ is changed into $\bar{\bar{C}}$ (Fig. 2.7.1) and $b(k_z)$ decomposed afterwards into $b(k_z) = b_+(k_z) + b_-(k_z)$ (cf.(2.4.10)). For b_+, b_- respectively, the integral along C_U (C_L) is again zero, see (2.4.11) and (2.4.24). The integral which has been left in (15) is $2\pi i$ times the sum of residues due to the poles enclosed $k_z = \pm k$, $\pm i\eta_\nu$, 0, $\pm 2\pi n/p$ ($n = 1,2,\ldots$) :

$$(V_o/E_1)\, S_1(k,r) - i\, b(k)\, I_o(k_r r)/I_o(k_r a) =$$

$$= (-i\, b_+(k) - i\, b_-(-k))\; I_o(k_r r)/I_o(k_r a)$$

$$+i \sum_{\nu=1}^{\infty} \frac{J_o(j_\nu r/a)}{J_1(j_\nu) a^2/j_\nu} \left[\frac{b_+(i\eta_\nu)}{i\eta_\nu} \left(\frac{1}{i\eta_\nu + k} - \frac{1}{i\eta_\nu + k} \right) - \frac{b_-(-i\eta_\nu)}{-i\eta_\nu} \left(\frac{1}{-i\eta_\nu + k} - \frac{1}{-i\eta_\nu - k} \right) \right]$$

$$+i\, 2\, B_o\, i^{-1}/k \;\; J_o(k_o r)/(J_o(k_o a))$$

$$+ \sum_{n=1}^{\infty} \frac{I_o(\mu_n r/p)}{I_o(\mu_n a/p)} \; B_n \left[\frac{1}{2\pi n/p + k} - \frac{1}{2\pi n/p - k} + \frac{1}{-2\pi n/p + k} - \frac{1}{-2\pi n/p - k} \right]$$

In the last two lines the residues (2.4.12) have been used. From (2.4.6) and (2.4.10) it is found :

$$i\left[b(k) - b_+(k) - b_-(-k)\right] = \sum_{s=\infty}^{-\infty} B_s(-1)^s\,(k-2\pi s/p)^{-1}\left[2i\,\sin(kp/2) - 2\,e^{ikp/2}\right]$$

$$= -\,b(k)\,\mathrm{ctg}(kp/2) \qquad = -\sum_{s=\infty}^{-\infty} B_s(-1)^s\,(k-2\pi ns/p)^{-1}\,2\,\cos(kp/2)$$

$$\text{(Note: } b_-(-k)\,\exp(-ikp/2) = i\sum_{s=\infty}^{-\infty} B_s(-1)^s(-k-2\pi s/p)^{-1} = -i\sum_{s=\infty}^{-\infty} B_s(-1)^s(k+2\pi s/p)^{-1}$$

$$= -i\sum_{s=\infty}^{-\infty} B_s(-1)^s\,(k-2\pi s/p)^{-1}\ )$$

All this together with equations (2.6.2) gives the series (8).

Similarly, for the radial S-coefficient :

$$V_o\,S_r(k,r) = -i\,\frac{E_1}{2\pi}\lim_{\ell\to\infty}\int_{\hat{C}} dk_z\left[\frac{e^{i\ell(k_z+k)}-1}{i(k_z+k)} + \frac{e^{i\ell(k_z-k)}-1}{i(k_z-k)}\right] b(k_z)\,\frac{k_z\,J_1(\gamma r)}{\gamma J_o(\gamma a)}$$

$$= -i\,E_1\,b(k)\,\frac{k\,I_1(k_r r)}{k_r\,I_o(k_r a)} + \frac{E_1}{2\pi}\int_{\hat{C}} dk_z\left[\frac{1}{k_z+k} + \frac{1}{k_z-k}\right] b(k_z)\,\frac{k_z\,J_1(\gamma r)}{\gamma\,J_o(\gamma a)}$$

$$= -i\,V_o\,T_r(k,r) \qquad + \quad \ldots \qquad (2.7.16)$$

The remaining integral is treated by the method already described after equation (15), and this finally yields the series (8).

Finally, the same method gives for the magnetic S-coefficient :

$$V_o\,S_m(k,r) = i\,V_o\,T_m(k,r) + \frac{E_1}{2\pi}\int_{\hat{C}} dk_z\left[\frac{1}{k_z+k} - \frac{1}{k-k_z}\right] b(k_z)\,\frac{J_1(\gamma r)}{\gamma J_o(\gamma a)}$$

(2.7.17)

and thereafter the series 2.7.10.

2.8 Series Expansions of the Field Starting from the Potential $U = -rH_\theta$.

In Section 2.4 and 2.5 it has been assumed that the field within the drift tube space $r < a$ is excited by the tangential electrical field :

$$E_z^a(z) = 2E_1 \left[1/2 + \sum_{n=1}^{\infty} B_n \cos(2\pi nz/p) \right] \qquad (2.4.5)$$

applied along the circumferential slot $r = a$, $|z| \leq p/2$. On the other hand, numerical methods usually give values of $U = -rH_\theta$ at discrete points. Therefore either these values must be interpolated to give values of the electrical field or, as has been described in Section 2.5, the series for $U = -rH_\theta$ (2.5.7c) derived from eq. (2.4.5) can be used to determine the coefficients B_n by solving a set of linear equations.

Still another approach may be based upon the fact that the electromagnetic field in the interior of a domain is completely determined if the magnetic field in this case H_θ, tangential to the boundary enclosing the domain, is given. This method is simpler than those described before as far as the evaluation of the Fourier coefficients is concerned, since these may be calculated by use of the Bessel formulae, see appendix 2.8A. On the other hand, this method has some drawbacks. Inspection of eq. (2.5.7) or Fig. 2.5.3 reveals that the magnetic field, H_θ, is nonzero along the wall of the drift tube, $r = a$, $|z| \geq p/2$. And experience shows that the contributions due to regions adjacent to the gap ($|z|$ slightly greater than $p/2$) are appreciable and cannot be neglected. Therefore in the present approach a cylinder $0 \leq r \leq \bar{a} < a$ entirely contained in the interior of the drift tube space with a circumferential gap $|z| \leq \bar{p}/2 = L/2$, whose length equals that of the cell, is selected as domain upon which Green's theorem is applied. The model (Fig. 2.8.1.) is an infinitely long circular wave guide of radius $\bar{a}$ in which an electromagnetic field is excited by the boundary field:

$$\begin{aligned} |z| \leq \bar{p}/2: \quad & -rH_\theta(z,\bar{a}) = U(z,\bar{a}) = U^{\bar{a}}(z) = A_o/2 + \sum_{n=1}^{\infty} A_n \cos(2\pi nz/\bar{p}) \\ |z| > \bar{p}/2: \quad & U(z,\bar{a}) = U^{\bar{a}}(z) = 0 \end{aligned} \qquad (2.8.1)$$

$\bar{p}$ instead of cell length L has been used in order to make the derivation slightly more general. But in the present applications $\bar{p} = L$ is used. The first objection which may be raised is the fact that the field $U(z,\bar{a})$ is cut away at $|z| = L/2$ where it begins to grow again. But coupling between different cavities is small and consequently the aforementioned approximation is not so serious. This is confirmed by the results of field comparisons. A more serious point is the fact that $kL - 2\pi$, a quantity which appears in the denominators of some terms of the series expressions of the transit time factor and of the S-coefficients, is very small. Care of this must be taken in computations.

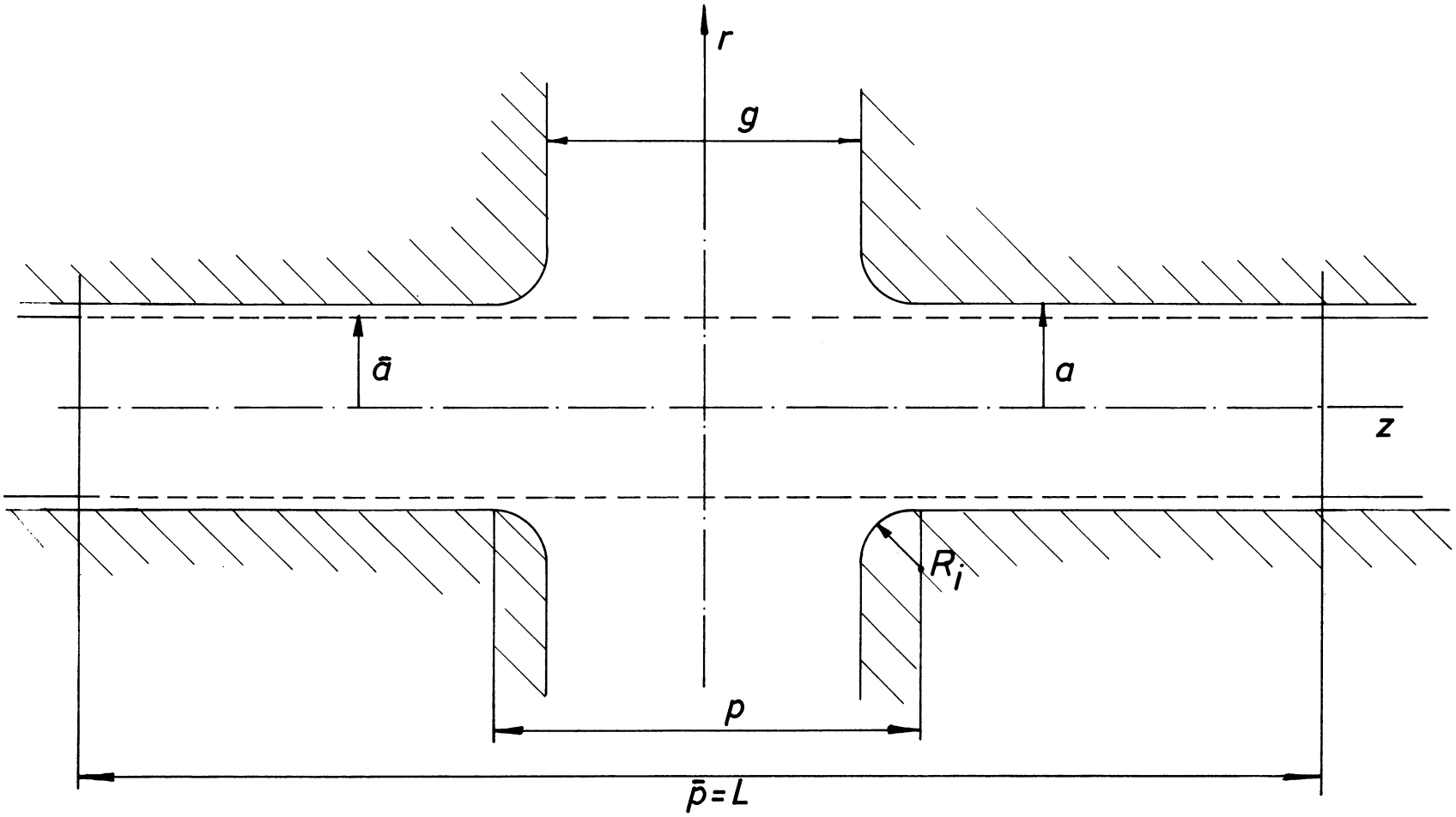

Fig. 2.8.1 Configuration for excitation of electromagnetic field by the boundary field $U(z,r=\bar{a}) = -\bar{a}\,H_\theta$. It consists of a wave guide of radius $\bar{a} < a$ with a slot $-L/2 = -\bar{p}/2 \leq z \leq \bar{p}/2 = L/2$ along which the field $U(z,r=\bar{a})$ is impressed.

The field in the interior as a functional of the boundary field, $\bar{U}^{\bar{a}}(z) = U(z,\bar{a})$ is found with the help of a Green's function, cf. eq. (23) :

$$U(z,r) = \frac{r}{\bar{a}} \frac{1}{2\pi} \int_{-\infty}^{\infty} d\bar{z} \int_{-\infty}^{\infty} dk_z \, e^{ik_z(z-\bar{z})} U^{\bar{a}}(\bar{z}) \, J_1(\gamma r)/J_1(\gamma \bar{a})$$

Inserting $U^{\bar{a}}(z)$ of (1) and performing the integration with respect to $\bar{z}$ gives:

$$- rH_\theta(z,r) = U(z,r) = \frac{r}{\bar{a}} \frac{1}{2\pi} \int_{-\infty}^{\infty} dk_z \, a(k_z) \, e^{ik_z z} \, J_1(\gamma r)/J_1(\gamma \bar{a}) \qquad (2.8.2)$$

with :

$$\gamma = (k_o^2 - k_z^2)^{\frac{1}{2}}$$

and :

$$a(k_z) = a(-k_z) = \sin(k_z p/2) \sum_{s=\infty}^{-\infty} A_s \, (-1)^s \, (k_z - 2\pi s/p)^{-1} \qquad (2.8.3)$$

$$= - 2p \, (k_z p) \sin(k_z p/2) \sum_{n=o}^{\infty} \frac{A_n \, (-1)^n}{1 + \delta_{no}} \frac{1}{(2\pi n)^2 - (k_z p)^2}$$

The longitudinal electrical field is found from (2) with the help of (2.3.4) :

$$E_z(z,r) = \frac{1}{\omega \varepsilon \bar{a}} \frac{1}{2\pi} \int_{-\infty}^{\infty} dk_z \, a(k_z) \, e^{ik_z z} \, \gamma J_o(\gamma r)/J_1(\gamma \bar{a}) \qquad (2.8.4)$$

The integrals (2) and (4) have simple poles at :

$$J_1(\gamma a) = J_1(j_\nu') = 0: \qquad k_z = \pm i\eta_\nu' = \pm i \left[(j_\nu'/\bar{a})^2 - k_o^2 \right]^{\frac{1}{2}} \qquad (2.8.5)$$

They can be evaluated by use of Cauchy's residue theorem as described in sections 2.5, 2.5A, 2.5B. If $z > \bar{p}/2$ ($z < -\bar{p}/2$) then the path of integrations is completed by a semicircle of infinite radius C_U (C_L , Fig. 2.2.1) and the integral equals the infinite sum of the residues enclosed. If $|z| < \bar{p}/2$ then the path of integration in the k_z-plane must be deformed into $\tilde{C}$ (cf. Fig. 2.5.1, where, however, for the present application p must be replaced by $\bar{p}$), $a(k_z)$ decomposed into the exponentials and $\tilde{C}$ completed by C_U, C_L resp. This gives an additional chain of simple poles at $k_z = \pm 2\pi n/\bar{p}$, n = o,1,2,... . The result of these calculations is the following series :

$|z| \leq \bar{p}/2$: $\quad U(z,r) = - r\, H_\theta(z,r) =$

$$= \frac{r}{\bar{a}}\left[\frac{A_o}{2}\frac{J_1(k_o r)}{J_1(k_o \bar{a})} + \sum_{n=1}^{\infty} A_n \cos(2\pi n\frac{z}{\bar{p}})\frac{I_1(\bar{\mu}_n r/\bar{p})}{I_1(\bar{\mu}_n \bar{a}/\bar{p})}\right. \tag{2.8.6a}$$

$$\left. + 2\left(\frac{\bar{p}}{\bar{a}}\right)^2 \sum_{n=o}^{\infty}\frac{A_n(-1)^n}{1+\delta_{no}} \sum_{v=1}^{\infty}\frac{J_1(j'_v r/\bar{a})}{J_o(j'_v)}\frac{j'_v \cosh(\eta'_v z)}{(\bar{p}\eta'_v)^2 + (2\pi n)^2} e^{-\eta'_v \bar{p}/2}\right]$$

$|z| = \bar{p}/2$: $\quad U(\frac{\bar{p}}{2},r) = - r\, H_\theta(\frac{\bar{p}}{2},r) =$

$$= \frac{r}{2\bar{a}}\left[\frac{A_o}{2}\frac{J_1(k_o r)}{J_1(k_o \bar{a})} + \sum_{n=1}^{\infty} A_n (-1)^n \frac{I_1(\bar{\mu}_n r/\bar{p})}{I_1(\bar{\mu}_n \bar{a}/\bar{p})}\right. \tag{2.8.6b}$$

$$\left. + 2\left(\frac{\bar{p}}{\bar{a}}\right)^2 \sum_{n=o}^{\infty}\frac{A_n(-1)^n}{1+\delta_{no}} \sum_{v=1}^{\infty}\frac{J_1(j'_v r/\bar{a})}{J_o(j'_v)}\frac{j'_v\, e^{-\eta'_v \bar{p}}}{(\bar{p}\eta'_v)^2 + (2\pi n)^2} + \delta_{\bar{a}r}\,\bar{D}\right]$$

$$\delta_{\bar{a}r} = \begin{cases} 1 & \bar{a}=r \\ 0 & \bar{a}\neq r \end{cases} \qquad \bar{D} = \sum_{n=o}^{\infty} A_n(-1)^n/(1+\delta_{no})$$

$(|z| \geq p/2:)$ $\quad U(z,r) = - r\, H_\theta(z,r) =$ (2.8.6c)

$$= -2\left(\frac{\bar{p}}{\bar{a}}\right)^2 \frac{r}{\bar{a}} \sum_{n=o}^{\infty}\frac{A_n(-1)^n}{1+\delta_{no}} \sum_{v=1}^{\infty}\frac{J_1(j'_v r/\bar{a})}{J_o(j'_v)}\frac{j'_v \sinh(\eta'_v \bar{p}/2)}{(\eta'_v \bar{p})^2 + (2\pi n)^2} e^{-\eta'_v |z|}$$

with

$$\mu_n = \left[(2\pi n)^2 - (k_o \bar{p})^2\right]^{\frac{1}{2}} \tag{2.8.7}$$

The expressions for the electrical field may be derived according to eqs. (2.3.4) and (2.3.5):

$|z| \leq \bar{p}/2$: $\quad \omega\varepsilon\bar{a}\bar{p}\; E_z(z,r) =$

$$= \frac{A_o}{2} k_o \bar{p}\,\frac{J_o(k_o r)}{J_1(k_o \bar{a})} + \sum_{n=1}^{\infty} A_n \cos(2\pi n\frac{z}{\bar{p}})\,\bar{\mu}_n \frac{I_o(\bar{\mu}_n r/\bar{p})}{I_1(\bar{\mu}_n \bar{a}/\bar{p})} \tag{2.8.8a}$$

$$+ 2\left(\frac{\bar{p}}{\bar{a}}\right)^3 \sum_{n=o}^{\infty}\frac{A_n(-1)^n}{1+\delta_{no}} \sum_{v=1}^{\infty}\frac{J_o(j'_v r/\bar{a})}{J_o(j'_v)}\frac{j'^2_v \cosh(\eta'_v z)}{(\eta'_v \bar{p})^2 + (2\pi n)^2} e^{-\eta'_v \bar{p}/2}$$

$$|z| = \bar{p}/2 \qquad 2 \quad \omega\varepsilon\bar{a}\bar{p}\ E_z(z,r) =$$

$$= \frac{A_o}{2}\ k_o p\ \frac{J_o(k_o r)}{J_1(k_o a)} + \sum_{n=1}^{\infty} A_n(-1)^n\ \bar{\mu}_n\ \frac{I_o(\bar{\mu}_n r/\bar{p})}{I_1(\bar{\mu}_n \bar{a}/\bar{p})} \qquad (2.8.8b)$$

$$+ 2\left(\frac{\bar{p}}{\bar{a}}\right)^3 \sum_{n=o}^{\infty} \frac{A_n(-1)^n}{1+\delta_{no}} \sum_{v=1}^{\infty} \frac{J_o(j'_v r/\bar{a})}{J_o(j'_v)}\ \frac{j'^2_v\ e^{-\eta'_v \bar{p}}}{(\eta'_v \bar{p})^2 + (2\pi n)^2}$$

$$(|z| \geq p/2:) \qquad E_z(z,r) = \qquad (2.8.8c)$$

$$-\frac{2}{\varepsilon\omega\bar{a}^2}\left(\frac{\bar{p}}{\bar{a}}\right)^2 \sum_{n=o}^{\infty} \frac{A_n(-1)^n}{1+\delta_{no}} \sum_{v=1}^{\infty} \frac{J_o(j'_v r/\bar{a})}{J_o(j'_v)}\ \frac{j'^2_v\ \sinh(\eta'_v \bar{p}/2)}{(\eta'_v \bar{p})^2 + (2\pi n)^2}\ e^{-\eta'_v |z|}$$

$$|z| < \bar{p}/2 \qquad \omega\varepsilon\bar{a}\bar{p}\ E_r(z,r) = \qquad (2.8.9a)$$

$$\sum_{n=1}^{\infty} 2\pi n\ A_n \sin(2\pi n \frac{z}{\bar{p}})\ \frac{I_1(\bar{\mu}_n r/\bar{p})}{I_1(\bar{\mu}_n \bar{a}/\bar{p})}$$

$$- 2\left(\frac{\bar{p}}{\bar{a}}\right)^2 \sum_{n=o}^{\infty} \frac{A_n(-1)^n}{1+\delta_{no}} \sum_{v=1}^{\infty} \frac{J_1(j'_v r/\bar{a})}{J_o(j'_v)}\ \frac{j'_v(\eta'_v p)\ \sinh(\eta'_v z)}{(\eta'_v \bar{p})^2 + (2\pi n)^2}\ e^{-\eta'_v p/2}$$

$$\begin{pmatrix} z > \bar{p}/2: \\ z < -p/2: \end{pmatrix} \qquad \omega\varepsilon\bar{a}\bar{p}\ E_r(z,r) = \qquad (2.8.9c)$$

$$= \mp 2\left(\frac{\bar{p}}{\bar{a}}\right)^2 \sum_{n=o}^{\infty} \frac{A_n(-1)^n}{1+\delta_{no}} \sum_{v=1}^{\infty} \frac{J_1(j'_v r/\bar{a})}{J_o(j'_v)}\ \frac{j'_v(\eta'_v \bar{p})\ \sinh(\eta'_v \bar{p}/2)}{(\eta'_v \bar{p})^2 + (2\pi n)^2}\ e^{-\eta'_v |z|}$$

Since in general $\bar{p}/2 = L$, the expressions of type (c) valid for $z > \bar{p}/2$ cannot be used. This has been indicated by bracketing the expressions giving their domain of validity. They are given here for the sake of completeness. If z is rather close to $\bar{p}/2$, then the series in v converge very slowly. The parts exhibiting these unpleasant features can be summed at $\bar{z} = \bar{p}/2$ for U and E_z.

The method has been applied in the following way: In general values of U of the last mesh line within the drift tube space are used to determine N Fourier coefficients A_n with the help of the Bessel formulae, cf. appendix A. N is the number of meshpoints per line. $\bar{a}$ is the radius of this line. Using these Fourier coefficients in formulae (6) the value of U ($\equiv U_C$) can be calculated for any point with $r < \bar{a}$ and is compared with the corresponding mesh value U_m. In the gap, $|z| \leq p/2$, (where $p = g + 2R_i$ is again the gap length as defined in Fig. 2.1.4 and as used in Section 2.5).

U_C/r and U_m/r agree to better than 1% ; for $|z| > p/2$, U_C/r becomes smaller than U_m/r and is only 50% of it at $|\bar{z}| = L/2$. As already explained in Section 2.5 and Fig. 2.5.2, this difference arises from the different boundary conditions at $z = L/2$, U_m being a cavity field and U_C a wave guide field. This discrepancy is not so serious as it appears since these values in the drift tube bore are smaller by several orders of magnitude compared with the values in the gap. The electrical fields, too, have been calculated with the help of (8) and (9). Agreement with the values due to the first approach (Section 2.5) and with those found by interpolation of meshvalues is satisfactory (a few % , in the gap, mostly as good as 1%). Near to $|z| \approx L/2$ the calculated values of E_z and E_r sometimes exhibit spurious oscillations.

In order to simplify the discussion, the method described in Section 2.5 is called the electric approach, the present method the magnetic one. Their degree of complexity is comparable, slightly higher for the electric approach where a system of linear equations must be solved whose degree equals the number of mesh points in the gap. Therefore, a simple interpolation procedure to give the field values appears more advantageous than both approaches. In the electric approach some field values at $|z| \approx p/2$ may be wrong due to insufficient convergence, while field values found by the magnetic approach are inaccurate only in the interior of the drift tube where they are small anyway. For this reason the latter method seems to be better for field calculations. But the Fourier coefficients, B_n , found in the electric approach describe the exciting field at the gap circumference and may be amenable to a physical interpretation which may also favour the understanding of beam dynamics coefficients.

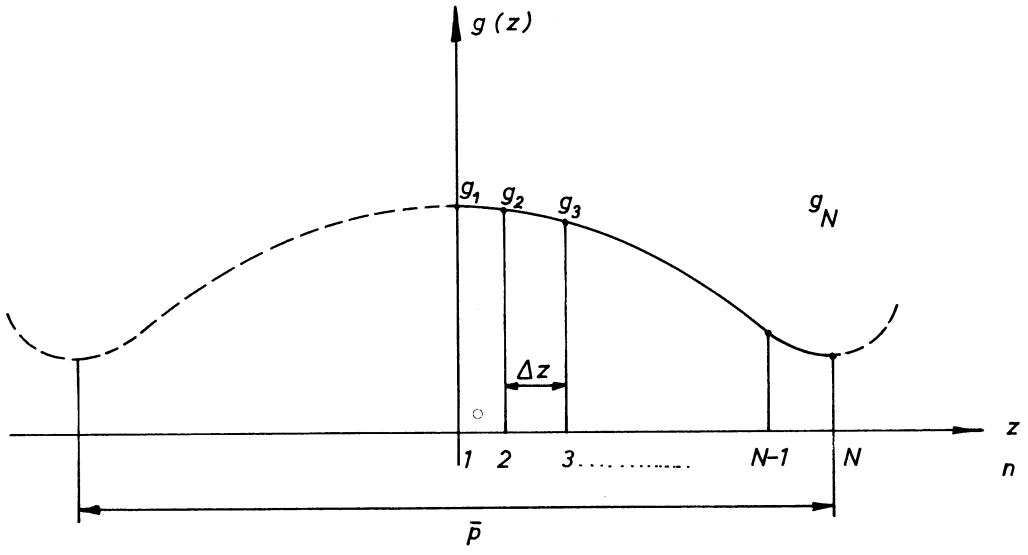

Fig. 2.8.2. Trigonometric interpolation of discrete values $g_1, g_2, \ldots g_N$ given at equidistant points 1, 2, ... N.

2.8.A Bessel Formulae for the Determination of Fourier Coefficients

At N equidistant points 1,2,3, ... N the values g_1, g_2, ... g_N of a periodic and even function are given. The point 1 is the centre of symmetry and the points 1 to N describe half a period of the function, see Fig. 2.8.2. These values can be interpolated by the finite trigonometric sum :

$$g(z) = A_o/2 + \sum_{v=1}^{N-1} A_v \cos(2\pi vz/\bar{p}) \qquad (2.8.10)$$

with period:

$$\bar{p} = 2(N - 1)\Delta z \qquad (2.8.11)$$

Δz is the distance of adjoining points. The Fourier coefficients A_v can be calculated according to the Bessel formula:[28)]

$$A_v = \left[(N-1)(1 + \delta_{v,N-1})\right]^{-1} \left[g_1 + (-1)^v g_N + 2 \sum_{n=2}^{N-1} g_n \cos\left[\pi v(n-1)/(N-1)\right]\right] \qquad (2.8.12)$$

Then the function g(z) assumes the prescribed values :

$$g_s = g((s-1)\,\Delta z) \qquad s = 1,2,\ldots N \qquad (2.8.13)$$

The derivation of (12) is easy[29)]. Inserting $\bar{p} = 2\,(N - 1)\,\Delta z$ and $z = (s - 1)\,\Delta z = \alpha\,\Delta z$, $s = \alpha + 1 = 1,2,\ldots N$ into (10) gives a linear system of equations:

$$g_s = g((s-1)\,\Delta z) = g(\alpha\Delta z) = \sum_{v=o}^{N-1\,''} A_v \cos\left[\pi v\alpha/(N-1)\right] \qquad (2.8.14)$$

The double prime at the summation sign indicates that the first and the last term must be multiplied by $\frac{1}{2}$ (cf. eq. (10) together with (12)). The system (13) is solved with the help of the orthogonality relations:

$$\sum_{\alpha=o}^{N-1\,''} \cos\left[\alpha\mu\pi/(N-1)\right] \cos\left[\alpha v\pi/(N-1)\right] = \tfrac{1}{2}\,(N - 1)\delta_{\mu v}\,(1 + \delta_{v,o} + \delta_{v,N-1}) \qquad (2.8.15)$$

to give (12). The same equation is obtained if the integral for the Fourier coefficients of an even integrable function g(z) :

$$A_v = \frac{2}{\bar{p}} \int_o^{\bar{p}} g(z) \cos(2\pi vz/\bar{p})\, dz$$

is approximately evaluated by the trapezoidal rule.

The programme for the calculation of Fourier coefficients given in ref. [30)] has been adapted for the present case.

2.8.B A second Green's Function of a Wave Guide. Derivation of Eq. (2.8.2)

The Green's function $G_2(z,r;\bar{z},\bar{r})$ is a solution of the inhomogeneous wave equation (2.4.30) obeying the boundary conditions (2.4.33):

$$\lim_{|z|\to\infty} G_2 = 0 \qquad \lim_{|z|\to\infty} \partial G_2/\partial z = 0 \quad (\text{if } \omega < \omega'_{c1}) \tag{2.8.16}$$

In place of (2.4.32) a different condition is prescribed :

$$r = \bar{a} : \qquad \partial G_2/\partial r = 0 \tag{2.8.17}$$

Inserting G_2 into Green's theorem, eq. (2.4.34), gives by use of (16) and (17):

$$\int_{\bar{z}=-\infty}^{\infty} d\bar{z} \int_{\bar{r}=0}^{\bar{a}} d\bar{r}\, \bar{r}\, (G_2\, \bar{\Delta} V(\bar{z},\bar{r}) - V(\bar{z},\bar{r})\, \bar{\Delta}\, G_2) = \int_{\bar{z}=-\infty}^{\infty} \bar{r}\, d\bar{z}\, \frac{\partial V}{\partial \bar{r}}\, G_2(z,r;\bar{z},\bar{r})\Big|_{\bar{r}=a} \tag{2.1.18}$$

Since V and (G_2) are solutions of the homogeneous wave equation (2.4.35) (of the inhomogeneous wave equation (2.4.30)), it follows:

$$r \le \bar{a} : V(z,r) = \bar{a} \int_{\bar{z}=-\infty}^{\infty} d\bar{z}\; G_2(z,r;\bar{z},\bar{a})\, \frac{\partial V}{\partial \bar{r}}\Big|_{\bar{r}=a} \tag{2.8.19}$$

G_2 can be represented by the Fourier integral :

$$G_2(z,r;\bar{z},\bar{r}) = G_2(\bar{z},\bar{r};z,r) =$$

$$= \frac{i}{4} \int_{\bar{C}} dk_z\, e^{ik_z(z-\bar{z})}\; J_o(\gamma r_<) \left[J_1(\gamma\bar{a})\, H_o^{(1)}(\gamma r_>) - H_1^{(1)}(\gamma\bar{a})\, J_o(\gamma r_>) \right] / J_1(\gamma\bar{a}) \tag{2.8.20}$$

The path $\bar{C}$ follows the real k_z-axis, except that it avoids the simple poles $k_z = \pm k_o$, see Fig. 2.2.1. For frequencies below the lowest cut-off frequency ($\omega < \omega'_{c1}$) the other poles, $k_z = \pm i\eta'_\nu$, eq. (5), lie on the k_{z2} -axis just between the η_ν's. The residue series belonging to (20) is :

$$G_2(z,r;\bar{z},\bar{r}) = \frac{1}{\bar{a}^2} \sum_{\nu=1}^{\infty} \frac{J_o(j'_\nu r/a)\, J_o(j'_\nu \bar{r}/a)}{\eta'_\nu\; J_o^2(j'_\nu)}\, e^{-\eta'_\nu|z-\bar{z}|} + \frac{i}{\bar{a}^2 k_o}\, e^{ik_o|z-\bar{z}|} \tag{2.8.21}$$

Deriving (19) with respect to r, inserting G_2 of equation (20) and using the Wronksian (2.4.42) gives:

$$\frac{\partial V}{\partial r} = \frac{1}{2\pi\bar{a}} \int_{-\infty}^{\infty} d\bar{z} \int_{-\infty}^{\infty} dk_z \, e^{ik_z(z-\bar{z})} \frac{J_1(\gamma r)}{J_1(\gamma a)} \bar{a} \frac{\partial V}{\partial \bar{r}}\bigg|_{\bar{r}=a} \tag{2.8.22}$$

Here the singularities at $k_z = \pm k_o$ have disappeared. V is identified with the Hertz potential V. $U = - r H_\theta = -\varepsilon\omega r \, \partial V/\partial r$, eq. (2.3.2) gives :

$$U(z,r) = \frac{r}{\bar{a}} \frac{1}{2\pi} \int_{-\infty}^{\infty} d\bar{z} \int_{-\infty}^{\infty} dk_z \, e^{ik_z(z-\bar{z})} \frac{J_1(\gamma r)}{J_1(\gamma\bar{a})} U(\bar{z},\bar{a}) \tag{2.8.23}$$

2.8.C Derivation and Summation of Series Expansions.

The derivation of the series expansions (6) to (9) is accomplished by the method described in Sections 2.5.A and 2.5.B with some slight modifications. The fact that the denominators of the integral representations (2) and (4) contain $J_1(\gamma\bar{a})$ in place of $J_o(\gamma a)$ (cf. eq. (2.5.12)) does not make a principal difference. Of course, the radius of the semicircles C_U and C_L must be chosen to pass about half-way between the points $k_z = \pm i\eta'_\nu$. The residues at these simple poles are computed according to (2.5.10) where, however, at the end of the calculations $J'_1(j'_\nu)$ is eliminated with the help of the differential equation of the Bessel functions :

$$J'_1(j'_\nu) = - J''_o(j'_\nu) = (1/j'_\nu)\, J'_o(j'_\nu) + J_o(j'_\nu) = J_o(j'_\nu) \qquad (2.8.24)$$

The summation of the series (6a) and (6c) at $|z| = \bar{p}/2$ is accomplished by use of :

$$2\left(\frac{\bar{p}}{a}\right)^2 \sum_{\nu=1}^{\infty} \frac{J_1(j'_\nu r/a)}{J_o(j'_\nu)} \frac{j'_\nu}{(2\pi n)^2 + (\eta'_\nu p)^2} = \delta_{\bar{a}r} - \frac{I_1(\bar{\mu}_n r/\bar{p})}{I_o(\bar{\mu}_n \bar{a}/\bar{p})} \qquad (2.8.25)$$

This series follows from the integral :

$$\lim_{R\to\infty} \frac{1}{2\pi i} \oint_{|k_z|=R} dk_z\, k_z\, J_1(\gamma r) \Big/ \left[J_1(\gamma\bar{a})\, (k_z^2 - (2\pi n/p)^2) \right] = \delta_{\bar{a}r} \qquad (2.8.26)$$

by Cauchy's residue theorem (cf. Section 2.5.C). By applying the operator $r^{-1}(\partial/\partial r)r$ to both sides of (25) results the series needed for the summation of (8a) and (8c).

2.9 Expressions for Voltage, Transit Time Factor and S-Coefficients Based on the Series for $U = - rH_\theta$.

The instantaneous peak voltage V(r) is found with the help of eq. (2.8.4) in the same way as in eqs. (2.6.13) till (2.6.15) :

$$V(r) = \lim_{\ell \to \infty} \int_{-\ell}^{\ell} E_z(z,r)\, dz = \frac{A_o/2}{\omega\varepsilon\bar{a}}\; k_o\bar{p}\; \frac{J_o(k_o r)}{J_1(k_o\bar{a})} \tag{2.9.1}$$

$a(k_z=0) = A_o\bar{p}/2$ has been used. In the usual method first the electric field along the axis, $E_z(z,0)$ is computed by interpolating the values of $U(z,r) = - rH_\theta(z,r)$. This is then integrated numerically to give the voltage $V_o = V(0)$. When V_o is computed with the help of (1) :

$$V_o = E_o/L = (A_o/2)\, k_o p/(\omega\varepsilon a\, J_1(k_o a)) \tag{2.9.1a}$$

there is no need for such an interpolation, since A_o is computed by numerical integration of $U(z,r) = - r\, H_\theta(z,r)$. The procedure is simpler, but less information on the field distribution is used, because here the values of only one mesh line, $r = \bar{a}$, are used while the interpolation to find E_z involves those of several lines.

The derivation of the transit time factor :

$$T_o(k) = \lim_{\ell \to \infty} \frac{1}{V_o} \int_{-\ell}^{\ell} E_z(z,0)\cos(kz)\, dz = \frac{a(k)}{\bar{p}A_o/2}\; \frac{k_r}{k_o}\; \frac{J_1(k_o\bar{a})}{I_1(k_r\bar{a})} \tag{2.9.2}$$

is analogous to that described in eqs. (2.6.16),(2.6.18). However there is an important difference as far as the application of formula (2) is concerned:
In general $\bar{p}$ is put equal to the total cell length L. Then the quantity:

$$\alpha = 2\pi - k\bar{p} = 2\pi - kL \tag{2.9.3}$$

contained in the coefficient of A_1 in a(k) is zero or at least very small. In order to take this into account, (2) is rewritten :

$$T_o(k) = \frac{k_r}{k_o}\frac{J_1(k_o a)}{I_1(k_r a)}\left[\frac{\sin(kL/2)}{kL/2} + \frac{A_1}{A_o/2}\;\frac{2kL}{2\pi + kL}\;\frac{\sin(\alpha/2)}{\alpha} - 2kL\sin\left(\frac{kL}{2}\right)\sum_{n=1}^{\infty}\frac{A_n}{A_o/2}\;\frac{(-1)^n}{(2\pi n)^2 - (kL)^2}\right] \tag{2.9.4}$$

This expression is tractable even if α is zero or very near to it. In that case the main contribution arises from the term proportional to $[\sin(\alpha/2)]/\alpha$ and all others are small compared to it. Agreement between the numerical value of T_o found in this way and those due to other methods is good. The arguments brought forward in the comparison of methods at the end of the preceeding paragraph apply here too.

The longitudinal S-coefficient :

$$S_1(k,r) = \lim_{\ell \to \infty} \frac{1}{V_o} \int_{-\infty}^{\infty} E_z(z,r) \sin(kz)\, dz$$

can be expressed by the following series :

$$S_1(k,r) = - T_o(k) \operatorname{ctg}(k\bar{p}/2)\, I_o(k_r r) + \frac{J_o(k_o r)}{k\bar{p}/2} - 2\frac{k}{k_o} J_1(k_o\bar{a}) \sum_{n=1}^{\infty} \frac{A_n}{A_o/2}\, \bar{\mu}_n \frac{I_o(\bar{\mu}_n r/\bar{p})}{I_1(\bar{\mu}_n \bar{a}/\bar{p})} \qquad (2.9.5)$$

$$+ 4\frac{k}{k_o} J_1(k_o\bar{a}) \left(\frac{\bar{p}}{\bar{a}}\right)^3 \sum_{n=o}^{\infty} \frac{A_n(-1)^n}{(A_o/2)(1+\delta_{no})} \sum_{v=1}^{\infty} \frac{J_o(j'_v r/a)}{J_o(j'_v)} \frac{e^{-\eta'_v p/2}}{(2\pi n)^2 + (\eta'_v p)^2} \frac{j'^2_v}{(kp)^2 + (\eta'_v p)^2}$$

with: $$\bar{\mu}_n = \left[(2\pi n)^2 - (k_o\bar{p})^2\right]^{\frac{1}{2}}$$

But this is very inconvenient if $\bar{p} = L$. S_1 is rewritten with $\alpha = 2\pi - kL$:

$$\frac{J_o(k_o r)}{kL/2} - I_o(k_r r)\frac{k_r}{k_o}\frac{J_1(k_o\bar{a})}{I_1(k_r\bar{a})}\left[\frac{\cos(kL/2)}{(kL/2)} - 2kL\cos\left(\frac{kL}{2}\right)\sum_{n=2}^{\infty}\frac{A_n}{A_o/2}\frac{(-1)^n}{(2\pi n)^2 + (kL)^2}\right]$$

$$+ \frac{2\,J_1(k_o\bar{a})}{2\pi + kL}\frac{kL}{k_o L}\frac{A_1}{A_o/2}\frac{1}{\alpha}\left[k_r L\frac{I_o(k_r r)}{I_1(k_r\bar{a})}\cos\frac{\alpha}{2} - \bar{\mu}_1\frac{I_o(\bar{\mu}_1 r/L)}{I_1(\bar{\mu}_1\bar{a}/L)}\right]$$

$$- 2\frac{kL}{k_o L} J_1(k_o\bar{a}) \sum_{n=2}^{\infty} \frac{A_n}{A_o/2}\, \bar{\mu}_n \frac{I_o(\bar{\mu}_n r/L)}{I_1(\bar{\mu}_n\bar{a}/L)} \qquad (2.9.6)$$

$$- 4\frac{kL}{k_o L} J_1(k_o\bar{a})\left(\frac{L}{\bar{a}}\right)^3 \sum_{n=o}^{\infty} \frac{A_n(-1)^n}{(A_o/2)(1+\delta_{no})} \sum_{v=1}^{\infty} \frac{J_o(j'_v r/\bar{a})}{J_o(j'_v)} \frac{j'^2_v}{(2\pi n)^2 + (\eta'_v L)^2} \frac{e^{-\eta'_v L/2}}{(kL)^2 + (\eta'_v L)^2}$$

with $$\bar{\mu}_n = \left[(2\pi n)^2 - (k_o L)^2\right]^{\frac{1}{2}}$$

If $2\pi = kL$, $\alpha = 0$ then $k_r L = \bar{\mu}_1$ and de l'Hospital's rule gives for the terms of the second line :

$$- \frac{2\pi}{k_o L} J_1(k_o \bar{a}) \frac{A_1}{A_o/2} \left[\frac{2}{\bar{\mu}_1} \frac{I_o(\bar{\mu}_1 r/L)}{I_1(\bar{\mu}_1 \bar{a}/L)} - \frac{\bar{a}}{L} \frac{[I_o(\bar{\mu}_1 r/L)]^2}{[I_1(\bar{\mu}_1 \bar{a}/L)]^2} \right] \qquad (2.9.7)$$

The expression (6) has been evaluated in one or two cases and there agreement with results of other computations was satisfactory. But it would be dangerous to generalize without checking the features which have been observed in these particular examples. The first two terms of the expression (6) are the most important ones. The first of them is almost constant. In the second only the first term of the infinite sum gives an appreciable contribution.

The third term is the difference of two great terms; but it is small. Greater than it is the term with n = 2 in the infinite sum giving the third expression while the other terms of it are small. The double series is smaller than 10^{-5} $S_1(k,r)$.

The expressions for the other S-Coefficients have not been derived and the whole approach has been abandoned in favour of that described in Sections 2.5 to 2.7. Some reasons for doing this were accidental. The other is that the approach where the longitudinal electric field $E_z^a(z)$ applied along the gap r = a, $|z| \leq p/2$ is assumed as the basic quantity, is more appealing from the physical point of view.

3. Motion of a Proton in a Spatially Uniform Time-Harmonic Field

This chapter is exclusively devoted to the motion of a proton in a uniform time-harmonic electric field. This is an unrealistic approximation to the real field in a linac gap. But it provides a simple example where many of the problems and notions prevailing in the realistic case can be studied easily. Also the various methods of solving the equations of motion are discussed. This may serve as an introduction for novices in the linac art and may be skipped by the adepts as an unnecessary diversion though some of the derivations included here might be new to them.

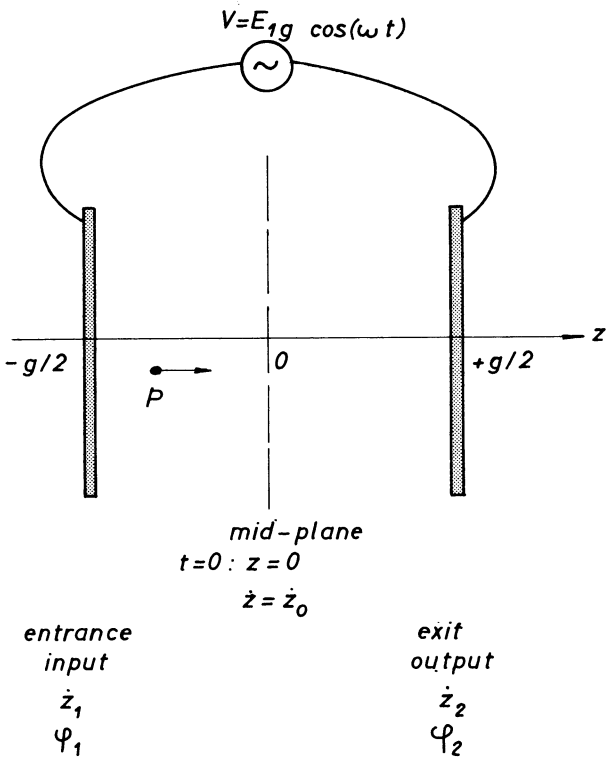

Fig. 3.1.1 Motion of a proton in a plane condensor as model of an accelerating gap.

3.1 Non-relativistic Treatment. The Pertubation Parameter κ.

The motion of a proton in the spatially homogeneous field :

$$E_z = E_1 \cos(\phi + \phi_o), \quad \phi = \omega t, \quad E_1 = \text{const.}$$

of a plane condensor (Fig.3.1.1) to whose plates an alternating voltage is applied, may serve as an admittedly oversimplified example. Such a field does not represent a very realistic approximation to the real field of an accelerating gap (cf. Fig. 1.1.5). In addition, it is only an approximate solution of Maxwells equations, contrary to the static homogeneous field, since $\Delta E_z + k_o^2 E_z = k_o^2 E_z \neq 0$. Even if the field is not Maxwellian, it is always permitted to assume such a field of force. The corresponding equation of motion :

$$m\,\ddot{z} = m\,\omega^2 z'' = eE_z = eE_1 \cos(\phi + \phi_o) \tag{3.1.1}$$

($' = d/d\phi = d/d(\omega t)$) with the initial conditions $\phi = \omega t = 0$: $z = 0, \dot{z} = \dot{z}_o$ (3.1.2)
has the solution :

$$z = (\dot{z}_o/\omega)\,\phi - eE_1 \left[\phi \sin\phi_o + \cos(\phi + \phi_o) - \cos\phi_o \right] \tag{3.1.3}$$

It is a peculiarity of the accelerator art that the conditions (2) specifying the solution of eq. (1) are given at the centre, z= 0, of the gap. Therefore they are called <u>mid-plane conditions .</u> The reason for this choice will become clear in the course of the treatment of particle dynamics in a realistic model of an accelerating gap, where the centre is a rather well defined point while entrance and exit are in general assumed at $z = -\infty, +\infty$ respectively. Of course, it is necessary to find these mid-gap values too. This is explained in Section 3.3.

Equation (3) is rewritten in dimensionless form:

$$kz = \phi - \kappa \left[\phi \sin\phi_o + \cos(\phi + \phi_o) - \cos\phi_o \right] \tag{3.1.3a}$$

with

$$k = \omega/\dot{z}_o \tag{3.1.4}$$

and:

$$\kappa = eE_1/(m\omega\dot{z}_o) \tag{3.1.5}$$

Equation (3) reveals a typical difficulty encountered in the treatment of dynamics in time-dependent fields: Trajectories and other quantities depending upon them (as e.g. kinetic energy) are given as functions of time t (or time angle (= phase) ϕ). But geometry singles out the longitudinal variable z (e.g. gap entrance and exit are situated at z = -g/2, g/2 respectively).

It is necessary to solve the trancendental equation (3a) for ϕ with given z. This cannot be done exactly. Thus successive approximations may be employed to invert equation (3a). If $E_1 \sim \kappa = 0$, then there is no field and the particle is moving freely :

$$\phi_{(o)}(z) = \phi^{(o)}(z) = kz \tag{3.1.6}$$

Higher approximations are obtained by iteration. In this way the influence of the electrical field upon particle motion is taken into account in successive steps:

$$\phi_{(i+1)}(z) = kz + \kappa\left[\cos(\phi_{(i)} + \phi_o) - \cos\phi_o + \phi_{(i)}\sin\phi_o\right] \tag{3.1.7}$$

This is written down explicitely for the first two iterations :

$$\phi_{(1)}(z) = kz + \kappa\left[\cos(\phi_{(o)}(z) + \phi_o) - \cos\phi_o + \phi_{(o)}(z)\,\sin\phi_o\right] \tag{3.1.7a}$$

$$= kz + \kappa\left[\cos(kz + \phi_o) - \cos\phi_o + kz\,\sin\phi_o\right] \tag{3.1.7b}$$

$$\phi_{(2)}(z) = kz + \kappa\left[\cos(\phi_{(1)}(z) + \phi_o) - \cos\phi_o + \phi_{(1)}(z)\,\sin\phi_o\right]$$

If the expression for $\phi_{(1)}(z)$ is inserted into the right hand side of (7b) this gives a rather clumsy expression. An approximation is introduced which is based upon the smallness of κ . (In a proton linac gap, typically $\kappa < 0.1$ ($\omega/2\pi$= 200 MHz, $E_1 \leq 14$ MV/m, $\dot{z}_o \geq 0.035$ c (~ 0.5 MeV)), in a proton synchrotron accelerating gap $\kappa < 0.01$ ($\omega/2\pi$ = 3 MHz, $E_1 \approx 0.1$ MV/m, $\dot{z}_o \geq 0.3$ c (~ 50 MeV))*). Due to the smallness of κ the results of (7a) and (7b) may be displayed by expanding them in a Taylor's series with regard to κ :

$$\phi_{(1)}(z) = \phi^{(o)}(z) + \kappa\phi^{(1)}(z) = \tag{3.1.8a}$$

$$= kz + \kappa\left[\cos(kz + \phi_o) - \cos\phi_o + kz\,\sin\phi_o\right]$$

$$\phi_{(2)}(z) = \phi^{(o)}(z) + \kappa\phi^{(1)}(z) + \kappa^2\phi^{(2)}(z) + \kappa^3 .. \tag{3.1.8b}$$

$$= kz + \kappa\left[\cos(kz + \phi_o) - \cos\phi_o + kz\,\sin\phi_o\right] - \kappa^2\phi^{(1)}(z)\left[\sin(kz + \phi_o) - \sin\phi_o\right]$$

$$+ \kappa^3 ..$$

*) In an electron linac $\kappa \gtrless 1$. Therefore expansions in powers of κ as displayed in equations (8) are inappropriate in this case. In addition, it is not reasonable to treat electron motion by non-relativistic equations as (1) and (3) .

In this and the following sections subscripts indicate the order of iteration; e.g. $\phi_{(1)}(z)$, eq. (7a), results from one iteration; $\phi_{(2)}(z)$, eq. (7b) from two iterations. Superscripts denote the order of derivation with respect to κ (or equally the power of κ accompanying the expression); e.g. $\phi^{(2)}(z) = (d^2\phi_{(2)}/d\kappa^2)_{\kappa=o} = (d^2\phi_{(3)}/d\kappa^2)_{\kappa=o} = \ldots$. The result of at least n iterations is needed to compute $\phi^{(n)}(z) = (d^n\phi_{(n)}(z)/d\kappa^n)_{\kappa=o}$; $\phi_{(n+1)}(z)$, $\phi_{(n+2)}(z)$ which result from even higher iterations, will give the same $\phi^{(n)}(z) = (d^n\phi_{(n+1)}(z)/d\kappa^n)_{\kappa=o} = (d^n\phi_{(n+2)}(z)/d\kappa^n)_{\kappa=o} = \ldots$

By this kind of expansion the solutions $\phi_{(1)}(z)$, $\phi_{(2)}(z)$ found by iteration assume a form which reminds one of another approximate method of solution, namely perturbation theory where solutions are found by expanding the solutions and all equations in powers of a small parameter (as here is κ). This view is supported by the physical interpretation which can be given to $\kappa = (eE_1/\omega)/(m\dot{z}_o)$. It may be regarded as the ratio of two momenta. The average force eE_1 times the time $1/\omega$ (~ 1 period) which equals the impact of the electrical field on the free particle with momentum $m\dot{z}_o$. *) .

It is assumed that $\phi^{(1)}(z)$ is not greater in absolute value than $\phi^{(o)}(z)$, that in turn $\phi^{(2)}(z)$ is not greater than $\phi^{(1)}(z)$ and $\phi^{(o)}(z)$, and so on. The first power of κ neglected should then give the order of magnitude of the error. Thus perturbation theory has in comparison with iterations the advantage that it gives an indication of the accuracy obtained, if the assumption just mentioned is fulfilled. However, in most cases it is not possible to prove this very basic assumption, since the calculation of higher order expressions becomes prohibitively complicated. In the present case it has been shown that the first order solution is already a good approximation to the exact one and that the second order corrections still improve the result. (See the end of this section).

---

*) This physical interpretation suggests that the parameter describing the magnitude of the impact of the accelerating field upon the particle crossing a linac gap, is even smaller than $\kappa = eE_1/m\omega\dot{z}_o$, since this quantity is derived from particle motion in a homogeneous field unlimited in its extension. Even such a time harmonic field has a direction accelerating a charge only during one half of a period, so its effect may be of the order of $\kappa/2$. In an accelerator gap the particle sees the field only during one quarter or one third of a period. Therefore the results of first order perturbation theory may be as accurate as those of power series in $\kappa/3 < 0.033$ or $\kappa/4 < 0.025$. This matches with the results of the numerical investigation reported at the end of this section where it is found that the coefficients accompanying the powers of κ in eq. (8) and (10) even decrease with increasing order n.

Inserting $\phi = \phi_{(1)}(z)$ from (8a) into the equation of motion,

$$m\ddot{z} = d/dz\ (\tfrac{1}{2}m\dot{z}^2) = dW/dz = eE_z = eE_1 \cos(\phi + \phi_o) \qquad (3.1.9)$$

expanding into powers of κ and integrating gives the energy gain across the gap:

$$\Delta W = eE_1 \int_{-g/2}^{g/2} \cos(\phi + \phi_o)\, dz =$$

$$= \Delta W^{(o)} + \kappa \Delta W^{(1)} + \kappa^2 \ldots \qquad (3.1.10)$$

$$= eV_o\, T_{oh}(k) \cos\phi_o + eV_o \kappa \tfrac{1}{2} \left[\cos(kg/2) - \frac{\sin(kg)}{kg}\right] \sin(2\phi_o) + eV_o\kappa^2 \ldots$$

where

$$V_o = \int_{-g/2}^{g/2} E_1\, dz = E_1 g \quad \text{is the instantaneous peak voltage across the gap}$$

and where

$$T_{oh}(k) = \frac{1}{E_1 g} \int_{-g/2}^{g/2} E_1 \cos(kz)\, dz = \frac{\sin(kg/2)}{(kg/2)} \qquad (3.1.11)$$

is the transit time factor ((2.6.8), (2.6.9), $k_o = 0$) for a field homogeneous in the z- and r-direction (therefore no $I_o(ka)$). In eq. (10) it accounts for the fact that the field strength is changing during the time the particle is crossing the gap, so that it cannot acquire an amount of kinetic energy equivalent to the "instantaneous potential difference" $eV_1 \cos\phi_o$. It would gain this amount only if its velocity were so great or the width of the gap so small that the transit time were small compared to the period of the field. In practice : $\pi/3 \leq kg \leq 2\pi/3$, $0.96 \geq T_{oh} \geq 0.83$ (Fig. 3.1.2). The transit time factor of a real gap $T_o(k)$, eq. (2.6.9), is divided by $I_o(k_r a) > 1$. Moreover, in cavities designed for rather high energies the electrical field along the axis exhibits a strong depression in the centre (cf. Fig. 2.5.4). This further diminishes T_o;e.g. $T_o = 0.56$ (197 MeV, MURA 31465 [26]).

The second term in (10) gives a correction. It is small, for it is multiplied by $\kappa (< 0.1)$ and, in addition, the trigonometric expression is small compared to $T_{oh}(k)$. (cf. Fig. 3.1.3).

Equation (10) represents a power series in κ . Even in the first gap of an Alvarez linac structure κ is not greater than 0.1 and it becomes smaller afterwards. By use of (8) all other dynamical variables may assume a similar form permitting to estimate the accuracy achieved, since there is the hope that the order of magnitude of each term is essentially determined by the power in κ , the accompanying coefficient not increasing in magnitude with increasing order.

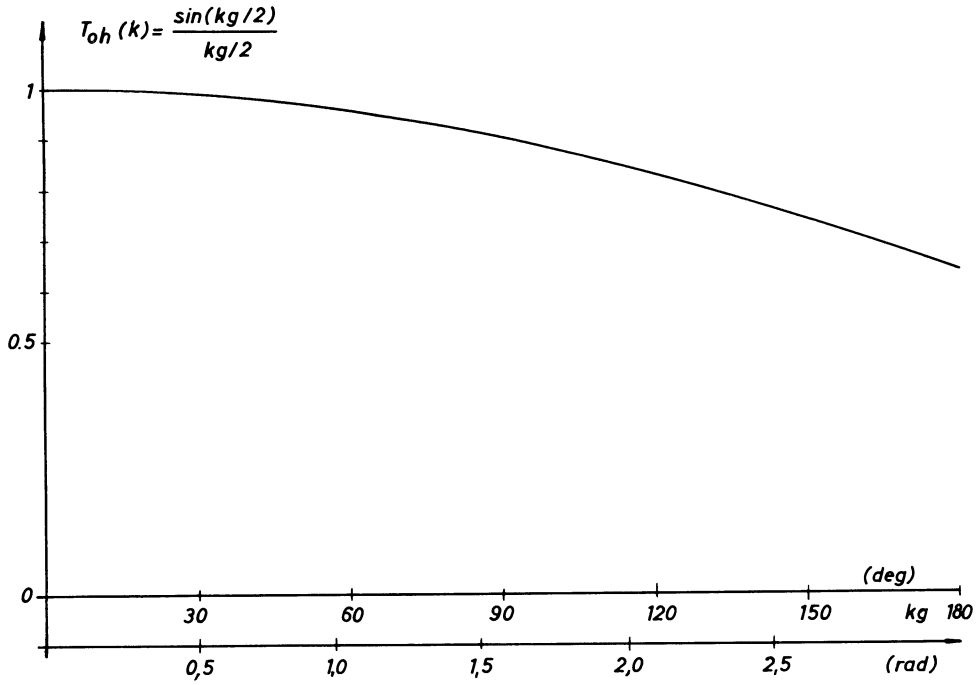

Fig. 3.1.2 Transit time factor for uniform field, $T_{oh}(k)$, as function of transit time angle, kg.

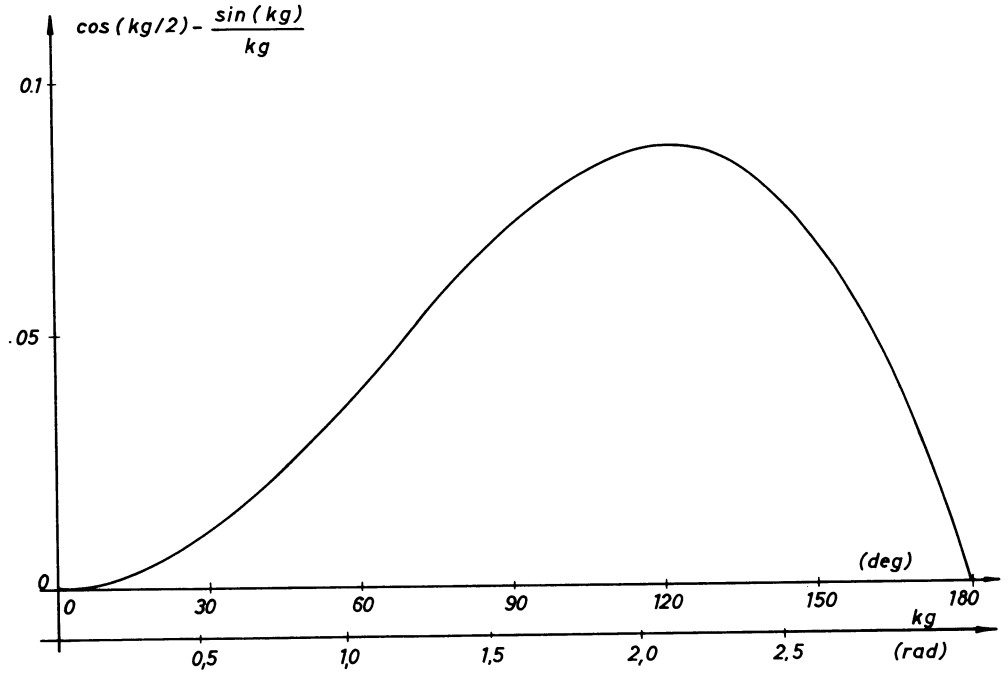

Fig. 3.1.3 Correction term for energy gain

In order to check this, a numerical investigation was undertaken [31]:

Repeating the iterations (7) sufficiently often for a given z, the corresponding value of the time-angle $\phi(z)$ is found to any desired accuracy. $\kappa = 0.1$ was chosen which corresponds to $\omega/2\pi = 200$ MHz, $E_1 = 14.2$ MV/m, $\dot{z}_o = 0.035\ c = 1.047 \times 10^7$ m/s (W = 0.5 MeV, 0.5 MeV protons). These values are even more unfavourable than those actually encountered at the entrance of a proton linac. Fig. 3.1.4 displays the difference between exact phase $\phi_{EX}(z)$ and the first order approximation $\phi_{(1)}(z)$, eqs (7a) and (8a), Fig. 3.1.5 the difference $\phi_{EX}(z) - \phi_{(2)}(z)$. In Figs. 3.1.6 , 3.1.7 is shown the deviation of the approximate phase changes $\Delta\phi_{(1)}$, $\Delta\phi_{(2)}$ respectively from the exact $\Delta\phi_{EX}$. Inserting the exact phases into the expression for gain in kinetic energy gives an accurate value of this quantity :

$$\Delta W_{EX} = (m/2)\left[\dot{z}^2(z=g/2) - \dot{z}^2(z=-g/2)\right] \tag{3.1.12}$$

$$= 2\,\kappa\,W\left[\sin(\phi_{EX}(z=g/2) + \phi_o) - \sin(\phi_{EX}(z=-g/2) + \phi_o)\right]$$

$$+ \kappa^2 W\left\{\left[\sin(\phi_{EX}(z=g/2) + \phi_o) - \sin\phi_o\right]^2 - \left[\sin(\phi_{EX}(z=-g/2) + \phi_o) - \sin\phi_o\right]^2\right\}$$

In table 3.1.1 these values are compared with the approximate results $\Delta W^{(o)} = \Delta W_{(o)}$ and $\Delta W_{(1)} = \Delta W^{(o)} + \kappa\Delta W^{(1)}$. First order results are accurate to better than 1%, second order results to better than 2 ‰ . Comparison of $\Delta W^{(o)}/\Delta W_{EX}$ with $\Delta W^{(1)}/\Delta W_{EX}$ reveals that $\kappa\Delta W^{(1)}$ is smaller than $\Delta W^{(o)}$ by a factor 50 to 100. This is more favourable than it was assumed at the beginning where it was postulated that $\Delta W^{(1)}$ is not greater than $\Delta W^{(o)}$. The same conclusion can be drawn from formula (10) and Figs. 3.1.2 and 3.1.3 . In addition the correction term has a sign such that it always improves the result.

3.1.A Roots of the Phase Equation (3.1.3a)

Equation (3) is rewritten as :

$$\phi = kz + \kappa\left[\cos(\phi + \phi_o) - \cos\phi_o + \phi \sin\phi_o\right] \qquad (3.1.13)$$

Roots of this equation for a given value of the parameter z may be interpreted as intersections of the straight line $\phi(1 - \kappa \sin\phi_o) - kz + \kappa \cos\phi_o$ with the sinusoidal curve $\kappa \cos(\phi + \phi_o)$. The slope of the former, $1 + |\kappa \sin\phi_o|$ ($0 \leq -\phi_o \leq \pi/2$, in order to ensure acceleration and phase stability [32]) is greater than that of $\kappa \cos(\phi + \phi_o)$, provided $0 < \kappa < 1$. Therefore, the two curves have exactly one point in common, i.e. (13) has one and only one root. The method of solution by iterations (7) is convergent. A sufficient condition that the iterations :

$$x_1 = f(x_o) \ , \ x_2 = f(x_1), \ \ldots$$

converge to the solution $x = f(x)$ is [33] :

$$|f'(x)| = \kappa \ | \ \sin(x + \phi_o) - \sin\phi_o| \leq 2 \kappa < 1 \ .$$

The speed of convergence of iterations can be estimated with the help of equations like (4.1.6) which indicate the relation between approximate solutions found by perturbation theory and those found by iterations. In the numerical example discussed just before where $\kappa = 0.1$, each iteration improves the accuracy of the solution by at least one order of magnitude. Convergence is slowest at the gap ends, $|z| = g/2$.

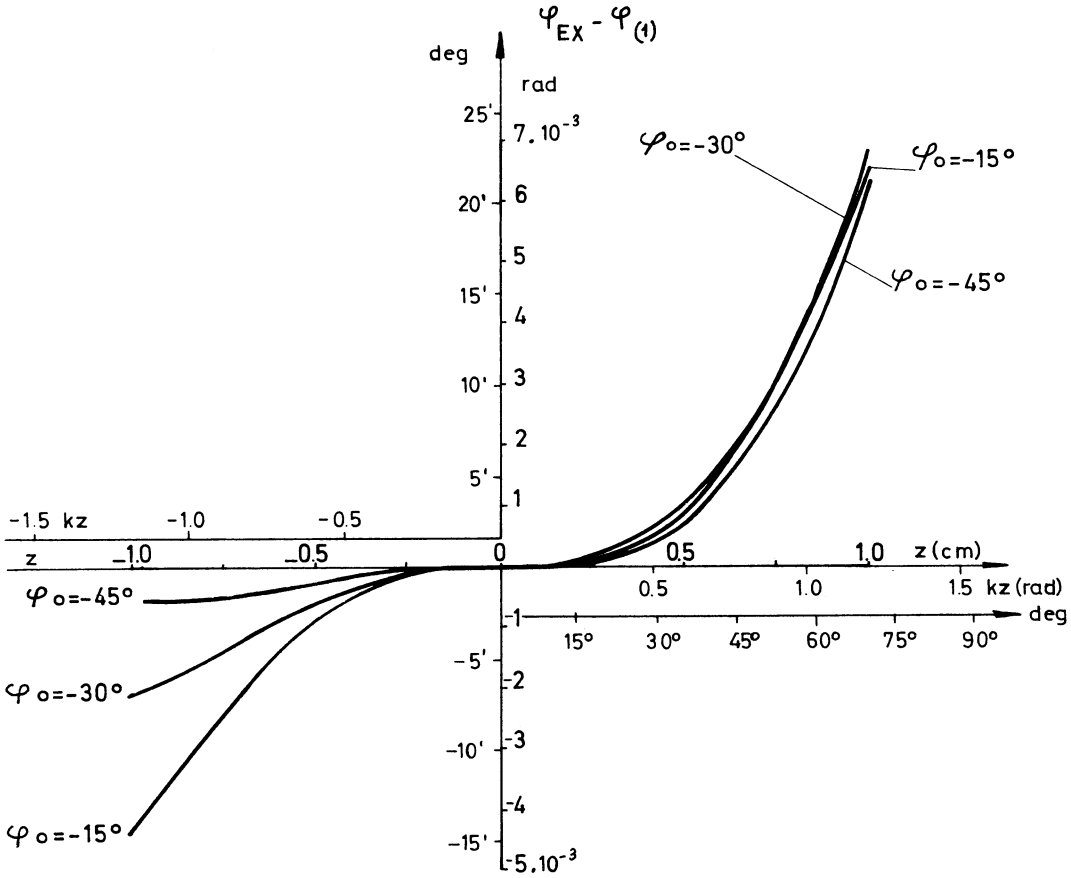

Fig. 3.1.4 Difference between exact phase, $\phi_{EX}(z)$, and first order approximation, $\phi_{(1)}(z)$, eq.(7a), versus zero order phase, $kz = \phi_{(o)}(z)$. Phase is fixed at centre, $z = 0$. $\kappa = eE_1/(m\omega\dot{z}_o) = 0.1$, $E_1 = 14.2$ MV/m, $\omega/2\pi = 200$ MHz, $\dot{z}_o = 0.035$ c (~0.5 MeV protons), $k = 119.65\ m^{-1}$.

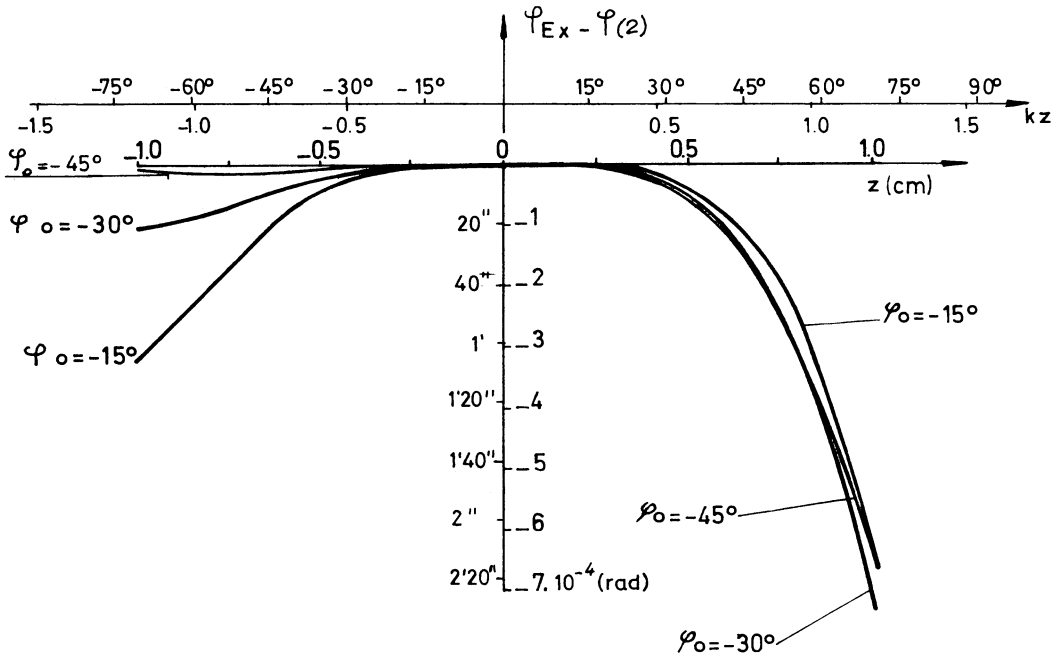

Fig. 3.1.5 Difference between exact phase, $\phi_{EX}(z)$, and second order approximation, $\phi_{(2)}(z)$, eq. (7b), versus zero order phase, $kz = \phi_{(o)}(z)$. Phase is fixed at centre, z = 0. Parameters same as in Fig. 3.1.4.

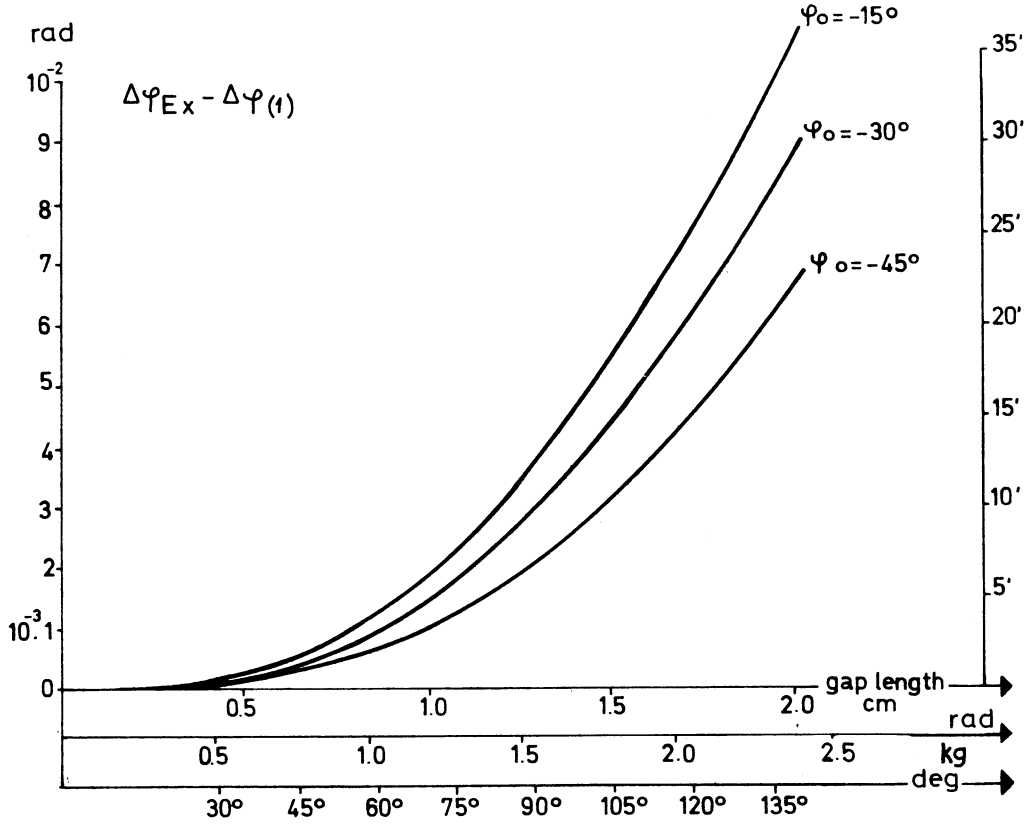

Fig. 3.1.6 Difference between exact phase change across gap, $\Delta\phi_{EX}$, and first order change, $\Delta\phi_{(1)}$, versus gap length and zero order phase change kg = $\Delta\phi_{(o)}$. - $\kappa = eE_1/(m\omega\dot{z}_o) = 0.1$, $E_1 = 14.2$ MV/m, $\omega/2\pi =$ 200 MHz, $\dot{z}_o = 0.035$ c (~ 0.5 MeV protons), k = 119,65 m^{-1}.

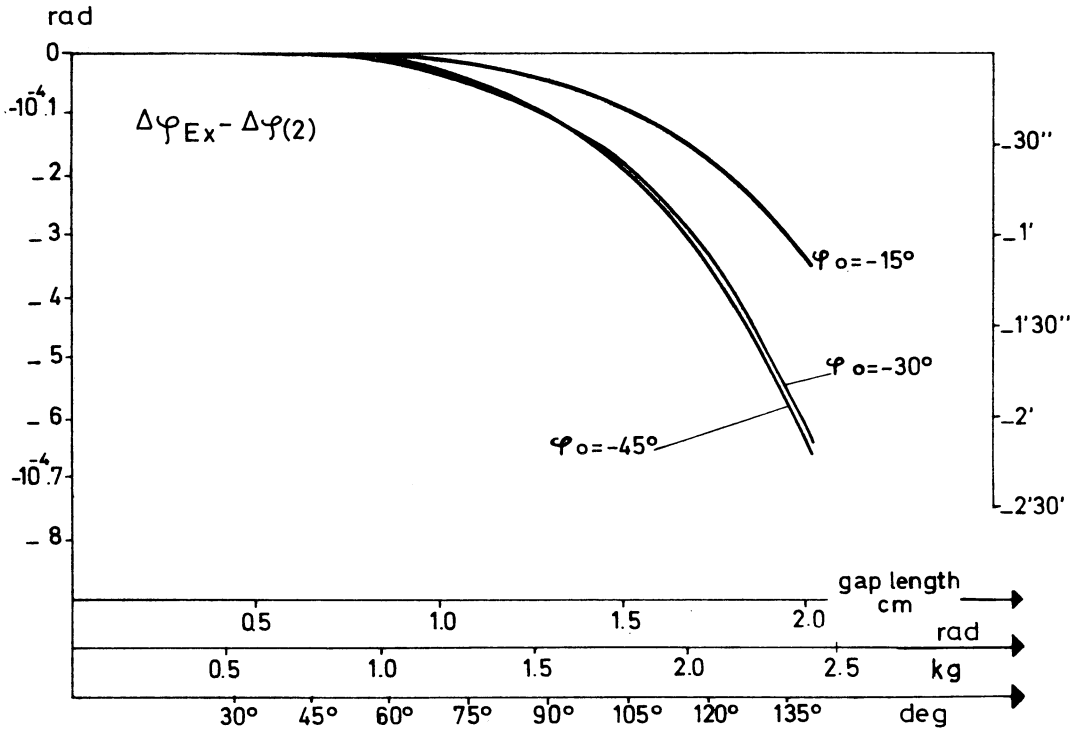

Fig. 3.1.7 Difference between exact phase change across the gap, $\Delta\phi_{EX}$, and second order change, $\Delta\phi_{(2)}$, versus gap length g and zero order phase change, $kg = \Delta\phi_{(o)}$. Numerical parameters same as in Fig. 3.1.6.

Table 3.1.1 Comparison of Exact and Approximate Results for Energy Gain and Phase Change.

φ_o	kg (deg)	g (cm)	ΔW_{EX} (in 500 keV units)	$\Delta W^{(o)}/\Delta W_{EX}$	$\kappa\Delta W^{(1)}/\Delta W_{EX}$	$(\Delta W^{(o)}+\kappa\Delta W^{(1)})/\Delta W_{EX}$	$\Delta W_{EX,1}$ (in 500keV units)	$\Delta W_{EX,2}$ (in 500keV units)
-15^o	60^o	0,88	0,192965	1,001141	-0,001059	1,000082	,089380	,103585
	90^o	1,31	0,272546	1,002420	-0,002031	1,000389	,120317	,152229
	120^o	1,75	0,333324	1,003848	-0,002718	1,001130	,138480	,194844
-30^o	60^o	,88	0,172841	1,002104	-0,002048	1,000056	,072898	,099944
	90^o	1,31	0,243924	1,004204	-0,003931	1,000273	,092078	,151846
	120^o	1,75	0,298186	1,006083	-0,005262	1,000821	,097377	,200810
-45^o	60^o	,88	0,141010	1,002919	-0,002899	1,000021	,051492	,089518
	90^o	1,31	0,198870	1,005684	-0,005568	1,000117	,057697	,141173
	120^o	1,75	0,243035	1,007875	-0,007455	1,000420	,049877	,193159

φ_o	kg (deg)	kg (rad)	$\Delta\varphi_{EX}$	$\Delta\varphi_{(1)} = kg + \kappa\Delta\varphi^{(1)}$	$\Delta\varphi_{(2)}$	$kg + \kappa\Delta\varphi^{(1)} + \kappa\Delta\varphi^{(1)}$	$\Delta\varphi_{EX,1}$	$\Delta\varphi_{EX,2}$
-15^o	60^o	1,04720*)	1,04722	1,04598	1,04723	1,04725	,53661	,51061
	90^o	1,57080	1,57057	1,56674	1,57062	1,57060	,81348	,75719
	120^o	2,09440	2,09296	2,08502	2,09314	2,09308	1,09425	,99880
-30^o	60^o	1,04720	1,04584	1,04484	1,04585	1,04585	,53442	,51142
	90^o	1,57080	1,56606	1,56297	1,56615	1,56612	,80790	,75815
	120^o	2,09440	2,08275	2,07628	2,08311	2,08301	1,08324	,92951
-45^o	60^o	1,04720	1,04454	1,04386	1,04456	1,04455	,53161	,51293
	90^o	1,57080	1,56189	1,55973	1,56199	1,56196	,80103	,74451
	120^o	2,09440	2,07352	2,06877	2,07389	2,07379	1,07043	1,00319

$\kappa = eE_1/(m\omega\hat{z}_o) = 0.1$, $E_1 = 14.2$ MV/m, $\omega/2\pi = 200$ MHz, $\hat{z}_o = 0.035$ c (~ 0.5 MeV protons), $k = 119{,}65\ m^{-1}$. $\Delta W_{EX,1}$, $\Delta\varphi_{EX,1}$ give the exact change of energy and phase across the first half of the gap, quantities with index 2 the same changes in the second half.

*) For $\varphi_o = -15^o$ and values of kg of about this magnitude the exact transit time angle, $\Delta\varphi_{EX}$, is slightly smaller than the zero order phase change, $kg = \omega g/v_o$. It should be remembered that kg is smaller than $\omega g/v_1$, the transit time angle of a particle crossing the gap in free motion with the entrance velocity v_1.

3.1. B Convergence of Perturbation Series

Here will be discussed the conditions which ensure convergence of the perturbation series for phase, eq. (8) and kinetic energy, eq. (10). It is convenient to transform the equation of motion (1) into a set of two first order equations:

$$d\phi/dz = d(\omega t)/dz = \omega\ (dz/dt)^{-1} = \omega(m/2)^{\frac{1}{2}}/(T)^{\frac{1}{2}} \qquad (3.1.14)$$

$$dT/dz = d/dz(\frac{m}{2}\dot{z}^2) = eE_1 \cos(\phi + \phi_o) \qquad (3.1.15)$$

where T is kinetic energy. Equation (14) is just an identity, eq. (15) agrees with (9). They may be derived by canonical transformations[38]. With the help of the solution (3), $(T)^{\frac{1}{2}}$ may be expressed by :

$$(T)^{\frac{1}{2}} = (m/2)^{\frac{1}{2}}\ \omega/k\left[1 + \kappa(\sin(\phi + \phi_o) - \sin\phi_o)\right] \qquad (3.1.16)$$

where k and κ are defined in eqs. (4), (5) respectively. Introducing the dimensionless variables :

$$\zeta = kz \qquad \eta = T/W = T/(m\ \dot{z}_o^2/2) \qquad (3.1.17)$$

and replacing $(T)^{\frac{1}{2}}$ by the expression (16), equations (14) and (15) are rewritten in dimensionless form :

$$\frac{d\phi}{d\zeta} = \frac{1}{1 + \kappa\left[\sin(\phi+\phi_o) - \sin\phi_o\right]} = 1 - \kappa\,\frac{\sin(\phi + \phi_o) - \sin\phi_o}{1 + \kappa\left[\sin(\phi + \phi_o) - \sin\phi_o\right]} \qquad (3.1.18a)$$

$$= g_1 + \kappa\ f_1(\phi;\ \kappa;\ \zeta)$$

$$\frac{d\eta}{d\zeta} = \kappa\ 2\cos(\phi + \phi_o) = 0 + \kappa\ 2\cos(\phi + \phi_o) \qquad (3.1.18b)$$

$$= g_2 + \kappa\ f_2\ (\phi\ ;\kappa\ ;\zeta\ )$$

Equation (18a) is particularly suggestive. At points where the denominator vanishes, $d\phi/d\zeta$ and with it all higher derivatives cease to exist. This cannot happen for any real ϕ, ϕ_o if $|\kappa| < 1/2$. On the contrary, if $|\kappa| \geq 1/2$, then the denominator may vanish for certain values of ϕ, ϕ_o and it may be expected that these singularities determine the radius of convergence of series expansions. It should be remembered that only equations (18a) and (18b) together describe the dynamical problem completely and that the singularities even if they occur in only one of the two equations limit the range of the solutions of both.

The rigorous demonstration of the convergence of the perturbation series solutions :

$$\phi(\zeta) = \phi^{(o)}(\zeta) + \kappa\phi^{(1)}(\zeta) + \kappa^2\phi^{(2)}(\zeta) + \kappa^3 \ldots$$
$$\eta(\zeta) = \eta^{(o)}(\zeta) + \kappa\eta^{(1)}(\zeta) + \kappa^2\eta^{(2)}(\zeta) + \kappa^3 \ldots \qquad (3.1.19)$$

is limited to the case where $0 \leq \kappa < 1/2$ which suffices for the present applications (where $0 < \kappa \leq 0.1$) . The corresponding theory may be found in ref.[34]. $g_1 = 0$, $g_2 = 1$ are just constants. $f_2(\phi; \kappa; \zeta)$ is analytical in ϕ and κ for any real values of ϕ, κ, ζ; and so is $f_1(\phi; \kappa; \zeta)$ provided $0 \leq \kappa < 1/2$. It follows from the theorems in that reference that the series (18) converge for any real ζ and ϕ if $|\kappa| < 1/2$.

The convergence of the perturbation series (18) has various aspects. Firstly, there is the question under which conditions they converge at all. This has been settled just before. For perturbation series the sole convergence which is a property concerning the tail of the series, is not so helpful. It is practically impossible to evaluated terms of too high an order; therefore the convergence must be sufficiently fast, so that the first few terms give sufficient accuracy. The third point regards the perturbation parameter κ . It should be chosen in such a way that the coefficients, e.g. $\phi^{(n)}(\zeta)$, accompanying the various powers, κ^n, do not increase with increasing n. Which property permits to estimate the accuracy which can be obtained by retaining the first N terms of the series, since the error should not be much greater than $\kappa^{n+1}\phi^{(n+1)}(\zeta)$.

3.2 Practical Application of Beam Dynamics Formulae. Evaluation of Mid-Gap Values by Use of S-coefficients.

The beam dynamics formulae derived in the preceeding section will first be cast into a form as they are used in practical applications. Of course, the expressions derived above for a uniform field represent an approximation too poor to be used in the treatment of particle dynamics in a real gap. Nevertheless it may be worthwhile to introduce already here the procedure employed in realistic cases. In the thin lens approximation which is explained in detail in Section 4.2, the real particle trajectory is replaced by a step function. Only first order *) expressions are used.

Afterwards the evaluation of the mid-gap values will also be discussed.

The expression for the energy gain across the gap may be taken over as it stands in eq. (3.1.9b) :

$$\Delta W = eV_o\, T_{oh}(k)\, \cos\phi_o + eV_o\kappa \ldots \tag{3.2.1}$$

where $k = \omega/\dot{z}_o$, eq. (4). How it is used in the thin lens approximation, is described in eqs. (4.2.2.) and Fig. 4.2.1 .

The change of total phase across the gap, $\Delta\phi$, however, is decomposed into three contributions (cf. Fig. 4.2.2 and eqs. (4.2.5)) :

$$\Delta\phi = \frac{\omega}{\dot{z}_1}\frac{g}{2} + \frac{\omega}{\dot{z}_2}\frac{g}{2} + \Delta\bar{\phi} = \frac{kg}{2}\left(\frac{\dot{z}_o}{\dot{z}_1} + \frac{\dot{z}_o}{\dot{z}_2}\right) + \Delta\bar{\phi} \tag{3.2.2}$$

The first (second) contribution corresponds to the phase change of a particle moving freely with the input velocity $\dot{z}_1 = \dot{z}(z=-g/2)$ through the first half of the gap up to the centre (with the output velocity $\dot{z}_2 = \dot{z}(z=g/2)$ through the second half of the gap). The last one $\Delta\bar{\phi}$, the change in reduced phase, is found from (3.1.8a) and from :

$$\begin{aligned}\dot{z}_o/\dot{z}(z) &= \left[1 + \kappa\left[\sin(\phi_o + \phi(z)) - \sin\phi_o\right]\right]^{-1} \\ &= \left[1 + \kappa\left[\sin(\phi_o + kz) - \sin\phi_o\right] + \kappa^2\ldots\right]^{-1} \\ &= 1 - \kappa\left[\sin(\phi_o + kz) - \sin\phi_o\right] + \kappa^2\ldots\end{aligned} \tag{3.2.3}$$

*) Note that $eV_o\kappa = eE_1 g\kappa$ in eq.(1) and $(eV_o/2W)\kappa$ in eq(4) are already of second order in the field.

to be :

$$\Delta\bar{\phi} = \frac{eV_o}{2W}\left[\cos(kg/2) - \frac{\sin(kg/2)}{kg/2}\right] + \frac{eV_o}{2W}\ \kappa\ \ldots$$

$$= \frac{eV_o k}{2W}\ \frac{d}{dk}\ T_{oh}(k) + \ldots \qquad (3.2.4)$$

$W = m\,\dot{z}_o^2/2$ is kinetic energy at the gap centre.

These beam dynamics equations permit to calculate the motion of the particle through the total gap only after the mid-gap values $\dot{z}_o$ and ϕ_o are known. This is due to the fact that in the preceeding section the general solution of the equation of motion has been specified by the initial conditions (3.1.2) where it is assumed that the particle is at the gap centre, $z = 0$, at time (phase) $\omega t = \phi = 0$ and there has velocity $\dot{z}_o$. At that instant the time harmonic accelerating field has the value $E_z = E_1 \cos\phi_o$. The choice of the initial data indicating the phase the field assumes at the instant where the particle passes at a certain reference point, is called the choice of the reference point for phase. The gap centre, $z = 0$, is this reference point with the initial conditions (3.1.2). Other reference points are discussed in the next section.

If a particle is traced through the whole linac , then the following method is applied: Assume the motion of this particle through the first n-1 gaps has been worked out: therefore the phase and energy it has in leaving the (n-1)-th gap, are known. After the phase change through the drift space before the n-th gap has been taken into account, the input values of phase and energy are known. Starting from these the mid-gap values of the same quantities must be found. The increments of phase and energy across the first half of the gap can be calculated with the help of the formulae containing S-coefficients given below. Afterwards the change in energy and phase across the whole gap is calculated according to eqs. (1),(2) and (4).

The gain in energy across the first half of the gap is found from eq.(3.1.9) where $\phi = \phi^{(o)}(z) = kz$, eq. (3.1.6), is inserted :

$$\Delta w_1 = eE_1 \int_{-g/2}^{o} \cos(\phi_o + kz)\, dz$$

$$\Delta w_1 = eV_o\ \frac{1}{2}\ \frac{\sin(kg/2)}{kg/2}\ \cos\phi_o + eV_o\ \frac{1}{2}\ \frac{1 - \cos(kg/2)}{kg/2}\ \sin\phi_o \qquad (3.2.5)$$

$$= eV_o\ \frac{1}{2}\ T_{oh}(k)\ \cos\phi_o + eV_o\ \frac{1}{2}\ S_{oh}(k)\ \sin\phi_o$$

$V_o = E_1 g$. The transit time factor $T_{oh}(k)$ is already known from formula (3.1.11). In the above expression appears a second coefficient, the (longitudinal) S-coefficient for a homogeneous field (cf. eq.(2.7.1)) :

$$S_{oh}(k) = \frac{2}{V_o} \int_o^{g/2} E_1 \sin(kz)\, dz = \frac{1 - \cos(kg/2)}{kg/2} \qquad (3.2.6)$$

The phase change across the first half of the gap, $\Delta\phi_1$, is similar to $\Delta\phi$, eq. (2), decomposed into two contributions:

$$\Delta\phi_1 = \frac{\omega}{\dot{z}_1}\frac{g}{2} + \Delta\bar{\phi}_1 \qquad (3.2.7)$$

$$= \phi(z=0) - \phi(z=-g/2) = \frac{kg}{2}\frac{\dot{z}_o}{\dot{z}_1} + \Delta\bar{\phi}_1$$

The first term, $\omega g/(2\dot{z}_1)$, is the phase change of a particle moving freely with the input velocity $\dot{z}_1 = \dot{z}(z=-g/2)$ from the entrance to the gap centre. The second, $\Delta\bar{\phi}_1$ is the change in reduced phase. $\Delta\phi_1$ is found from (3.1.8a). From this expression and from the definition (7) $\Delta\bar{\phi}_1$ is calculated with the help of (3):

$$\Delta\bar{\phi}_1 = \frac{1}{2}\frac{eV_ok}{2W}\left\{\left[-\frac{\sin(kg/2)}{k^2g/2} + \frac{\cos(kg/2)}{k}\right]\sin\phi_o - \left[-\frac{1-\cos(kg/2)}{k^2g/2} + \frac{\sin(kg/2)}{k}\right]\cos\phi_o\right\} \qquad (3.2.8)$$

$$= \frac{1}{2}\frac{eV_ok}{2W}\left\{\frac{d}{dk}T_{oh}(k)\sin\phi_o - \frac{d}{dk}S_{oh}(k)\cos\phi_o\right\}$$

$$= \frac{\Delta\bar{\phi}}{2} - \frac{eV_ok}{2W}\,\frac{1}{2}\,\frac{d}{dk}S_{oh}(k)\cos\phi_o$$

The procedure to find the wanted mid-gap values $\dot{z}_o$, $(\phi_o + \phi(0)) = \phi_o$ from the known input values $\dot{z}_1$, $\phi_1 = (\phi_o + \phi(z=-g/2))$ uses the equations:

$$\frac{m}{2}(\dot{z}_o^2 - \dot{z}_1^2) = \Delta w_1 \qquad (3.2.9)$$

$$\phi_o - \phi_1 = \frac{\omega}{\dot{z}_1}\frac{g}{2} + \Delta\bar{\phi}_1 \qquad (3.2.10)$$

$$k = \omega/\dot{z}_o \qquad W = m\,\dot{z}_o/2 \qquad (3.2.11)$$

For Δw_1 and $\Delta\bar{\phi}_1$ the expressions (5) and (8) (where k and W of eq. (11) are inserted) are employed. This then gives a system of implicit transcendental equations for $\dot{z}_o$ and ϕ_o which is solved by iteration. The exit velocity z_2, is found from :

$$m\,\dot{z}_2/2 = W + \Delta W - \Delta w_1 \qquad (3.2.12)$$

3.3 The Choice of the Reference Point for Phase and Zero Order Velocity

The problem investigated here is a rather intriguing one. Therefore it may be explained with an example. The evaluation of the zero order energy gain $\Delta W^{(o)}$ as calculated in eq. (3.1.10) may be interpreted in the following way : A charge is carried through the accelerating gap with constant velocity, $\dot{z}_o$. The force the time-dependent field exerts upon this charge at each point is registered and the integral of these values across the gap is assumed to be approximately equal to the gain in energy the proton acquires in the corresponding real (accelerated) motion. The scanning velocity used in Section 3.1 is $\dot{z}_o$, the velocity the particle really has in the centre of the gap. In the same way the initial conditions given at the gap centre, z = 0, determine the whole zero order solution describing free particle motion and enter thereby in the higher approximations. Approximate solutions are exact at this point. It is held in wide belief that approximate solutions chosen in this way describe the motion through the whole gap most accurately. But one may ask if another fictitious scanning velocity which equals the velocity the particle assumes at a different point in the gap, say at the entrance, will give better results. Of course, all initial conditions must be chosen accordingly. This point in the gap where initial conditions for solutions are prescribed and where approximate solutions are exact, is called the reference point. The motion of a proton in a time-harmonic uniform field offers a simple example to investigate the influence of the choice of the reference point upon approximate results numerically. Results confirm that approximate solutions give best accuracy for reference points near to the gap centre, though the differences are not very appreciable.

However, when mid-gap conditions are used, it is necessary to find these mid-gap values, ϕ_o and $W = m\,\dot{z}_o^2/2$, starting from the input values of these quantities given at the gap entrance. This step where the S-coefficients come into the play, described in section 3.2, is again of an asymmetric nature and it may be that its results are not more accurate than those of the second so that the overall accuracy of both steps may not be better than that of a method where the energy gain and phase change across the whole gap would be computed directly from the input data. This problem has, however, not yet been investigated.

Some care must be taken to choose the conditions determining the arbitrary constants in the solution of the equation of motion (which correspond to the initial or mid-plane conditions) appropriately so that the different expressions always describe the same motion. The initial conditions as chosen in eq. (3.1.2) imply that the field has the value $E_z = E_1 \cos\phi_o$ when the particle is at the gap centre. If another point within the gap, say with coordinate $z = \alpha g/2$ (entrance = $-1 \leq \alpha \leq 1$ = exit)(Fig. 3.2.1) together with the exact velocity the particle assumes in it, is chosen to specify the solution, then the phase constant in the electric field must be adjusted accordingly.

The example is the same which already has been studied in the preceding section . The treatment consists of two steps: i) equation (3.1.7) belonging to the initial data (3.1.2) is repeated sufficiently often for all $z = \alpha g/2$ in order to give exact values for

the phase $\phi_{EX}(z=\alpha g/2) \equiv \psi_o(\alpha)$. The step width for α is 1/60 to 1/30 depending on gap length. Thereafter the exact particle velocity at this point:

$$\dot{z}(z=\alpha g/2) = \dot{z}_o \left\{ 1 + \kappa \left[\sin(\phi_o + \psi_o(\alpha)) - \sin \phi_o \right] \right\} \equiv v(\alpha) \qquad (3.3.1)$$

is calculated. ii) Then a certain reference point (i.e. a certain value for α) is chosen. The equation of motion with the appropriate phase constant :

$$m\ddot{z} = eE_1 \cos(\omega t + \psi_o(\alpha)) \qquad (3.3.2)$$

is solved with the (initial) conditions :

$$t = 0: \quad z = \alpha g/2 \quad \dot{z} = v(\alpha) \qquad (3.3.3)$$

This ensures that the particle feels at the same space point and the same "physical" time the same force irrespective of the choice of the reference point α (or of the origin of the time scale). Solving (2) under the conditions (3):

$$\omega z = \omega\alpha g/2 + v(\alpha)\, \omega t - \kappa \dot{z}_o \left[\omega t \sin \psi_o(\alpha) + \cos(\omega t + \psi_o(\alpha)) - \cos\psi_o(\alpha) \right] \qquad (3.3.4)$$

therefore gives the same exact values for phase, energy gain and all other quantities; on the contrary, the results of approximate formulae and procedures will depend on α . For example, if an approximate expression for phase ωt is inserted into the velocity formula:

$$\dot{z}(\omega t) = (eE_1/\omega) \left[\sin(\omega t + \psi_o) - \sin \psi_o \right] \qquad (3.3.5)$$

different values for the entrance velocity will be found depending on α ; this also applies to the velocity at any other point except for the point $z = \alpha g/2$ where the velocity $v(\alpha)$ will be reproduced. $\alpha = 0$ gives the results of the preceding section .

The zero and first order expression for the entrance (t_i) and exit time (t_e) are found by iteration :

$$\left.\begin{matrix} \omega t_{i(o)} \\ \omega t_{e(o)} \end{matrix}\right\} = \mp \frac{1 \pm \alpha}{2} \frac{\omega g}{v(\alpha)} \qquad (3.3.6)$$

$$\left.\begin{matrix}\omega t_{i(1)}\\ \omega t_{e(1)}\end{matrix}\right\} = \left\langle \begin{matrix}\omega t_{i(o)}\\ \omega t_{e(o)}\end{matrix} \right\rangle + \kappa \frac{\dot{z}_o}{v(\alpha)} \left\{ \mp \frac{1 \pm \alpha}{2} \frac{\omega g}{v(\alpha)} \sin \psi_o(\alpha) + \cos\left[\psi_o(\alpha) \mp \frac{1 \pm \alpha}{2} \frac{\omega g}{v(\alpha)}\right] - \cos\psi_o(\alpha) \right\} \tag{3.3.7}$$

$\omega t_{i(1)}$ and $\omega t_{e(1)}$ are inserted into the velocity formula (5) which in turn gives the gain in kinetic energy $\Delta W(\alpha) = m/2\ (\dot{z}^2(\omega t_{e(1)}) - \dot{z}^2(\omega t_{i(1)}))$. Subsequent expansion into powers of $\kappa \dot{z}_o / v(\alpha)$ gives zero and first order energy gain, $\Delta W^{(o)}(\alpha)$ and $\Delta W^{(o)} + \kappa \Delta W^{(1)}(\alpha)$:

$$\Delta W^{(o)}(\alpha) = e V_o \frac{v(\alpha)}{\dot{z}_o} \frac{1}{kg/2} \sin\left(\frac{kg}{2} \frac{\dot{z}_o}{v(\alpha)}\right) \cos\left(\psi_o(\alpha) - \alpha \frac{kg}{2} \frac{\dot{z}_o}{v(\alpha)}\right) \tag{3.3.8}$$

$$= e V_o \frac{v(\alpha)}{\dot{z}_o} \left[\sin\left(\frac{kg}{2} \frac{v(\alpha)}{\dot{z}_o}(1-\alpha) + \psi_o\right) - \sin\left(\psi_o - \frac{kg}{2} \frac{v(\alpha)}{\dot{z}_o}(1+\alpha)\right)\right]$$

$\Delta W^{(o)} + \kappa \Delta W^{(1)}$ is rather clumsy and may be found in ref.[31]. The factorization of the dependence of $\Delta W(\alpha)$ on phase on the one hand and on velocity and gap length (transit time factor) on the other, is only possible if $\alpha = 0$, eq. (3.1.10) where the centre is reference point. If the entrance is reference point, $\alpha = -1$, then $\Delta W^{(o)}(\alpha)$ becomes ($v(\alpha = -1) = z_1$ = entrance velocity, $\psi_o(-\alpha) = \phi_1$ = input phase) :

$$\Delta W^{(o)}(\alpha=-1) = e V_o \frac{1}{\dot{z}_1 g/2\omega} \sin\frac{\dot{z}_1 g}{2\omega} \cos\left(\phi_1 + \frac{\dot{z}_1 g}{2\omega}\right) \tag{3.3.9}$$

The first and second order energy gain are compared with the exact value ΔW_{EX} for all α. The value of α where the approximate results come closest to the exact one, is called the optimal reference point α_{opt}. Its position is $z_{ro} = (g/2)\alpha_{opt}$. Results are displayed in Tables 3.3.1, 3.3.2 and in Figs. 3.3.2 - 3.3.4. The optimal reference point is always situated in the first half of the gap, not very far from the centre. But the accuracy of the approximate formulae is in general as good as 1% even if the entrance is taken as reference point.

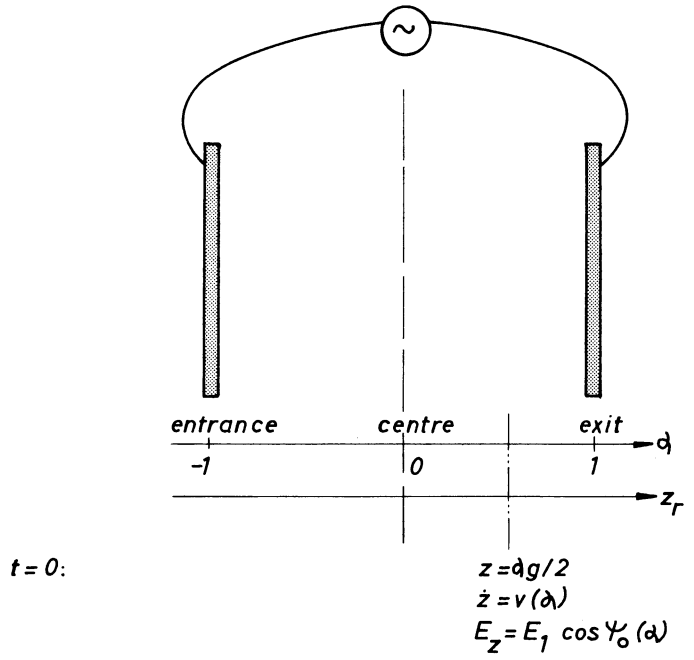

Fig. 3.3.1 Position of the reference point for phase in the gap.

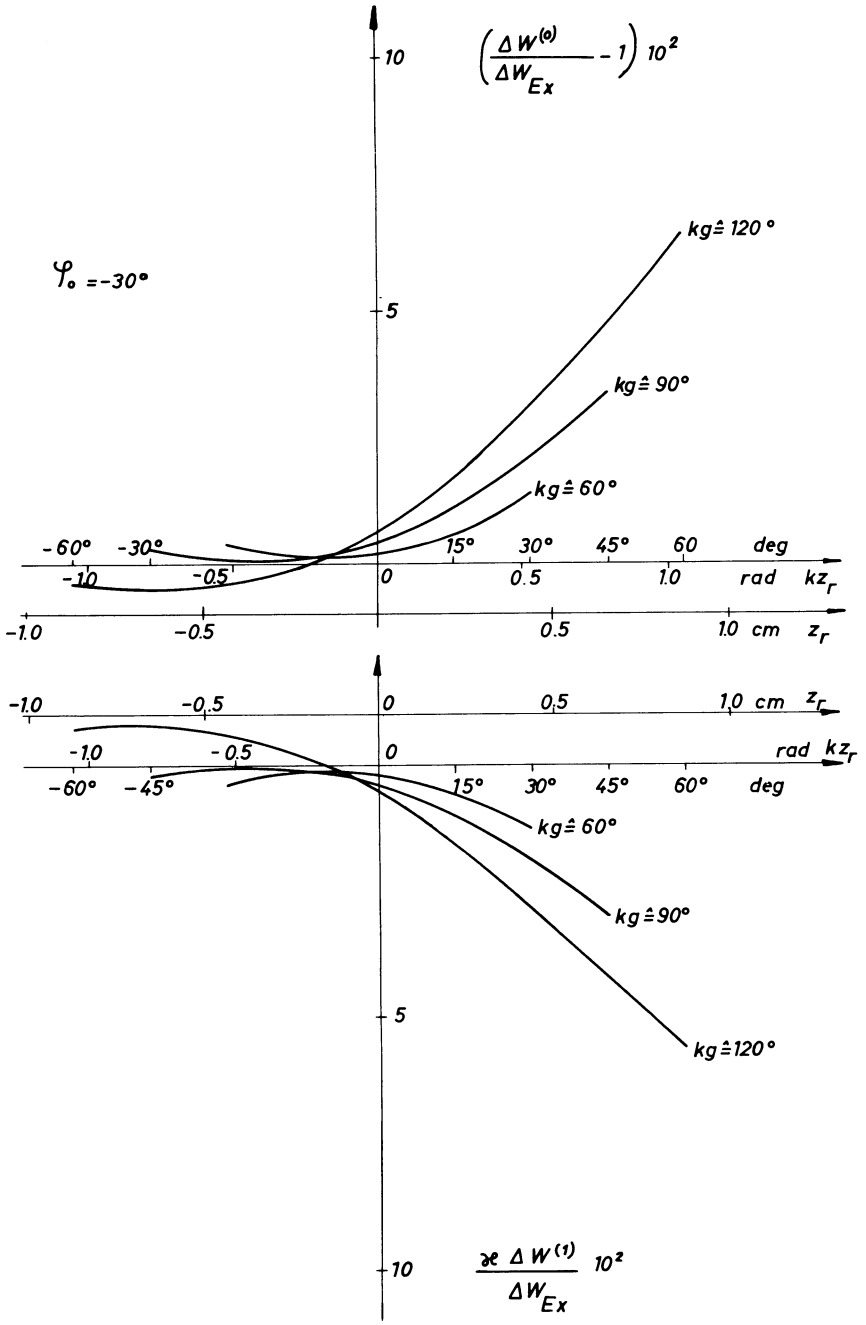

Fig. 3.3.2 Relative deviation of first order energy gain, $\Delta W^{(o)}/\Delta W_{EX}$, versus position of reference point.

Fig. 3.3.3 Relative magnitude of correction term, $\Delta W^{(1)}/\Delta W_{EX}$. It is smallest where first order energy gain is most accurate. $\kappa = eE_1/(m\omega\dot{z}_o) = 0.1$, $E_1 = 14.2$ MV/m, $\omega/2\pi = 200$ MHz, $\dot{z}_o = 0.035\ c$ (~0.5 MeV protons), $k = 119{,}65\ m^{-1}$.

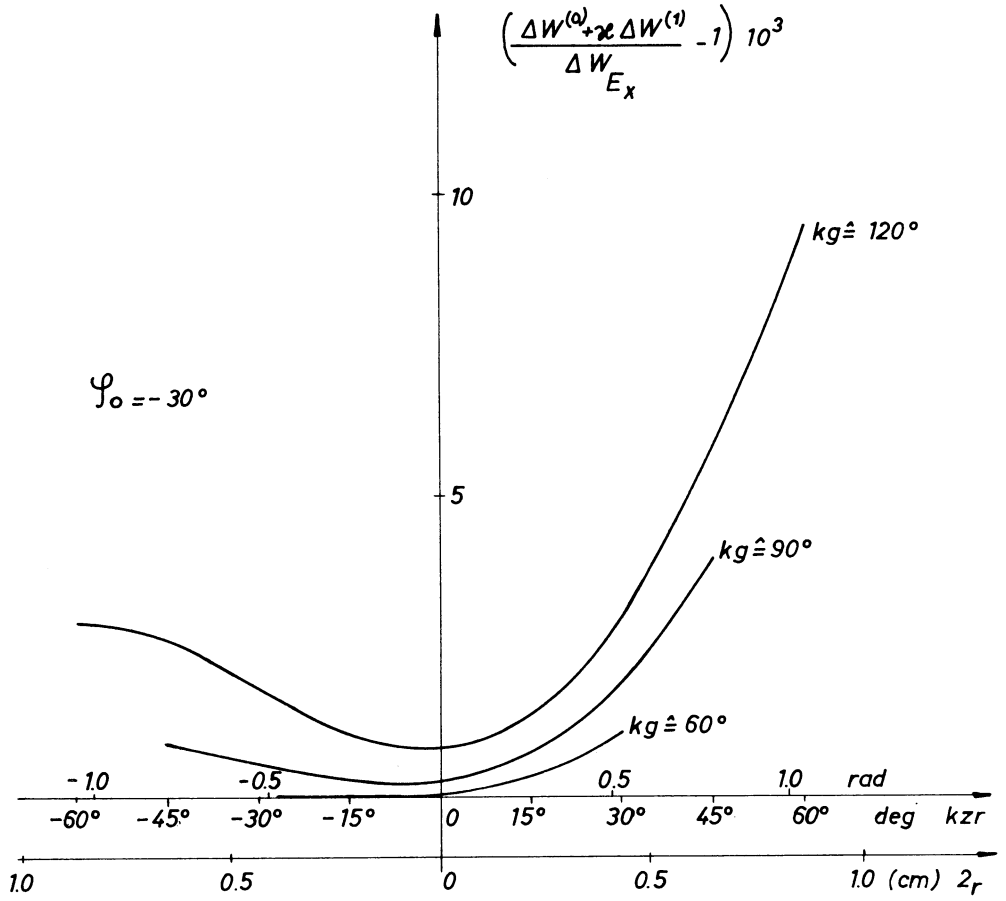

Fig. 3.3.4 Second order energy gain over exact energy gain, $(\Delta W^{(o)} + \kappa \Delta W^{(1)})/\Delta W_{EX}$, versus position of reference point. - $\kappa = eE_1/(m\omega \dot{z}_o) = 0.1$, $E_1 = 14.2$ MV/m, $\omega/2\pi = 200$ MHz, $\dot{z}_o = 0.035$ c (~0.5 MeV protons), k = 119,65 m^{-1}.

TABLE 3.3.1. Position of Optimal Reference point and Energy Gain for 1st order.

φ_o	kg (deg)	g (cm)	α_{opt}	z_{ro} position of optimal reference point (cm)	$\Delta W^{(o)}/\Delta W_{EX}$ $\alpha = \alpha_{opt}$ optimal reference point	$\Delta W^{(o)}/\Delta W_{EX}$ $\alpha = 0$ centre reference point	$\Delta W^{(o)}/\Delta W_{EX}$ $\alpha = -1$ entrance reference point
-15^o	60^o	.88	-0.30	-0.06	1.00004	1.00114	.99975
	90^o	1.31	-0.18	-0.04	0.99976	1.00242	.99384
	120^o	1.75	-0.10	-0.01	0.99996	1.00385	.98055
-30^o	60^o	.88	-0.30	-0.25	1.00146	1.00210	1.00360
	90^o	1.31	-0.49	-0.10	1.00081	1.00420	1.00256
	120^o	1.75	-0.20	-0.04	1.00016	1.00669	0.99538
-45^o	60^o	.88	-0.17	-0.03	1.00262	1.00292	1.00638
	90^o	1.31	-0.27	-0.31	1.00413	1.00569	1.00711
	120^o	1.75	-0.38 (-1.00)*	-0.04	1.00287 (1.00143)*	1.00788	1.00143

$\kappa = eE_1/(m\omega\dot{z}_o) = 0.1$, $E_1 = 14.2$ MV/m, $\omega/2\pi = 200$ MHz, $\dot{z}_o = 0.035$ c ($\sim$0.5 MeV protons), $k = 119{,}65\ m^{-1}$

* In this case the proton is first retarded and then accelerated. This is the reason why there are two values of α ($\alpha = -1$ and -0.38) for which the deviation of the approximate from the exact results has a minimum.

TABLE 3.3.2. Position of Optimal Reference Point and Energy Gain for 2nd Order

ϕ_o	kg (deg)	g (cm)	α_{opt}	z_{ro} position of optimal reference point (cm)	$(\Delta W^{(o)} + \kappa\Delta W^{(1)})/\Delta W_{EX}$ $\alpha = \alpha_{opt}$ optimal reference point	$(\Delta W^{(o)} + \kappa\Delta W^{(1)})/\Delta W_{EX}$ $\alpha = 0$ centre reference point	$(\Delta W^{(o)} + \kappa\Delta W^{(1)})/\Delta W_{EX}$ $\alpha = -1$ entrance reference point
-15^o	60^o	.88	-0.13	-.13	1.00007	1.00008	1.00038
	90^o	1.31	-0.07	-.12	1.00038	1.00039	1.00230
	120^o	1.75	-0.02	-.09	1.00113	1.00113	1.00658
-30^o	60^o	.88	-0.57	-.13	1.00001	1.00005	1.00002
	90^o	1.31	-0.16	-.32	1.00023	1.00027	1.00086
	120^o	1.57	-0.05	-.18	1.00081	1.00082	1.00289
-45^o	60^o	.88	-0.17	-.07	1.00000	1.00002	.99983
	90^o	1.31	-0.44	-.17	1.00001	1.00012	1.00002
	120^o	1.75	-0.05	-.34	1.00040	1.00042	1.00067
			-(1.00)*	(-.88)*	(1.00067)*		

$\kappa = eE_1/(m\omega\dot{z}_o) = 0.1$, $E_1 = 14.2$ MV/m, $\omega/2\pi = 200$ MHz, $\dot{z}_o = 0.035$ c (~ 0.5 MeV protons), $k = 119{,}65\ m^{-1}$.

*) Same footnote as in Table 3.3.1.

3.4 Relativistic Treatment

It is not a very realistic approximation to take into account the relativistic mass variation while neglecting the effect of the magnetic field which necessarily accompanies a time-dependent electric field. Nevertheless it may be useful to treat this example in order to expose the method which is applied to a realistic field in chapter 6.

The relativistic equation of motion :

$$\frac{d}{dt}\ \frac{m\,\vec{v}}{(1-\beta^2)^{\frac{1}{2}}} = \vec{e}_z\ eE_1\cos(\omega t + \phi_o) \qquad (3.4.1)$$

where m is rest mass, is integrated once. With the initial conditions:

$$t = 0 : \quad (x,y,z) = 0\ ,\ (\dot{x},\dot{y},\dot{z}) = \vec{v} = \vec{v}_o = (\dot{x}_o,\dot{y}_o,\dot{z}_o) \qquad (3.4.2)$$

this gives :

$$m\,\vec{v}\,(1-\beta^2)^{-\frac{1}{2}} = m\,\vec{v}_o\,(1-\beta_o^2)^{-\frac{1}{2}} + \vec{e}_z(eE_1/\omega)\left[\sin(\phi+\phi_o) - \sin\phi_o\right] \qquad (3.4.3)$$

where $\phi = \omega t$. This equation cannot be solved exactly. The most annoying feature is the root $(1-\beta^2)^{-\frac{1}{2}}$ on the left hand side. It can be removed by the following method. (3) is divided by mc and squared, i.e. the inner product is formed of the left hand side and of the right hand side respectively :

$$\beta^2(1-\beta^2)^{-1} = \beta_o^2\,(1-\beta_o^2)^{-1} + 2\,(1-\beta_o^2)^{-\frac{1}{2}}\,\frac{\dot{z}_o}{c}\,\kappa_c\left[\sin(\phi+\phi_o) - \sin\phi_o\right] \qquad (3.4.4)$$

$$+\,\kappa_c^2\left[\sin(\phi+\phi_o) - \sin\phi_o\right]^2 \equiv F$$

with $\kappa_c = eE_1/(m\omega c) \approx \kappa\,\beta_o$. This is solved for β^2 and $(1-\beta^2)^{\frac{1}{2}}$ is evaluated:

$$\beta^2/(1-\beta^2) = F \qquad \beta^2 = F/(1+F) \qquad (1-\beta^2)^{\frac{1}{2}} = (1+F)^{-\frac{1}{2}} \qquad (3.4.5)$$

$$(1-\beta^2)^{\frac{1}{2}} = (1-\beta_o^2)^{\frac{1}{2}}\left[1 + 2(1-\beta_o^2)^{\frac{1}{2}}\,\frac{\dot{z}_o}{c}\,\kappa_c\left[\sin(\phi+\phi_o) - \sin\phi_o\right] + (1-\beta_o^2)\,\kappa_c^2\left[\sin(\phi+\phi_o) - \sin\phi_o\right]^2\right]^{-\frac{1}{2}}$$

Multiplying the left hand side of (3) by that of (5) and the right hand side of (3) by that of (5) gives an equation $m\vec{v} = \ldots.$ where the right hand side is a pure function of t (or ϕ) though a quite complicated one. Since κ_c is small

$$\kappa = eE_1/(m\omega\dot{z}_o) < 0.1 \qquad \kappa_c = eE_1/(m\omega c) < 3.6 \times 10^{-3} \qquad (3.4.6)$$

the root in (5) is expanded in powers of κ_c. The resulting simplification permits to integrate the equation of motion $m\vec{v} = \ldots.$ by integrating the right hand side term by term:

$$\left.\begin{matrix} x \\ y \end{matrix}\right\} = \left.\begin{matrix} \dot{x}_o \\ \dot{y}_o \end{matrix}\right\} \cdot \frac{1}{\omega} \Bigg\{ \phi + \kappa_c \frac{\dot{z}_o}{c} (1 - \beta_o^2)^{\frac{1}{2}} \left[\cos(\phi + \phi_o) - \cos\phi_o + \phi \sin\phi_o \right] \qquad (3.4.7)$$

$$+ \kappa_c^2 (1 - \beta_o^2) \left(\frac{3}{2} \frac{\dot{z}_o^2}{c^2} - \frac{1}{2} \right) \Bigg(\phi \left(\frac{1}{2} + \sin^2\phi_o \right) + 2 \sin\phi_o \left[\cos(\phi + \phi_o) - \cos\phi_o \right] - \frac{1}{4} \left[\sin\left[2(\phi + \phi_o) \right] - \sin(2\phi_o) \right] \Bigg) + \ldots \Bigg\}$$

$$z = \frac{\dot{z}_o}{\omega} \Bigg\{ \phi - \left(\kappa - \frac{\dot{z}_o}{c} \kappa_c \right) (1 - \beta_o^2)^{\frac{1}{2}} \left[\cos(\phi + \phi_o) - \cos\phi_o + \phi \sin\phi_o \right]$$

$$- \kappa_c^2 (1 - \beta_o^2) \frac{3}{2} \left(1 - \frac{\dot{z}_o^2}{c^2} \right) \Bigg(\phi \left(\tfrac{1}{2} + \sin^2\phi_o \right) + 2 \sin\phi_o \left[\cos(\phi + \phi_o) - \cos\phi_o \right] - \frac{1}{4} \left[\sin\left[2(\phi + \phi_o) \right] - \sin(2\phi_o) \right] \Bigg) + \ldots \Bigg\}$$

(3.4.8)

with $k = \omega/\dot{z}_o$, eq. (3.1.4). The equation for the transverse coordinates displays the coupling between longitudinal and transverse motion due to the relativistic mass variation. Solving equation (8) for phase ϕ by iteration as in (3.1.6), (3.1.7) gives :

$$\phi_{(2)}(z) = kz + \left(\kappa - \frac{\dot{z}_o}{c} \kappa_c \right) (1 - \beta_o^2)^{\frac{1}{2}} \left[\cos(kz + \phi_o) - \cos\phi_o + kz \sin\phi_o \right]$$

$$- \left(\kappa - \frac{\dot{z}_o}{c} \kappa_c \right)^2 (1 - \beta_o^2) \left[\cos(kz + \phi_o) - \cos\phi_o + kz \sin\phi_o \right] \times$$

$$\left[\sin(kz + \phi_o) - \sin\phi_o \right] \qquad (3.4.9)$$

$$+ \kappa_c^2 (1 - \beta_o^2) \frac{3}{2}\left(1 - \frac{\dot{z}_o^2}{c^2}\right) \left(kz \left(\frac{1}{2} + \sin^2\phi_o\right) + 2 \sin\phi_o \left[\cos(kz + \phi_o) - \cos\phi_o\right] - \frac{1}{4}\left[\sin(2kz + 2\phi_o) - \sin(2\phi_o)\right]\right) + \ldots$$

If $\dot{z}_o \approx \beta c$ approaches the velocity of light, phase ϕ becomes :

$$\lim_{\dot{z}_o \to c} \phi(z) = kz \qquad (3.4.10)$$

The velocity no longer increases and the phase increases linearly with distance. Reduced phase $\bar{\phi} = \phi - z\, d\phi/dz = k = \omega/\dot{z}_o$ (cf. Section 4.2) is constant . Inserting (5) into the relativistic expression for the change in total kinetic energy :

$$\Delta W_{tot} = mc^2 \left[(1 - \beta_e^2)^{-\frac{1}{2}} - (1 - \beta_i^2)^{-\frac{1}{2}} \right] \qquad (3.4.11)$$

(the subscripts i and e denote the $\beta = v/c$ of entrance and exit) and subsequent expansion in powersof κ_c gives :

$$\Delta W_{tot} = mc^2 \left\{ \frac{\dot{z}_o}{c} \kappa \left[\sin\left[\phi(g/2) + \phi_o\right] - \sin\left[\phi(-g/2) + \phi_o\right] \right] + \kappa_c^2 (1 - \beta^2)^{\frac{1}{2}} \frac{1}{2} \left(1 - \frac{\dot{z}_o^2}{c^2}\right) \left(\left[\sin\left[\phi(g/2) + \phi_o\right] - \sin\phi_o\right]^2 - \left[\sin\left[\phi(-g/2) + \phi_o\right] - \sin\phi_o\right]^2 \right) + \ldots \right\} \qquad (3.4.12)$$

Introducing $\phi_{(2)}(\pm g/2)$ from (9) gives the increase in total kinetic energy:

$$\Delta W_{tot} = e V_o T_{oh}(k) \cos\phi_o + e V_o \kappa (1 - \beta_o^2)^{\frac{1}{2}} \left(1 - \frac{\dot{z}_o^2}{c^2}\right) \left[\frac{1}{2} \cos\left(\frac{kg}{2}\right) - \frac{\sin(kg)}{kg} \right] + \kappa^2 \ldots \qquad (3.4.13)^{*)}$$

with the high relativistic limit :

$$\lim_{\dot{z}_o \to c} \Delta W_{tot} = \Delta W = e V_o T_{oh}(k) \cos\phi_o \qquad (3.4.14)$$

---

*) Equations (36), (37), (39) and (40) of ref.[31] (corresponding to equations (8), (9) and (13) of this section) contain an error.

The same result follows from (3.1.9) with the help of (10).

The second term of (13) may be split up into two parts, one proportional to κ which arises from the second iteration, the other proportional to $\kappa\dot{z}_o^2/c^2$ which is due to the mass variation. This already hints to the fact that relativistic contributions are of the order $\kappa\beta_o^2$.

4. Approximation Schemes

In the first section of this chapter the general methods of solving approximately the equations of motion are explained. In Section 4.2 the thin lens approximation is described. This is a method generally employed but scarcely described in full. The end of this section treats shortly the canonically conjugate thin lens variables and may help to correct some wide-spread misconception about them.

4.1. General Considerations on Perturbation Theory

In this section are presented the somewhat different methods of approximation employed in solving equations of motion with a field too complicated to permit an exact solution. For simplicity the discussion will be restricted to the one-dimensional problem. As in chapter three, subscripts indicate the order of iteration; superscripts denote the order of the perturbation equation, i.e. the power of the perturbation parameter κ accompanying the expression.

In one method the equation of motion :

$$\ddot{z} = F(z,t) \tag{4.1.1}$$

containing the force term $F(z,t)$ is solved by iteration: a zero order approximation $z_o(t)$ is assumed for the trajectory; this is inserted into the right hand side of (1), which becomes a pure function of t, and the differential equation can be integrated by quadratures. This procedure can be repeated :

$$\ddot{z}_1 = F(z_o(t),t) \equiv G_1(t) \ , \ \ddot{z}_2 = F(z_1(t),t) \equiv G_2(t) \ , \ \ldots \tag{4.1.2}$$

In the present application the initial trajectory is that of a free particle, i.e. $z_o(t) = \dot{z}_o t = z^{(o)}(t)$.

The other approach, perturbation theory, is at first explained in a problem which is somewhat different in nature from that to which the method is applied in Chapters 5 and 6. The peculiarities which arise if the unperturbed motion is free particle motion, will be discussed after the general principle has been described. In perturbation theory it is assumed that the problem to be solved :

$$\ddot{z} = g(z,t) + \kappa f(z,t) = F(z,t) \tag{4.1.3}$$

belonging to the external force $F(z,t) = g(z,t) + \kappa f(z,t)$, with $g \neq 0$), is not very much different from one with the external force $g(z,t)$:

$$\ddot{z} = g(z,t) \tag{4.1.3a}$$

whose solution $z^{(o)}(t)$ is known :

$$\ddot{z}^{(o)}(t) = g(z^{(o)}(t),t) \tag{4.1.3b}$$

In other words: The term κf in eq. (3), the perturbation is small compared to g, the unperturbed force. It is not indispensible, but very advantageous to express the

smallness of the perturbation by a perturbation parameter κ as indicated in equation (3), where it is assumed that g and f are of about the same order of magnitude while κ is small compared to unity.

An example of this kind is the motion of an artificial satellite (with an orbit not too far from earth) in the joint gravitational field of earth and moon. The unperturbed motion is that of the satellite in the sole field of the earth, $g \sim m_e/r^2$ where m_e is earth mass and r the distance of these two bodies. The solution corresponding to $z^{(o)}(t)$ is a Kepler ellipse. The perturbation is the additional gravitational field due to the moon. The perturbation parameter κ is the ratio $m_m/(m_e + m_m)$ where m_m is the moon mass. Before the advent of the space age the standard example of this so-called restricted three body problem was the motion of a planetoid in the common gravitational field of sun and Jupiter [36].

The solution of (3) is expressed as a power series in κ :

$$z(t) = z^{(o)}(t) + \kappa z^{(1)}(t) + \kappa^2 z^{(2)}(t) + \ldots \qquad (4.1.4)$$

For the further treatment the basic assumption is made that all functions are analytic in κ ; each equation must be fulfilled separately in each power of κ. Inserting (4) into (3) , expanding into powers of κ and comparing coefficients of equal powers of κ , gives :

$$\begin{aligned}
\kappa^o &: \ddot{z}^{(o)} = g(z^{(o)}(t),t) \\
\kappa &: \ddot{z}^{(1)} - z^{(o)}(t)\, g_z(z^{(o)}(t),t) = f(z^{(o)}(t),t) \qquad (4.1.5) \\
\kappa^2 &: \ddot{z}^{(2)} - z^{(2)}(t)\, g_z(z^{(o)}(t),t) = \frac{1}{2} z^{(1)2} g_{zz}(z^{(o)},t) + z^{(1)} f_z(z^{(o)},t)
\end{aligned}$$

The subscript, z, of g and f denotes partial derivation with respect to the independent variable z. The solution of the zero order equation is known by assumption; in the succeeding ones the n^{th} right hand side contains only functions already found in the preceding steps. The whole equation is solved to get the n^{th} approximation, $z^{(n)}(t)$. It is assumed that $z^{(n+1)}(t)$ is not greater than $z^{(n)}(t)$ for the range of t considered, so that the choice of κ , and the assumption of the series (4), are reasonable and allow an estimate of the accuracy attained with the first n terms of (4).

Now it is necessary to generalize the method just described for the present applications where the zero order approximation is assumed to be motion without force, i.e. free particle motion : $g = o$, $F = \kappa f$. It is no longer possible to compare forces and to suppose that $|\kappa f| \ll |g|$. Still it is conceivable that the motion of a fast moving particle is not changed very much by a weak field of force to which it is exposed during a short time; and that the difference between the two trajectories is not very great. This vague notion of smallness of the influence the field exerts upon the otherwise free particle passing it,

may be sharpened by the statement : The impulse transmitted to the particle during the time it traverses the interaction region, should be small compared to the free particle momentum. In the case where $g = 0$ it is no longer possible to find a suitable perturbation parameter, κ, by inspection of the equations of motion in Newtonian form (3). Other forms of them may be more suitable, as for example the system in canonical form (3.1.18) which is equivalent to the Newtonian form (3.1.1). The right hand side of (3.1.18a) appears again as the sum of two terms, the second being multiplied by $\kappa = (eE_1/\omega)/(m\dot{z}_o)$ while g and f are of about the same order of magnitude, provided $\kappa \ll 1$.

In order to guess κ, it is necessary to rely on physical considerations of the kind given above, on equations already containing the result (e.g. (3.1.8) to (3.1.10)) and on the relations which connect in the case $g \equiv 0$ the solutions of the systems (2) with those of (5), namely :

$$z_o(t) = z^{(o)}(t) \ , \ z_1(t) = z^{(o)}(t) + \kappa z^{(1)}(t)$$
$$z_2(t) = z^{(o)}(t) + \kappa z^{(1)}(t) + \kappa^2 z^{(2)}(t) + \kappa^3 \ldots \qquad (4.1.6)$$

They are derived in appendix A.

From this comparison and from the results of chapters 3 and 5, it may be concluded that $\kappa = eE_1/(m\omega\dot{z}_o)$ of (3.1.5), (5.1.4) is a suitable parameter to describe the influence of the electric field upon the motion of an otherwise free particle, where to each power of κ corresponds an order in iteration and where the power of κ gives the order of magnitude of the whole term. It may also be concluded from the relativistic treatment in Section 3.3 and Chapter 6 that the order of magnitude of relativistic effects (force of the magnetic radio frequency field and mass variation) is given by $\kappa k_o^2/k^2 \approx \kappa \beta^2$. Fig. 4.1.1 shows the relative magnitude of these various parameters depending on particle velocity which nearly equals the longitudinal velocity.

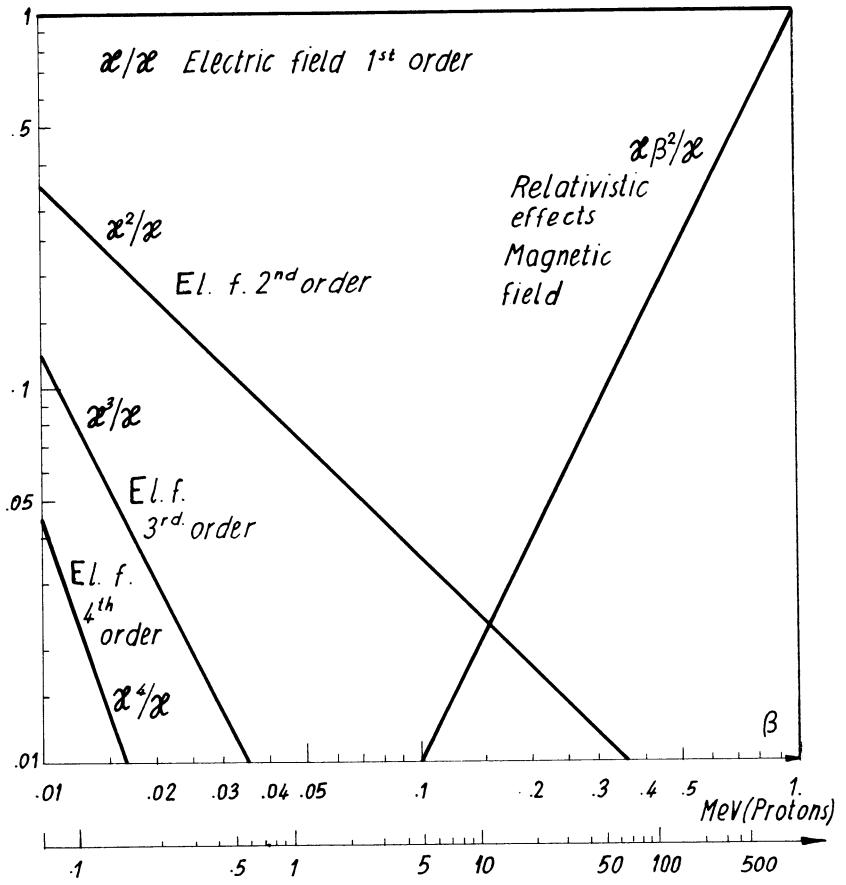

Fig. 4.1.1 Relative magnitude of perturbation parameters κ, κ^2, ..., $\kappa\beta^2$, versus (longitudinal) particle velocity. First order contributions ($\sim\kappa$) have been normalized to unity. $\kappa = eE_1/(m\omega\dot{z}_o)$, $\dot{z}_o \approx \beta$, $\omega/2\pi$ = 200 MHz, E_1 = 14.2 MV/m, m = proton rest mass.

4. 1.A Relation between Iterative and Perturbation Theoretic Solution

The following considerations where the solutions found by iterations are compared with those due to perturbation theory, do not represent a mathematical proof. Formal expansions are employed, and the question of convergence is not touched. The convergence of such series is discussed in ref. [34]. (Cf. Section 3.1.B).

The equation of motion :

$$\ddot{z} = F(z,t) \tag{4.1.1}$$

with initial conditions :

$$t = 0 \; : \; z = 0 \; , \; \dot{z} = \dot{z}_o \tag{4.1.7}$$

is solved by iteration. At the beginning the trial solution $z_{(o)}(t)$ is inserted and the resulting equation is integrated twice with respect to time. This gives in view of the initial conditions (7) :

$$\ddot{z}_{(1)} = F(z_{(o)}(t),t) \tag{4.1.8a}$$

$$\dot{z}_{(1)}(t) = \int_o^t d\bar{t} \; F(z_{(o)}(\bar{t}),\bar{t}) + \dot{z}_o \tag{4.1.8b}$$

$$z_{(1)}(t) = \int_o^t d\bar{t} \int_o^{\bar{t}} d\bar{\bar{t}} \; F(z_{(o)}(\bar{\bar{t}}),\bar{\bar{t}}) + \dot{z}_o t \tag{4.1.8c}$$

Then the solution $z_{(1)}(t)$ is used to give the second approximation :

$$\ddot{z}_{(2)} = F(z_{(1)}(t),t) \tag{4.1.9a}$$

$$\dot{z}_{(2)} = \ldots \tag{4.1.9b}$$

$$z_{(2)}(t) = \int_o^t d\bar{t} \int_o^{\bar{t}} d\bar{\bar{t}} \; F(z_{(1)}(\bar{\bar{t}}),\bar{\bar{t}}) + \dot{z}_o t \tag{4.1.9c}$$

Another set of solutions is found by perturbation theory. At present the total force acting upon the particle is regarded as a perturbation $\kappa f(z,t)$. There is no unperturbed force $g(z,t)$ in the equation of motion (3) :

$$\ddot{z} = F(z,t) \equiv \kappa \, f(z,t) \qquad g(z,t) \equiv 0 \tag{4.1.10}$$

Assuming the perturbation expansion :

$$z(t) = z^{(o)}(t) + \kappa z^{(1)}(t) + \kappa^2 z^{(2)}(t) + \kappa^3 \ldots \qquad (4.1.11)$$

eq. (10) is split into the system of perturbation equations :

$$\ddot{z}^{(o)} = 0 \qquad (4.1.12$$

$$\ddot{z}^{(1)} = f(z^{(o)}(t),t) \qquad (4.1.13)$$

$$\ddot{z}^{(2)} = f_z(z^{(o)}(t),t) \qquad (4.1.14)$$

where the subscript, z, denotes partial derivation with respect to the independent variable z. Its solution belonging to the initial conditions (7) are :

$$z^{(o)} = \dot{z}_o t = z_o(t) \qquad (4.1.12a)$$

$$z^{(1)}(t) = \int_o^t d\bar{t} \int_o^{\bar{t}} d\bar{\bar{t}} \; f(z^{(o)}(\bar{\bar{t}}),\bar{\bar{t}}) \qquad (4.1.13a)$$

$$z^{(2)}(t) = \int_o^t d\bar{t} \int_o^{\bar{t}} d\bar{\bar{t}} \; f_z(z^{(o)}(\bar{\bar{t}}),\bar{\bar{t}}) \qquad (4.1.14a)$$

Now the two sets are put in relation to each other under the assumption that the trial solution $z_{(o)}(t)$ used in eq. (8) describes free particle motion :

$$z_{(o)}(t) = z^{(o)}(t) = \dot{z}_o t \qquad (4.1.15)$$

Take the first two terms of (11) and insert into this expression the solutions (12a) and (13a). Comparing this with (8c) given in view of $F \equiv \kappa f$:

$$z_{(1)}(t) = z^{(o)}(t) + \kappa z^{(1)}(t) \qquad (4.1.16)$$

This is inserted into (9c) and the resulting equation is expanded into a Taylor's series with respect to κ :

$$z_{(2)}(t) = \dot{z}_o t + \int_o^t d\bar{t} \int_o^{\bar{t}} d\bar{\bar{t}} \; F(z^{(o)}(\bar{\bar{t}}) + \kappa z^{(1)}(\bar{\bar{t}}),\bar{\bar{t}}) \qquad (4.1.17)$$

$$= z^{(o)}(t) + \int_o^t d\bar{t} \int_o^{\bar{t}} d\bar{\bar{t}} \; \{F(z^{(o)},\bar{\bar{t}}) + \kappa z^{(1)}(\bar{\bar{t}}) \; F_z(z^{(o)},\bar{\bar{t}}) + \kappa^2 \ldots\}$$

Comparing this with (11) where now the first three terms are retained, gives with $F \equiv \kappa f$:

$$z_{(2)}(t) = z^{(o)}(t) + \kappa z^{(1)}(t) + \kappa^2 z^{(2)}(t) + \kappa^3 \ldots \qquad (4.1.18)$$

Eqs. (15), (16) and (18) are the three equations quoted in eq. (6).

The results of the first iteration equals that of first order perturbation theory. The solution found by the second iteration is not exactly equal to that found by second order perturbation theory : Second order perturbation theory gives only terms which are proportional to κ^0, κ^1 and κ^2 . The second iteration solution may be expanded into a Taylors series in κ and the terms proportional to κ^0, κ^1, κ^2 will be the same as those due to perturbation theory; but it still contains terms of higher powers by which it differs from the perturbation theoretic solution. The same situation is observed in higher orders.

For a uniform field $F_z = 0$, and the first order approximation gives already the exact solution, eq. (3.1.3). All higher approximations just reproduce this solution. However, if z is chosen as the independent variable the solutions no longer can be given exactly. In this case the equivalence between iterations and perturbation theory is again restricted to that described just before. For example, second order results are not exactly equal, as is revealed by the comparison in eq. (3.1.8b).

4.2 Treatment of Particle Trajectories. The Thin Lens Approximation

The numerical integration of particle trajectories through a linac gap makes use of two different methods : One employs step by step integration of Newton's equations :

$$m\, d/dt\, \vec{v}/(1 - \beta^2)^{\frac{1}{2}} = e\vec{E}(z,r,t) + e\, \vec{v} \times \mu\vec{H}(z,r,t) \qquad (4.2.1)$$

Nowadays programmes for a Runge-Kutta (or similar) treatment of differential equations are available in almost every computer library. However, such an approach has certain disadvantages, it is time-consuming and, in addition, it may require large amounts of storage capacity to provide information on the fields accelerating the particle. These drawbacks become prohibitively severe in case of computations following particles through the whole linac. (The travelling wave approach not considered here, is not sufficiently accurate to give more than qualitative results). For this reason, this method is now rarely used, its application is in general limited to checks of consistency and accuracy of the second [9) 37)].

The second method has been proposed by PANOFSKY[1)] to compute longitudinal motion of a proton in an Alvarez type linear accelerator. Considering the successive gaps as really independent, and separated by drift space where the r.f. field is practically zero, PANOFSKY derived an expression for the energy gain of a particle in such a gap as if it were reduced to its median plane. The longitudinal motion can then be computed in a way similar to beam optics with thin lenses, i.e. at each gap particles receive an energy which they keep along the drift space up to the centre of the next gap. This approach has been refined by several authors (e.g.[4) 5) 9)] and extended to include transverse motion. It is somewhat of a matrix type (but not necessarily linear) and is extensively used in the design and analysis of proton linear accelerators [11)].

In this Section the "thin lens approximation" will be described. (Chapter 5 is devoted to the explicit derivation of the pertinent matrix elements (or difference equations) which is accomplished by approximate solution of the equation of motion in a linac gap.) The real path of a particle crossing a cell ($-L_1 \leq z \leq L_2$), or the quadrupole field-free part of a cell, is replaced by a fictitious one in which the whole change of motion (in both longitudinal and transverse planes) takes place in the median plane, i.e. the gap centre,and outside of this plane the particle moves as if it were free. The term "lens" as used in this context does not describe a physically realizable device ; it is only a mathematical prescription for treating fictitious trajectories.

It may be worthwhile to stress the difference between this method used in particle optics and those used in ordinary (light) optics. In ordinary (geometrical) optics a thick lens is described by two principal planes. To each of them belongs a focal point. If the position of these planes and the focal length are known, it is possible to construct for each ray entering the system the corresponding one leaving it. The intermediate ray connecting the

external ones may be again fictitious, but it is continuous. If the optical lens is sufficiently thin so that the two principal planes coincide, or are at least very near to each other, it is possible to represent this lens by just one principal plane with two foci. This is the thin lens approximation as the term is used in ordinary optics. The term thin lens approximation given to the method used here in particle optics covers a different description. In a proton linac the accelerating gap regarded as a beam optical lens is a thick lens, i.e. it cannot be described by only one principal plane in the sense this word is used in light optics. However, it is more convenient to represent it by one plane situated in the gap centre in place of two principal planes. But this beam optical thin lens approximation must use discontinuous "rays" as shown in the figures below. There is also a two lens method, where the fictitious trajectory is continuous, but is bent at two planes which are again called "lenses" [12].

In any approach of this kind the spatial coordinate z (measured along the linac axis) is singled out and it is envisaged to introduce it as the independent variable; in consequence, time t (or time-angle (phase) $\phi = \omega t$) becomes a dependent variable, $\phi = \phi(z)$, and together with total energy E ($-E/\omega$) it gives the pair of canonically conjugate longitudinal coordinates.* Either the equations of motion must be appropriately transformed from the beginning; or if the common shape (1) of Newton's equations is retained, as is done here, the change of variables must be carried out in the composition of the difference equations. At low energy the substitution dt = const. dz provides a poor approximation to this requirement.

Momentum-like coordinates (e.g. radial momentum p_r, total (or longitudinal) kinetic energy or total energy) are constant in force-free regions and the fictitious trajectory is just a step function (see Fig. 4.2.1) :

$$\begin{aligned} -L_1 \leq z \leq -0 &: T(z) = W_- \\ +0 \leq z \leq L_2 &: T(z) = W_+ = W_- + \Delta W \end{aligned} \qquad (4.2.2)$$

In place of radial momentum :

$$\begin{aligned} -L_1 \leq z \leq -0 &: p_r = p_{r-} \\ +0 \leq z \leq L_2 &: p_r = p_{r+} = p_{r-} + \Delta p_r \end{aligned} \qquad (4.2.3)$$

radial slope, $r' = dr/dz$, often is preferred because it is accessible to direct measurement by slits. Its difference equations are :

$$\begin{aligned} -L_1 \leq z \leq -0 &: r' = r'_- \\ +0 \leq z \leq L_2 &: r' = r'_+ = r'_- + \Delta r' \end{aligned} \qquad (4.2.4)$$

---

* Another pair are reduced phase, $\bar{\phi}$, and $-T/\omega$, longitudinal kinetic energy divided by ω.

The other variables (e.g. time-angle (phase) $\phi(z)$ or radial position r) linearly increase with z in domains free from fields. In fact, in such regions z and r vary linearly with time t (or ϕ) and the inverse of a linear function is also linear. The fictitious thin lens trajectory is (cf. Fig. 4.2.2) ; $' = d/dz$) :

$$\begin{aligned} -L_1 \leq z \leq -0 \quad &: \phi(z) = \phi(-L_1) + (z + L_1)\phi'(-L_1) \\ -0 \leq z \leq +0 \quad &: \phi_- = \phi(-0) \rightarrow \phi_+ = \phi(+0) = \phi(-0) + \Delta\bar{\phi} \\ +0 \leq z \leq L_2 \quad &: \phi(z) = \phi(+0) + z\,\phi'(L_2) \end{aligned} \tag{4.2.5}$$

and (Fig. 4.2.3)

$$\begin{aligned} -L_1 \leq z \leq -0 \quad &: r(z) = r(-L_1) + (z + L_1)r'(-L_1) \\ -0 \leq z \leq +0 \quad &: r = r(-0) \rightarrow r = r(+0) = r(-0) + \Delta\bar{r} \\ +0 \leq z \leq L_2 \quad &: r(z) = r(+0) + z\,r'(L_2) \end{aligned} \tag{4.2.6}$$

The fictitious trajectory is discontinuous in $\phi(z)$ and $r(z)$. However, the jumps $\Delta\bar{\phi}$ and $\Delta\bar{r}$ do not correspond to the total change of phase and radial position across the gap, but only to the difference in reduced phase:

$$\bar{\phi}(z) = \phi(z) - z\,\phi'(z) \tag{4.2.7}$$

$$\Delta\bar{\phi} = \bar{\phi}(+0) - \bar{\phi}(-0) = \phi(+0) - \phi(-0) = \phi(L_2) - L_2\phi'(L_2) - \phi(-L_1) - L_1\phi'(-L_1) \tag{4.2.8}$$

and reduced radial position :

$$\bar{r}(z) = r(z) - z\,r'(z) \tag{4.2.9}$$

$$\Delta\bar{r} = \bar{r}(+0) - \bar{r}(-0) = r(+0) - r(-0) = r(L_2) - L_2r'(L_2) - r(-L_1) - L_1r'(-L_1) \tag{4.2.10}$$

$\Delta\phi$ and Δr become infinite if one or both L_j tend to infinity, while $\Delta\bar{\phi}$ and $\Delta\bar{r}$ approach finite limits. These jumps account for the fact that the field accelerating the particle is distributed throughout the gap. This has been overlooked in earlier work[1]. The error has been detected by J.S. BELL[2] and later by PROME [6) 9)] for phase. In the paper just quoted [9)] radial position has been correctly treated; PARMILA had to be cured from this defect [37)]. An equivalent alternative method introduced by PROME [11) 12)] employs two lenses, one at each gap end (see Fig. 4.2.3).

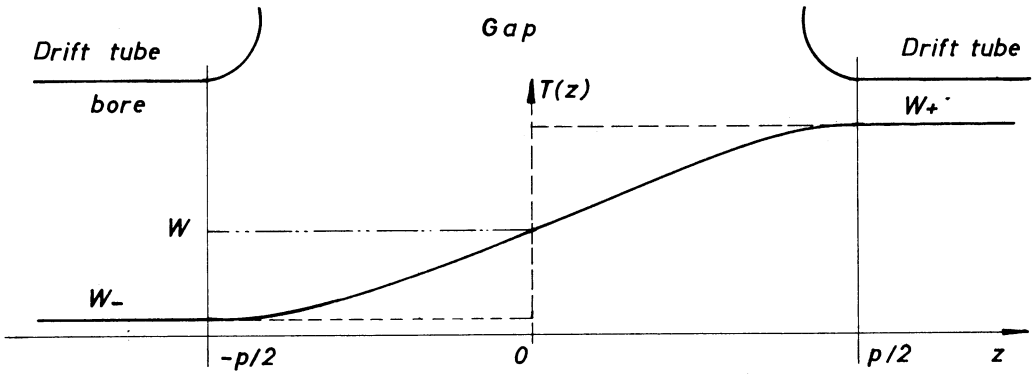

Fig. 4.2.1. Thin lens approximation for longitudinal kinetic energy. The real trajectory (———) is replaced by the step function (---). W is the mid-gap value of T. The same procedure applies to other momentum-like variables.

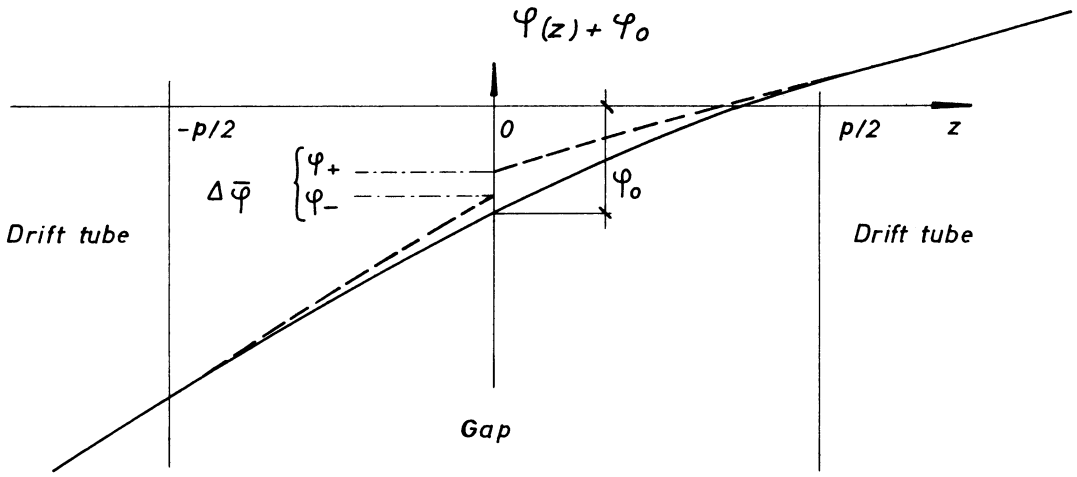

Fig. 4.2.2 Thin lens approximation for phase (or time-angle), $\phi(z) + \phi_o = \omega t + \phi_o$. The real trajectory (———) is replaced by two straight lines (---) with input slope $d\phi/dz|_{z=-L_1}$ and output slope $d\phi/dz|_{z=L_2}$ respectively connected by $\Delta\bar{\phi}$ which is only the change in reduced phase.

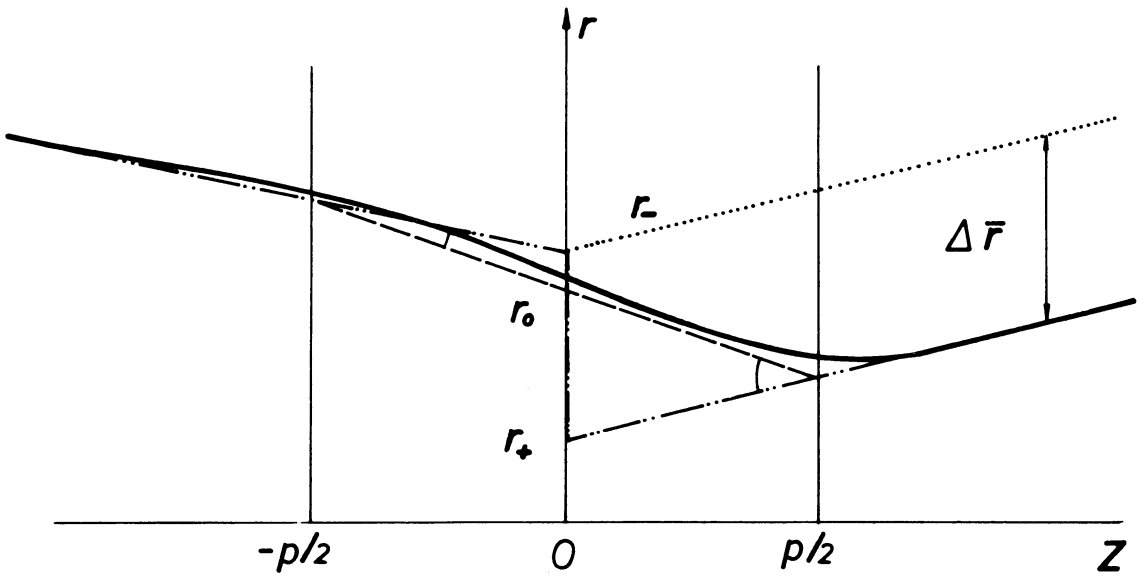

Fig. 4.2.3 Thin lens and two lens approximation for radius. The action of the radial electrical field E_r distributed throughout the gap can be approximated by one "lens" situated at the centre (z = 0) producing a discontinuous trajectory (-..-..) or by two lenses (one at each gap end $z = \pm p/2$) yielding a continous trajectory (- - -). Both methods give trajectories equivalent to the real one (———). Earlier methods (e.g. PARMILA 1) which employed one lens, but retained a continuous trajectory (....) could not account for the fact that the force is distributed throughout the gap, and yielded incorrect results.

The action of the accelerating field upon the particle trajectories is incorporated both into the increments ΔW, Δp_r (or $\Delta r'$), $\Delta\bar{\phi}$, $\Delta\bar{r}$ and into the slopes ϕ' and r' in equations (5),(6) respectively, which are different before and after the lens situated at z = 0.

In this context arises the question whether it is possible to set up a thin lens Hamiltonian H_{TL} from which the increments $\Delta(-W/\omega)$, $\Delta\bar{\phi}$, Δp_r, $\Delta\bar{\bar{r}}$ may be derived by differentiations with respect to mid-gap values :

$$\begin{aligned} \Delta(-W/\omega) &= -\,\partial H_{TL}/\partial\bar{\phi}_o \\ \Delta\bar{\phi} &= \partial H_{TL}/\partial(-W_o/\omega) \\ \Delta p_r &= -\,\partial H_{TL}/\partial\bar{\bar{r}}_o \\ \Delta\bar{\bar{r}} &= \partial H_{TL}/\partial p_{ro} \end{aligned} \qquad (4.2.11)$$

The principles how to find such a Hamiltonian have been explained by the author [38]. It is necessary to introduce canonically conjugate reduced variables by canonical transformations. A set of such canonically conjugate variables is :

$$\begin{aligned} Q_\phi &= \bar{\phi} = \phi - z\, d\phi/dz \\ P_\phi &= -\,T/\omega \\ P_r &= p_r + \ldots \\ Q_r &= r - \phi\, p_r/(m\omega) + \ldots = r - \phi\, dr/d\phi + \ldots = \bar{\bar{r}} + \ldots \end{aligned} \qquad (4.2.12)$$

T is longitudinal kinetic energy, $m\,\dot{z}^2/2$. The dots in the equations for the radial variables Q_r, P_r indicates that there have been omitted terms involving the potential of the accelerating field which vanish in the limit $|z| \to \infty$. Therefore in the limit $L_j \to \infty$ the increments of all four variables across the whole gap agree with those of the left hand sides of (11). Unfortunately, the derivation of the thin lens Hamiltonian belonging to the set of equations (11) by canonical transformations meets some practical difficulties. The canonically conjugate radial variables as indicated above, can be given only after the potential has been approximated by the first terms of a power series in r (same expansion as in eq. (5.1.12)). This entails further complications rendering the procedure impractical in applications, (see also ref. 41 which is an improved version of ref. 38).

The canonically conjugate radial variables as given in eq. (12) differ from $r' = dr/dz$, eq. (4) and $\bar{r} = r - z\, dr/dz$, eq. (9), the radial variables usually employed in the treatment of particle dynamics. In fact, r' and $\bar{r}$ are not canonically conjugate variables since their

Poisson bracket is different from unity already to the first order in κ, i.e. in the fields. By the method developed in ref. [38] it can be shown that the Poisson bracket for the two variables αr , $\beta r'$ (α,β constants) is :

$$(\alpha r,\beta r') = \alpha\beta/(m\dot{z})\left[1 + (dr/dz)^2\right] = (\dot{z}_o/\dot{z})\left[1 + (dr/dz)^2\right] \qquad (4.2.13)$$

$$= 1 + \kappa \ldots$$

where for convenience $\alpha\beta = m\,\dot{z}_o$ has been taken and where the coefficient of κ is different from zero. In addition, the Poisson brackets between any one of the two longitudinal coordinates $\phi = Q_\phi$, $P_y = -T/\omega$ on the one hand and any one of the pair r', $\bar{r}$ on the other are different from zero already to the first order in κ. In consequence, these variables do not fulfil Liouville's theorem, even not to the first order in the field. Of course it is completely admissible to describe particle dynamics by variables which lack this property.

5. Non-Relativistic Motion of a Proton in a Realistic Field

Here the non-relativistic equations of motion containing the real field of a gap are solved and the beam dynamics difference equations are derived. Calculations are lengthy and involved. An easy way is described at the beginning of Section 5.2; unfortunately, it was not possible to derive all necessary equations by it .

5.1. Approximate Solution of the Non-relativistic Equations of Motion

The treatment starts with the equations of motion :

$$m\ddot{z} = m\omega^2 z'' = e\,E_z \qquad m\ddot{r} = m\omega^2 r'' = e\,E_r \tag{5.1.1}$$

where $' = d/d\phi = d/d(\omega t)$ denotes derivation with respect to phase and where m is rest mass. The magnetic field is omitted since, as will be seen in Chapter 6 the effect of the mass variation is of the same order of magnitude . "Mid plane conditions" (given at the centre of the gap) are now employed instead of initial conditions :

$$\begin{aligned} t = \phi = 0: \quad & z = 0\ , \ z' = \dot{z}/\omega = \dot{z}_o/\omega = 1/k \\ & r = r_o\ , \ r' = \dot{r}_o/\omega = r'_o/k = (dr/dz)_o/k \\ & \theta = \theta_o = 0 \qquad \dot{\theta} = \dot{\theta}_o = 0 \qquad \theta(\phi) \equiv 0 \end{aligned} \tag{5.1.2}$$

to specify the solutions of the differential equations (1). There are no forces acting in the azimuthal direction, and planar motion can be assumed. Equations (1) will be solved by the perturbation theory of section 4.1.

After insertion of the field representations (2.2.11), (2.2.12) they are rewritten in a shape more suitable for this purpose :

$$\begin{aligned} k\,z'' &= \kappa \cos(\phi + \phi_o)\,\frac{1}{2\pi} \int_{-\infty}^{\infty} dk_z\, b(k_z)\, e^{ik_z z} \quad J_o(\gamma r)/J_o(\gamma a) \\ k\,r'' &= \kappa \cos(\phi + \phi_o)\,\frac{-i}{2\pi} \int_{-\infty}^{\infty} dk_z\, b(k_z)\, e^{ik_z z} \quad k_z\, J_1(\gamma r)/(\gamma J_o(\gamma a)) \end{aligned} \tag{5.1.3}$$

κ is the perturbation parameter (cf. (3.1.5)) :

$$\kappa = eE_1/(m\omega\dot{z}_o) = eE_1 k/(m\omega^2) \tag{5.1.4}$$

Assuming the perturbation series :

$$\begin{aligned} z(\phi) &= z^{(o)}(\phi) + \kappa\, z^{(1)}(\phi) + \kappa^2 z^{(2)}(\phi) + \kappa^3 \ldots \\ r(\phi) &= r^{(o)}(\phi) + \quad r^{(1)}(\phi) + \kappa^2 r^{(2)}(\phi) + \kappa^3 \ldots \end{aligned} \tag{5.1.5}$$

equations (3) are split up into the system :

$$\kappa^o : \quad z^{(o)''} = \ddot{z}^{(o)}/\omega^2 = 0 \qquad r^{(o)''} = \ddot{r}^{(o)}/\omega^2 = 0 \tag{5.1.6}$$

$$\kappa^1 : k\, z^{(1)\backprime\backprime} = \cos(\phi + \phi_o)\, \frac{1}{2\pi} \int_{-\infty}^{\infty} dk_z\, b(k_z)\, e^{ik_z z^{(o)}} J_o(\gamma r^{(o)})/J_o(\gamma a)$$

$$k\, r^{(1)\backprime\backprime} = \cos(\phi + \phi_o)\, \frac{-i}{2\pi} \int_{-\infty}^{\infty} dk_z\, b(k_z)\, e^{ik_z z^{(o)}} k_z\, J_1(\gamma r^{(o)})/(\gamma J_o(\gamma a)) \qquad (5.1.7)$$

$$\kappa^2 : k\, z^{(2)\backprime\backprime} = \cos(\phi + \phi_o)\, \frac{1}{2\pi} \int_{-\infty}^{\infty} dk_z\, b(k_z)\, e^{ik_z z^{(o)}} \Big[\gamma J_o'(\gamma r^{(o)})\, r^{(1)} + k_z\, J_o(r^{(o)})\, iz^{(1)}\Big] \Big/ J_o(\gamma a)$$

$$k\, r^{(2)\backprime\backprime} = \cos(\phi + \phi_o)\, \frac{-i}{2\pi} \int_{-\infty}^{\infty} dk_z b(k_z)\, e^{ik_z z^{(o)}} k_z \Big[\gamma J_1'(\gamma r^{(o)})\, r^{(1)} + ik_z\, J_1(\gamma r^{(o)}) z^{(1)}\Big] \Big/ (\gamma J_o(\gamma a)) \qquad (5.1.8)$$

κ^3 : .....

by expansion in powers of κ , and equating coefficients of equal powers of κ. One may compare (6) to (8) with the system (4.1.12) to (4.1.14). The corresponding pair of mid-plane conditions is required for each pair of equations (6), (7), (8). Inserting (2) into (5), and equating coefficients of equal power of κ gives :

$$\kappa^o : \omega t = \phi = 0: \quad z^{(o)} = 0,\ z^{(o)\backprime} = 1/k,\ r^{(o)} = r_o,\ r^{(o)\backprime} = r_o^{\backprime} = r_o'/k \qquad (5.1.9)$$

$$\kappa^n : \omega t = \phi = 0: \quad z^{(n)} = z^{(n)\backprime} = r^{(n)} = r^{(n)\backprime} = 0,\ n = 1,2,\ldots \qquad (5.1.10)$$

Equations (6) describe the motion of a free particle whose solutions corresponding to (9) are :

$$r^{(o)}(\phi) = r_o^{\backprime}\phi + r_o\ ,\ z^{(o)}(\phi) = \phi/k \qquad (5.1.11)$$

Introducing (11) into (7), the right hand side becomes a pure function of ϕ . The arising integrals must be further approximatedby expansion of the Bessel functions into powers of $r_o^{\backprime}$:

$$J_n\Big(\gamma\Big[r_o^{\backprime}\phi + r_o\Big]\Big) = J_n(\gamma r_o) + r_o^{\backprime}\phi\, \gamma J_n'(\gamma r_o) + r_o^{\backprime 2} \ldots \qquad (5.1.12)$$

Terms of second or higher order in $r_o^{\backprime}$ are neglected. Equations (7) are integrated twice with respect to ϕ:

$$z^{(1)}\tilde{}(\phi) = \frac{1}{2\pi} \int_{\hat{C}} dk_z\, b(k_z) \frac{J_o(\gamma r_o)}{J_o(\gamma a)} \left[\frac{e^{i\phi_o}}{2} \frac{e^{i\phi(k_z/k+1)}}{i(k_z + k)} + \frac{e^{-i\phi_o}}{2} \frac{e^{i\phi(k_z/k-1)}}{i(k_z - k)} \right] + A_z$$

$$+ r\tilde{}_o \frac{1}{2\pi} \int_{\hat{C}} dk_z\, b(k_z) \frac{\gamma J_o'(\gamma r_o)}{J_o(\gamma a)} \left[\frac{e^{i\phi_o}}{2} \frac{e^{i\phi(k_z/k+1)}}{i(k_z + k)} \phi + k \frac{e^{i\phi_o}}{2} \frac{e^{i\phi(k_z/k+1)}}{(k_z + k)^2} \right.$$

$$\left. + \frac{e^{-i\phi_o} e^{i\phi(k_z/k-1)}}{2\, i(k_z - k)} \phi + k \frac{e^{-i\phi_o}}{2} \frac{e^{i\phi(k_z/k-1)}}{(k_z - k)^2} \right]$$

(5.1.13)

$$z^{(1)}(\phi) = A_z \phi + B_z$$

$$-k \frac{1}{2\pi} \int_{\hat{C}} dk_z\, b(k_z) \frac{J_o(\gamma r_o)}{J_o(\gamma a)} \left[\frac{e^{i\phi_o}}{2} \frac{e^{i\phi(k_z/k + 1)}}{(k_z + k)^2} + \frac{e^{-i\phi_o}}{2} \frac{e^{i\phi(k_z/k-1)}}{(k_z - k)^2} \right]$$

$$- kr\tilde{}_o \frac{1}{2\pi} \int_{\hat{C}} dk_z\, b(k_z) \frac{\gamma J_o'(\gamma r_o)}{J_o(\gamma a)} \left[\frac{e^{i\phi_o}}{2} \frac{e^{i\phi(k_z/k+1)}}{(k_z + k)^2} \phi + 2ik \frac{e^{i\phi_o}}{2} \frac{e^{i\phi(k_z/k+1)}}{(k_z + k)^3} \right.$$

$$\left. + \frac{e^{-i\phi_o}}{2} \frac{e^{i\phi(k_z/k-1)}}{(k_z - k)^2} \phi + 2ik \frac{e^{-i\phi_o}}{2} \frac{e^{i\phi(k_z/k-1)}}{(k_z - k)^3} \right]$$

(5.1.14)

$$\hat{r}^{(1)}\tilde{}(\phi) = \frac{-i}{2\pi} \int_{\hat{C}} dk_z\, b(k_z) \frac{k_z J_1(\gamma r_o)}{\gamma J_o(\gamma a)} \left[\quad .... \quad \right] + A_r$$

$$+ r\tilde{}_o \frac{-i}{2\pi} \int_{\hat{C}} dk_z\, b(k_z) \frac{k_z J_1'(\gamma r_o)}{J_o(\gamma a)} \left[\quad .... \quad \right]$$

(5.1.15)

$$r^{(1)}(\phi) = A_r \phi + B_r + \frac{i}{2\pi} k \int_{\hat{C}} dk_z\, b(k_z) \frac{k_z J_1(\gamma r_o)}{\gamma J_o(\gamma a)} \left[.... \right]$$

$$+ \frac{i}{2\pi} kr\tilde{}_o \int_{\hat{C}} dk_z\, b(k_z) \frac{k_z J_1'(\gamma r_o)}{J_o(\gamma a)} \left[.... \right]$$

(5.1.16)

The new integrands in (13) to (16) are singular at $k_z = \pm k$. Therefore the path of integration in the k_z-plane has been indented at $k_z = \pm k$ ($\hat{C}$ in Fig. (2.2.1)) before performing integrations with respect to ϕ .

The constants of integration, A_z , B_z , A_r , B_r are uniquely determined by (10). However, they need not be determined here since all quantities considered in this section are differences of such a kind that these constants drop out. They are evaluated in appendix 5.2.A. The above solutions provide the basis for the derivation of the difference equations describing the influence of the gap field upon the particle crossing it. This is done in the next two sections.

Before that, however, it is necessary to derive the transformations already mentioned in Section 4.2 treating the thin lens approximation, which lead from ϕ to z as independent variable, and to express them afterwards by the solutions (13) to (16). These transformations cannot be performed exactly, expansions in powers of κ are employed. An accuracy of first order (in κ) only is required. In an expression already multiplied by κ (e.g. $\kappa z^{(1)}(\phi)$) the substitutions $\phi^{(o)} = kz$, $z^{(o)} = \phi/k$ suffice to change from ϕ to z (e.g. $\kappa z^{(1)}(kz)$) and vice versa.

Longitudinal kinetic energy is given from (5) and (11) :

$$T = \frac{m}{2}\dot{z}^2(\phi) = \frac{m}{2}\omega^2\left[z'(\phi)\right]^2 = \frac{m}{2}\omega^2\left[\frac{1}{k^2} + \kappa\frac{2}{k}z^{(1)\prime}(\phi) + \kappa^2\ldots\right]$$

$$= (m\omega^2/2k^2) + m\omega^2/k \;\; \kappa z^{(1)\prime}(\phi) + \kappa^2 \ldots \qquad (5.1.17)$$

$$T = W \qquad + 2\,Wk \;\; \kappa z^{(1)\prime}(kz) + \kappa^2 \ldots$$

To find the phase variation, the equation $z = z(\phi)$ must be solved for a given z : with the help of (5) and (11), this leads to :

$$kz = \phi + \kappa\, kz^{(1)}(\phi) + \kappa^2\ldots$$

$$\phi = kz - \kappa\, kz^{(1)}(\phi) - \kappa^2\ldots$$

which is now solved by iteration :

$$\phi = kz - \kappa\, k\, z^{(1)}(\phi^{(o)}) - \kappa^2 \ldots$$

$$\phi(z) = kz - \kappa\, k\, z^{(1)}(kz) \quad - \kappa^2 \ldots \tag{5.1.18}$$

Its derivative :

$$\phi' = d\phi/dz = k - \kappa k^2\, z^{(1)\wedge}(kz) - \kappa^2 \ldots. \tag{5.1.19}$$

is needed to express reduced phase (4.2.5) :

$$\bar{\phi}(z) = \phi(z) - z\phi'(z)$$

$$= - \kappa\, k \left[z^{(1)}(kz) - kz\, z^{(1)\wedge}(kz) \right] + \kappa^2 \ldots \tag{5.1.20}$$

In these equations the letter z denotes two different things:z is just the position of the particle, while $z^{(1)}(\ )$, $z^{(1)\wedge}(\ )$ are the function operators defined by equations (13), (14) respectively.

Radial velocity is given by :

$$\dot{r}(\phi) = \omega\, r\hat{}(\phi) = \omega \left[r\hat{}_o + \kappa\, r^{(1)\wedge}(\phi) + \kappa^2 \ldots \right] \tag{5.1.21}$$

$$= \omega \left[r\hat{}_o + \kappa\, r^{(1)\wedge}(kz) + \kappa^2 \ldots \right]$$

For the transition from $\dot{r}(\phi) = \omega\, r\hat{}(\phi)$ to :

$$r' = dr/dz = (dr/d\phi)(d\phi/dz) = r\hat{}\phi' \tag{5.1.22}$$

(5), (11) and (19) are used :

$$r'(\phi) = r'_o + \kappa \left[k\, r^{(1)\wedge}(kz) - r'_o\, k\, z^{(1)\wedge}(kz) \right] + \kappa^2 \ldots \tag{5.1.23}$$

In an earlier paper [39] the variation of ϕ' in equation (22) had been overlooked and $\phi'(\phi)$ erroneously replaced by the constant $k = \phi'(0)$. Therefore the expressions arising from the second term in the square bracket of (23) are missing in the difference equations of this ref.[39]. This mistake has been detected by PROME [40]. Similar objections may be raised against the treatment in refs.[4], 7) - 9).

Reduced radius (4.2.9) is found with the help of (5), (11), (18) and (13) :

$$
\begin{aligned}
\bar{r} &= r - z\, r' \\
&= r_o \dot{\phi} + r_o + \kappa r^{(1)}(\phi) + \kappa^2 \ldots \\
&\quad - \left[z^{(o)}(\phi) + \kappa\, z^{(1)}(\phi) + \kappa^2 \ldots \right] \left[r'_o + \kappa\, k r^{(1)\cdot}(\phi) - r'_o\, \kappa\, k\, z^{(1)\cdot}(\phi) + \kappa^2 \ldots \right] \\
&= r_o + \kappa \left[r^{(1)}(kz) - kz\, r^{(1)\cdot}(kz) \right] - r'_o\, \kappa \left[z^{(1)}(kz) - kz\, z^{(1)\cdot}(kz) \right] + \kappa^2 \ldots \\
&= r_o + \kappa \left[r^{(1)}(kz) - kz\, r^{(1)\cdot}(kz) \right] + r'_o\, \bar{\phi}(z)/k + \kappa^2 \ldots \\
&= \underset{=}{r} + r'_o\, \bar{\phi}(z)/k + \kappa^2 \ldots
\end{aligned}
\qquad (5.1.24)
$$

In the last line but one equation (20) has been used.

Again, the reduced radius as defined in the paper just mentioned[39]:

$$
\begin{aligned}
\underset{=}{r} &= r - \phi\, dr/d\phi = r - \phi\, r' \\
&= r_o + \kappa \left[r^{(1)}(kz) - (kz)\, r^{(1)\cdot}(kz) \right] + \kappa^2 \ldots
\end{aligned}
\qquad (5.1.25)
$$

has not been entirely correct.

5.2. Difference Equations Across the Whole Gap

Before making use of the equations listed above to derive the difference equations for change in energy, phase, radial slope and radial position across the gap it may be pointed out that difference equations for ΔW and Δp_r can be obtained in a simpler way. This is shown for ΔW. Equation (5.1.1) gives :

$$m\,\ddot{z} = \frac{m}{2}\frac{d}{dz}\,\dot{z}^2 = \frac{d}{dz}\,W = e\,E_z(z,r,\phi) \qquad (5.2.1.)$$

It is permitted to insert in the right hand side the zero order solutions (cf. (5.1.11)) :

$$\phi^{(o)} = kz \qquad r^{(o)} = r_o' z + r_o \qquad (5.2.2)$$

to get the gain in energy to first order (in κ). Expanding in powers of r_o' and subsequent integration gives :

$$\Delta W/e = \int_{-\infty}^{\infty} E_z(z,r_o,kz)\,dz + r_o' \int_{-\infty}^{\infty} \frac{\partial E_z(z,r_o,kz)}{\partial r_o}\,z\,dz + \ldots$$

$$= \cos\phi_o \int_{-\infty}^{\infty} E_z(z,r_o)\cos(kz)\,dz - r_o' \sin\phi_o \int_{-\infty}^{\infty} \frac{\partial E_z(z,r_o)}{\partial r_o}\,z\sin(kz)\,dz$$

In the second line the equations (2.2.11) and (2.2.12) and the symmetry properties (2.5.2) have been used. Comparison with (2.6.4) leads to :

$$\Delta W = eV_o\;T_1(k,r_o)\cos\phi_o + eV_o\;d/dk\;\partial T_1(k,r_o)/\partial r_o\;\;r_o'\sin\phi_o \qquad (5.2.3)$$

The second equation (5.1.1), when treated similarly, yields the change in radial momentum. This kind of treatment is easy for ΔW and Δp_r where only one integration with respect to ϕ is involved. In the other cases the use of equations (5.1.13) to (5.1.16) appears more advantageous.

The gain in the longitudinal kinetic energy between $z = -\ell$ and $z = \ell$, $\Delta W(\ell)$, is given from (5.1.17):

$$\Delta W(\ell) = m(\omega^2/k)\,\kappa\left[z^{(1)}\tilde{}(k\ell) - z^{(1)}\tilde{}(-k\ell)\right] + \kappa^2 \ldots \qquad (5.2.4)$$

The evaluation of $z^{(1)}\tilde{}(\phi)$,(5.1.13) for $\phi = \pm k\ell$ is accomplished in Appendix A. This is easy, provided $\ell > p/2$. $\hat{C}$ is completed by C_U, C_L respectively (cf. Fig. 2.2.1) for $+\ell(-\ell)$ and Cauchy's residue theorem is used. The poles $k_z = \pm k$ (see (11)) give again ΔW of (3); the poles $k_z = \pm i\eta_\nu$ ($J_o(\gamma a) = 0$, cf. (2.5.1)) give an additional series whose terms are

proportional to $\exp(-\eta_v \ell)$. Consequently, in the limit $\ell \to \infty$ there remains ΔW of (3) only. In appendix B the additional series just mentioned is given. Its expressions are complicated; it is doubtful whether its inclusion would be rewarded by a proportional increase in accuracy.

At least, it gives some insight under which condition the limit $\ell \to \infty$ represents a good approximation, namely

$$2{,}4 \times (L - p)/(2a) \gg 1$$

where L is cell length and a the radius of the drift tube bore.

The integral representations (2.2.11) to (2.2.13) may be regarded as a superposition of waves of all phase velocities. The poles $k_z = k$ (for $\phi = k\ell$) and $k_z = -k$ (for $\phi = -k\ell$) which correspond to the singular behaviour of the Fourier Dirichlet integral in refs.[7)-9)], cut out from the continuous spectrum the wave whose phase velocity equals the particle velocity. It appears as if the particle interacts with that wave only which has the same velocity. This statement must not be taken too literally. In an evaluation of the integrals (5.1.13) to (5.1.16) where $\ell < p/2$ which may be accomplished in the same way as that of the fields (cf. (2.5.19)), there appear additional poles at $k_z = \pm 2\pi n/p$ representing standing waves.

The change in reduced phase between the points $z = -\ell$ and $z = \ell$ is according to (5.1.20):

$$\Delta\bar{\phi}(\ell) = -\kappa k\left[\left[z^{(1)}(k\ell) - (k\ell)\, z^{(1)\sim}(k\ell)\right] - \left[z^{(1)}(-k\ell) - (-k\ell)\, z^{(1)\sim}(-k\ell)\right]\right] + \kappa^2 \ldots$$

and in the limit $\ell \to \infty$

$$\Delta\bar{\phi} = \frac{eV_o}{2W} k\left[\, d/dk\; T_1(k,r_o)\, \sin\phi_o + d/dk\; \partial T_1(k,r_o)/\partial r_o\; r'_o \cos\phi_o \,\right] \tag{5.2.5}$$

In order to get the last expression, (16) has been used. The treatment of the transverse quantities is similar.

$$\begin{aligned} \Delta r^{\sim} = \Delta(dr/d\phi) &= \kappa \lim_{\ell \to \infty} \left[r^{(1)\sim}(k\ell) - r^{(1)\sim}(-k\ell)\right] \\ &= \frac{eV_o}{2Wk}\left[-T_r(k,r_o)\, \sin\phi_o + d/dk\; \partial T_r(k,r_o)/\partial r_o\; r'_o \cos\phi_o\right] \end{aligned} \tag{5.2.6}$$

$$\begin{aligned} \Delta r' = \Delta(dr/dz) &= k\, \Delta r^{\sim} - r'_o\, \Delta W/(2W) \\ &= \frac{eV_o}{2W}\left[-T_r(k,r_o)\, \sin\phi_o + \left(d/dk\; \partial T_r(k,r_o)/\partial r_o - T_1(k,r_o)\right) r'_o \cos\phi_o\right] \end{aligned} \tag{5.2.7}$$

$$\Delta\bar{\bar{r}} = \Delta(r - \phi\, dr/d\phi) =$$

$$= \kappa \lim_{\ell \to \infty} \left[\left[(r^{(1)}(k\ell) - (k\ell)\, r^{(1)}\text{`}(k\ell) \right] - \left[ r^{(1)}(-k\ell) - (-k\ell)\, r^{(1)}\text{`}(-k\ell) \right] \right] + \kappa^2 \ldots$$

$$= -\frac{eV_o}{2W} \left[d/dk\, T_r(k,r_o)\, \cos\phi_o + d^2/dk^2\, \partial T_r(k,r_o)/\partial r_o\, r'_o\, \sin\phi_o \right] \tag{5.2.8}$$

$$\Delta\bar{r} = \Delta(r - z\, dr/dz) = \Delta\bar{\bar{r}} + r'_o\, \Delta\bar{\phi}/k \tag{5.2.9}$$

$$= -\frac{eV_o}{2W} \left[d/dk\, T_r(k,r_o)\, \cos\phi_o + \left(d^2/dk^2\, \partial T_r(k,r_o)/\partial r_o - d/dk\, T_1(k,r_o) \right) r'_o\, \sin\phi_o \right]$$

ΔW, $\Delta\bar{\phi}$, $\Delta r'$, $\Delta\bar{r}$ are listed in Table I.

5.2.A Evaluation of Beam Dynamics Integrals

The evaluation of the integrals in k_z arising from (5.1.13) to (5.1.16) is simple in the case where the particle crosses the whole gap, $\phi = k\ell$ ($-k\ell$) respectively with $\ell > p/2$. A rigorous proof has to proceed along the lines exposed in Section 2.5.B, and this will not be repeated here. The evaluation is accomplished by Cauchy's residue theorem, after the path $\hat{C}$ has been completed to a closed contour by adding C_U , C_L respectively. Besides the simple poles $k_z = i\eta_v$ ($-i\eta_v$) (cf. (2.5.10)) (whose contributions will in general be disregarded), there are poles of various orders at $k_z = +k$ ($-k$). The residue of a pole of order n is easily found by:

$$\text{Res}\left(h(x)/(x-x_o)^n \; ; \; x=x_o\right) = \left[(n-1)!\right]^{-1} \left(d^{n-1}h(x)/dx^{n-1}\right)\Big|_{x=x_o} \qquad (5.2.10)$$

For convenience, the integrals involving the magnetic field which are needed in the relativistic treatment, are treated here together with those containing the electric field components, and all are combined into one equation. Curly brackets contain three lines, one valid for E_z, E_r, H_θ respectively. $z^{(1)\sim}(\,)$, $r^{(1)\sim}(\,)$, $m^{(1)\sim}(\,)$, $z^{(1)}(\,)$, $r^{(1)}(\,)$ and $m^{(1)}(\,)$ should be regarded as function operators defined by integrals in k_z . They are used to express the coordinates of a particle, see equations (5.1.17) to (5.1.25), but they should not be confused with the coordinates themselves.

$$\left\{ \begin{matrix} z^{(1)\sim}(\phi) \\ r^{(1)\sim}(\phi) \\ m^{(1)\sim}(\phi) \end{matrix} \right\} = \frac{1}{kE_1} \int_0^{\phi} d\bar{\phi} \left\langle \left\{ \begin{matrix} E_z(z^{(o)}, r^{(o)}, \bar{\phi}) \\ E_r(z^{(o)}, r^{(o)}, \bar{\phi}) \\ H_\theta(z^{(o)}, r^{(o)}, \bar{\phi}) \quad \mu c/k_o \end{matrix} \right\} \right\rangle = \qquad (5.2.11)$$

$$= \frac{1}{2\pi} \int_{\hat{C}} dk_z \, f(k_z) \left[\frac{e^{i\phi_o}}{2} \frac{e^{i\phi(k_z/k+1)}}{i(k_z+k)} + \left\langle \left\{ \begin{matrix} + \\ + \\ - \end{matrix} \right\} \right\rangle \frac{e^{-i\phi_o}}{2} \frac{e^{i\phi(k_z/k-1)}}{i(k_z-k)} \right] + \left\langle \left\{ \begin{matrix} A_z \\ A_r \\ A_m \end{matrix} \right\} \right\rangle$$

$$+ \frac{\tilde{r_o}}{2\pi} \int_{\hat{C}} dk_z \, f_r(k_z) \left[\left[\frac{e^{i\phi_o}}{2} \frac{e^{i\phi(k_z/k+1)}}{i(k_z+k)} \phi + k \frac{e^{i\phi_o}}{2} \frac{e^{i\phi(k_z/k+1)}}{(k_z+k)^2} \right] \right.$$

$$\left. + \left\{ \begin{matrix} + \\ + \\ - \end{matrix} \right\} \left[\frac{e^{-i\phi_o}}{2} \frac{e^{i\phi(k_z/k-1)}}{i(k_z-k)} \phi + k \frac{e^{-i\phi_o}}{2} \frac{e^{i\phi(k_z/k-1)}}{(k_z-k)^2} \right] \right]$$

where f and f_r must be chosen according to the following table:

function	field	$f(k_z)$	$f_r(k_z)$
$z^{(1)}$	E_z	$b(k_z)\ J_o(\gamma r_o)/J_o(\gamma a)$	$-b(k_z)\ \gamma\ J_1(\gamma r_o)/J_o(\gamma a)$
$r^{(1)}$	E_r	$-ib(k_z)\ k_z\ J_1(\gamma r_o)/(\gamma J_o(\gamma a))$	$-ib(k_z)\ k_z\ J_1'(\gamma r_o)/J_o(\gamma a)$
$m^{(1)}$	H_θ	$ib(k_z)\ J_1(\gamma r_o)/(\gamma J_o(\gamma a))$	$ib(k_z)\ J_1'(\gamma r_o)/J_o(\gamma a)$

Table 5.2.1 Abbreviations for Field and Beam Dynamics Integrals.

Evaluation as described above gives for $\phi = \pm k\ell$ ($\ell > p/2$) :

(5.2.12)

$$\begin{Bmatrix} z^{(1)}(\pm k\ell) \\ r^{(1)}(\pm k\ell) \\ \\ \\ m^{(1)}(\pm k\ell) \end{Bmatrix} = \begin{Bmatrix} A_z \\ A_r \\ \\ \\ A_m \end{Bmatrix} + \begin{Bmatrix} (\pm) \\ (\pm) \\ \\ \\ - \end{Bmatrix} \frac{e^{(\mp i\phi_o)}}{2} f(\pm k) + \begin{Bmatrix} (\pm) \\ (\pm) \\ \\ \\ - \end{Bmatrix} r_o \frac{e^{(\mp i\phi_o)}}{2} \Big((\pm k\ell)\ f_r(\pm k) \\ -(\pm k\ell)\ f_r(\pm k) + ik\ d/dk_z\ f_r(k_z)\big|_{k_z = \pm k} \Big)$$

In all the small round brackets either the upper or the lower sign must be chosen consistently. Note that terms containing ℓ cancel. Taking into account the (even or odd) symmetry of $f(k_z)$ gives together with (2.6.10) :

$$E_1\ b(k)/I_o(k_r a) = V_o\ T_o(k) \qquad \kappa b(k)/J_o(\gamma a) = (eV_o/2Wk)\ T_o(k)$$

(5.2.13)

the result :

$$\begin{Bmatrix} \kappa z^{(1)}(\pm k\ell) \\ \kappa r^{(1)}(\pm k\ell) \\ \kappa m^{(1)}(\pm k\ell) \end{Bmatrix} = \left\langle \begin{Bmatrix} \kappa A_z \\ \kappa A_r \\ \kappa A_m \end{Bmatrix} \right\rangle + \tag{5.2.14}$$

$$+ \begin{Bmatrix} (\pm)\, T_o(k)\, I_o(k_r r_o) \\ -iT_o(k)\, k\, I_1(k_r r_o)/k_r \\ -i\, T_o(k)\, I_1(k_r r_o)/k_r \end{Bmatrix} \frac{e^{(\mp i\phi_o)}}{2} \frac{eV_o}{2Wk} + \left\{ \begin{matrix} i\ d/dk\ T_o(k) k_r I_1(k_r r_o) \\ (\pm)\ d/dk\ T_o(k)\, k\, I_1'(k_r r_o) \\ (\pm)\ d/dk\ T_o(k)\, I_1'(k_r r_o) \end{matrix} \right\} e^{\frac{(\mp i\phi_o)}{2}} \frac{eV_o}{2Wk} r_o'$$

The expressions in the curly brackets in the last line are T-coefficients, and the two blocks may be replaced by the following ones:

$$\begin{Bmatrix} (\pm)\, T_1(k,r_o) \\ -i\ \ T_r(k,r_o) \\ -i\ \ T_m(k,r_o) \end{Bmatrix} \qquad \begin{Bmatrix} i\ d/dk\ \partial T_1(k,r_o)/\partial r_o \\ (\pm)\ d/dk\ \partial T_r(k,r_o)/\partial r_o \\ (\pm)\ d/dk\ \partial T_m(k,r_o)/\partial r_o \end{Bmatrix}$$

In place of the functions :

$$\begin{Bmatrix} z^{(1)}(\phi) \\ r^{(1)}(\phi) \\ m^{(1)}(\phi) \end{Bmatrix} = \int_o^{\phi} d\bar{\phi} \left\{ \begin{matrix} z^{(1)}(\bar{\phi}) \\ r^{(1)}(\bar{\phi}) \\ m^{(1)}(\bar{\phi}) \end{matrix} \right\} = \left\langle \begin{Bmatrix} A_z\phi + B_z \\ A_r\phi + B_r \\ A_m\phi + B_m \end{Bmatrix} \right\rangle - \tag{5.2.15}$$

$$- \frac{k}{2\pi} \int_{\hat{C}} dk_z\, f(k_z) \left[\frac{e^{i\phi_o}}{2} \frac{e^{i\phi(k_z/k+1)}}{(k_z+k)^2} + \left\langle \begin{matrix} + \\ + \\ - \end{matrix} \right\rangle \frac{e^{-i\phi_o}}{2} \frac{e^{i\phi(k_z/k-1)}}{(k_z-k)^2} \right]$$

$$- \frac{kr_o'}{2\pi} \int_{\hat{C}} dk_z\, f_r(k_z) \left[\left[\frac{e^{i\phi_o}}{2} \frac{e^{i\phi(k_z/k+1)}}{(k_z+k)^2}\, \phi + 2ik \frac{e^{i\phi_o}}{2} \frac{e^{i\phi(k_z/k+1)}}{(k_z+k)^3} \right] \right.$$

$$\left. + \left\langle \begin{matrix} + \\ + \\ - \end{matrix} \right\rangle \left[\frac{e^{-i\phi_o}}{2} \frac{e^{i\phi(k_z/k-1)}}{(k_z-k)^2}\, \phi + 2ik \frac{e^{-i\phi_o}}{2} \frac{e^{i\phi(k_z/k-1)}}{(k_z-k)^3} \right] \right]$$

only the reduced quantities are given :

$$\left\langle \begin{Bmatrix} \kappa \left[z^{(1)}(\underline{+}k\ell) - (\underline{+}k\ell)\, z^{(1)}\tilde{}(\underline{+}k\ell) \right] \\ \kappa \left[r^{(1)}(\underline{+}k\ell) - (\underline{+}k\ell)\, r^{(1)}\tilde{}(\underline{+}k\ell) \right] \\ \kappa \left[m^{(1)}(\underline{+}k\ell) - (\underline{+}k\ell)\, m^{(1)}\tilde{}(\underline{+}k\ell) \right] \end{Bmatrix} \right\rangle = \left\langle \begin{Bmatrix} \kappa\, B_z \\ \kappa\, B_r \\ \kappa\, B_m \end{Bmatrix} \right\rangle + \tag{5.2.16}$$

$$+ \left\langle \begin{bmatrix} -i & d/dk\ T_o(k) & I_o(k_r r_o) \\ (\bar{+}) & d/dk\ T_o(k)\ k & I_1(k_r r_o)/k_r \\ (\bar{+}) & d/dk\ T_o(k) & I_1(k_r r_o)/k_r \end{bmatrix} \right\rangle \frac{e^{(\bar{+}i\phi_o)}}{2} \frac{eV_o}{2W} + \left\langle \begin{bmatrix} (\underline{+}) & d^2/dk^2\ T_o(k) k_r & I_1(k_r r_o) \\ -i & d^2/dk^2\ T_o(k)\ k & I_1'(k_r r_o) \\ -i & d^2/dk^2\ T_o(k) & I_1'(k_r r_o) \end{bmatrix} \right\rangle \frac{e^{(\bar{+}i\phi_o)}}{2} \frac{eV_o}{2W} r_o'$$

Again, the two blocks of formulae given in the last line may be replaced by the following ones :

$$\left\langle \begin{bmatrix} -i & d/dk\ T_1(k,r_o) \\ (\bar{+}) & d/dk\ T_r(k,r_o) \\ (\bar{+}) & d/dk\ T_m(k,r_o) \end{bmatrix} \right\rangle \qquad \left\langle \begin{bmatrix} (\underline{+}) & d^2/dk^2\ \partial T_1(k,r_o)/\partial r_o \\ -i & d^2/dk^2\ \partial T_r(k,r_o)/\partial r_o \\ -i & d^2/dk^2\ \partial T_m(k,r_o)/\partial r_o \end{bmatrix} \right\rangle$$

5.2.B Correction terms for finite cell length

In the above appendix differences of all quantities have been evaluated in the limit $\ell \to \infty$. If the length of the drift tubes or (of their quadrupole field free part) is not large in comparison with their inner diameter, the contributions due to the first poles $k_z = \pm i\eta_1 , \pm i\eta_2, \ldots$ ($J_o(\gamma a) = 0$) (cf.(2.5.1)) may no longer be negligible. In physical terms: the field of the evanescent modes has not yet sufficiently died off. Unfortunately, these correction terms are complicated and, in addition, it is questionable whether they describe beam dynamics correctly, since the series (c) which have been derived in Section 2.5 from the same integral representations of wave guide fields, strongly differ from the cavity fields found by mesh calculations for $|z| > p/2$.

Therefore only an example, the change in kinetic energy between $z = -\ell$ and $z = \ell$, ℓ being finite, is given. Residues for $k_z = \pm i\eta_\nu$ are evaluated by use of (2.5.10). This gives :

$$\Delta W(\ell) = \Delta W + \frac{eV_o}{pa^2} J_o(k_o a)\left\{ \sum_{\nu=1}^{\infty} j_\nu J_o(j_\nu r/a)\left[R_\nu(k\ell) - R_\nu(-k\ell)\right] \right.$$
$$\left. - r_o'/a \sum_{\nu=1}^{\infty} j_\nu^2 J_1(j_\nu r/a)\left[\ell\left(R_\nu(k\ell) + R_\nu(-k\ell)\right) - \left(P_\nu(k\ell) - P_\nu(-k\ell)\right)\right] \right\} \qquad (5.2.17)$$

ΔW is the change for $\ell \to \infty$, equation (3). R_ν and P_ν are abbreviations for the following expressions :

$$R_\nu(\pm k\ell) = \frac{b(i\eta_\nu)\, e^{-\eta_\nu|\ell|}}{\eta_\nu J_1(j_\nu)(\eta_\nu^2 + k^2)}\left[k \sin(\phi_o \pm k\ell) \mp \eta_\nu \cos(\phi_o \pm k\ell)\right]$$
$$P_\nu(\pm k\ell) = \frac{b(i\eta_\nu)\, e^{-\eta_\nu|\ell|}}{\eta_\nu J_1(j_\nu)(\eta_\nu^2 + k^2)^2}\left[(\eta_\nu^2 - k^2)\cos(\phi_o \pm k\ell) - 2\eta_\nu k \sin(\phi_o \pm k\ell)\right] \qquad (5.2.18)$$

$$b(i\eta_\nu) = 4\,\eta_\nu \sinh(\eta_\nu p/2) \sum_{n=o}^{\infty} \frac{(-1)^{n_B n}}{1 + \delta_{no}}\left[\eta_\nu^2 + (2\pi n/p)^2\right]^{-1}$$

By use of this formula it is possible to indicate under which conditions the contributions due to the poles $k_z = \pm i\eta_\nu$ can be safely neglected. It may be expected that the magnitude of the terms of the series in (17) is mainly determined by the greater of the two exponentials contained in P_ν and R_ν :

$$2\, b(i\eta_\nu)\, e^{-\eta_\nu|\ell|} \approx e^{-\eta_\nu(|\ell| - p/2)} - \ldots$$

and this will be small if :

$$\eta_\nu (|\ell| - p/2) \approx j_\nu(|\ell| - p/2)/a \approx (\nu - 1/4)\,\pi\,(|\ell| - p/2)/a \gg 1. \qquad (5.2.19)$$

Here the static approximation (2.5.8) has been used. For v = 1 this condition gives :

$$2{,}4 \times (|\ell| - p/2)/a \gg 1 \qquad (5.2.19)$$

For ℓ a value must be used which is representative for the distance of the boundary where the regime of the accelerating gap ends and a new (accelerating or focusing) zone begins, from the gap centre.

5.3 Difference Equations for the First Half of the Gap

The increments ΔW, $\Delta\bar{\phi}$, $\Delta r'$, $\Delta\bar{r}$ as derived in the preceeding section and displayed in Table I, are given as functions of the mid-gap values W, ϕ_o, r'_o, r_o. Mid-gap values are preferred to initial values for several reasons: One is the belief supported by some examples (cf. Section 3.2.) that the accuracy of approximate formulae is better in the first case. Another is convenience of design.

Still it is necessary to find them for a particle entering the gap so that the transformations across the whole gap can be performed. For this purpose are needed equations describing the change of kinetic energy Δw_1, phase $\Delta\bar{\phi}_1$, radial slope $\Delta r'_1$ and position $\Delta\bar{r}_1$ across the first half of the gap. These equations are solved for W, ϕ_o, r'_o, r_o by iterations. A question which has not yet been cleared up, is whether the gain in accuracy acquired by the employment of mid-gap values is not lost in this step. The half gap equations also have applications in the design of linac cells [11].

The gain in kinetic energy through the first half of the gap is found from (5.1.17) :

$$\Delta w_1 = 2Wk\kappa\left[z^{(1)\sim}(0) - z^{(1)\sim}(-k\ell)\right] + \kappa^2 \quad .. \qquad (5.3.1)$$

$z^{(1)\sim}(0)$ is zero according to (5.1.10). For $z^{(1)\sim}(-k\ell)$ the representation (5.1.13) may be used with the argument $\phi = -k\ell$. This gives terms of two kinds. The first ones are the integrals of (5.1.13) with argument $\phi = -k\ell$. They have been evaluated in Appendix 5.2.A and can be expressed by T-coefficients and their derivatives. The second type is represented by the constant A_z. It is found from equation (5.1.13) by the mid-gap condition $z^{(1)\sim}(0) = 0$ and is the negative of the integrals on the right hand side of (5.1.13) with the argument $\phi = 0$. These integrals, however, cannot be so easily evaluated than those with $|\phi| = k\ell > kp/2$. The same difficulty has already been faced in Section 2.5 when there the field representations have been evaluated for points in the interior of the gap. But instead of proceeding immediately by the method described in the first paragraph of Section 2.5 and in equation (2. 5.19), it is preferred to perform this task in two steps. The first consists of expressing these integrals by the longitudinal S-coefficient, $S_1(k,r)$ and its derivatives defined in Section 2.7. This is done in Appendix 5.3.A. The second step where the explicit expression for these integrals with $\phi = 0$, i.e. for the S-coefficients, are derived, has already been accomplished in Section 2.7 and appendix 2.7.B where also approximations are discussed.

In this way, the gain in the kinetic energy through the first half of the gap is found with the help of (5.2.14) and of eq. (8) given in Appendix 5.3.A :

$$\Delta w_1 = \lim_{\ell \to \infty} 2\,Wk\,\kappa\left[z^{(1)\sim}(0) - z^{(1)\sim}(-k\ell)\right]$$

$$= eV_o \frac{1}{2}\left[S_1(k,r_o)\sin\phi_o - T_1(k,r_o)\cos\phi_o + T_1(k,r_o)\,e^{i\phi_o}\right] \qquad (5.3.1a)$$

$$+ eV_o \frac{r_o'}{2}(-d/dk\;\partial/\partial r_o)\left[S_1\cos\phi_o - i\,T_1\cos\phi_o + iT_1\,e^{i\phi_o}\right]$$

The T_1 coefficient is given in eq. (2.6.4). This gives the first equation of Table III. The procedure is analogous for all other quantities :

$$\Delta\bar{\phi}_1 = \kappa k\left[-z^{(1)}(0) + \left\{z^{(1)}(-k\ell) - (-k\ell)\,z^{(1)\sim}(-k\ell)\right\}\right] + \kappa^2 \ldots$$

$$= \frac{1}{2}\frac{eV_o}{2W}\,k\left\{d/dk\left[T_1(k,r_o)\sin\phi_o - S_1(k,r_o)\cos\phi_o\right]\right. \qquad (5.3.2)$$

$$\left. - r_o'\,d^2/dk^2\;\partial/\partial r_o\left[T_1\cos\phi_o + S_1\sin\phi_o\right]\right\}$$

$$\Delta\hat{r}_1 = \kappa\left[r^{(1)\sim}(0) - r^{(1)\sim}(-k\ell)\right] + \kappa^2 \ldots$$

$$= \frac{1}{2}\frac{eV_o}{2Wk}\left\{\left[-T_r(k,r_o)\sin\phi_o - S_r(k,r_o)\cos\phi_o\right]\right. \qquad (5.3.3)$$

$$\left. + r_o'\,d/dk\;\partial/\partial r_o\left[T_r\cos\phi_o - S_r\sin\phi_o\right]\right\}$$

$$\Delta r_1' = k\,\Delta\hat{r}_1 - r_o'\;\Delta w_1/(2W) \qquad (5.3.4)$$

$$\Delta\bar{\bar{r}}_1 = \kappa\left[r^{(1)}(0) - \left\{r^{(1)}(-k\ell) - (-k\ell)\,r^{(1)\sim}(-k\ell)\right\}\right] + \kappa^2 \ldots$$

$$= \frac{1}{2}\frac{eV_o}{2W}\left\{d/dk\left[-T_r(k,r_o)\cos\phi_o + S_r(k,r_o)\sin\phi_o\right]\right. \qquad (5.3.5)$$

$$\left. - r_o'\,d^2/dk^2\;\partial/\partial r_o\left[T_r\sin\phi_o + S_r\cos\phi_o\right]\right\}$$

$$\Delta\bar{r}_1 = \Delta\bar{\bar{r}}_1 + r_o'\;\Delta\bar{\phi}_1/k \qquad (5.3.6)$$

5.3.A Mid-Gap Values expressed by S-coefficients

The method of presentation introduced in Section 5.2 A by which expressions arising from E_z, E_r, H_θ are simultaneously displayed in the three rows of one equation, is again used here together with the definition of the f 's given in Table 5.2.1. The evaluation, however, employs a different approach, but is rather simple.

Putting $\phi = 0$ in the integrals of equations (5.2.10) gives:

$$0 = \begin{Bmatrix} z^{(1)}(0) \\ r^{(1)}(0) \\ m^{(1)}(0) \end{Bmatrix} = \frac{1}{2\pi} \int_{\hat{C}} dk_z\, f(k_z) \left[\frac{e^{i\phi_o}}{2} \frac{1}{i(k_z + k)} + \begin{Bmatrix} + \\ + \\ - \end{Bmatrix} \frac{e^{-i\phi_o}}{2} \frac{1}{i(k_z - k)} \right] \tag{5.3.7}$$

$$+ \begin{Bmatrix} A_z \\ A_r \\ A_m \end{Bmatrix} + \frac{r\hat{}k}{2} \int_{\hat{C}} dk_z\, f_r(k_z) \left[\frac{e^{i\phi_o}}{2} \frac{1}{(k_z + k)^2} + \begin{Bmatrix} + \\ + \\ - \end{Bmatrix} \frac{e^{-i\phi_o}}{2} \frac{1}{(k_z - k)^2} \right]$$

Exponentials are eliminated by use of the Euler formula. The path of integration is symmetric, i.e. apart from its direction it is not changed by the substitution $k_z \to -k_z$. Thus integrals over odd functions in k_z vanish; there remain only integrals which can be replaced by the integrals (and their derivatives) discussed in Section 2.7.B.

$$\begin{Bmatrix} -\kappa A_z \\ -\kappa A_r \\ -\kappa A_m \end{Bmatrix} = \frac{e}{2Wk} \frac{1}{2} \frac{E_1}{2\pi} \int_{\hat{C}} dk_z \frac{b(k_z)}{J_o(\gamma a)} \begin{Bmatrix} J_o(\gamma r_o) \left[\dots - \dots \right] \sin\phi_o \\ (-k_z) \frac{J_1(\gamma r_o)}{\gamma} \left[\frac{1}{k_z + k} + \frac{1}{k_z - k} \right] \cos\phi_o \\ \frac{J_1(\gamma r_o)}{\gamma} \left[\dots - \dots \right] \cos\phi_o \end{Bmatrix}$$

$$+ \frac{e}{2Wk} \frac{r'_o}{2} \frac{E_1}{2\pi} \int_{\hat{C}} dk_z \frac{b(k_z)}{J_o(\gamma a)} \begin{Bmatrix} \gamma\, J_o'(\gamma r) \left[\dots + \dots \right] \cos\phi_o \\ k_z\, J_1'(\gamma r_o) \left[\frac{1}{(k_z + k)^2} - \frac{1}{(k_z - k)^2} \right] \sin\phi_o \\ (-1)\, J_1'(\gamma r_o) \left[\dots + \dots \right] \sin\phi_o \end{Bmatrix}$$

$$\left\langle \begin{Bmatrix} -\kappa A_z \\ -\kappa A_r \\ -\kappa A_m \end{Bmatrix} \right\rangle = \frac{1}{2}\frac{eV_o}{2Wk} \left\langle \begin{Bmatrix} \left[S_l(k,r_o) - i\ T_l(k,r_o)\right] \sin\phi_o \\ \left[-S_r(k,r_o) - i\ T_r(k,r_o)\right] \cos\phi_o \\ \left[S_m(k,r_o) - i\ T_m(k,r_o)\right] \cos\phi_o \end{Bmatrix} \right\rangle +$$

$$+ \frac{r_o'}{2}\frac{eV_o}{2Wk}\, d/dk\ \partial/\partial r_o \left\langle \begin{Bmatrix} \left[-S_l + i\ T_l\right] \cos\phi_o \\ \left[-S_r - i\ T_r\right] \sin\phi_o \\ \left[S_m - i\ T_m\right] \sin\phi_o \end{Bmatrix} \right\rangle \tag{5.3.8}$$

The same procedure is used to evaluate (5.2.15) for $\phi = 0$ and gives in view of (5.1.10)

$$\left\langle \begin{Bmatrix} -\kappa B_z \\ -\kappa B_r \\ -\kappa B_m \end{Bmatrix} \right\rangle = +\frac{1}{2}\frac{eV}{2W}\, d/dk \left\langle \begin{Bmatrix} \left[S_l(k,r_o) - i\ T_l(k,r_o)\right] \cos\phi_o \\ \left[S_r(k,r_o) + i\ T_r(k,r_o)\right] \sin\phi_o \\ \left[-S_m(k,r_o) + i\ T_m(k,r_o)\right] \sin\phi_o \end{Bmatrix} \right\rangle +$$

$$+ \frac{r_o'}{2}\frac{eV_o}{2W}\, d^2/dk^2\ \partial/\partial r_o \left\langle \begin{Bmatrix} \left[S_l - i\ T_l\right] \sin\phi_o \\ \left[-S_r - i\ T_r\right] \cos\phi_o \\ \left[S_m - i\ T_m\right] \cos\phi_o \end{Bmatrix} \right\rangle \tag{5.3.9}$$

5.4 A Method to avoid S-Coefficients

In the preceding sections the mid-gap conditions (5.1.2) have been used to specify the solution of the equations of motion from which the difference equations across the whole gap have been deduced. Before these can be used the mid-gap values must be found with the help of the formula derived in Section 5.3 which involve the S-coefficients. Since the S-coefficients are rather complicated functions of $k = \omega/\dot{z}_o$ and r, it may be worthwhile indicating that there exists a possibility of avoiding them if the input coordinates are used to express the change of kinetic energy, phase,... across the gap. The expressions for the differences of these quantities are similar to those derived before. They involve the transit time factor T_o, eq. (2.6.7), where, however, the argument is

$$\bar{k} = \omega/\dot{z}_1 \tag{5.4.1}$$

($\dot{z}_1$ = longitudinal input velocity) in place of $k = \omega/\dot{z}_o$.

It is not possible to give here the complete set of difference equations.* The discussion is limited to the formula for the energy gain which is derived from the equation of motion :

$$m\,\ddot{z} = dW/dz = e\,E_z(z,r)\cos(\phi + \psi_1) \tag{5.4.2}$$

$E_z(z,r)$ is the field representation (2.2.11). It is assumed that at time zero the particle is at the cell entrance which has a distance $z = -\ell < -p/2$ from the gap (and cell) centre $z = 0$:

$$\begin{aligned} \omega t = \phi = 0: \quad z &= -\ell \quad \dot{z} = \dot{z}_1 \\ r &= r_1 \quad \dot{r} = \dot{r}_1 = r_1' \dot{z}_1 \end{aligned} \tag{5.4.3}$$

At that instant the longitudinal field distribution is $E_z = E_z(z,r)\cos\psi_1$. The relation between the phase constant ϕ_o introduced in eq. (5.1.3) and the present phase constant ψ_1 must be rather complicated and depends on ℓ, the radius and the velocities.

The equations of motion are again solved by perturbation theory. The zero order solutions describing free particle motion are in view of the initial conditions (3) :

$$\begin{aligned} \omega t = \phi &= \bar{k}z + \bar{k}\ell \\ r &= r_1 + r_1'(z + \ell) \end{aligned} \tag{5.4.4}$$

this is inserted into (2) where, as usual, a Taylor expansion with respect to r_1' is performed. Integration from $z = -\ell$ to $z = \ell$ gives :

---

* The complete set is given in [42].

$$\Delta W/e = \int_{-\ell}^{\ell} E_z(z,r_1)\cos(\bar{k}z + \bar{k}\ell + \psi_1)\,dz + r_1' \int_{-\ell}^{\ell} \frac{\partial E_z(z,r_1)}{\partial r_1}(z+\ell)\cos(\bar{k}z + \bar{k}\ell + \psi_1)\,dz$$

$$= \cos(\bar{k}\ell + \psi_1) \int_{-\ell}^{\ell} E_z(z,r_1)\cos(\bar{k}z)\,dz$$

$$+ r_1'\ell\cos(\bar{k}\ell + \psi_1) \int_{-\ell}^{\ell} \frac{\partial E_z(z,r_1)}{\partial r_1}\cos(\bar{k}z)\,dz$$

$$- r_1' \sin(\bar{k}\ell + \psi_1) \int_{-\ell}^{\ell} \frac{\partial E_z(z,r_1)}{\partial r_1} z \sin(\bar{k}z)\,dz$$

In the last step the symmetry $E_z(z,r) = E_z(-z,r)$ has been used. The limits of the integrals may be replaced by $\ell \to \infty$ while in the trigonometric functions the finite value of ℓ must be retained. Comparison with (2.6.4) gives for the gain in kinetic energy across th e whole gap:

$$\Delta W = eV_o\, T_1(\bar{k},r_1)\cos(\bar{k}\ell + \psi_1) + eV_o\left[\ell \frac{\partial}{\partial r_1} T_1(\bar{k},r_1) + \frac{d}{d\bar{k}}\frac{\partial}{\partial r_1} T_1(\bar{k},r_1)\right] r_1' \sin(\bar{k}\ell + \psi_1) \tag{5.4.5}$$

$$= eV_o\, T_o(\bar{k})\, I_o(k_r r_1)\cos(\bar{k}\ell + \psi_1) + eV_o\left[\left(\ell + \frac{d}{dk}\right) T_o(\bar{k})\, k_r\, I_1(k_r r_1)\right] r_1' \sin(\bar{k}\ell + \psi_1)$$

with

$$k_r = \left[\bar{k}^2 - k_o^2\right]^{\frac{1}{2}} \tag{5.4.6}$$

$T_o(\bar{k})$ is the transit time factor, eq. (2.6.8), depending on the longitudinal input velocity $\dot{z}_1$ by $\bar{k} = \omega/\dot{z}_1$.

The above formula shows the form of dynamics equations typical for this approach which differs from that presently employed. It is obvious that the whole linac design procedure must be changed from the very start if this new set of difference equations is employed.

6. Relativistic Motion

Here the relativistic equations of motion are solved approximately and the ensuing difference equations are derived. The method by which the relativistic mass variation is treated, may be new.

6.1 Approximate Solution of the Relativistic Equations of Motion

In a relativistic treatment of the equations of motion, the most troublesome thing is the root expressing the variation of mass with velocity. In order to circumvent this obstacle, it is assumed that the solutions $z(\phi)$ and $r(\phi)$ are already known and can be inserted into the equation of motion

$$m\omega \, d/d\phi \, \vec{v}(1-\beta^2)^{-1/2} = e\vec{E}(z,r,\phi) + e(\vec{v} \times \mu\vec{H}(z,r,\phi)) \qquad (6.1.1)$$

where m = rest mass. Integrating once with respect to ϕ leads to :

$$\vec{v}(1 - \beta^2)^{-1/2} = \vec{v}_o(1 - \beta_o^2)^{-1/2} + \int_o^\phi d\phi \left[e\vec{E} + e(\vec{v} \times \vec{H}\mu) \right] /m\omega \qquad (6.1.2)$$

$\vec{v}_o$ contains the constants of integration. The above equation is squared, i.e. the inner product is formed of the vector on each side, and divided by $c^2(\vec{\beta} = \vec{v}/c)$:

$$\beta^2(1 - \beta^2)^{-1} = \beta_o^2(1 - \beta_o^2)^{-1} + 2\kappa_c(1 - \beta_o^2)^{-\frac{1}{2}} \int_o^\phi d\phi \left[\vec{\beta}_o \cdot \vec{E}/E_1 + \vec{\beta}_o \cdot (\vec{v} \times \vec{H}\mu/E_1) \right] + \kappa_c^2 \ldots \equiv F$$

with (6.1.3)

$$\kappa_c = eE_1/(m\omega c) \approx \kappa\beta_o \, . \qquad (6.1.4)$$

$\kappa\beta_o < 0.004$, see (3.4.6). Taylor's expansions in this quantity are used, but they are more of a formal nature. For, as opposed to κ, κ_c itself is not the parameter indicating the order of magnitude of relativistic effects. Solving (3) for β^2, forming the expression for $(1 - \beta^2)^{\frac{1}{2}}$ and expanding into powers of κ_c gives :

$$\beta^2/(1 - \beta^2)^{-1} = F \qquad \beta^2 = F/(1 + F) \qquad (1 - \beta^2)^{\frac{1}{2}} = (1 + F)^{-\frac{1}{2}}$$

$$(1 - \beta^2)^{\frac{1}{2}} = (1 - \beta_o^2)^{\frac{1}{2}} \left\{ 1 - \kappa_c(1 - \beta_o^2)^{\frac{1}{2}} \int_o^\phi d\phi \left[\vec{\beta}_o \cdot E/E_1 + \vec{\beta}_o \cdot (v \times H\mu/E_1) \right] + \kappa_c^2 \ldots \right\} \qquad (6.1.5)$$

Multiplying eq. (2) by (5) gives:

$$k\vec{v} = k\vec{v}_o + \omega(1 - \beta_o^2)^{\frac{1}{2}} \kappa \int_o^\phi d\phi \left[\vec{E}/E_1 + (\vec{v} \times \mu\vec{H}/E_1) \right]$$
$$- k\vec{v}_o(1 - \beta_o^2)^{\frac{1}{2}} \kappa_c \int_o^\phi d\phi \left[\vec{\beta}_o \cdot E/E_1 + \vec{\beta}_o \cdot (v \times H\mu/E_1) \right] + (1 - \beta_o^2)^{\frac{1}{2}} \kappa_c\kappa \ldots \qquad (6.1.6)$$

The first integral arises from the force on the right hand side of equation (1). The second one has been introduced by the manipulations performed to get rid of $(1 - \beta^2)^{-\frac{1}{2}}$ on the left hand side. Therefore it is admissible to say that it accounts for the mass variation. The increase (or decrease) of the particle mass is expressed by the effect of the forces having acted upon it.

Plane motion is assumed, $0 = \dot{\theta} \equiv 0$, and the vector $\vec{v}$ has two components only :

$$\vec{v} = (\dot{r} \ , \ \dot{z}) = \omega(dr/d\phi, \ dz/d\phi) = \omega(\grave{r} \ , \ \grave{\phi}) \tag{6.1.7}$$

Perturbation series similar to (5.1.5) are assumed:

$$\begin{aligned} z(\phi) &= z^{(o)}(\phi) + \kappa \, z^{(r)}(\phi) + \ \kappa^2 .. \\ r(\phi) &= r^{(o)}(\phi) + \kappa \, r^{(r)}(\phi) + \ \kappa^2 .. \end{aligned} \tag{6.1.8}$$

$z^{(o)}(\phi)$, $r^{(o)}(\phi)$, $\vec{v}^{(o)}(\phi)$ correspond to free-particle motion and are determined by the mid-plane conditions (5.1.2) :

$$\begin{aligned} \vec{v}^{(o)} &= \vec{v}_o = (\dot{r}_o, \dot{z}_o) = \omega \ (\grave{r}_o, \grave{z}_o) = (\omega/k) \ (r'_o, 1) \\ z^{(o)} &= \phi/k \qquad r^{(o)} = \grave{r}_o \phi + r_o \end{aligned} \tag{6.1.9}$$

where $k = \omega/\dot{z}_o$. The first order terms are labelled by the superscript r to indicate that after inserting (8) into (6), terms proportional to κ and κ_c must be retained since these two quantities are not so different in magnitude for higher velocities $\dot{z}_o$. This gives:

$$\begin{aligned} \frac{\vec{v}^{(r)}(\phi)}{\omega(1-\beta_o^2)^{\frac{1}{2}}} = \frac{1}{k} \int_o^\phi \frac{\vec{E}}{E_1}(z^{(o)}, r^{(o)}, \phi) \ d\phi + \frac{\omega}{k} \int_o^\phi d\phi \ \frac{\vec{v}^{(o)}}{\omega} \times \frac{\vec{\mu H}}{E_1}(z^{(o)}, r^{(o)}, \phi) \\ - \frac{\vec{v}_o}{\omega} \, k_o^2 \, \frac{1}{k} \int_o^\phi d\phi \ \frac{\vec{v}_o}{\omega} \cdot \frac{\vec{E}}{E_1}(z^{(o)}, r^{(o)}, \phi) \end{aligned} \tag{6.1.10}$$

where $\kappa_c \omega k/(\kappa c) = \omega^2/c^2 = k_o^2$ has been used. The term of the second line of eq. (6) involving the magnetic field does not contribute to that order of approximation. (10) is split up into components and terms non-linear in r'_o are dropped :

$$z^{(r)\backprime}(\phi) =$$

$$(1-\beta_o^2)^{\frac{1}{2}} \left\{ \frac{1}{k} \int_o^\phi \frac{E_z}{E_1}(z^{(o)},r^{(o)},\phi)\, d\phi + \frac{k_o^2}{k^2}\, r_o' k\, \frac{1}{k} \int_o^\phi \frac{\mu H_\Theta(z^{(o)},r^{(o)},\phi)}{E_1 k_o/c}\, d\phi \right.$$
$$\left. - \frac{k_o^2}{k^2}\left(\frac{1}{k} \int_o^\phi \frac{E_z}{E_1}(z^{(o)},r^{(o)},\phi)\, d\phi + r_o' \frac{1}{k} \int_o^\phi \frac{E_r}{E_1}(z^{(o)},r^{(o)},\phi)\, d\phi + r_o'^2 \ldots \right) \right\}$$
$$= (1-\beta_o^2)^{\frac{1}{2}} \left\{ z^{(1)\backprime}(\phi) + \frac{k_o^2}{k^2} r_o' k\, m^{(1)\backprime}(\phi) - \frac{k_o^2}{k^2}\left(z^{(1)\backprime}(\phi) + r_o' r^{(1)\backprime}(\phi) \right) \right\}$$

(6.1.11)

$$r^{(r)\backprime}(\phi) =$$

$$(1-\beta_o^2)^{\frac{1}{2}} \left\{ \frac{1}{k} \int_o^\phi \frac{E_r}{E_1}(z^{(o)},r^{(o)},\phi)\, d\phi - \frac{k_o^2}{k^2} k \frac{1}{k} \int_o^\phi \frac{\mu H_\Theta(z^{(o)},r^{(o)},\phi)}{E_1 k_o/c}\, d\phi - \frac{k_o^2}{k^2} r_o' \frac{1}{k} \int_o^\phi \frac{E_z}{E_1}(z^{(o)},r^{(o)},\phi)\, d\phi \right\}$$
$$= (1-\beta_o^2)^{\frac{1}{2}} \left\{ r^{(1)\backprime}(\phi) - \frac{k_o^2}{k^2} k\, m^{(1)\backprime}(\phi) - \frac{k_o^2}{k^2} r_o' z^{(1)\backprime}(\phi) \right\}$$

The reduction of the relativistic equations of motion is completed. The first order relativistic solutions are expressed by functions already defined in the non-relativistic treatment, see (5.2.11), where the integral representations (2.2.11) to (2.2.13) for $E_z(z,r,\phi)$, E_r and H_Θ have been used. The second integration with respect to ϕ is easy, it amounts to dropping the grave accents in the above equations. The first term in each line is due to the electrical field and is the only one included in the non-relativistic solutions. All other terms are preceded by $k_o^2/k^2 \approx \beta_o^2$ which hints to the fact that all relativistic contributions are of the order $\kappa\beta_o^2$. This is confirmed by the outcome of the evaluations which follow. The second term in each line arises from the magnetic field, the remaining ones account for the relativistic mass variation.

The thin lens variables $\bar{\phi}(z)$, $r'(z)$, $\bar{r}(z)$ as well as $r^{\backprime}(\phi)$ and $\bar{\bar{r}}(\phi)$ may be taken from (5.1.20) to (5.1.25) except that in these equations $z^{(1)\backprime}(\phi)$, $z^{(1)}(\phi)$, $r^{(1)\backprime}(\phi)$ and $r^{(1)}(\phi)$ must be replaced by $z^{(r)\backprime}(\phi)$, $z^{(r)}(\phi)$, $r^{(r)\backprime}(\phi)$ and $r^{(r)}(\phi)$ respectively. Kinetic energy T deserves special attention. In the non-relativistic case only longitudinal kinetic energy has been used, while in the relativistic domain longitudinal and transverse kinetic energy in general are coupled. In addition, the relativistic and non-relativistic expresssions for

total kinetic energy are different. To the degree of approximation here employed, however, they are not coupled, and equal the non-relativistic expressions. In order to demonstrate this, (5) is inserted into

$$T_{tot} = m\,c^2 \left[(1 - \beta^2)^{-1/2} - 1 \right]$$

and this is afterwards expanded in powers of κ_c :

$$T_{tot} = m\,c^2 \left[(1 - \beta_o^2)^{-1/2} - 1 \right] + m\,c^2\,\kappa_c \int_o^{\phi} d\phi\ \vec{\beta}_o \cdot \vec{E}/E_1 + \kappa_c^2 \ldots \qquad (6.1.12)$$

$$= \text{const.} + (m\omega^2/k)\,\kappa \left[z^{(1)}(\phi) + r_o' r^{(1)}(\phi) \right] + \kappa_c^2 \ldots$$

The constant cancels when differences are formed. The first term in the square bracket equals the second term of (5.1.17), the essential term of non-relativistic longitudinal kinetic energy. The last term in the above bracket is radial kinetic energy, provided $\dot{\theta} \equiv 0$ and the magnetic field force is neglected.

6.2 Relativistic Difference Equations

For simplicity, in this section the relativistic difference equations across the whole gap and along the first half of it are derived together. It is known from the non-relativistic treatment that each of the difference equations consists of two parts, one containing T-coefficients and giving half of the change of the corresponding quantity across the total gap, the second part containing S-coefficients. Of course, this has been checked here and the simplified procedure is mainly employed in order to save space.

The change in kinetic energy is found from (6.1.12), (5.3.8) and (5.2.14):

$$\Delta w_1^{(r)} = 2\,Wk\,\kappa \left\{ \left[z^{(1)\sim}(0) - z^{(1)\sim}(-k\ell) \right] + r_o' \left[r^{(1)\sim}(0) - r^{(1)\sim}(-k\ell) \right]^* \right\} + \kappa^2 \ldots$$

$$= \frac{1}{2} eV_o \left\{ \left[T_1 \cos\phi_o + S_1 \sin\phi_o \right] + r_o' \, d/dk \;\; \partial/\partial r_o \left[T_1 \sin\phi_o - S_1 \cos\phi_o \right] \right.$$

$$\left. + r_o' \left[- T_r \sin\phi_o - S_r \cos\phi_o \right]^* \right\} + \kappa^2 \ldots$$

The argument (k, r_o) of the T- and S-coefficients is suppressed throughout this section. Terms containing the T-coefficients are combined to give the energy gain across the whole gap:

$$\Delta W^{(r)} = eV_o \left\{ T_1 \cos\phi_o + d/dk \;\; \partial/\partial r_o \; T_1 \, r_o' \sin\phi_o + \left[-T_r \, r_o' \sin\phi_o \right]^* \right\} + \kappa^2 \ldots \tag{6.2.1}$$

and thereafter the change in the first half :

$$\Delta W_1^{(r)} = \Delta W^{(r)}/2 + \frac{1}{2} \; eV_o \left\{ S_1 \sin\phi_o - d/dk \;\; \partial/\partial r_o \; S_1 \, r_o' \cos\phi_o + \left[-S_r \, r_o' \cos\phi_o \right]^* \right\} \tag{6.2.2}$$

$$= \Delta w_1 + \frac{1}{2} eV_o \left[- T_r \sin\phi_o - S_r \cos\phi_o \right]^*$$

For the derivation of the other difference equations, equations (5.1.18) to (5.1.25) may be used where, however, the superscript $^{(1)}$ must be replaced by $^{(r)}$ and the corresponding functions be taken from (6.1.11). The arising integrals have already been evaluated in equations (5.2.14), (5.2.16) and (5.3.8), (5.3.9).

---

* The starred brackets give, as always, radial kinetic energy.

This gives for the change in reduced phase :

$$\bar{\Delta\phi}_1^{(r)} = -\kappa k \left\{ z^{(r)}(0) - \left[z^{(r)}(-k\ell) - (-k\ell)\, z^{(r)\cdot}(-k\ell) \right] \right\} + \kappa^2 \ldots$$

$$\frac{\bar{\Delta\phi}_1^{(r)}}{(1-\beta_o^2)^{\frac{1}{2}}} = -\kappa k \left\{ \left(1 - \frac{k_o^2}{k^2}\right) \left(z^{(1)}(0) - \left[z^{(1)}(-k\ell) - (-k\ell)\, z^{(1)\cdot}(-k\ell) \right] \right) \right.$$

$$+ \frac{k_o^2}{k^2} r'_o \left(k\, m^{(1)}(0) - k\left[m^{(1)}(-k\ell) - (-k\ell)\, m^{(1)\cdot}(-k\ell) \right] \right.$$

$$\left. \left. - r^{(1)}(0) + \left[r^{(1)}(-k\ell) - (-k\ell)\, r^{(1)\cdot}(-k\ell) \right] \right) \right\}$$

$$= -\frac{1}{2}\frac{eV_o}{2W} k \left\{ \left(1 - \frac{k_o^2}{k^2}\right) \left(\frac{d}{dk} \left[-T_1 \sin\phi_o + S_1 \cos\phi_o \right] \right.\right.$$

$$\left. + r'_o \frac{d^2}{dk^2} \frac{\partial}{\partial r_o} \left[T_1 \cos\phi_o + S_1 \sin\phi_o \right] \right)$$

$$\left. + \frac{k_o^2}{k^2} \left(r'_o k \frac{d}{dk} \left[T_m \cos\phi_o + S_m \sin\phi_o \right] - \frac{d}{dk} \left[-T_r \cos\phi_o + S_r \sin\phi_o \right] \right) \right\}$$

With

$$k \frac{d}{dk} T_m - \frac{d}{dk} T_r = k \frac{d}{dk} T_o \frac{1}{k_r} I_1 - \frac{d}{dk} T_o \frac{k}{k_r} I_1 = -T_o \frac{1}{k_r} I_1$$

(6.2.3)

$$= -T_m$$

the total reduced phase, $\bar{\Delta\phi}^{(r)}$, can be written:

$$\frac{\bar{\Delta\phi}^{(r)}}{(1-\beta_o)^{\frac{1}{2}}} = \frac{eV_o}{2W} k \left\{ \left(1 - \frac{k_o^2}{k^2}\right) \left(\frac{d}{dk} T_1 \sin\phi_o - \frac{d^2}{dk^2} \frac{\partial}{\partial r_o} T_1 r'_o \cos\phi_o \right) \right.$$

$$\left. - \frac{k_o^2}{k^2} \left(\qquad\qquad T_m r'_o \cos\phi_o \right) \right\}$$

(6.2.4)

$$= \left(1 - \frac{k_o^2}{k^2}\right) \bar{\Delta\phi} - \frac{eV_o}{2W} k \frac{k_o^2}{k^2} \left(T_o \frac{1}{k_r} I_1 \right) r'_o \cos\phi_o$$

and thereafter the change in the first half :

$$\bar{\Delta\phi}_1^{(r)} = \bar{\Delta\phi}^{(r)}/2 - (1 - \beta_o^2)^{\frac{1}{2}} \frac{1}{2} \frac{eV_o}{2W} k \left\{ \left(1 - \frac{k_o^2}{k^2}\right) \left(\frac{d}{dk} S_1 \cos\phi_o + \frac{d^2}{dk^2} \frac{\partial}{\partial r_o} S_1 r'_o \sin\phi_o \right) \right.$$

$$\left. + \frac{k_o^2}{k^2} \left(-k \frac{d}{dk} S_m - \frac{d}{dk} S_r \right) r'_o \sin\phi_o \right\} \quad (6.2.5)$$

$$\frac{\Delta\bar{\phi}_1^{(r)}}{(1-\beta_o^2)^{\frac{1}{2}}} = \left(1 - \frac{k_o^2}{k^2}\right)\Delta\bar{\phi}_1 - \frac{k_o^2}{k^2}\frac{1}{2}\frac{eV_o}{2W} k r_o' \left(T_m \cos\phi_o - \left[k \frac{d}{dk} S_m + \frac{d}{dk} S_r \right] \sin\phi_o \right)$$

The change in radial velocity is :

$$\Delta r_1^{\wedge(r)} = \kappa \left[r^{(r)\wedge}(0) - r^{(r)\wedge}(-k\ell) \right] + \kappa^2 \ldots$$

$$\frac{\Delta r_1^{\wedge(r)}}{(1-\beta_o^2)^{\frac{1}{2}}} = \kappa \left\{ \left[r^{(1)\wedge}(0) - r^{(1)\wedge}(-k\ell) \right] - \frac{k_o^2}{k^2} \left(\left[km^{(1)\wedge}(0) - km^{(1)\wedge}(-k\ell) \right] + r_o' \left[z^{(1)\wedge}(0) - z^{(1)\wedge}(-k\ell) \right] \right) \right\}$$

$$= \frac{1}{2}\frac{eV_o}{2Wk} \left\{ \left[- T_r \sin\phi_o - S_r \cos\phi_o \right] + r_o' \frac{d}{dk} \frac{\partial}{\partial r_o} \left[T_r \cos\phi_o - S_r \sin\phi_o \right] - \frac{k_o^2}{k^2} \left(\begin{array}{l} \left[-k\, T_m \sin\phi_o + k\, S_m \cos\phi_o \right] + r_o' k \frac{d}{dk} \frac{\partial}{\partial r_o} \left[T_m \cos\phi_o + S_m \sin\phi_o \right] \\ \qquad + r_o' \left[T_1 \cos\phi_o + S_1 \sin\phi_o \right] \end{array} \right) \right\}$$

With (3) and $k\, T_m = T_r$ the difference $\Delta r^{\wedge(r)}$ can be written :

$$\Delta r^{\wedge(r)} = (1 - \beta_o^2)^{\frac{1}{2}} \frac{eV_o}{2Wk} \left\{ \left(1 - \frac{k_o^2}{k^2}\right) \left(- T_r \sin\phi_o + \frac{d}{dk} \frac{\partial}{\partial r_o} T_r \, r_o' \cos\phi_o \right) - \frac{k_o^2}{k^2} \left(\left[T_1 - \frac{\partial}{\partial r_o} T_m \right] r_o' \cos\phi_o \right) \right\} \qquad (6.2.6)$$

and with this one gets for $\Delta r_1^{\wedge(r)}$: (6.2.7)

$$\Delta r_1^{\wedge(r)} = \Delta r^{\wedge(r)}/2 + (1 - \beta_o^2)^{\frac{1}{2}} \frac{1}{2} \frac{eV_o}{2Wk} \left\{ - S_r \cos\phi_o - \frac{d}{dk} \frac{\partial}{\partial r_o} S_r \, r_o' \sin\phi_o - \frac{k_o^2}{k^2} \left(\begin{array}{l} k\, S_m \cos\phi_o + k \frac{d}{dk} \frac{\partial}{\partial r_o} S_m \, r_o' \sin\phi_o \\ \qquad + \quad S_1 \qquad r_o' \sin\phi_o \end{array} \right) \right\}$$

The transformation from $r^{\wedge} = dr/d\phi$ to $r' = dr/dz$ is accomplished by use of :

$$\Delta r'^{(r)} = k \;\; \Delta r^{\wedge(r)} - r_o' \kappa k \left[z^{(r)\wedge}(k\ell) - z^{(r)\wedge}(-k\ell) \right]$$

$$= k \;\; \Delta r^{\wedge(r)} - r_o' (1 - \beta_o^2)^{\frac{1}{2}} (1 - k_o^2/k^2) \;\; \Delta W/(2W) + r_o'^2 \ldots \qquad (6.2.8)$$

$$\Delta r_1'^{(r)} = k \;\; \Delta r_1^{\wedge(r)} - r_o' (1 - \beta_o^2)^{\frac{1}{2}} (1 - k_o^2/k^2) \;\; \Delta w_1/(2W) + r_o'^2 \ldots$$

This gives :

$$\frac{\Delta r'^{(r)}}{(1-\beta)^{\frac{1}{2}}} = \frac{eV_o}{2W}\left\{\left(1-\frac{k_o^2}{k^2}\right)\left(-T_r\sin\phi_o + \left[\frac{d}{dk}\frac{\partial}{\partial r_o}T_r - T_1\right]r'_o\cos\phi_o\right)\right.$$
$$\left. - \frac{k_o^2}{k^2}\left(\left[T_1 - \frac{\partial}{\partial r_o}T_m\right]r'_o\cos\phi_o\right)\right\}$$
$$= \left(1-\frac{k_o^2}{k^2}\right)\Delta r' - \frac{eV_o}{2W}\frac{k_o^2}{k^2}\left[T_o(I_o - I'_1)\right]r'_o\cos\phi_o$$

$$\Delta r_1'^{(r)} = \Delta r'^{(r)}/2 - (1-\beta_o^2)^{\frac{1}{2}}\frac{1}{2}\frac{eV_o}{2W}\left\{\left(S_r + \frac{k_o^2}{k^2}k\,S_m\right)\cos\phi_o\right.$$
$$\left. + \left[\frac{\partial}{\partial r_o}\left(\frac{d}{dk}S_r + \frac{k_o^2}{k^2}k\frac{d}{dk}S_m\right) + S_1\right]r'_o\sin\phi_o\right\} \qquad (6.2.10)$$

The change of reduced radius is calculated in two steps, at first the change in $\bar{\bar{r}} = r - \phi\, dr/d\phi$ is found, and then that of $\bar{r} = r - z\, dr/dz$.

$$\Delta\bar{\bar{r}}_1^{(r)} = \kappa\left\{r^{(r)}(0) - \left[r^{(r)}(-k\ell) - (-k\ell)\,r'^{(r)}(-k\ell)\right]\right\} + \kappa^2\ldots$$

$$\frac{\Delta\bar{\bar{r}}_1^{(r)}}{(1-\beta_o^2)^{\frac{1}{2}}} = \frac{1}{2}\frac{eV_o}{2W}\left\{\frac{d}{dk}\left[-T_r\cos\phi_o + S_r\sin\phi_o\right] + r'_o\frac{d^2}{dk^2}\frac{\partial}{\partial r_o}\left[-T_r\sin\phi_o - S_r\cos\phi_o\right]\right.$$
$$\left. - \frac{k_o^2}{k^2}\left(k\frac{d}{dk}\left[-T_m\cos\phi_o - S_m\sin\phi_o\right] + r'_o\,k\frac{d^2}{dk^2}\frac{\partial}{\partial r_o}\left[-T_m\sin\phi_o + S_m\cos\phi_o\right]\right.\right.$$
$$\left.\left. + r'_o\frac{d}{dk}\left[-T_1\sin\phi_o + S_1\cos\phi_o\right]\right)\right\}$$

In the expression for $\bar{\bar{\Delta r}}^{(r)}$ the T-coefficients can be combined

$$\frac{d}{dk}T_r - \frac{k_o^2}{k^2}k\frac{d}{dk}T_m = \left(1-\frac{k_o^2}{k^2}\right)\frac{d}{dk}T_r + \frac{k_o^2}{k^2}T_m$$
$$\frac{d^2}{dk^2}T_r - \frac{k_o^2}{k^2}k\frac{d^2}{dk^2}T_m = \left(1-\frac{k_o^2}{k^2}\right)\frac{d^2}{dk^2}T_r + \frac{k_o^2}{k^2}2\frac{d}{dk}T_m \qquad (6.2.11)$$

to give:

$$\frac{\Delta\bar{\bar{r}}'(r)}{(1-\beta_o^2)^{\frac{1}{2}}} = \frac{eV_o}{2W}\left\{-\left(1-\frac{k_o^2}{k^2}\right)\left(\frac{d}{dk}\,T_r\cos\phi_o + \frac{d^2}{dk^2}\frac{\partial}{\partial r_o}\,T_r\; r_o'\sin\phi_o\right)\right.$$
$$\left. - \frac{k_o^2}{k^2}\left(T_m\cos\phi_o - \left[\frac{d}{dk}\,T_1 - 2\,\frac{d}{dk}\frac{\partial}{\partial r_o}\,T_m\right] r_o'\sin\phi_o\right)\right\} \qquad (6.2.12)$$

$$= \left(1-\frac{k_o^2}{k^2}\right)\Delta\bar{\bar{r}} - \frac{k_o^2}{k^2}\left[\left(T_o\,\frac{1}{k_r}\;\; I_1\right)\cos\phi_o - \frac{d}{dk}\left(T_o(I_o - 2\,I_1')\right) r_o'\sin\phi_o\right]$$

$$\Delta\bar{\bar{r}}_1(r) = \Delta\bar{\bar{r}}(r)/2 + (1-\beta_o^2)^{\frac{1}{2}}\,\frac{1}{2}\,\frac{eV_o}{2W}\left\{\left[\frac{d}{dk}\;S_r + \frac{k_o^2}{k^2}\,k\,\frac{d}{dk}\,S_m\right]\sin\phi_o\right.$$
$$- \frac{\partial}{\partial r_o}\left[\frac{d^2}{dk^2}S_r + \frac{k_o^2}{k^2}\,k\,\frac{d^2}{dk^2}S_m\right] r_o'\;\cos\phi_o$$
$$\left. - \frac{k_o^2}{k^2}\;\frac{d}{dk}\,S_1\;\; r_o'\;\cos\phi_o\right\} \qquad (6.2.13)$$

The transition $\bar{\bar{r}} = r - \phi\; dr/d\phi \to \bar{r} = r - z\; dr/dz$ is analogous to the last line of equation (5.1.24) :

$$\Delta\bar{r}(r) = \Delta\bar{\bar{r}}(r) + r_o'\,\Delta\bar{\phi}(r)/k$$

$$\frac{\Delta\bar{r}'(r)}{(1-\beta_o^2)^{\frac{1}{2}}} = \left(1-\frac{k_o^2}{k^2}\right)\Delta\bar{r}' - \frac{k_o^2}{k^2}\,\frac{eV_o}{2W}\left\{T_m\cos\phi_o + \frac{d}{dk}\left[\,2\,\frac{\partial T_m}{\partial r_o} - T_1\,\right] r_o'\sin\phi_o\right\} \qquad (6.2.14)$$

$$\Delta\bar{r}_1(r) = \Delta\bar{r}(r)/2 + (1-\beta_o^2)^{\frac{1}{2}}\,\frac{1}{2}\,\frac{eV_o}{2W}\left\{\left(\frac{d}{dk}\,S_r + \frac{k_o^2}{k^2}\,k\,\frac{d}{dk}\;S_m\right)\sin\phi_o\right.$$
$$\left. - \left(\frac{\partial}{\partial r_o}\left[\,\frac{d^2}{dk^2}\;S_r + \frac{k_o^2}{k^2}\,k\,\frac{d^2}{dk^2}S_m\,\right] + \frac{d}{dk}\,S_1\right) r_o'\cos\phi_o\right\} \qquad (6.2.15)$$

The four quantities used ΔW, $\Delta\bar{\phi}$, $\Delta r'$, $\Delta\bar{r}$; Δw_1, $\Delta\bar{\phi}_1$, $\Delta r_1'$, $\Delta\bar{r}_1$ when treating particle trajectories in the thin lens approximation are listed in Tables II and IV.

ACKNOWLEDGMENTS

The author is very indebted to Dr. P.M. Lapostolle for suggesting this topic, his advice and many helpful discussions. Dr. M. Martini read parts of the draft and suggested improvements. Dr. K. Katz, Saclay, and Drs. M. Martini and D.J. Warner provided the results of their cavity calculations. The various programmes and the drawings have been prepared by Mme Y. Marti who also checked part of the formulae.

Table I - The Transit Time Factor and its Derivatives

$$T_o(k) = \frac{2}{V_o}\int_o^\infty E_z(z,o)\cos(kz)\,dz = T_{oo}(1+Y)$$

$$T'_o(k) = -\frac{2}{V_o}\int_o^\infty E_z(z,o)\, z\sin(kz)\,dz = T'_{oo}(1+Y) + T_{oo}\,Y'$$

$$T''_o(k) = -\frac{2}{V_o}\int_o^\infty E_z(z,o)\, z^2\cos(kz)\,dz = T''_{oo}(1+Y) + 2\,T'_o\,Y' + T_o\,Y''$$

$$k_r = \left[k^2 - k_o^2\right]^{\frac{1}{2}} \qquad p = g + 2R_i \qquad \text{(Fig. 2.1.4)}$$

$$T_{oo}(k) = \frac{J_o(k_o a)}{I_o(k_r a)}\,\frac{\sin(kp/2)}{(kp/2)}$$

$$T'_{oo} = p\,T_{oo}\left[\frac{1}{2}\operatorname{ctg}(kp/2) - \frac{1}{kp} - \frac{a}{p}\frac{kp}{k_r p}\,\frac{I_1(k_r a)}{I_o(k_r a)}\right]$$

$$T''_{oo} = p\,T'_{oo}\left[\quad''\quad\right]$$

$$+ p^2\,T_{oo}\left[-\frac{1}{4}\frac{1}{\sin^2(kp/2)} + \frac{1}{(kp)^2} - \left(\frac{a}{p}\frac{kp}{k_r p}\right)^2\left\{1 - \left(\frac{I_1(k_r a)}{I_o(k_r a)}\right)^2\right\} - \frac{a}{p}\frac{I_1(k_r a)}{I_o(k_r a)}\left(\frac{1}{k_r p} - 2\frac{(kp)^2}{(k_r p)^3}\right)\right]$$

$$Y = -2(kp)^2\sum_{n=1}^{\infty}(-1)^n B_n\left[(2\pi n)^2 - (kp)^2\right]^{-1}$$

$$Y' = 2p\left[\frac{Y}{kp} - 2(kp)^3\sum_{n=1}^{\infty}(-1)^n B_n\left[(2\pi n)^2 - (kp)^2\right]^{-2}\right]$$

$$Y'' = 8p^2\left[-\frac{Y}{(kp)^2} + \frac{5}{8}\frac{1}{kp}\frac{Y'}{p} - 2(kp)^4\sum_{n=1}^{\infty}(-1)^n B_n\left[(2\pi n)^2 - (kp)^2\right]^{-3}\right]$$

The apostrophe (') denotes derivation with respect to $k(=\omega/\dot{z}_o)$. It is customary to normalize the derivatives by multiplying them by $2\pi/L$ or k. This has not been done in the above expressions.

Table II - Expressions for T- and S-coefficients

$$T_1(k,r) = T_o(k)\, I_1(k_r r) \qquad T_m(k,r) = T_o(k)\, I_1(k_r r)/k_r$$

$$T_r(k,r) = T_o(k)\, k\, I_1(k_r r)/k_r \qquad k_r = (k^2 - k_o^2)^{1/2}$$

$$S_1(k,r) = -\operatorname{ctg}(kp/2)\, T_o\, I_o(k_r r) + \frac{J_o(k_o r)}{pk/2} - 4\, J_o(k_o a) \sum_{n=1}^{\infty} \frac{pk\, B_n}{(2\pi n)^2 - (kp)^2} \frac{I_o(\mu_n r/p)}{I_o(\mu_n a/p)}$$

$$- 8\, J_o(k_o a)\, (kp) \left(\frac{p}{a}\right)^2 \sum_{n=0}^{\infty} \frac{B_n(-1)^n}{1+\delta_{no}} \sum_{\nu=1}^{\infty} \frac{J_o(j_\nu r/a)}{J_1(j_\nu)} \frac{\exp(-\eta_\nu p/2)}{(kp)^2 + (\eta_\nu p)^2} \frac{j_\nu}{(2\pi n)^2 + (\eta_\nu p)^2}$$

$$S_r(k,r) = \operatorname{ctg}(kp/2)\, T_o(k)\, k\, I_1(k_r r)/k_r + 4\, J_o(k_o a) \sum_{n=1}^{\infty} \frac{B_n (2\pi n)^2}{(2\pi n)^2 - (kp)^2} \frac{1}{\mu_n} \frac{I_1(\mu_n r/p)}{I_o(\mu_n a/p)}$$

$$- 8\, J_o(k_o a) \frac{p}{a} \sum_{n=0}^{\infty} \frac{B_n(-1)^n}{1+\delta_{no}} \sum_{\nu=1}^{\infty} \frac{J_1(j_\nu r/a)}{J_1(j_\nu)} \frac{\exp(-\eta_\nu p/2)}{(kp)^2 + (\eta_\nu p)^2} \frac{(\eta_\nu p)^2}{(kp)^2 + (\eta_\nu p)^2}$$

$$\frac{1}{p} S_m(k,r) = -\operatorname{ctg}(kp/2)\, T_o(k) \frac{1}{k_r p} I_1(k_r r) + \frac{2}{kp} \frac{J_o(k_o r)}{k_o p} - 4\, J_o(k_o a) kp \sum_{n=1}^{\infty} \frac{B_n}{(2\pi n)^2 - (kp)^2} \frac{1}{\mu_n} \frac{I_1(\mu_n r/p)}{I_o(\mu_n a/p)}$$

$$- 8\, J_o(k_o a)\, kp \frac{p}{a} \sum_{n=0}^{\infty} \frac{B_n(-1)^n}{1+\delta_{no}} \sum_{\nu=1}^{\infty} \frac{J_1(j_\nu r/a)}{J_1(j_\nu)} \frac{\exp(-\eta_\nu p/2)}{(kp)^2 + (\eta_\nu p)^2} \frac{1}{(2\pi n)^2 + (\eta_\nu p)^2}$$

$$\eta_\nu p = \left[(j_\nu p/a)^2 - (k_o p)^2 \right]^{\frac{1}{2}} \qquad \mu_n = \left[(2\pi n)^2 - (k_o p)^2 \right]^{\frac{1}{2}} \qquad p = g + 2 R_i$$

S_m and T_m are not dimensionless. Concerning their normalization see p. 53.
p, g, R_i are defined in Fig. 2.1.4.

Table III - Non-relativistic change of longitudinal kinetic energy, reduced phase, radial slope and reduced radial position across a gap

$$\Delta W = eV_o \; T_o I_o \cos\phi + eV_o \; d/dk(T_o k_r I_1) \; r' \sin\phi$$

$$\Delta\bar{\phi} = \alpha k \; d/dk(T_o I_o) \sin\phi - \alpha k \; d^2/dk^2(T_o k_r I_1) \; r' \cos\phi$$

$$\Delta r' = -\alpha \; (T_o k \, I_1/k_r) \sin\phi + \alpha \left[d/dk(T_o k \, I_1') - T_o I_o \right] r' \cos\phi$$

$$\Delta\bar{r} = -\alpha \; d/dk(T_o \, k \, I_1/k_r) \cos\phi - \alpha \left[d^2/dk^2(T_o k \, I_1') - d/dk(T_o I_o) \right] r' \sin\phi$$

Table IV - Change of the Same Quantities in the Relativistic Case

$$\Delta W_r = \Delta W + \left[- eV_o \; (T_o k \, I_1/k_r) \; r' \sin\phi \right]^*$$

$$\Delta\bar{\phi}_r/(1 - \beta_o^2)^{\frac{1}{2}} = \Delta\bar{\phi} \; (1 - k_o^2/k^2) - \alpha k (k_o^2/k^2) \; (T_o I_1/k_r) \; r' \cos\phi$$

$$\Delta r_r'/(1 - \beta_o^2)^{\frac{1}{2}} = \Delta r' (1 - k_o^2/k^2) + \alpha \; (k_o^2/k^2) \; T_o \; (I_1' - I_o) \; r' \cos\phi$$

$$\Delta\bar{r}_r/(1 - \beta_o^2)^{\frac{1}{2}} = \Delta r \; (1 - k_o^2/k^2) - \alpha (k_o^2/k^2) \; (T_o I_1/k_r) \cos\phi - \alpha \; (k_o^2/k^2) \; d/dk(2T_o I_1' - T_o I_o) \; r' \sin\phi$$

* Adding the term in the square brackets gives the gain in total kinetic energy . (cf. eq. (6. 1. 12) and (6.2.1)).

Table V - Change of Kinetic Energy, Reduced Phase, Radial Slope and Reduced Position along the First Half of the Gap

$$\Delta w_1 = \Delta W/2 + (eV_o/2)\left[S_1 \sin\phi - d/dk\ \partial S_1/\partial r\ r' \cos\phi \right]$$

$$\Delta \bar{\phi}_1 = \Delta \bar{\phi}/2 - (\alpha k/2)\left[dS_1/dk \cos\phi + d^2/dk^2\ \partial S_1/\partial r\ r' \sin\phi \right]$$

$$\Delta r'_1 = \Delta r'/2 - (\alpha/2)\left[S_r \cos\phi + (d/dk\ \partial S_r/\partial r + S_1)\ r' \sin\phi \right]$$

$$\Delta \bar{r}_1 = \Delta \bar{r}/2 + (\alpha/2)\left[dS_r/dk \sin\phi - (d^2/dk^2\ \partial S_r/\partial r + dS_1/dk)\ r' \cos\phi \right]$$

Table VI - Change of the Same Quantities in the Relativistic Case

$$\Delta w_{rl} = \Delta W_r/2 + (eV_o/2)\left\{ S_l \sin\phi - \left(\frac{\partial}{\partial r}\frac{dS_l}{dk} + \left[S_r \right]^* \right) r' \cos\phi \right\}$$

$$= \Delta w_l + r' \left[- T_r \sin\phi - S_r \cos\phi \right]^*$$

$$\Delta\bar{\phi}_{rl} = \Delta\bar{\phi}_r/2 - (1-\beta_o^2)^{\frac{1}{2}} \frac{\alpha k}{2} \left\{ \left(1 - \frac{k_o^2}{k^2}\right)\left(\frac{dS_l}{dk}\cos\phi + \frac{\partial}{\partial r}\frac{d^2S_l}{dk^2} r' \sin\phi\right) - \frac{k_o^2}{k^2}\left(\frac{dS_r}{dk} + k\frac{dS_m}{dk}\right) r' \sin\phi \right\}$$

$$= (1-\beta_o^2)^{\frac{1}{2}} \left\{ \left(1 - \frac{k_o^2}{k^2}\right)\Delta\bar{\phi}_l - \frac{k_o^2}{k^2}\frac{\alpha k}{2} \left(\frac{T_o I_l}{k_r} r' \cos\phi - \left[\frac{dS_r}{dk} + k\frac{dS_m}{dk} \right] r' \sin\phi \right) \right\}$$

$$\Delta r'_{rl} = \Delta r'_r/2 - (1-\beta_o^2)^{\frac{1}{2}} \frac{\alpha}{2} \left\{ \left(S_r + \frac{k_o^2}{k^2} k S_m \right)\cos\phi + \left(\frac{\partial}{\partial r}\left[\frac{dS_r}{dk} + \frac{k_o^2}{k^2} k \frac{dS_m}{dk} \right] + S_l \right) r' \sin\phi \right\}$$

$$\Delta\bar{r}_{rl} = \Delta\bar{r}_r/2 + (1-\beta_o^2)^{\frac{1}{2}} \frac{\alpha}{2} \left\{ \left(\frac{dS_r}{dk} + \frac{k_o^2}{k^2} k \frac{dS_m}{dk} \right) \sin\phi - \left(\frac{\partial}{\partial r}\left[\frac{d^2S_r}{dk^2} + \frac{k_o^2}{k^2} k \frac{d^2S_m}{dk^2} \right] + \frac{dS_l}{dk} \right) r' \cos\phi \right\}$$

* Adding the term in the square bracket gives the gain in total kinetic energy (cf. eq.(6.1.12))

Common to Tables III to VI

$\alpha = eV_o/(2W)$ $\qquad k_o^2/k^2 = (dz/dt)_o^2/c^2 \approx \beta_o^2$

$W = m/2\ (dz/dt)_o^2 = (m/2)\ \dot{z}_o^2$ $\quad$ m = rest mass $\qquad 1 - k_o^2/k^2 = k_r^2/k^2 \approx 1 - \beta_o^2$

The argument $k = \omega/\dot{z}_o$ of $T_o(k)$, $k_r r_o$ of the modified Bessel functions $I_n(k_r r)$ and k,r_o of $S_l(k,r_o)$, $S_r(k,r_o)$, $S_m(k,r_o)$ and the subscript $_o$ of ϕ_o, r_o and $r_o' = (dr/dz)_o$ have been dropped. In all the expressions of Tables III and VI all these parameters refer to mid-gap values.

	Name of Cavity	Energy (MeV)	Frequency (MHz)	Cell length L (cm)	cavity radius R (cm)	gap length g(cm)	inner rim curvature R_i(cm)	drift tube bore a(cm)	references
CERN 3 MeV Linac	70001	.558	203.07	5.090	53.00	1.274	.15	.824	13) 24)
	70203	.738	203.04	5.470	53.80	1.369	.15	.840	
	51112	1.891	202.94	9.364	53.80	1.769	.20	1.185	
	51415	2.395	203.00	10.531	53.80	2.634	.25	1.306	
	51617	2.764	203.06	11.308	53.80	2.828	.25	1.363	
KATZ	15141	.644	202.19	5.491	48.10	1.302	.73	.743	25)
	15034	7.981	202.40	19.200	48.10	6.248	.73	1.250	
MURA	31335	5.469	201.30	16.010	47.00	4.42	1.00	1.000	26) 24)
	20241	10.860	201.00	22.500	46.10	7.00	1.00	1.000	26)
	30941	19.463	200.44	30.000	49.00	9.50	1.00	1.000	27)
	30830	47.756	200.37	46.000	44.00	14.00	1.00	1.500	27)
	20242	63.784	202.40	52.000	44.00	19.00	1.00	1.500	26)
	30736	84.098	196.98	60.450	43.00	22.00	1.00	2.000	27)
	31465	197.011	200.93	84.000	42.00	40.00	1.00	2.000	26)

Table VII. Geometries of the Cavities investigated.

REFERENCES

1) W.H.K. Panofsky, UCRL-1216, (1951).
L.W. Alvarez et al., Rev. Sc. Instr. 26, 111 - 133 (1955)

2) J.S. Bell, AERE T/M 114, (1954).

3) R. Taylor, AERE R 3012 (1959).

4) D.A. Swenson, 1964 Conf. Proton Lin. Acc. MURA 714, p. 328 - 340.
P.B. Austin et al., MURA 713 (1965).

5) M. Rich, MURA 714, p. 341 - 352.

6) M. Promé, No. SEFS TD 65 /12, CEA, Saclay, (1965).

7) P.M. Lapostolle, CERN internal report AR/Int.SG/65-11, (1965).

8) P.M. Lapostolle, CERN 66-20, (1966).

9) A. Carne, P.M. Lapostolle, M. Promé, in: Proc. 5th Int. Conf. High Energy Acc., Frascati 1965, Ed. M. Grilli, CNEN, Roma 1966, p. 656 - 662.

10) A. Carne and P.M. Lapostolle, Proc. 1966 Linear Acc. Conf. Los Alamos, LA-3609, p. 201 - 204.

11) Linear Accelerators, Eds., P.M. Lapostolle and A.Septier, North Holland Publ. Co., Chap. C.1.2.b (A. Carne et al.) (in preparation).

12) M. Promé, CEA - R - 3261, Saclay, 1968.

13) M. Martini, D.J. Warner, CERN 68-11, (1968).

14) J.A. Stratton, Electromagnetic Theory, McGraw Hill, New York, 1951, pp. 28, 349.

15) F. Borgnis and Ch. Papas, in: Handbuch der Physik, Springer 1956, 16, 415 - 420.
K. Kurokawa, IRE Trans. MTT-6, 178 - 187 (1958).

16) W. Glaser, in: Handbuch der Physik, Ed. S. Flügge, 33, p. 167, Springer 1956.

17) Reference 11), Chap. C.1.1.d (A. Katz).

18) V.I. Smirnov, A Course on Higher Mathematics, Pergamon Press 1964, Vol. II, Chaps. 143, 151, 157.

19) H.S. Carslaw, Introduction to the Theory of Fourier's Series and Integrals, 3rd ed., Dover, 104, 106.

20) Cooke, Proc. London Math. Soc. 28, 207 - 241 (1928).
Erdelyi, Magnus, Oberhettinger, Tricomi: Higher Transcendental Functions, McGraw Hill, New York, N.Y., 1953, Vol. 2, p. 103, eq.(52)(contains misprints).

21) G.N. Watson, Treatise on the Theory of Bessel Functions, Cambridge 1922, University Press, p. 199 - 203.

22) B. Schnizer, Green's Functions and Green's Tensors for the Electromagnetic Field in a Wave Guide (in preparation).

23) P.M. Lapostolle, CERN int. rep. ISR-300/LI-67-36, (1967).

24) M. Martini, J.D. Warner. Private communication.

25) A. Katz, private communication.

26) MURA Linac Cavity Calculations, 0.75 - 200 MeV. March 1967.

27) University of Wisconsin, Physical Sciences Laboratory; MURA linac cavity calculations, 0.75 - 200 MeV, July 1966, Revised July 1967.

28) Handbook of Mathematical Functions, Ed. M. Abramowitz and I.A. Stegun, National Bureau of Standards, 1964, p. 881.
L. Collatz in: Handbuch der Physik, Ed. S. Flügge, Springer 1955, Vol. 2, p. 411.

29) L. Fox and I.B. Parker, Chebychev Polynomials in Numerical Analysis. Oxford London 1968. Oxford University Press, p. 27.

30) A. Ralston et W.S. Wolf : Méthodes mathématiques pour calculateurs arithmétiques, Dunod, Paris, 1965, Chap. 24.

31) B. Schnizer, CERN internal report, ISR-300/LIN/66-36, (1966).

32) K. Johnsen in: R. Kollath, Teilchenbeschleuniger, Braunschweig 1962, Vieweg, p. 273 ref. 8) Chap 2.2 - 2.7.

33) R. Courant, Differential and Integral Calculus, Vol. 1, Chap.III, 3, Interscience Publ.

34) F.R. Moulton, Differential Equations, Dover Publ. (1958). Arts. 27 - 29.

35) Ref. 14) sect. 3.14 - 3.17.

36) E.T. Whittaker, A Treatise on the Analytical Dynamics of Particles and Rigid Bodies. Cambridge University Press, 4th ed. (1959), p. 355.

37) D.A. Swenson, D.E. Young and B. Austin, LA-3609, p. 229 - 232, (1966).
D.A. Swenson, Los Alamos, MP-3/DAS-1 (1967).

38) B. Schnizer, CERN internal report ISR-300/LI-67-45, (1967).

39) B. Schnizer, Proc. US National Particle Acc. Conf. Washington 1967, IEEE Trans. NS-14 557 - 561 (1967).

40) M. Promé, private communication (March 1967).

41) B. Schnizer, Canonical thin lens approximation for an accelerating gap (to be published).

42) B. Schnizer, A new approach to Proton Linac beam dynamics calculations (to be published).

43) J.D. Jackson, Classical Electrodynamics, New York 1962, Wiley, Chap. 3.10.